



**PHARMACOKINETIC INFLUENCES OF SELECTED PHYTOCHEMICAL
COMPOUNDS FROM HERBAL MEDICINES USED BY HIV-POSITIVE PATIENTS
ON DRUG-METABOLISING PROTEINS OF HIV-1 PROTEASE INHIBITOR
DRUGS**

Submitted by

**IDOWU KEHINDE ADEMOLA
Student Number: 218068180**

**In fulfilment of the requirements for the degree of
DOCTOR OF PHILOSOPHY
(MEDICINE)**

**In the
DISCIPLINE OF VIROLOGY**

**School of Laboratory Medicine and Medical Sciences, College of Health Sciences,
University of KwaZulu-Natal, Durban, South Africa.**

July 2020

Supervised by

**Prof. Michelle Gordon
(Supervisor)**

**Prof. Manimbulu Nlooto
(Co-supervisor)**

PREFACE

The experimental work described in this dissertation was carried out in two different laboratories, namely, drug design and computational chemistry laboratory, Discipline of Pharmaceutical Sciences, University of KwaZulu-Natal, Westville campus, and Medical Biochemistry laboratory, University of KwaZulu-Natal, Howard campus from June 2018 to January 2020.

The thesis represents the original work by the author and has not been submitted in any other form for any degree or diploma to another University. Where use has been made of the work of others, it has been duly acknowledged in the text.



Idowu Kehinde Ademola (Candidate)

08 July 2020

Date



Prof. Michelle Gordon (Supervisor)

08 July 2020

Date



Prof. Manimbulu Nlooto (Co-supervisor)

11 July 2020

Date

DECLARATION

I, Idowu Kehinde Ademola, declare that:

- (i) The research reported in this dissertation, except where otherwise indicated, and is my original work.
- (ii) The work described in this dissertation has not been previously submitted to UKZN or any other tertiary institution for purposes of obtaining a degree or any other academic qualification, whether by I or any other party.
- (iii) This dissertation does not contain other person's data, pictures, graph or other information unless specifically acknowledged as being sourced from other researchers. Where other written sources have been quoted, then:
 - (a) Their words have been re-written, but the general information attributed to them has been referenced.
 - (b) Where their exact words have been used, their writing has been placed inside quotation marks and referenced.
- (iv) Where I have produced publication, I drafted the article and together with my supervisors' guidance, input and support submitted the article to the journal. I have completed the dissertation with the guidance and support of my supervisors.
- (v) This dissertation does not contain text, graphics or tables copied and pasted from the internet unless specifically acknowledged, and the source being detailed in the dissertation and the references section.



Idowu Kehinde Ademola (Candidate)

08 July 2020

Date



Prof. Michelle Gordon (Supervisor)

08 July 2020

Date



Prof. Manimbulu Nlooto (Co-supervisor)

11 July 2020

Date

DEDICATION

I dedicate this whole work to God Almighty (the giver of life), my strength at all times and my redeemer.

To my wonderful and beautiful wife, Idowu Deborah (Anike-Ade) and my son, Idowu Mayer for all your support, prayers and understanding, for being there many times, for those inspirational words and encouragement. Thanks a lot; I will always love you guys.

My appreciation also goes to my family (especially my parents, mother-in-law, and siblings), my late Twin sister (Taiwo Idowu), friends and prayer partners.

ACKNOWLEDGMENTS

Words are not enough to appreciate my indefatigable supervisors, Prof. Michelle Gordon and Prof. Manimbulu Nlooto for giving me the privilege to learn from you. Thanks for all the constant coaching and support.

I cannot but appreciate Dr. Rene Khan and Dr. R. Pritika for your assistance, advices and supervision with the experimental and computational works. I say a big thank you.

I also want to appreciate families and friends that God has used during the period of the program, the persons of Dr. Tim Govender, Engr. and Mrs. Akinmejiwa, Prof. and Dr (Mrs) Francis Shode, Dr. John, Dr and Dr (Mrs) Alese, Dr. O. A. Oseni, Dr. Shalie, Mrs. Mamukuyomi, Mr. Ola, the Gbadeyan's family, the Samms' family, Mr. and Rev. (Dr) Timm, Pastor and Pastor (Mrs) Adejimi, Ogunbanwo Adeleke, Simeon Eche, Angela Sinyani, Zola and my other colleagues. God in His infinite mercy will be with you all.

This work was made possible by funding from the College of Health Sciences.

TABLE OF CONTENTS:

PRELIMINARY PAGES.....i - xxiv

GENERAL ABSTRACT.....xxv

CHAPTER ONE.....1

1.0 Introduction.....2

1.1 Background and context of the study.....2

1.2 Problem Statement or Justification for the study.....3

1.3 Research Questions, Aim and Objectives.....4

 1.3.1 General Research Question.....4

 1.3.2 Specific Research Questions.....4

 1.3.2 Aim.....4

 1.3.3 Specific Objectives.....5

1.4 General Methodology.....5

 1.4.1 Study Design.....5

 1.4.2 Materials.....5

 1.4.3 Data Collection and Tools.....6

 1.4.4 Ethical considerations.....7

 1.4.5 Dissemination plan.....7

1.4.6	Statistical Analysis.....	7
1.5	Layout of the dissertation/structure of the dissertation.....	8
1.6	References.....	10
CHAPTER 2.....		12
2.0	LITERATURE REVIEW.....	13
2.1	HIV	13
2.1.1	The Epidemiology and prevalence of HIV in Africa.....	13
2.1.2	The Classification and geographical distribution of HIV.....	14
2.1.3	The Structure of HIV-1.....	16
2.1.4	HIV-1 Life Cycle	17
2.1.5	Inhibitory steps of the HIV-1 life cycle and Antiretroviral Drugs.....	19
2.2	HIV-1 Protease Enzyme.....	20
2.3	HIV-1 Protease Inhibitors.....	22
2.4	Antiretroviral therapy in South Africa.....	23
2.5	Metabolising Enzymes/Transporters and Protease Inhibitors drugs.....	25
2.5.1	Solute Carrier (SLCO) and ATP-Binding Cassette (ABC).....	26
2.5.1.1	P-glycoproteins.....	26
2.5.1.2	Cytochrome P450 (CYP).....	28

2.5.2	CYP3A4 and P-gp Substrate Overlapping.....	30
2.6	Traditional Herbal Medicine and Its Global Usage.....	31
2.6.1	Use of THMs in Africa and South Africa.....	31
2.6.2	Concomitant use of Antiretroviral Therapy and African Traditional Medicine.....	33
2.6.3.	Herb-drug interactions from Concomitant Use of ARVs and THMs.....	33
2.6.4	PI drugs and THMs Interaction.....	34
2.7	Traditional Herbal Medicine Used by HIV-1 Positive Patients in South Africa	35
2.7.1	Antiviral PCs in African Traditional Component Plants from THMs and Their Antiviral Mode of Actions.....	39
2.8	References.....	48
CHAPTER THREE.....		71
	The pharmacokinetic properties of HIV-1 protease inhibitors: A computational perspective on herbal phytochemicals.....	72
CHAPTER FOUR.....		109
	Molecular Dynamic Mechanism(s) of inhibition of Bioactive Phytochemical Compounds targeting Cytochrome P450 3A4 and P-glycoprotein.....	110

CHAPTER FIVE.....	136
Evaluation of Cytotoxicity, Cell Viability and Modulatory Influences of Antiviral Bioactive Compounds on Gene Expressions and Protein Activities of Cytochrome P450 3A4 and P-glycoprotein in HepG2 and HEK293 cell lines.....	137
CHAPTER SIX.....	166
Synthesis.....	167
CHAPTER SEVEN.....	175
Conclusion.....	176
Recommendations.....	177
APPENDICES.....	179
Appendix A: Chapter 3 supporting information.....	180
Appendix B: Chapter 4 supporting information.....	187
Appendix C: Input files for MD simulations for Chapter 3 and 4.....	191
Appendix D: Chapter 5 supporting information.....	198
Appendix E: Published manuscript (Chapter 3).....	201
Appendix F: Published manuscript (Chapter 3).....	213
Appendix G: Ethical Approval.....	225

LIST OF TABLES

CHAPTER TWO

Table 1.1: Classes of antiretroviral agents and the inhibitory step of HIV-1 life Cycle.....	20
Table 1.2: ARVs available in Southern Africa and their Dosages.....	24
Table 1.3: Commercial Herbal Mixtures Commonly Used by HIV-Patients in South Africa.....	37
Table 1.4: Antiviral Activities of PCs from Component Plants Present in Some THMs.....	40

CHAPTER THREE

Table 1: Selected Phytochemicals with antiviral activities present COA [®] -FS herbal medicine and its component plants.....	76
Table 2: Predicted targets involved in the metabolism of the four FDA-approved PI drugs and selected phytochemical compounds.....	83
Table 3: Pharmacokinetic effects of phytochemical compounds on the enzyme and transporter involved in the metabolism of the four FDA-approved PIs.....	86
Table 4: Predicted ADME parameters, drug-likeness, pharmacokinetic and physicochemical properties of phytochemical and four FDA-approved drugs using SWISSADME server.....	88
Table 5: Docking scores for the four FDA-approved PI drugs and phytochemical compounds.....	89
Table 6. Thermodynamic binding free energy for phytochemical compounds and FDA-approved drugs to <i>HIVpro</i>	91

CHAPTER FOUR

Table 1. Thermodynamic Binding Free Energy for PCs and Inhibitors of ABCB1 and CYP3A4.....	123
--	-----

CHAPTER FIVE

Table 1. Result of analysis of the dose dependent curve showing IC ₂₀ and IC ₅₀ of the compounds on HepG2 and HEK293 cells.....	146
---	-----

LIST OF FIGURES

CHAPTER TWO

Figure 1.1: Distribution of HIV-1 subtypes across different geographical locations.....	15
Figure 1.2: The structure of HIV virion particle.....	16
Figure 1.3: The structure illustrating the RNA genome of HIV-1.....	17
Figure 1.4: The viral life cycle of HIV.....	18
Figure 1.5: Crystal structure of homodimer of HIV-1 Subtype C Protease enzyme with the three domains labelled. The flexible structures (flap) open and close to allow the entry of the large-gag poly proteins and the aspartates (ASP 25) allow hydrolytic activity of PR.....	21
Figure 1.6: The protease region is being flanked at the N-terminus by the P ^{6pol} -protease site and the C-terminus by the reverse transcriptase.....	22
Figure 1.7: Mechanism of action of PIs. The HIV PR is the target of PIs; they prevent the cleavage of the polypeptide and maturation of the virion.....	23
Figure 1.8: Illustration of the localization of transport proteins in translocation of PIs.....	25
Figure 1.9: The structure of drug transporting P-gp illustrating the TMD and NBD 1 and 2.....	28
Figure 1.10: The cartoon representation of CYP3A4 structure with different channels.....	30

CHAPTER THREE

Figure 1: 2D Structures of the fifteen selected phytochemical compounds and 2D structures of the Four FDA approved drugs and Crystal structure of South African HIV-1 sub-type C (PDB code 3U71).....	75
Figure 2: RMSD profile of protein backbone atoms calculated over the course of 100 ns molecular dynamics of <i>HIVpro</i> bound to the four different ligands and FDA-approved PI drugs.....	92

Figure 3: RoG profile of protein backbone atoms calculated over the course of 100 ns molecular dynamics of <i>HIVpro</i> bound to different ligands and drugs.....	93
Figure 4: RMSF profile of protein backbone atoms calculated over the course of 100 ns molecular dynamics of <i>HIVpro</i> bound to four different ligands and FDA-approved drugs.....	94
Figure 5: Representation of ligand- <i>HIVpro</i> interactions with different amino acid residues.....	95

CHAPTER FOUR

Figure 1. Superpositions of the crystalized structures of the natural substrates (in red) of the proteins and the ligand-complexes (in green). a) ABCB1 b) CYP3A4 and their respective RMSD values.....	114
Figure 2: Comparative RMSD profile plots of C-a atoms of the ABCB1, RTV and LPV with ligands, a) K7G, b) EGCG, c) EGA and d) LUT systems and CYP3A4, RTV and LPV with e) K7G, f) EGCG, g) EGA and h) LUT calculated throughout 100 ns molecular dynamics.....	118
Figure 3: RoG profile of protein backbone atoms calculated throughout 100 ns molecular dynamics of ABCB1 bound RTV, LPV and ligands, a) K7G, b) EGCG, c) EGA and d) LUT and CYP3A4 bound to RTV, LPV and ligands, e) K7G, f) EGCG, g) EGA and h) LUT systems calculated throughout 100 ns molecular dynamics.....	119
Figure 4: Comparative RMSF plots of Residue-based average C-a fluctuations of the apo (ABCB1), and bound with RTV, LPV and ligands, a) K7G, b) EGCG, c) EGA and d) LUT and CYP3A4 bound to RTV, LPV and ligands, e) K7G, f) EGCG, g) EGA and h) LUT systems calculated throughout 100 ns molecular dynamics.....	121
Figure 5: Solvent accessible surface area of apo (ABCB1) RTV, LPV and ligands, a) K7G, b) EGCG, c) EGA and d) LUT, and CYP3A4 bound to RTV, LPV and ligands, e) K7G, f) EGCG, g) EGA and h) LUT systems calculated throughout 100 ns molecular dynamics.....	122

Figure 6: Amino acid Residues at the NBD of ABCB1 (A) and catalytic site of CYP3A4 (B)....125

Figure 7: Representation of Protein (ABCB1)-ligand interactions plots with different amino acid residues.....126

Figure 8: Representation of Protein (CYP3A4)-ligand interaction plots with different amino acid residues.....128

CHAPTER FIVE

Figure 1. Molecular structures of Epigallocatechin gallate, Luteolin, Kaempferol-7-glucoside and Ellagic acid.....139

Figure 2: Cell viability (MTT assay) of HepG2 cells treated with (A) K7G, (B) EGA, (C) LUT and (D) EGCG.....145

Figure 3: Cell viability (MTT assay) of HEK-293 cells treated with (A) K7G, (B) EGA, (C) LUT and (D) EGCG.....146

Figure 4. Intracellular ATP levels (A and B) and Extracellular LDH levels (C and D) in HepG2 and HEK293 cells treated with both IC₂₀ and IC₅₀ of EGCG, K7G, LUT and EGA.....148

Figure 5: Effects of the compounds at IC₂₀ and IC₅₀ concentrations on ABCB1 mRNA and protein expressions in HepG2 cells (A and B) and in HEK293 cells (C and D).....150

Figure 6: Effects of the compounds at IC₂₀ and IC₅₀ concentrations on CYP3A4 mRNA and protein expression in HepG2 cells (A and B) and in HEK293 cells (C and D).....152

ETHICAL APPROVAL

The Biomedical Research Ethic Committee (BREC) of the College of Health Sciences, University of KwaZulu-Natal considered and granted this thesis titled ‘Pharmacokinetic Influences of Selected Phytochemical Compounds From Herbal Medicines Used By HIV-Positive Patients On Drug-Metabolising Proteins of HIV-1 Protease Inhibitor Drugs’ full ethical approved (BREC Ref No: BE566/18).

LIST OF ABBREVIATIONS

Å	Amstrong
ABCB1	ATP-binding cassette gene 1
Ags	Antigens
AIDS	Acquired Immune Deficiency Syndrome
AMPK α	AMP-dependent protein kinase α
AMV	Amprenavir
APG	Apigenin
ART	Antiretroviral therapy
ARVs	Antiretroviral drugs
ASP25	Aspartate residue 25
ATP	Adenosine Triphosphate
ATV	Ritonavir
ATZ	Atazanavir
BA	Bile acids
BCA	Bicinchoninic Acid
BREC	Biomedical Research Ethic Committee
BSEP	Bile Salt Export Pump

CA	Capsid
cART	Combination of Antiretroviral Therapy
CCM	Complete Culture Media
CCRC5	CC chemokine receptor 5
CD4	Cluster of Differentiation 4
cDNAs	Complimentary Deoxyribonuclie Acids
CHIKV	Chikungunya Virus
CHPC	Center for High Performance Computing
CM	Cryptococcal Meningitis
Cmax	Plasma Concentration
AUC	Plasma Concentration-Time Curve
COA [®] -FS	Centre of Awareness- food supplement
CPE	Cytopathic Effect
CRFs	Circulating Recombinant Forms
CYP450	Cytochrome P450
CYP1	Cytochrome P450 1
CYP2	Cytochrome P4502
CYP2C19	Cytochrome P450 2C 19

CYP3	Cytochrome P450 3
CYP4	Cytochrome P450 4
CYP5	Cytochrome P450 5
CYP7	Cytochrome P450 7
CYP8	Cytochrome P450 8
CYP11	Cytochrome P450 11
CYP17	Cytochrome P450 17
CYP19	Cytochrome P450 19
CYP20	Cytochrome P450 20
CYP21	Cytochrome P450 21
CYP24	Cytochrome P450 24
CYP26	Cytochrome P450 26
CYP27	Cytochrome P450 27
CYP39	Cytochrome P450 39
CYP46	Cytochrome P450 46
CYP51	Cytochrome P450 51
CYP3A4	Cytochrome P450 3A4
DCCM	Dynamic Cross-Correlation Matrix

DENV	Dengue Virus
DMEM	Dulbecco's Modified Eagle Medium
DNA	Deoxyribonucleic acid
DRV	Darunavir
EGA	Ellagic acid
EGCG	Epigallocatechin-3-gallate
EHV	Equine Herpes Virus
ELISA	Enzyme-Linked Immunosorbent Assay
EMEM	Eagle's Minimum Essential Medium
env	Envelope gene
EV	Enterovirus
FDA	Food and Drug Administration
FP	Full-Length Promoter
FPR	Fosamprenavir
FST	Fisetin
GAFF	General Amber Force Field
gag	Capsid Proteins
GER	Geranin

HAART	Highly Active Antiretroviral Therapy
HBsAg	HBV antigen
HBsAg	Hepatitis B Antigen
HBV	Hepatitis B Virus
HBV	Hepatitis B Virus
HCV	Hepatitis C Virus
HCV	Hepatitis C Virus
HEK-293	Human Embryonic Kidney cells
HEP-G2	Human liver Hepatocellular cell line
HBP	High blood pressure
HIV	Human Immunodeficiency Virus
HSV	Herpes Simplex Virus
IAV	Influenzas A virus
IC	Inhibitory Concentration
IDV	Indinavir
InSTIs	Integrase inhibitors
IST	Isosteviol
K7G	Kaemperol-7-glucoside

KZN	Province of KwaZulu-Natal
LDH	Lactate Dehydrogenase
LNT	Lanosterol
LPV	Lopinavir
LUT	Luteolin
MA	Matrix
MD	Molecular dynamics
MDR1	Multidrug Resistance Proteins 1
MM/GBSA	Molecular Mechanics Energies/Generalized Born and Surface Area
mRNAs	Messenger Ribonucleic Acid
MTT	3-(4,5-dimethylthiazol-2-yl)-2,5-diphenyltetrazolium bromide
NAD ⁺	Nicotinamide adenine dinucleotide
NADH/H ⁺	Nicotinamide adenine dinucleotide Hydrogen
NBD	Nucleotide-Binding Domains
NC	Nucleocapsid
NFR	Nelfinavir
NGN	Naringenin
NNRTIs	Non-nucleoside reverse transcriptase inhibitor

NRTIs	Nucleoside reverse transcriptase inhibitors
ns	Nanosecond
NTCP	Sodium-taurocholate co-transporting polypeptide
NtRTIs	Nucleotide reverse transcriptase inhibitors
OAPTs	Organic anion transporting polypeptides
OCTs	Organic Cation Transporters
OD	Optical density
PCs	Phytochemical Compounds
PDB	Protein Data Bank
P-gp	P-glycoprotein
PI-3	Parainfluenza virus
PIs	Protease Inhibitor Drugs
pol	Polymerase gene
PR	Protease enzyme
PTA	Phthalic acid
PV	Polio Virus
PXR	Pregnane X receptor
RBD	Relative Band Density

RESP	Restrained Electrostatic Potential
RLU	Relative Light Units
RMSD	Root Means Square Deviation
RMSF	Root Means Square Fluctuation
RNA	Ribonucleic Acid
RoG	Radius of Gyration
RSV	Respiratory syncytial virus
RT	Reverse Transcriptase Enzyme
RT-PCR	Real-Time Polymerase Chain Reaction
RV	Rabies Virus
RXR	Retinoid X-receptor- α
SARS	Severe Acute Respiratory Syndrome
SASA	Solvent accessible surface area
SIV	Simian Immunodeficiency Virus
SLC	Solute Carrier
SPS	Strengthening Pharmaceutical Systems
SQV	Saquinavir
SV	Sindbis Virus

TB	Tuberculous
TBM	Tuberculous Meningitis
THMs	Traditional Herbal Medicines
TPV	Tipranavir
UNAIDS	The Joint United Nation Programme on HIV and AIDS
USA	United States of America
VCT	Voluntary Counselling and Testing
VL	Viral Load
WHO	World Health Organization
ZIKV	Zika Virus
μl	microlitre
μmol	micromole

General Abstract

Introduction: Sub-Saharan Africa has the highest incidence of HIV/AIDS and AIDS-related deaths in the world. Although there is currently no cure for the disease, significant progress has been made in developing antiretroviral drugs (ARVs) that can inhibit disease progression. However, despite the availability of these ARVs, HIV-positive patients use traditional herbal medicines (THMs) either alone or simultaneously with conventional ARVs. This simultaneous usage may cause serious adverse effects due to herb-drug interactions, although there are also possible positive effects such as the enhanced bioavailability of the ARVs or possible antiviral activity.

Aim: These potential interactions prompted this study which examined the pharmacokinetic properties and influences of selected phytochemical compounds (PCs) commonly found in THMs on drug-metabolising proteins involved in the metabolism of protease inhibitor drugs (PIs) as well as their potential as inhibitors of HIV-1 protease.

Method: The potential inhibitory activities of fifteen PCs (Epigallocatechin gallate (EGCG), Fisetin (FST), Ellagic acid (EGA), Cholesta-4,6-dien-3-ol (CHD), Lanosteol (LNT), Benzyl Isothiocyanate (BIT), Gallic acid, (GA), Isosteviol (IST), Stigmasterol (STG), Phthalic acid (PTA), Naringenin (NGN), Kaempferol-7-glucoside (K7G), Luteolin (LUT), Geranin (GER), Apigenin (APG)) against the South African sub-type C HIV-1 protease enzyme and PIs' drug-metabolizing proteins were investigated, using molecular dynamic (*in-silico*) techniques. Furthermore, an *in vitro* evaluation of the cytotoxicity assays, cell viability profiles and modulatory influences of the most promising antiviral PCs on the mRNA and protein expressions of the drug-metabolising proteins in two human cell lines (liver (HepG2) and kidney (HEK293)) was carried out.

Result: Four of the fifteen PCs (EGCG, K7G, LUT and EGA) were predicted to be potential inhibitors of HIV-1 protease, as well as inhibitors of cytochrome P450 3A4 (CYP3A4) and P-glycoprotein P-gp/ABCB1. Results from the *in vitro* study showed that these four PCs were not toxic to HepG2 cells at their IC₅₀ (50% cell viability) and IC₂₀ (80% cell viability). ATP (adenosine triphosphate) levels increased at IC₂₀, with no significant change at IC₅₀. In addition, no significant change in LDH (lactate dehydrogenase) was seen (with the exception of LUT). In the HepG2 cells, ABCB1 protein expression (western blot) decreased overall. While all PCs decreased CYP3A4 protein expression at IC₂₀, (with the exception of LUT)

protein expression increased at IC₅₀. mRNA levels were decreased for EGCG and K7G at IC₂₀. In HEK293 cells, all PCs were non-toxic. ATP concentrations were similar to the control except for EGCG which decreased at IC₂₀, and K7G which increased at IC₅₀. LDH concentration decreased when exposed to the PCs at IC₂₀, but a significant ($p < 0.05$) increase was recorded in LUT IC₅₀. ABCB1 protein expression increased at both IC₂₀ and IC₅₀ concentrations, although LUT and EGA mRNA expression decreased at IC₅₀. The decreased protein activities of CYP3A4 in K7G IC₅₀ and LUT IC₂₀ correlates with increased intracellular ATP.

Conclusion: The study therefore suggests that EGCG, K7G, LUT and EGA could decrease the biotransformation of drugs, and eventually increase drug plasma concentrations in the systemic circulation. These natural compounds that can serve as inhibitors of drug-metabolizing proteins and the HIV-1 protease enzyme could be useful in the treatment of HIV-1.

Keywords: Pharmacokinetic, HIV-1 protease inhibitor, Drug-metabolising proteins, Molecular simulations.

CHAPTER ONE

Chapter one of this thesis gives a brief introduction and the rationale behind the overall thesis, defining research questions, the aim and objectives of the study and a summary of the methodology.

1.0 INTRODUCTION

1.1 Background and context of the study

Acquired Immune Deficiency Syndrome (AIDS) is caused by Human Immunodeficiency Virus (HIV) [1]. At the end of 2018, approximately 38 million people were reported to be HIV-positive globally [2]. Sub-Saharan Africa is the most severely affected region in the world, and accounts for over 68% (25.8 million) of infections, and likewise the region with the highest number of AIDS-related deaths [2]. Among the 25.8 million, 20.6 million are living in East and Southern Africa [2]. Currently, there is no cure for HIV/AIDS; however the use of conventional antiretroviral drugs (ARVs) can significantly repress viral replication, with 23 million people currently accessing antiretroviral therapy (ART) worldwide [3]. Unfortunately, the emergence of resistant strains of the virus and complications caused by drug toxicity may compromise the effectiveness of these regimens. Despite the significant progress and advances made in the treatment of HIV infections with orthodox medicine, HIV positive patients all around the world still practice the concurrent use of prescribed ARVs and many traditional herbal medicines (THMs) [4].

The use of THMs is gaining more acceptance and recognition in the treatment of numerous diseases like HIV in several countries [5]. The World Health Organization (WHO) reported that about 80% of African and Asian populations depend on THMs for treatment of various diseases [6]. In South Africa, there are over 200,000 THMs countrywide [7-10]. This increased usage has prompted the South African Department of Health to involve THMs in the fight against HIV/AIDS and other related diseases. THMs are used to treat the side effects of ARVs as well as fungal infections, stomach upsets, pain and dizziness. Other reasons for the use of THMs by

patients are to complement dietary intake, improve energy levels, boost the immune response and the belief that these THMs could cure HIV/AIDS [11].

The significant increase in the usage of THMs in both developing and developed has caused considerable public health concern among scientists and physicians who are sometimes not sure about the safety of these herbal preparations especially when used concurrently with regular orthodox medications such as ARVs [12] because of herbal-medicine: drug interactions that could lead to severe toxicities and adverse reactions. Aside from the interaction between ARVs and THMs, toxicities arising from the usage of THMs can be erroneously attributed to ARVs complicating the clinical management of the patients.

1.2 Problem Statement or Justification for the study

In their health-seeking behavior, HIV positive patients either use THMs alone or in combination with ARVs. This habit is significantly gaining more popularity all around the world among people living with HIV [7, 10]. However, there are very few studies on the use of THMs and its impact on the efficacy of ARVs. The few available studies did not investigate the direct impact of the bioactive phytochemical compounds (PCs) of these THMs on the pharmacokinetic properties of ARVs or drug-metabolizing proteins of these ARVs. This dissertation therefore examined and described the pharmacokinetic influence(s) of some bioactive PCs present in THMs used by HIV-positive patients (in South Africa) on the drug-metabolizing proteins involved in the metabolism of commonly prescribed protease inhibitor drugs (PIs), as well as their potential as inhibitors of HIV-1 protease.

1.3 Research Questions, Aim and Objectives

1.3.1 General Research question

The general research question of this study is: “*What are the pharmacokinetic influences of selected phytochemical compounds from herbal medicines used by HIV-positive patients on drug-metabolising proteins of HIV-1 protease inhibitor drugs?*” To answer this general research question, specific research questions have been developed below.

1.3.2 Specific Research Questions

1.3.2.1 What are the pharmacokinetic properties and antiviral potentials of selected bioactive PCs against the South African subtype C HIV-1 protease enzyme (PR)?

1.3.2.2 What are the pharmacokinetic influence and structural mechanisms of inhibition/induction of the selected bioactive PCs on the drug-metabolizing proteins involved in the metabolism of the PIs?

1.3.2.3 What are the cytotoxicity, cell viability profiles, and modulatory influences of the selected PCs on mRNA and protein expressions of drug-metabolizing proteins involved in the metabolism of HIV-1 PIs?

1.3.3 Aim

To determine the pharmacokinetic influence(s) of bioactive PCs present in THMs used by HIV-positive patients on drug-metabolizing proteins involved in the metabolism of commonly prescribed PIs and to investigate their potential as HIV-1 protease inhibitors.

1.3.4 Specific Objectives

1.3.4.1 To determine the pharmacokinetic properties of selected bioactive PCs and their antiviral potentials against the South African subtype C HIV-1 protease enzyme (PR).

1.3.4.2 To determine the pharmacokinetic influence and structural mechanisms of inhibition/induction of the selected bioactive PCs on the drug-metabolizing proteins involved in the metabolism of the PIs using *in-silico* tools,

1.3.4.3 To evaluate the cytotoxicity, cell viability profiles, and modulatory influences of the selected PCs on mRNA and protein expressions of drug-metabolizing proteins involved in the metabolism of HIV-1 PIs.

1.4 GENERAL METHODOLOGY

1.4.1 Study Design

This study was carried out in two phases; the first phase was a virtual experimental study using *in silico* techniques, while phase two involves *in vitro* validatory experimentation using cell line models (liver, HepG2 and kidney, HEK293).

1.4.2 Materials

1.4.2.1 Phase 1: The materials used for the first phase of the study include, a laptop computer, SWISSPREDICT Software to identify specific enzymatic targets of the PCs, SWISSADME Software, to determine the pharmacokinetics properties of the PCs, and Chimera software for molecular docking to establish a molecular complex between the drug-metabolising proteins, South African sub-type C HIV protease and the PCs.

1.4.2.2 Phase 2: The materials used for this phase of the study are two specific cell line models for *in vitro* experiment. Other materials include, culture growth medium for cells, QuantiTect SYBR Green PCR kit (Qiagen) and primers for quantitative polymerase chain reaction (qPCR) for gene expression experiment and antibodies for western blotting.

1.4.3 Data Collection and Tools

1.4.3.1 Phase 1 (Computational Analysis): Computational analysis was carried out on the selected PCs; the first procedure was to identify specific enzymatic targets of the phytochemicals. Following this prediction, the pharmacokinetic properties of the PCs were determined. Once the protein(s) have been identified, molecular docking using the Chimera software was carried out to establish a molecular complex between the specific drug-metabolising proteins, South African sub-type C HIV protease and the PCs. Molecular dynamic stimulations, using the centre for high performance computing (CHPC), then established the conformational modifications of the proteins upon binding of the PC. As computational studies are strictly predictive, *in vitro* analysis will be required (toxicity test and gene expression analysis).

1.4.3.2 Phase Two (Cytotoxicity study, Protein and mRNA Expression analysis).

The *in vitro* analysis was conducted using two cell line models (liver, HepG2 and kidney, HEK293) cell lines. The four best compounds with better inhibitory activities were selected for this phase. All tests were conducted in triplicate to ensure unbiased results. Toxicity analysis using the MTT (3-(4, 5-dimethylthiazol-2-yl)-2, 5-diphenyltetrazolium bromide) assay at an acute (24 hours) period was assessed. Base on this assay, the PCs IC₅₀ (50% cell viability) and IC₂₀ (80% cell viability) were calculated. The cells were

treated with both IC₂₀ and IC₅₀ concentrations of the PCs. Both mRNA and protein expression for the drug-metabolising proteins were analysed using optimized real time polymerase chain reaction (RT-PCR) and western blotting, respectively.

1.4.4 Ethical considerations

This study proposal was submitted to the Biomedical Research Ethic Committee (BREC) of the University of KwaZulu-Natal for ethical approval before the commencement of the study, and was fully approved by BREC (Ref No: BE566/18).

1.4.5 Dissemination plan

The findings of this study are presented in publishable manuscripts. Chapter 3 consists of a peer-reviewed published article in an Elsevier Journal (Heliyon, 5; e02565, Appendix E) and chapter 4 consists of a peer-reviewed published article in Journal of Biomolecular Structure and Dynamics (DOI: 10.1080/07391102.2020.1821780).

1.4.6 Statistical Analysis

Statistical analyses were performed using GraphPad Prism version 5.00 software package (GraphPad PRISM®) and Microsoft excel 2010. Data are expressed as mean ± standard error of the mean (SEM). Dose-response-Inhibition (Log(inhibitor) vs. normalized response) was used for the MTT assay. Comparisons were made using the unpaired Student *t*-tests using Welch correction. Statistical significance was set at 0.05. All computational raw data plots were generated using the Origin data analysis software.

1.5 Layout of the dissertation/structure of the dissertation

Chapter One: Chapter one of this thesis, gives a brief introduction and the rationale behind the overall thesis, defining the research questions, aim and objectives. The layout of the thesis is described, and a summary of the methodology. However, each data chapter of the thesis has full description of its methodology.

Chapter Two: This chapter contains a general literature review that informs the background to the approach of this thesis.

Chapter Three: This chapter presents the published manuscript in Heliyon, 5; e02565 (Appendix E) that described the pharmacokinetic properties of the selected bioactive PCs and their antiviral potential activity against South African sub-type C HIV-1 PR.

Chapter Four: This chapter examines the inhibitory activities and molecular dynamic mechanisms of inhibition of the bioactive PCs targeting CYP3A4 and P-gp. (Manuscript published in the Journal of Biomolecular Structure & Dynamics (DOI: 10.1080/07391102.2020.1821780, Appendix F).

Chapter Five: This chapter describes the cytotoxicity, cell viability profile and modulatory influence(s) of the selected antiviral bioactive PCs on CYP3A4 and P-gp mRNA and protein expressions in two human cell lines (liver (HEPG2) and kidney (HEK293)). (Manuscript submitted to Journal Bioorganic Chemistry under manuscript number BIOORG-D-20-00966).

Chapter Six: This is a synthesis chapter, where we piece together and highlight the different findings from the study and place the study in the broader context. And the summary of the research questions and the main findings presented.

Chapter Seven: This is the concluding chapter of the thesis, where the study conclusion and recommendations for further research are presented.

References

1. Gurib-Fakim, A. *Medicinal plants: Traditions of yesterday and drugs of tomorrow*. Mol. Aspect of Med. 2006. 27:1-93.
2. UNAIDS. AIDSinfo.unaids.org. 2019. https://www.avert.org/global-hiv-and-aids-statistics#footnote1_qlt481t. (Accessed 10/01//2020).
3. Antonia, N.J., Tabuti, R. S., Mohammed, L.B. K., Yahaya, S., Philip, R. A. *Medicinal plants and traditional treatment practices used in the management of HIV/AIDS clients in Mpigi District, Uganda*. J. of Ethnopharmacology. 2017. 130, (1), 43-53.
4. Gyasi, R. M., Tagoe-Darko, E., Mensah, C. M. *Use of Traditional Medicine by HIV/AIDS Patients in Kumasi Metropolis, Ghana: A Cross-sectional Survey*. American Int. J. of Contemp. Res. 2013. 3:117–129.
5. AIDS InfoNet. *Alternative and complementary therapies*. 2014. http://www.aidsinfonet.org/fact_sheets/view/700. (Accessed 10/01//2020)
6. World Health Organization. *Traditional medicine*. WHO, Geneva. 2008. <http://www.who.int/mediacentre/factsheets/fs134/en/>.(Accessed 10/01/2020).
7. Hughes, G., Puoane, T., Clark, B., Wondwossen, T., Johnson, Q., Folk, W. *Prevalence and predictors of traditional medicine utilization among persons living with AIDS on antiretroviral and prophylaxis treatment on both rural and urban areas in South Africa*. Afr. J. Traditional, Complementary and Alternative Med. 2012. 9(4): 470-484.
8. Pretorius, E. *South African Health Review*. 5th Edition. Durban: Health Systems Trust; ‘Traditional Healers. 1999. pp. 249–256.
9. Razak, M. A., Eva, T., Charlotte, M. M. *Use of Traditional Medicine by HIV/AIDS Patients in Kumasi Metropolis, Ghana: A Cross-sectional Survey*. American Intern. J. of Contemporary Res; 2013.3, (4), 117-129.
10. Richter, M. *Traditional medicine and traditional healers in South Africa*. Treatment Action Campaign and AIDS Law Project. 2003. 4(10):45-78).

11. Sibanda, M., Nlooto, M. M., Naidoo, P. *Concurrent use of Antiretroviral and African traditional medicines amongst people living with HIV/AIDS in the eThekweni Metropolitan area of KwaZulu Natal*. *Afr. Health Sci*; 2016. 16(4): 1118–1130.
12. World Health Organization. *The Use of Stems in the Selection of International Nonproprietary Names (INN) for Pharmaceutical Substances*. 2016. https://www.who.int/medicines/services/inn/StemBook_2018.pdf?ua=1. (Accessed 10/01/2020).

CHAPTER TWO

Chapter two contains a general literature review that informs the background to the approach of this thesis.

2.0 LITERATURE REVIEW

2.1 HIV

2.1.1 The Epidemiology and Prevalence of HIV in Africa

At the end of 2018, the United Nations program on HIV/AIDS reported that approximately 38 million people were living with HIV worldwide [1]. The endemic of HIV differs from one country or region to another, according to a UNAIDS special report, Sub-Saharan Africa being the most affected region, accounts for approximately 26 million people living with HIV [1]. Studies have attributed the high spread of HIV/AIDS across sub-Saharan Africa to many significant factors such as; numerous sex partners, late or few usage of condom, low occurrence of circumcision, sex work, early exposure to sexual life, poverty, strong cultural beliefs in witchcraft, economic uncertainty in some countries, and colonialism practices (such as hard labour, harsh condition, and unsafe injection and vaccination practices), long latency period of the virus, lack of immediate symptomatology, denial of the existence of HIV/AIDS by governments and infected individuals, late or lack of preventive efforts, poverty and economic hardship, war or political instability and lack of education [2, 3].

From retrospective studies, it was determined that the first case of HIV in Africa occurred in Kinshasa, Democratic Republic of Congo in 1970 [4]. The disease rapidly spread to West and East Africa in the 1980s [5-7]. The spread was influenced by the booming commercial sex industry between industry services truckers, merchants, and migrant workers along the highway between Tanzania and Zambia. As a result, the second highest occurrence rate of HIV in the continent was found in Tanzam, a highway and railway station between Tanzania and Zambia in 1988 (www.avert.org/history-aids-africa.htm).

In Sub-Saharan Africa, South Africa has the highest number of HIV-1 infected people (estimate of 7.7 million by the end of 2018 [8], with approximately 240,000 new case of HIV infections reported at the end of 2018. In 2018, the number of HIV/AIDS-related death was 71,000 [8]. The first case of HIV in the country was reported in a homosexual air steward from the USA, who died of pneumonia in 1982 [9]. In South Africa, HIV-1 prevalence varies significantly by province [10]. For example, KwaZulu–Natal with a prevalence of almost 12.2% has the highest number of people living with HIV [11]. Moreover, Northern Cape and Western Cape have the least prevalence of 6.8% and 5.6% respectively [12, 13].

2.1.2 The Classification and geographical distribution of HIV

HIV is subdivided into two types, namely, HIV-1 and HIV-2 [14]. HIV-1 is spread across the world, while HIV-2 is primarily restricted to West Africa [15], but has been reported in other countries with connections to West Africa countries. Of these two types of HIV, HIV-1 is accountable for approximately 95% of all infections in the world [16]. HIV-2 accounts for fewer deaths than HIV-1, due to its less infectious nature than HIV-1 [17]. The two types were reported to have different origins, HIV-1 was assumed to have its origin from three cross-species transmissions of the simian immunodeficiency virus (SIV) that infected chimpanzees, and HIV-2 is assumed to have originated from sooty mangabey monkeys [18]. Four classifications of genetic diversity were reported for HIV-1, namely: Major (M), Outlier (O), N (non-M/N) and Putative (P) [19, 20]. The group M is responsible for more than 90% of HIV-1 infections and is split into nine genetic subtypes (A, B, C, D, F, E, H, J, and K), six subtypes (A1–A4, and F1–F2) and a range of circulating recombinant forms (CRFs) [20, 21]. Subtype C is found mostly in Southern and Eastern Africa, while Subtype A is found mostly in East Africa [18]. Subtype D is predominant in East Africa, and B in Northern Africa and Western world [22]. Subtype F is

subdivided into F1 and F2, and has been reported in South America, Africa and Eastern Europe [23, 24]. Subtype G and A/G recombinants also occur in Eastern Africa and in Central Europe, while H and K only occur in Central Europe. Subtype J has been found in Central America [23]. The Geographical distribution of the HIV-1 subtypes is illustrated in figure 1.1 below.

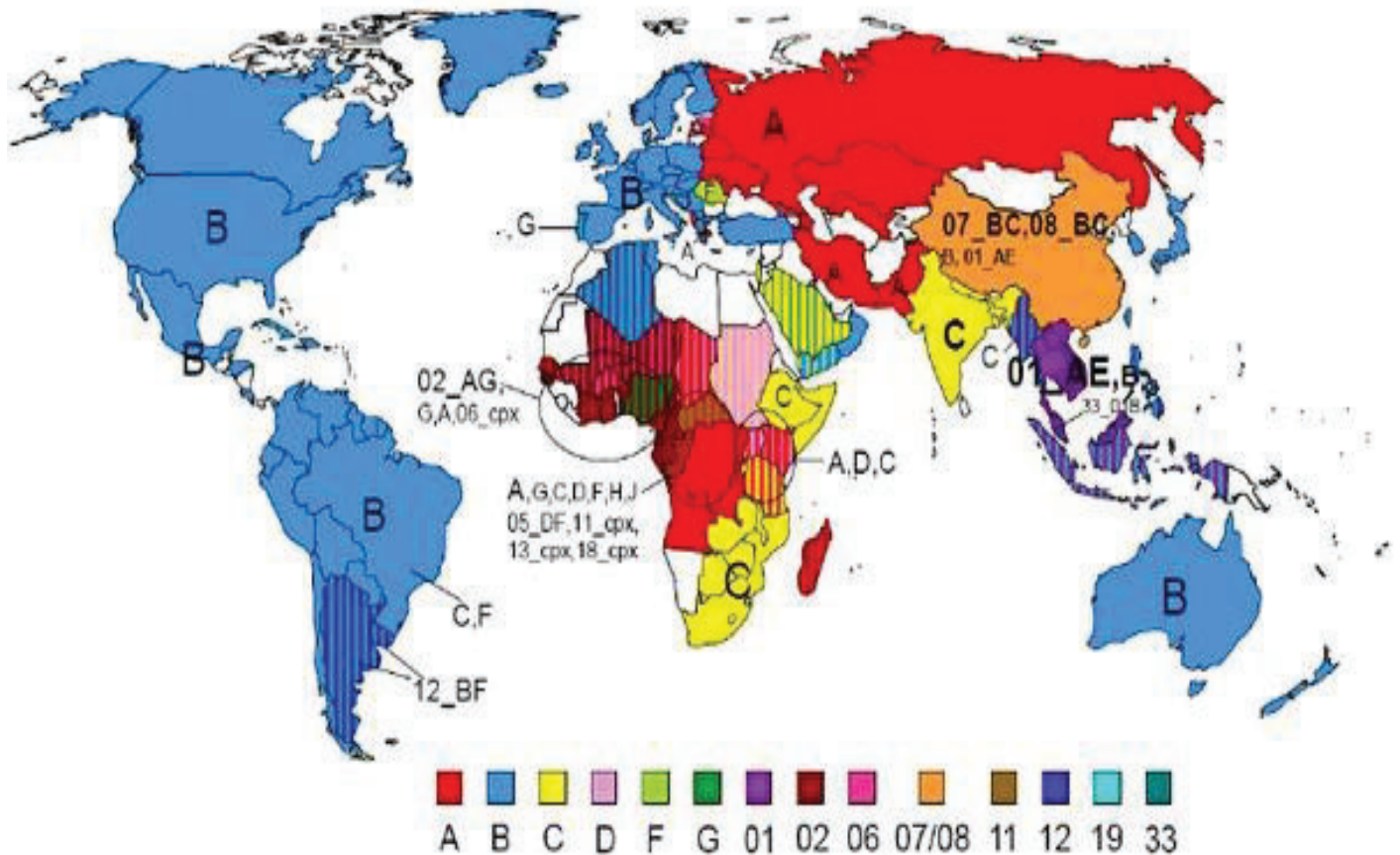


Figure 1.1: Distribution of HIV-1 subtypes across different geographical locations (Adopted from Michael, 2011 [25]).

2.1.3 The Structure of HIV-1

HIV-1 virions have a spherical shape and consist of two essential components: the core genetic component and the protein component called the capsid, which surrounds the genetic component [26]. The genetic information of the virus is housed in the genome, while the capsid protects the virus and gives it shape. The lipid bilayer membrane of the virus surrounds the viral Env glycoprotein and a number of cellular proteins [26].

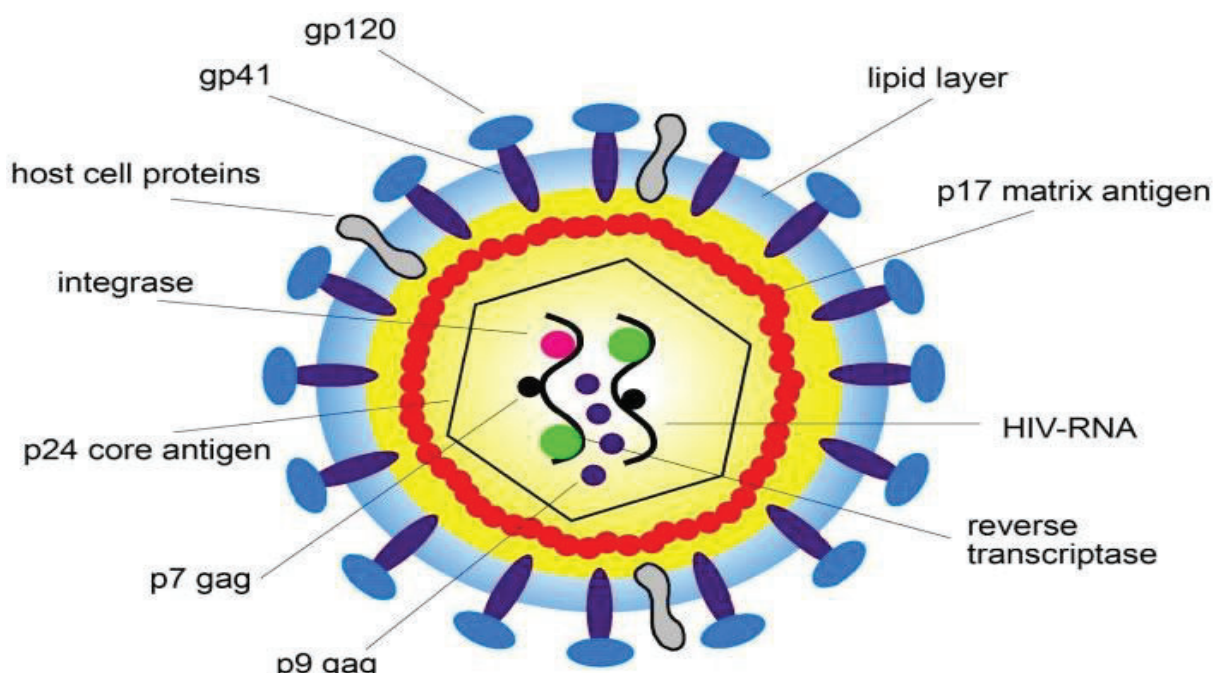


Figure 1.2: The structure of HIV virion particle. Source: www.HIVbook.com/2011/10/28/3-pathogenesis-of-hiv-1-infection/.

Matrix (MA), p6, capsid (p24) and nucleocapsid (NC/p7) form the structural proteins [27]. The Matrix (MA) forms a shell that connects to inner side of the membrane. The capsid has the N-terminal domains that are arranged in a hexameric ring to form a capsid. The NC is involved in the formation of the genomic RNA dimers as well as the stabilization of the NC assembly. The p6 is essential for the last stage of viral assembly and the release of the *vpr* protein. Both the

structural components, enzymes and genomic. Infected cells will then begin to produce immature virions [26]. These newly formed viruses leave the cell by budding. The HIV-1 protease enzyme then cleaves to the Gag and Gag pol polyprotein to produce mature viruses [26]. Many more CD4 cells are then infected by the newly produced and released viruses (virions) to repeat the whole process. The life cycle of HIV-1 is summarized in figure 1.4 below:

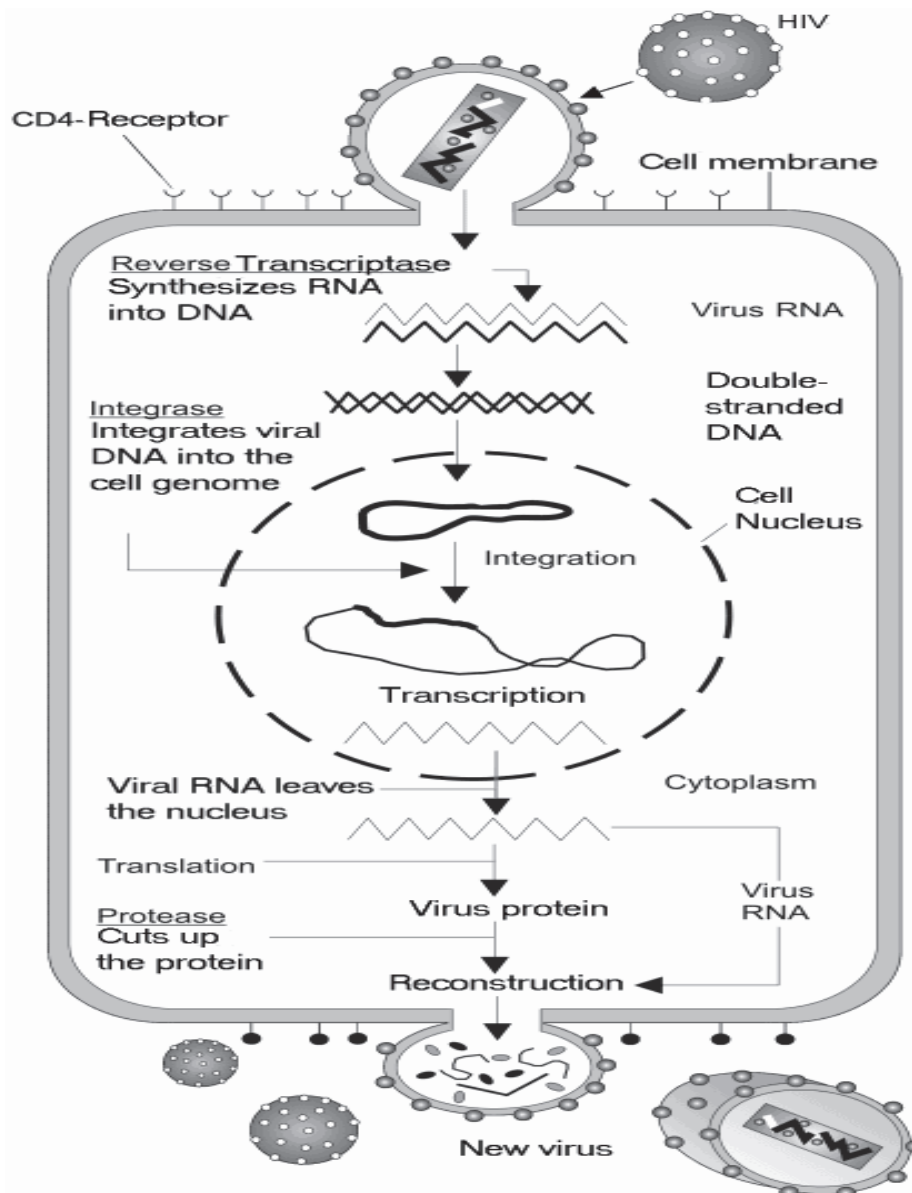


Figure 1.4: The viral life cycle of HIV. Source: www.aidsinfonet.org.

2.1.5 Inhibitory steps of HIV-1 life cycle and Antiretroviral Drugs

The Food and Drug Administration (FDA) has approved not less than twenty drugs for anti-HIV-1 therapy [31]. ARV therapy is the use of anti-HIV drugs (ARVs) to treat HIV infections to repress the replication of the HIV by disturbing or inhibiting the vital steps of HIV life circle [32] and, have been reported to be the most efficient and successful therapy to achieve a durable viral load suppression and restoring the immune system [33]. The key objectives of ART is to deliver the highest and long-lasting suppression of viral load (VL), reinstate the immune function, decrease HIV/AIDS-related death, improve life expectancy and quality of life, prevent the transmission of the virus, and reduce adverse side effects of the treatment [34]. There are five classes of HIV-1 inhibitor drugs available; Protease Inhibitors (PIs), Nucleoside, Nucleotide and Non-nucleoside reverse transcriptase inhibitors (NRTIs, NtRTIs, NNRTIs), Integrase inhibitors (InSTIs), and Entry inhibitors (CCR5) [34-36]. Stavudine, lamivudine, emtricitabine, abacavir, zidovudine and tenofovir are commercially available NRTIs. While, darunavir, atazanavir and lopinavir/ritonavir are known HIV-1 protease inhibitor drugs. NNRTI drugs include efavirenz, delavirdine, etravirine, and nevirapine [35, 36].

ART is usually a combination of two NTRIs and one PI or NNTRI [34, 37]. Studies revealed that ART has significantly increased both the emotional and physical quality of life for people living with HIV/AIDS and subsequently reduced HIV/AIDS-related deaths [38].

Table 1.1: Classes of antiretroviral agents and the inhibitory step of HIV-1 life Cycle [34].

Class	Mechanism of inhibiting HIV-1 life cycle	Specific action
NRTIs, NtRTIs	Inhibit reverse transcriptase	Mimic the structure of DNA, thereby stopping transcription HIV-1 RNA to DNA
NNRTIs	Inhibit reverse transcriptase	Modify the catalytic site (conformational change) and inhibits activity of reverse transcriptase
PIs	Inhibit protease	Inhibition of the final developmental stages of the virus replication, subsequently leading to the formation of immature virion
InSTIs	Inhibit viral integration	Inhibit the transmission of pro-viral DNA strands into the chromosomal DNA of the host
Entry Inhibitors	Inhibit viral entry	Bind to HIV-1 gp41/gp120 or host cell CD4+/chemokine receptors

2.2 HIV-1 Protease Enzyme (PR)

As seen in figure 1.4, several enzymes are important for successful replication of HIV-1. The HIV-1 PR is crucial enzyme that catalyzes the production of matured, viable and infectious virions [39]. HIV-1 PR is a C₂-symmetric active homodimer (two monomers of 99 amino acids each) and is from the family of aspartic proteases [32, 40]. The two monomeric chains assemble to form an enclosed tunnel covered by two flaps that characteristically "open and close" upon substrate binding [40]. The active site (amino acid position 25-27), the dimerization (amino acid position 94-95) and the flap domains (amino acid position 46–56) are the three crucial domains of the HIV-1 protease enzyme (Figure 1.5). The active site confers the hydrophilic activity of the enzyme while the flap domain allows the entry of the large gag polyproteins. The dimerization

domain is responsible for dimer formation as well as stabilization of an active protease [32]. This is an auto-processing mechanism that is categorized into two intramolecular and successive steps. The first step is the cleaving of the N-terminus at the P6pol-protease site and the cleaving of the C-terminus at the PR-RT cleavage site is the second step [41, 42].

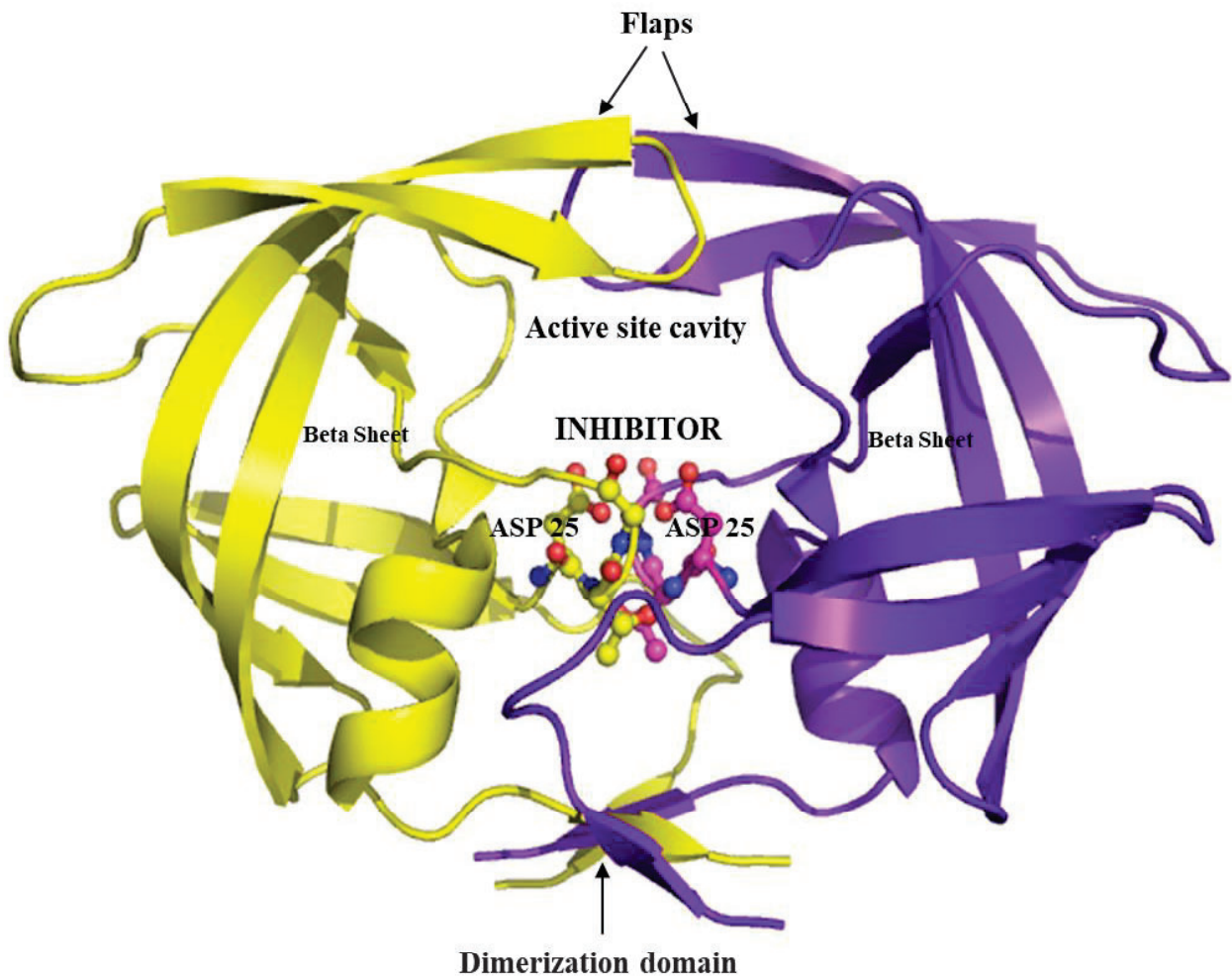


Figure 1.5: Crystal structure of homodimer of HIV-1 Subtype C Protease enzyme with the three domains labelled. The flexible structures (flap) open and close to allow the entry of the large-gag poly proteins and the aspartates (ASP 25) allow hydrolytic activity of PR (Adopted from Brik and Wong, 2003) [39].

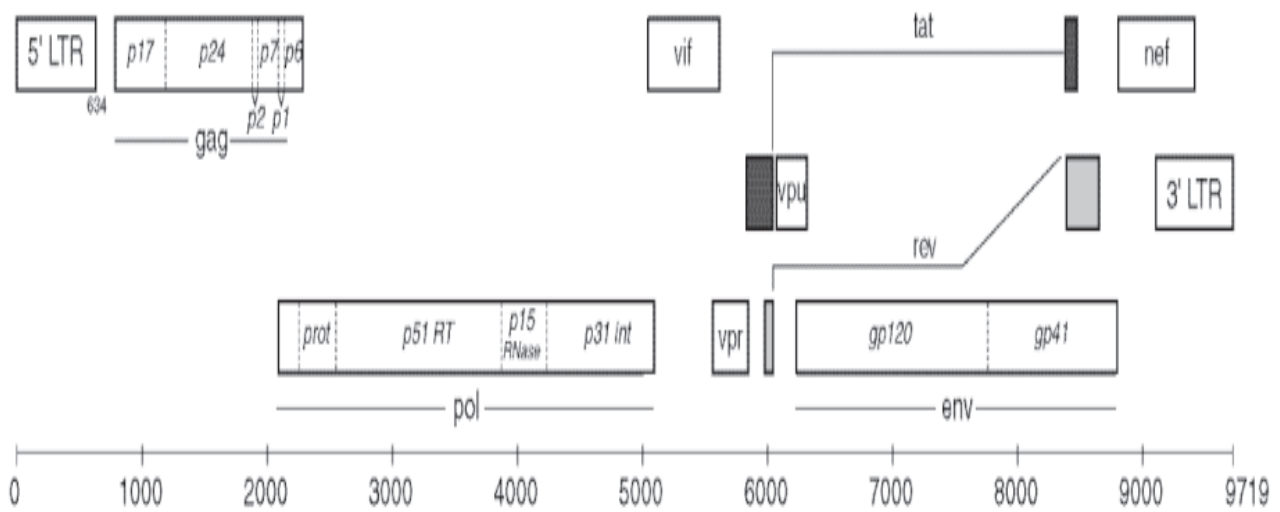


Figure 1.6: The protease region is being flanked at the N-terminus by the P^{6pol}-protease site and the C-terminus by the reverse transcriptase [41, 42].

2.3 HIV-1 Protease Inhibitors

With the significant role of PR in the life cycle of HIV-1, PR is a key target of drug therapy against HIV. Protease inhibitor drugs (PIs) are structurally similar to the natural substrate of HIV-1 PR, thereby competing with PR natural substrates for, binding to the active site. Therefore, inhibited PR cannot cleave the Gag and Gag pol polyprotein to produce mature, infectious virions [37, 42, 43].

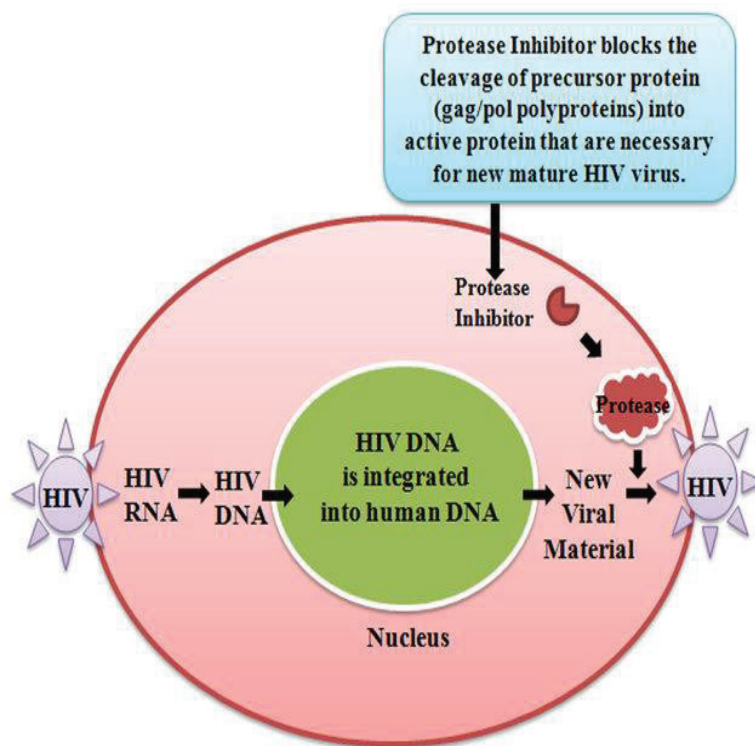


Figure 1.7: Mechanism of action of PIs. The HIV PR is the target of PIs; they prevent the cleavage of the polypeptide and maturation of the virion. (Adopted from Bhargava et al., 2017) [44].

2.4 Antiretroviral therapy in South Africa

According to 2019 ART clinical guidelines for South African, all HIV-positive individuals are eligible to begin ART. The guidelines further stated that ART should be initiated for every patient without contra-indications within 7 days, or if possible, on the same day of diagnosis. More importance and urgency are given to children (less than five years old) and patients with advanced HIV disease and pregnant women. Pregnant women without any clinical complication are to begin ART on the same day as their HIV diagnosis (<https://sahivsoc.org/Files/2019%20Abridged%20ART%20Guidelines%2010%20October%202019.pdf>). Table 1.2 below showed the ARVs currently available in Southern Africa and their recommended dosage.

Table 1.2: ARVs available in Southern Africa and their Dosages [34].

Generic name	Drug Class	Recommended dosage
Tenofovir	NtRTI	300 mg per day
Lamivudine	NRTI	300 mg per day
Emtricitabine	NRTI	200 mg per day
Abacavir	NRTI	300 mg half a day (Twice daily)
Zidovudine	NRTI	300 mg half a day (Twice daily)
Stavudine	NRTI	30 mg half a day (Twice daily)
Didanosine	NRTI	400 mg per day taken on an empty stomach
Efavirenz	NNRTI	600 mg at night
Nevirapine	NNRTI	200 mg per day for 2 weeks, follow by 200 mg half a day (Twice daily)
Rilpivirine	NNRTI	25 mg per day with food
Etravirine	NNRTI	200 mg half a day (Twice daily)
Atazanavir	PI	400 mg per day or 300 mg with RTV 100 mg per day
Lopinavir/RTV	Boosted PI	400/100 mg half a day (Twice daily)
Darunavir	PI	600 mg half a day with 100 mg RTV half a day
Raltegravir	InSTI	400 mg half a day (Twice daily)
Dolutegravir	InSTI	50 mg per day
Maraviroc	CCCR5 blocker	150 mg, 300 mg or 600 mg half a day (Twice daily) (doses depend on concomitant medication and interactions)

2.5 Metabolising Enzymes/Transporters and Protease Inhibitors drugs

The absorption and distribution of PIs determine their pharmacological and toxicological effects, and enzyme/transporter-mediated processes influence them. Figure 1.8 shows the localization of membrane transport proteins and intracellular enzymes in a normal cell. Solute carrier (SLC) and ATP-binding cassette (ABC) are membrane transporters involved in the uptake and pumping out of PIs, while the cytochrome P450 system biotransforms PIs in human liver microsomes [45].

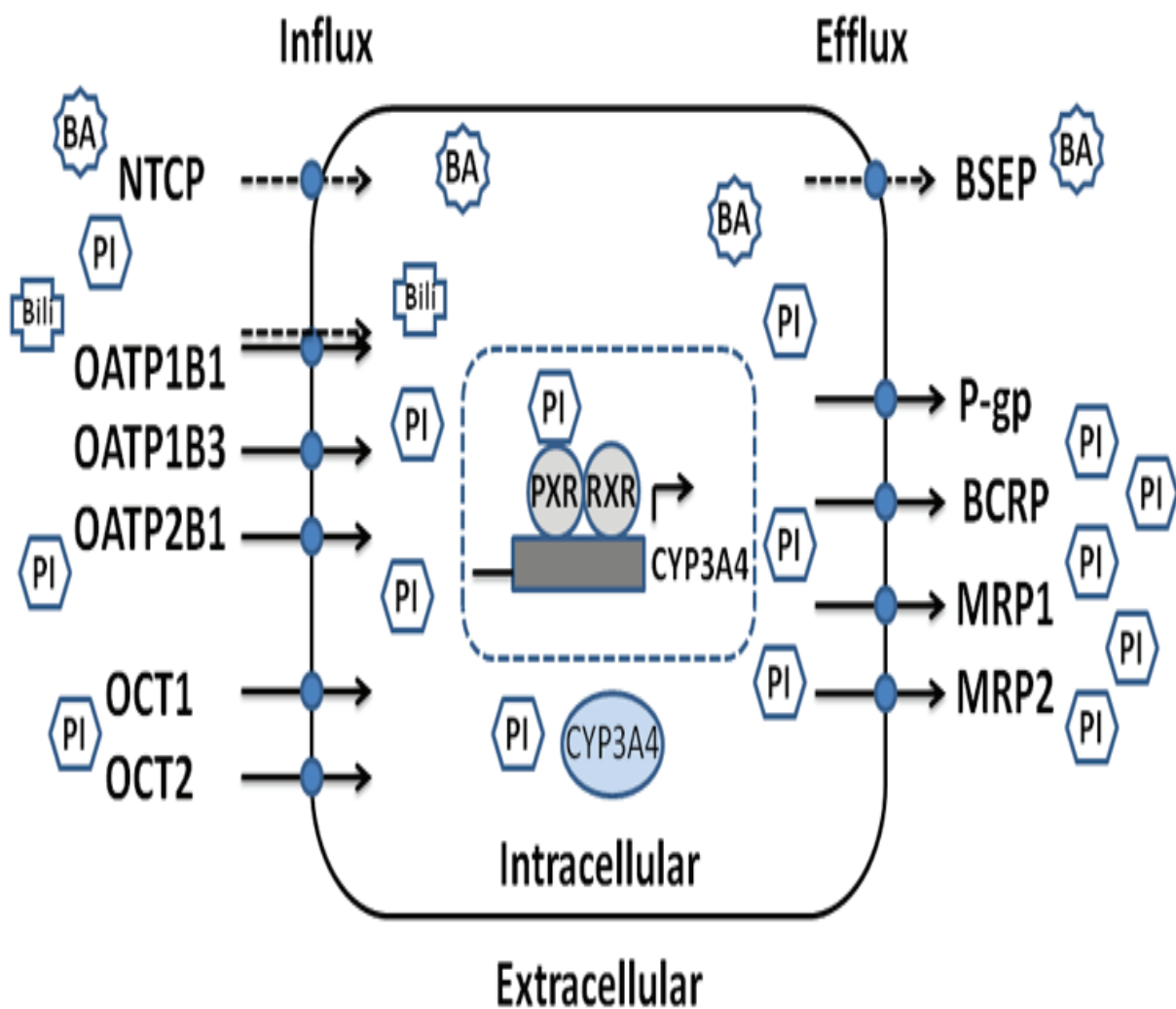


Figure 1.8: Illustration of the localization of transport proteins in translocation of PIs. (Adopted from Griffin et al., 2010) [46].

PIs inhibit other transport proteins such as Sodium-taurocholate co-transporting polypeptide, bile salt export pump (BSEP) and Organic anion-transporting polypeptides (OATP1B1). PIs can also bind to pregnane X receptor (PXR) and subsequently mediates the induction of cytochrome P450 3A4 (CYP3A4) [46].

2.5.1 Solute Carrier and ATP-Binding Cassette

Transporter-mediated influx is governed by the SLC superfamily, and is the rate-limiting step in the bioavailability of drugs and hepatobiliary clearance [46]. Organic anion-transporting polypeptides (OATPs) and organic cation transporters (OCTs) are the most important of this superfamily and are the transporters involved in interacting with drugs, as shown in figure 1.8. OATPs facilitate the bidirectional transportation of various compounds/drugs including Bile acid (BA), and other xenobiotics [47].

The ABC transporters are the most abundant protein families, present in all living organisms. Their role and structure are fairly well preserved across organism's species. The transport proteins mediate the transmembrane movement of biomolecules by making use of the energy created by hydrolysis of ATP [48]. Findings suggest that these transport proteins are highly involved in the metabolism of PIs and alter PIs pharmacokinetics by reducing bioavailability, thereby reducing concentrations in organs and tissues. The inadequate plasma concentration of the PIs has been associated with the development of drug resistance [49].

2.5.1.1 P-glycoproteins (P-gp)

P-glycoproteins are the most studied members of the ABC superfamily. They are the most significant drug transporter in the central nervous system and other tissues. They are referred to

as multidrug resistance proteins 1 (MDR1) because studies have shown that they are the cause of drug resistance to cancer drugs and major cause of treatment failures [49]. They are essential proteins present in the cell membrane, encoded in humans by the ABCB1 gene (van Waterschoot et al., 2010) [50]. Their primary role is to pump many potentially toxic substances out of the cells. Other functions include controlling the transportation and bioavailability of drugs. P-gps have wide substrate specificity, and they are an ATP-dependent efflux pump, consisting of 1242 amino acids. All known PIs are reported to be substrates of P-gp [50] and over-expression of P-gp genes was reported to reduce the plasma concentration of PIs [49, 51].

The comparison of the results from amino acid sequences from cloned complementary DNAs (cDNAs) with another member of the ABC family suggests that human P-gp has two symmetrical halves (two homologous segments). Each of these halves has six transmembrane (TM) domains that interrelated to one another via an intracellular and flexible polypeptide loop (Figure 1.9). In the cytoplasm, two ATP-binding domains, identified as nucleotide-binding domains (NBDs) comprise the power units of P-gp. These ATP-binding domains (NBDs) with energy transfer, transport substrates across the membrane in the cytoplasm. Similar to several other ABC transporters, P-gp alternates between two different conformational states during the transportation cycle. Firstly, at a conformational state (inward-facing conformation) with the potential to bind intracellular substrates and at the second conformational state (outward-facing conformation), the transporter is capable of transmembrane transportation of substrates. For the transportation of substrate, two molecules of ATP bind to P-gp at the NBDs. The binding of

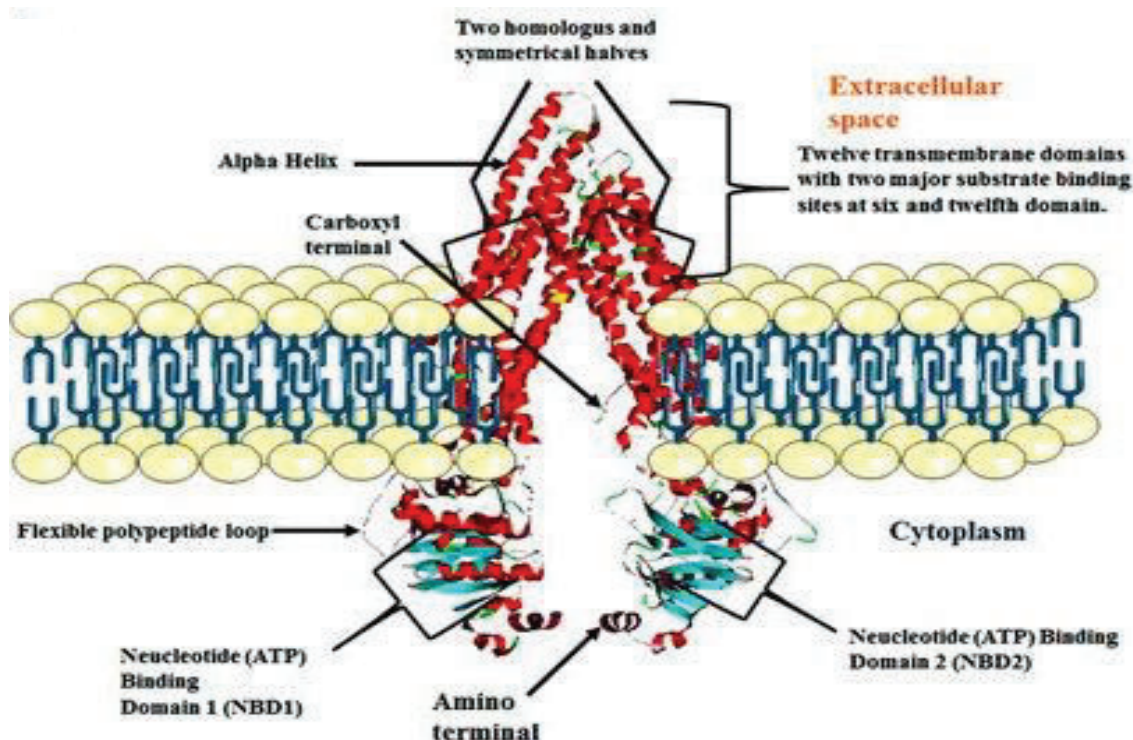


Figure 1.9: The structure of drug transporting P-gp illustrating the TMD and NBD 1 and 2 (Adopted from Dewanjee, et al., 2017) [52].

ATPs to NBDs result in the dimerization of the NBDs, and eventual occlusion of the binding site of P-gp. Hydrolysis of ATP and the resulting post-transport outward-facing conformation were the results of dimerization [52].

2.5.1.2 Cytochrome P450 (CYP)

Cytochrome P450 (CYP450) belongs to a superfamily of closely related, and membrane bound CYP450 enzymes containing heme as a cofactor [53] CYP450 enzymes are the major enzymes involved in the metabolism of drugs and are responsible for almost 75% of total drug metabolisms [54]. CYP450 deactivates drugs, either directly or by facilitated elimination from the system, and can also bioactivate several substances to form their active compounds [45]. In mammals, CYP450 oxidizes xenobiotics, steroids, and other metabolites. CYP450 are also

involved in the catabolism and synthesis of hormones and play essential role in the biosynthesis of fatty acid, hormones and defensive compounds in plants.

In humans, CYP450 are membrane-bound proteins found in the inner membrane of the mitochondria or in the endoplasmic reticulum [55]. Cytochrome P450 enzymes metabolize several substrates. Some metabolize a small number of substrates, for example CYP19, whereas others metabolize numerous substrates, for example CYP3A4. CYP450 enzymes are present in the liver, kidney and intestine where they are involved in numerous biological activities.

Eighteen mammalian cytochrome P450 families that encode for 57 genes in the human genome have been reported [56]. The CYP450 families are CYP1, CYP2, CYP3, CYP4, CYP5, CYP7, CYP8, CYP11, CYP17, CYP19, CYP20, CYP21, CYP24, CYP26, CYP27, CYP39, CYP46 and CYP51. Several drugs may inhibit or induce CYP450 3A enzymes, and it is vital to understand their regulation and expression in the context of HIV-1 infection [57]. For instance, RTV inhibits CYP3A4, resulting in decreased hepatic metabolism and an increase in the concentration of drugs metabolized by the same isoenzymes [57]. This inhibitory activity of RTV is the reason many PIs are used in combination with RTV because it inhibits CYP3A4 in order to maintain an optimal plasma concentration of PIs. In separate studies by Fabbiani et al., 2011 and Daniel et al., 2013 sub-therapeutic plasma drug concentrations of PIs were reported in HIV positive patients failing therapy [58, 59], and may be attributed to either over-expression or over induction of CYP3A4 genes and protein activities respectively.

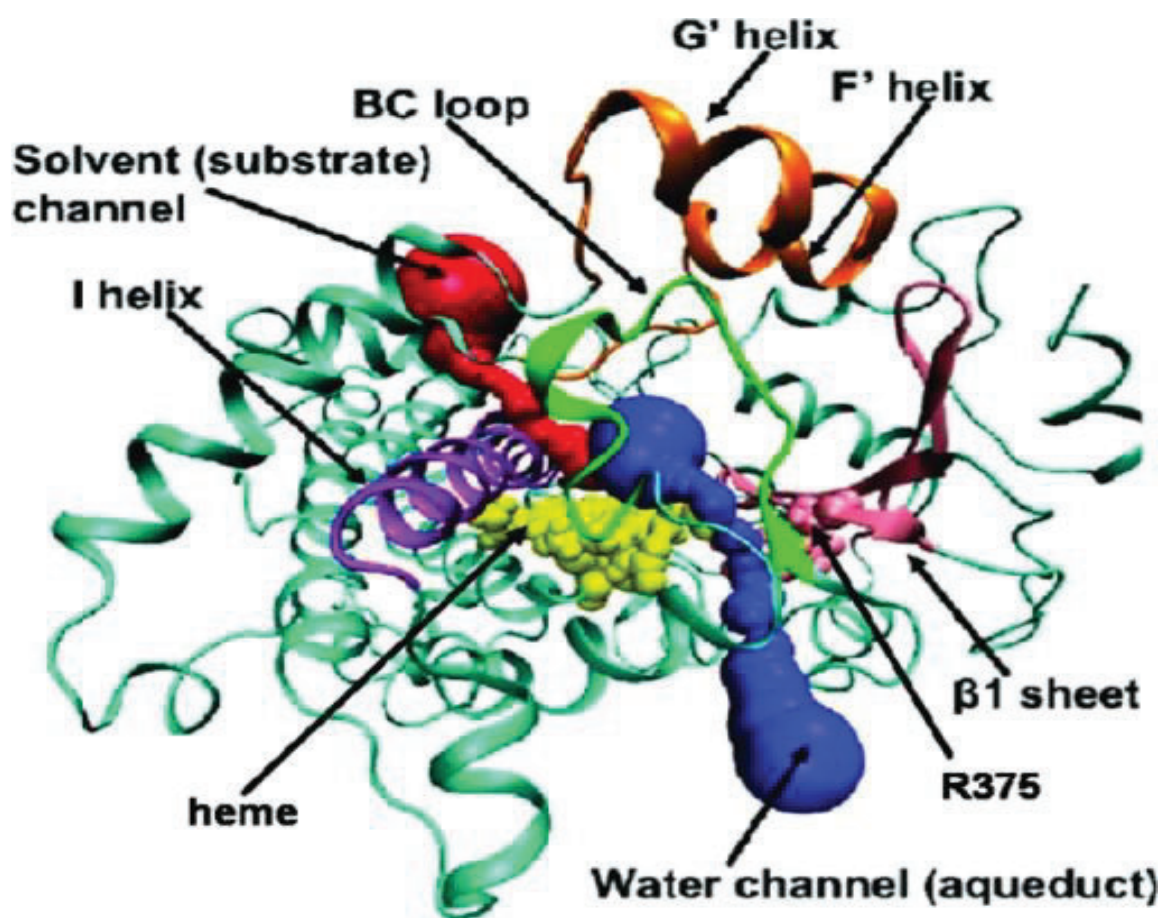


Figure 1.10: The cartoon representation of CYP3A4 structure with different channels, the heme and residue 375 are characterized by spheres and coloured yellow and pink, respectively (Adopted from Fishelovitch et al., 2010)[60].

2.5.2 CYP3A4 and P-gp Substrate Overlapping

CYP450 and P-gp form a critical and essential cascade in the metabolism and elimination of foreign substances in the body. Interestingly, numerous studies have reported that both P-gp and CYP3A4 have broad and overlapping substrate specificity [51, 61-63]. As several P-gp substrates or modulators are also substrates or modulators of CYP3A4, and P-gp inhibitors were also reported to be inhibitors of CYP3A4. For example, cyclosporin and RTV are inhibitors of P-gp as well as CYP3A4 [51, 63-65]. The inhibition or induction of both P-gp and CYP3A4 has been associated with several drug-drug and herbal-drug interactions [61].

2.6 TRADITIONAL HERBAL MEDICINE AND ITS GLOBAL USAGE

World Health Organization defined THMs as any health procedures, methods, beliefs, as well as knowledge, integrating plant-based medications, manual techniques, utilized singly or in combination, to cure, make a diagnosis and avoid diseases or improve well-being [66]. In other words, THMs are plant-derived ingredients with minimum or no industrial handling used for the treatment of infection within regional healing practices. THMs are getting substantial consideration and attention in global health. In 2008, WHO reported that 80% of the population of Africa and Asia depend on THMs not only for treatment and diagnosis of diseases but for other primary healthcare purposes [67, 68]. In New Zealand, 48% of patients in a provincial hospital reported having used THMs [69]. A similar study in Sri Lanka showed 67.4% among the studied population of 500 cancer patients uses THMs [70].

THM products play substantial roles in the control and treatment of several diseases such as HIV, diabetes, severe acute respiratory syndrome (SARS), hypertension and many more diseases. For example, the use of THMs was significant in the control and treatment of SARS in China [71]. Several countries like United States of America (USA), Nigeria, South Africa, Japan, Germany, China, and India have committed substantial and considerable research investments in THMs [66], believing that THMs research will play a crucial role in enhancing global health care. Pharmaceutical Industries and scientist all around the world have also invested a substantial amount of money looking for lead medicinal herbs and PCs [72].

2.6.1 Use of THMs in Africa and South Africa

The use of THMs in the continent of Africa has been traced back to the Stone Age and is older than some traditional medical sciences [73], and its usage is significantly increasing [74, 75].

THMs are used in all African societies and are universal to all cultures and traditions in Africa to cure various diseases. The majority of Africans either use THMs alone or in combination with other conventional medicines. Tabuti et al. 2012 reported that many people in Uganda had an immense understanding of the use of traditional medicines and used them as first-line treatment options before using conventional medicines [76]. In a similar study conducted in Lagos, Nigeria, 58% of the studied population believes that THMs are safer and efficient to use. Majority of the studied population believe that because the THMs are plant products, they do not possess any harmful effect [77]. In another study among people living with HIV, Puoane et al. 2012 reported that between 15% to 79% of people living with HIV in Africa use traditional medicine either alone or in combination with ARVs [78].

In South Africa, a multi-racial society with diverse approaches to treatment of illness and diseases based on different ethnic beliefs, approximately 70% – 80% of the South African population was reported to see traditional healers and make use of plant-derived herbal medicine for the control and treatment of various diseases [79-80]. Among the Black South African community, the majority use THMs rather than conventional medicines because they believe they are cheap, culturally appropriate and more individualized than the conventional drugs [81].

Several factors such as poverty, cultural beliefs, illiteracy, limited access to medical facilities, religious beliefs, HIV-1 infection and related illnesses, the adverse effects of ARVs, nausea and pain [82] are believed to be responsible for the significant use of THMs over conventional medicines. In addition, the limited number of orthodox doctors available in the medical sector who are unable to meet the need of the large population of African people is assumed to add to the soaring prevalence of THMs usage [83]. People with limited access to health care facilities mainly use traditional remedies [83].

2.6.2 Concomitant use of ART and African Traditional Medicine

Among people living with HIV, there are several reports of significant and concomitant use of THMs with ARVs. Peltzer et al. 2008 reported that there is an increase in the use of THMs among HIV-positive patients living in the province of KwaZulu-Natal in South Africa [79]. In a study from three ART facilities in the Kumasi Metropolis of Ghana, it was reported that 53.2% of the surveyed HIV-positive population used ARVs and THMs at the same time [82]. A high percentage of HIV-positive patients (98.2%) out of 388 patients interrogated at a Family Care Centre (FCC) in Harare, Zimbabwe reported using THMs concomitantly with ARVs [84]. A separate study in Uganda by Namuddu et al. 2011 reported that 33.7% of patients on ART were using THMs [85]. Also, in Uganda in the district of Kabarole, 38% of HIV-positive individuals were found to concomitantly use ARVs and THMs to manage HIV infections [86]. In a hospital in Kano, North-West Nigeria, a similar study showed that 4.25% of the 430 patients studied used ARV and THMs concurrently [87]. These and many more studies have confirmed the significant number of HIV-positive patients that use ARVs and THMs simultaneously in Africa. However, out of these high percentage of HIV-positive patients using ARVs and THMs concurrently, only a very few patients notified their health care providers of their usage of THMs. This validated Owen-Smith et al. suggestion that unambiguous dialogues between HIV-positive patients and health care providers on how to successfully and effectively incorporate THMs into ART treatment regimens in order to ensure the safety and health of patients living with HIV [88].

2.6.3. Herb-Drug Interactions from Concomitant Use of ARVs and THMs

The herb-drug interactions occur because several THMs alter the activities of drug-metabolizing proteins of many conventional medicines, thereby affecting the drugs' plasma blood

concentrations and therapeutic effects. There are little documentation with regard to the interaction between conventional medicines and plant-derived herbal products. Those limited studies have shown that simultaneous use of THMs may affect or resist the therapeutic effect of conventional drugs, thereby, exhibiting significant herb-drug interactions and causing the manifestation of adverse drug reactions [89, 90]. Either the crude extracts of these herbal medicines or their PCs can interact directly or indirectly to influence the pharmacokinetic and toxicological properties of conventional drugs. These herbs could interact with drug-metabolizing enzymes and transporters by either inhibiting or activating them, thereby altering the drugs bioavailability and pharmacological properties.

Interactions between herbal medicine and conventional drugs can lead to serious adverse effects [91]. For example, simultaneous use of Ginkgo (*Ginkgo biloba*) with Aspirin and Warfarin causes spontaneous hyphema and intracerebral haemorrhage respectively [92, 93]. Studies also showed that simultaneous usage of St John's wort with contraceptives such as ethinylestradiol and desogestrel causes inter-menstrual bleeding [94]. It also causes serotonin syndrome when used together with trazodone, sertraline or nefazodone [95, 96]. Bleeding and increased blood pressures are the adverse effect of simultaneous use of Ginkgo with warfarin and a thiazide diuretic, respectively [97]. Yong and Loh, 2004 reported altered pharmacokinetic properties of paracetamol and hypoglycaemia when Galic acid was taken together with chlorpropamide [90].

2.6.4 PI drugs and THMs Interactions

The therapeutic outcome of HIV PIs depends on the relationship between membrane transport proteins and drug-metabolizing enzymes expressed in the intestine and liver. As discussed earlier, these enzymes and transporters are capable of influencing the absorption, distribution,

and excretion of PIs, which in turn determined the pharmacological and toxicological effects of PIs. Alterations in the activities of these proteins significantly affect the therapeutic effect of HIV PIs [49, 98]. However, different herbal medicines have been reported to modify the activities of these drug-metabolizing proteins.

An *in vitro* study has shown that Cat's claw (*Uncaria tomentosa*), a therapeutic plant with antiviral activity, inhibits CYP3A4 activity and subsequently raises the concentration of PIs such as ATV, RTV and SQV in the plasma [98]. In another study, decreased blood concentration of indinavir by St. John's wort (*Hypericum perforatum*) was reported due to induction of CYP3A4. Hajda et al. 2010 reported that Garlic extract induced P-gp expression in the intestine and a significant reduction of approximately 50% SQV plasma concentration was detected in 10 healthy volunteers after 21 days of administering of garlic (Garlipure, two capsules/day) [100]. Fatal adverse reactions can also occur when herbal medicine is used with PIs. For example, a study by Gallicano et al. 2003 reported gastrointestinal toxicity when RTV and garlic were used concurrently [101]. Therefore, the combination of herbal medicine with PIs that are metabolized by CYP3A4 or P-gp may lead to drug failure and serious adverse effects.

2.7 THMs USED BY HIV-1 POSITIVE PATIENTS IN SOUTH AFRICA

Table 1.3 shows some of the commonly used and commercially available THMs used by HIV positive patients. These herbal medicines have been reported to boost the immune system, increase CD4 cell count and decrease viral load. Medicinal use of Ingungumbane Mahlabizifo herbal mixture was reported to improve CD4 cell count and reduce viral load [102]. In a preliminary and yet unpublished observational study conducted on 18 participants, COA[®]-FS herbal medicine was reported to significantly boost CD4 cell count and lower viral load when

administered alone to 18 HIV-positive participants.

(<http://ndabaonline.ukzn.ac.za/UkzndabaStory/Vol4-Issue15-CHS/HIV%20Traditional%20Complementary%20and%20Alternative%20Medicine%20Use%20Investigated/>). S'mangaliso herbal mixture was also reported to possess anti-HIV activity [102].

These THMs consists of several African plants, for example Ngoma herbal tonic consists of *Echinacea* sp., *Dandelion* sp., *Alfalfa* sp., *Aloe ferox* and *Harpagophytum* sp [103]. Table 1.3 summarised the TMs and there plant components. These are traditional African plants used in the treatment of various diseases. *Vernonia amygdalina*, *Azadirachta indica* and *Carica papaya* are being used to treat diseases in African countries such as South Africa, Uganda and Kenya [104, 105]. Likewise, *Sutherlandiaf rutescens* and *Hypoxis hemerocallide* are used for treatment of viral diseases [86, 106]. Langlois-Klassen et al. further reported the use of *Vernonia amygdalina*, *Aloe barbadensis*, *Ocimum* sp and many more plants in the treatment of HIV [86].

Table 1.3: Commercial Herbal Mixtures Commonly Used by HIV-Patients in South Africa.

Product Name	Medicinal uses	Ingredients (as listed on the label)
Imbiza Herbal Tonic	Increase sexual prowess, relieve general body pains and constipation, reduce stress and high blood pressure (HBP), boost energy and vitality	Twenty-one (21) herbal plants were used to make the mixture [102]
COA®-FS herbal Medicine	Use as food supplement and immune booster for treatment of HIV/AIDS symptoms.	<i>A. indica</i> , <i>P. americana</i> , <i>C. papaya</i> , <i>S. mombin</i> , <i>O. viride</i> and <i>V. amygdalina</i> [107]
Ingungumbane Mahlabezifo	Used to boost CD4 count, lower viral load, cleanses blood and improve sexual drive.	<i>Sutherlandia</i> , <i>Aloe</i> extracts, African potato, (vitamins B, C and yeast added) [102].
Ngoma herbal tonic	Boost the immune, reduce diabetic and HBP, relief arthritis, hypertension, stress and influenza.	<i>Sutherlandia</i> , <i>Echinacea</i> sp., <i>Dandelion</i> sp., <i>Alfalfa</i> sp., <i>Aloe ferox</i> , <i>Harpagophytum</i> sp. and 13.5% alcohol [102].
Stameta™ BODicare®	Immune booster, used to cure high blood pressure, heart problems, back pain, persistent tiredness, skin conditions, poor blood quality, fever and flu, nervous disorders, body sores, and Strengthens bones.	<i>H. rooperi</i> , <i>M. piperital</i> , <i>P. anisum</i> , <i>Aloe</i> (unspecified). (multivitamins (unspecified), calcium, magnesium, potassium, phosphorus and iron added) [102].

NL means not listed on the packaging

Table 1.3 cont'd.

Product Name	Medicinal uses	Ingredients (as listed on the label)
Uvukahlale 100901713	Increases red blood cell production, sex enhancer and aphrodisiacs.	<i>Aloe ferox</i> , vitamins, trace elements (unspecified), natural Tribulus and sodium benzoate and potassium sorbate [102].
Amandla esambane No. 1	To relieve HIV/AIDS symptoms, kidney infections, back pain, sores, rash, diarrhoea and chickenpox	NL [102]
S'mangaliso herbal mixture	To treat HIV/AIDS, HBP, period pain and cancer.	NL [102]
Ingwe muthi mixture and Lion izifozonke	Used to treat chest infections, sexually transmitted diseases (STDs), arthritis, heart burn, relieving constipation, and increasing sexual prowess.	NL [102]
Mvusaunkunzi	Sexual prowess booster and energiser.	NL [102]
Sejeso herbal mixture	To treat heartburn, constipation, stomach aches and, cramps.	NL [102]
Umpatisankosi	To improve sexual prowess, an energiser, to treat STDs and high blood pressure	NL [102]
UmuthiwekukhwehleIne zilonda	To treat cough and chest infections	NL [102]

NL means not listed on the packaging

Table 1.3 cont'd.

Product Name	Medicinal uses	Ingredients (as listed on the label)
Umzimbaomubi	Treatment for wounds and fungal infections.	NL [102]
Vuka Uphile 6009814670007	Treatment for kidney infections, TB, diabetes, HBP, arthritis, influenza, period pains, ulcers, painful eyes, painful ears and diarrhoea, boost erection and purify blood	NL [102]
Vusaumzimba Ingwe AMM 0016	Treatment for wounds and fungal infections (e.g rashes). To treat boils and chest infections, stop/relief menstrual pains, increase stamina and anti-influenza virus.	NL [102]

NL means not listed on the packaging

2.7.1 Antiviral PCs in African Traditional Component Plants from THMs and Their Antiviral Mode of Actions

Several studies have reported different antiviral activities and modes of actions of PCs present in many African Traditional component plants of herbal medicines against different viruses. These modes of action include inhibition of viral entry, reductions in virus replications, elevation of CD4 count, inhibition of important viral enzymes and many more.

Table 1.4: Antiviral Activities of PCs from Component Plants Present in Some THMs.

PCs	THMs	Viral Target	Mode of Action(s)	Ref.
Quinic acid	COA [®] -FS, Imbiza Herbal	HBV	Inhibition of replication of HBV-DNA and HBsAg production	[108]
Geranin	Imbiza Herbal, COA [®] -FS, Ngoma herbal	HIV-1	Inhibition of RNA tumor virus reverse transcriptase, HIV-1 protease, HIV-1 replication and HIV-1 entry into cells	[109, 110]
		HBV	Inhibit CD4-gp120 binding, HIV-1 integrase, and HIV-1 reverse transcriptase	[109, 111]
		HBV	Inhibition of HBV, HBV antigens (HBeAg) and surface (HbsAg) antigens	[112]
Stigmasterol	Imbiza Herbal, COA [®] -FS, Ingungumbane Mahlabezifo, Ngoma herbal, Stameta [™] BODicare [®]	HSV-1	Inhibition of HSV-1 replication after cell infected	[113]
		EHV-1	Inhibits viral fusion, entry into cell and irretrievable inactivation of infectivity	[114]

Table 1.4 cont'd.

Gallic acid	COA [®] -FS, Ngoma herbal, Imbiza Herbal	HSV-2	Reduction of replication of HSV-2 inhibits virus add-on to cells and its subsequent cell-to-cell spread activity.	[115-117]
		HIV	Inhibition of HIV-1 integrase and reverse transcriptase activities	[118]
Lanosterol	Imbiza Herbal, COA [®] -FS, Ingungumbane Mahlabezifo, Ngoma herbal, Stameta™ BODicare®	HCV	Down-regulates HCV replication and level of viral proteins in hepatoma cells	[119]
		HSV-1	Suppression of the expression of viral proteins of HSV-1 in Vero cells	[116]
		HSV-1	Inhibiting HSV-1 multiplication by inhibiting reverse transcriptase activity	[120]
		HIV-1	HIV-1 replication inhibited by inhibiting reverse transcriptase activity	[121]
Isosteviol and derivatives	COA [®] -FS, Ingungumbane Mahlabezifo, Ngoma herbal	HBV	Inhibit the host TLR2/NF-κB signalling pathway thereby interrupting the HBV replication and gene expression	[120]
		HSV	Antiretroviral activity against HSV and Cocksakie B viruses	[122]

Table 1.4 cont'd.

Phthalic acid	COA [®] -FS, Imbiza Herbal	DENV-1, PI-3, CHIKV, HSV-1 and 2	Antiretroviral activity against DENV-1, Parainfluenza virus (PI-3), CHIKV, HSV-1 and 2, cytomegalovirus	[123-126]
Caffeoyl esters	Ingungumbane Mahlabizifo, Ngoma herbal	HSV	Antiretroviral activity against herpes simplex	[127]
Caffeine	Imbiza Herbal, COA [®] -FS, Ngoma herbal, Stameta™ BODicare®	HIV-1	Suppression of integration step of the HIV-1 lifecycle, reverse transcriptase, integrase.	[128-130]
Benzyl Isothiocyanate	COA [®] -FS, Ngoma herbal	Murine AIDs	Inhibits leukemia retrovirus-induced death by down regulation of free radicals and restoration of the immune system	[131]
		HIV-1	Inhibition of viral transduction by HIV-1 based vectors	[128]
			Inhibit HIV-1 transduction.	[130]
			Inhibitory effect on HIV-1 integrase	[129]
			Targets Reverse transcriptase	[129]

Table 1.4 cont'd.

Theophylline	Imbiza Herbal, COA®-FS, Ngoma herbal, Stameta™ BODicare®	HIV-1	Suppression of replication of HIV-1	[132]
Caffeic acid	Imbiza Herbal, COA®-FS, Ngoma herbal, Stameta™ BODicare®	HIV-1	Inhibits HIV-1 integrase	[129]
		HBV	Inhibits HBV-DNA replication and HBsAg production	[133-134]
Ferulic acid	COA®-FS, Ngoma herbal, Stameta™ BODicare®	HCV	Inhibition of HCV replication through the induction of IFN α and antiviral response via p62-mediated Keap1/Nrf2 signalling pathway	[135]
		HIV-1	Reduction of the release and activity of the p24 antigen (protein from the virus capsid) Inhibits replication of the HIV	[136]
3,5-dicaffeoylquinic acid	Stameta™ BODicare®, Imbiza Herbal	HIV-1	Inhibition of catalytic activities of integrase enzymes	[137, 138]
		RSV	Inhibited virus-cell fusion in the early stage as well as cell-cell fusion at the end of replication cycle	[139]
D-chicoric acid	Ngoma herbal, Imbiza Herbal	HIV-1	Inhibition of integrase enzyme	[138, 140]
		HSV	Inhibits HSV-1 replication	[141]
Chlorogenic acid	Ingungumbane Mahlabizifo, Ngoma herbal, Imbiza Herbal	IAV	Blocks neuraminidase to inhibit influenza A virus in cell lines and animal models.	[142]
		HBV	Inhibits HBV-DNA replication as well as HBsAg production	[143]

Table 1.4 cont'd.

<i>p</i> -Coumaric acid	Imbiza Herbal, COA [®] - FS, Ngoma herbal	HCV	Inhibition of the early stage of viral infection	[144]
		IAV	It prolongs survival times and reduces virus titres in bronchoalveolar lavage fluids.	[145]
Rutin	Imbiza Herbal, Ingungumbane Mahlabizifo	PI-3	Inhibitory effect on the RNA of <i>PI-3</i>	[146]
		EV	Inhibition of 3C protease (3Cpro) enzymatic activity and replication of EV-A71 in cells.	[147]
Naringenin	Imbiza Herbal, Ingungumbane Mahlabizifo, Ngoma herbal	DENV-2	Virucidal activity against DENV-2.	[148]
		HSV-1 and 2	Stimulates virus-induced cytopathic effect (CPE) inhibitory activity.	[149]
Quercetin	Imbiza Herbal, COA [®] - FS, Ngoma herbal	HIV-1	Inhibits HIV-1 integrase	[150, 151]
		HSV-1, PV-1, RSV	Reduction in the infectivity of the viruses, reduction of intracellular replication of each virus	[152, 153]
		HIV	Inhibit HIV-1 protease enzyme	[154]
		HSV-1 and 2	Induces virus-induced cytopathic effect (CPE) inhibitory activity	[149]
		HSV	reduction of intracellular replication of the virus strains	[155]
Kaempferol	Imbiza Herbal, Ingungumbane Mahlabizifo	HIV-1	Inhibits early stage of HIV infection and reverse transcriptase activity.	[120]

Table 1.4 cont'd.

kaempferol-7-O-glucoside	Imbiza Herbal, Ingungumbane Mahlabizifo	HIV-1	Inhibits early stage of HIV infection and reverse transcriptase activity.	[120]
Apigenin	Ingungumbane Mahlabizifo, Imbiza Herbal	EV	Inhibits EV71 (Enterovirus 71)-mediated cytopathogenic effect, viral polyprotein expression, EV71 replication and cytokines up-regulation.	[156]
Ellagic acid	COA [®] -FS, Ngoma herbal, Stameta [™] BODicare [®] , Imbiza Herbal	HBV	Inhibits activities against host immune, blocks effectively HBV antigen (HBeAg) secretion	[157, 158]
		HIV-1	Inhibit integrase enzyme engaged in the insertion of viral genomic material to host cells	[159]
Catechins	Imbiza Herbal, Ingungumbane Mahlabizifo, Ngoma herbal	HIV-1, HSB, RSV, PV, SV	Inhibited DNA polymerases of HIV-1, HSB, RSV, polio virus and Sindbis virus activities. Inhibits binding of viral capsid proteins.	[148, 160]
Protocatechuic acid	Stameta [™] BODicare [®] , Imbiza Herbal	HBV	Decreases the secretion of HBsAg and release of the HBV DNA, inhibit replications of HBV.	[161, 162]

Table 1.4 cont'd.

Luteolin	Ingungumbane Mahlabizifo, Stameta™ BODicare®, Imbiza Herbal	HIV-1	Moderate inhibition against HIV-1 protease	[154]
		EV	Inhibition of EV71 (Enterovirus 71)-mediated cytopathogenic effect (CPE), viral polyprotein expression, EV71 replication and cytokines up-regulation. less inhibitory activity against 2Apro and 3Cpro activity	[156]
Epigallocatechin gallate	Imbiza Herbal, Ingungumbane Mahlabizifo, Ngoma herbal	HCV	Inhibition of HCV RNA replication, HCV entry and protein.	[144]
		HIV-1	Inhibitory activity on the life cycle of HIV-1. Interacts with different steps of HIV-1 life cycle.	[163]
		EV	inhibits enterovirus 71 (EV71) replication	[149]
		ZIKV	Inhibits the virus entry	[164]
Epigallocatechin	Imbiza Herbal, Ingungumbane Mahlabizifo, Ngoma herbal	EV	inhibits enterovirus 71 (EV71) replication	[149]

Table 1.4 cont'd.

Fisetin	Imbiza Herbal, Ingungumbane Mahlabizifo, Stameta™ BODicare®	CHIKV	Inhibits CHIKV RNA production and viral protein expression (intracellular anti-CHIKV activity).	[165]
Ursolic acid	COA®-FS, Imbiza Herbal	EV	Inhibition of replication of EV-A71 and 3Cpro activity.	[166]
Curcumin	COA®-FS, Imbiza Herbal	HIV-1	Inhibition of HIV-1 protease.	[167]
Lutein	Ingungumbane Mahlabizifo	ZIKV, CHIKV	It interferes with the binding of the enveloped viruses to cells	[167]
		HBV	Suppression of secretion of HBsAg and suppression of amount of extracellular HBV DNA. Inhibition of the activity of HBV full-length promoter (Fp) and HBV transcription	[133]

References

1. UNAIDS. [AIDSinfo.unaids.org](https://www.unaids.org/). 2019. https://www.avert.org/global-hiv-and-aids-statistics#footnote1_qlt481t. (Accessed 10/01/2020).
2. Chitnis, A., Rawls, D., Moore, J. *Origin of HIV Type 1 in Colonial French Equatorial Africa*. AIDS Res. and Human Retroviruses. 2000. 16(1), 5–8.
3. Kalpenia, E., Mbugua, N. *A review of Preventive Efforts in the Fight against HIV and AIDS in Africa*. Norwegian J. Geog. 2005. 59, 26-36.
4. Wolfe, N.D., Switzer, W.M., Carr, J.K., Bhullar, V.B. *Natural acquired simian retrovirus infections in Central Hunters*. The Lancet. 2004. 363(9413), 932-937.
5. Delaporte, E. *Epidemiological and molecular characteristics of HIV infection in Gabon, 1986-1994*. AIDS. 10(8), 903-10.
6. Garenne, M., Madison, M., Tarantola, D, Zanou, B., Aka, J., Dogore, R. *Mortality impact of AIDS in Abidjan, 1986-1992*. AIDS. 10 (11), 1283-1286.
7. Serwadda, D. *Slim disease: a new disease in Uganda and its association with HTLV-III infection*. The Lancet. 1985. 2, 849-52.
8. UNAIDS Special Report. *Ending AIDS: Progress towards 90-90-90 targets*. 2019. https://www.avert.org/professionals/hiv-around-world/sub-saharan-africa/south-africa#footnote6_9xeo01h. (Accessed 10/01/2020).
9. Sher, R. *HIV infection in South Africa, 1982-1988--a review*. S. Afr. Med. J. 76 (7), 314 – 318.

10. UNAIDS Data. 2017
https://www.unaids.org/sites/default/files/media_asset/20170720_Data_book_2017_en.pdf.
(Accessed 10/01/2020).
11. KwaZulu Natal Province AIDS council. *Annual Progress Report 2015/16*. 2017.
https://www.avert.org/professionals/hiv-around-world/sub-saharan-africa/south-africa#footnote6_9xeo01h. (Accessed 10/01/2020).
12. Northern Cape Provincial AIDS Council. *Annual Progress Report*. 2017.
<https://sanac.org.za/provincial-progress-reports/>. (Accessed 29/02/2020).
13. Western Cape Provincial AIDS Council. *Annual Progress Report 2015/16*. 2017.
<https://sanac.org.za/provincial-progress-reports/>. (Accessed 29/02/2020).
14. Cohen, M. S., Hellmann, N., Levy, J. A., Decock, K., Lange, J. *The spread, treatment, and prevention of HIV-1: evolution of a global pandemic*. The J. of Clin. Investigation. 2008. 118, 1244-1254.
15. Lemey, P., Pybus, O.G., Wang, B., Saksena, N.K., Salemi, M., Vandamme, A.M. *Tracing the origin and history of the HIV-2 epidemic*. Proc. Natl. Acad. Sci. USA. 2003. 100:6588–6592.
16. NAM Aidsmap. *HIV-1 and HIV-2*. 2019. <https://www.aidsmap.com/about-hiv/hiv-1-and-hiv-2>. (Accessed 10.01/2020).

17. Esbjörnsson, E., Joakim, A. *Long-term follow-up of HIV-2-related AIDS and mortality in Guinea-Bissau: a prospective open cohort study.* The Lancet HIV. 2019. S2352-3018, (18), 30254-6.
18. Lihana, R. W., Ssemwanga, D., Abimiku, A., Ndembi, N. *Update on HIV-1 diversity in Africa: a decade in review.* AIDS Rev. 2012. 14, 83-100.
19. San Mauro, D., Agorreta, A. *Molecular systematics: A synthesis of the common methods and the state of knowledge.* Cellul. and Mol. Biol. Letters. 2010. 15(2):311-41
20. Sharp, P. M., Hahn, B. H. *Origins of HIV and the AIDS pandemic.* Cold Spring Harb. Perspect. Med. 2011. 1:a006841.
21. Vidal, N., Peeters, M., Mulanga-Kabeya, C., Nzilambi, N., Robertson D., Ilunga W., Sema H., Tshimanga, K., Bongo B., Delaporte, E. *Unprecedented degree of human immunodeficiency virus type 1 (HIV-1) group M genetic diversity in the Democratic Republic of Congo suggests that the HIV-1 pandemic originated in Central Africa.* J. Virol. 2000. 74:10498–10507.
22. Soares, E. A., Santos, J. M., Sousa, A. F. A., Sprinz, T. M., Martinez, E., Silveira, A. M. B., Tanuri, J., Soares, M. A. *Differential Drug Resistance Acquisition in HIV-1 of Subtypes B and C.* PLoS ONE. 2007. 2, e730.
23. Wainberg, M. A. *HIV-1 subtype distribution and the problem of drug resistance.* AIDS. 2004. 18, S63-S68.

24. Jülg, B., Goebel, F. D. *HIV Genetic Diversity: Any Implications for Drug Resistance. infection.* 2005. 33, 299-301.
25. Michael, K. *The Changing Trends of HIV Subtypes and Its Implication on Mother-to-Child Transmission.* Recent Translational Res. in HIV/AIDS. 2011. Chapter 3. www.intechopen.com. 1224-1324.
26. Sierra, S., Kupfer, B., Kaiser, R. *Basics of the virology of HIV-1 and its replication.* J. of Clinical Virol. 2005. 34, 233-244.
27. Mushahwar, I. K. *Human Immunodeficiency Viruses: Molecular Virology, pathogenesis, diagnosis and treatment.* Perspectives in Med. Virol. 2007. 13: 75-87.
28. Arts, E. J., Hazuda, D. J. *HIV-1 antiretroviral drug therapy.* Cold Spring Harbor perspectives in med. 2012. 2(4), a007161.
29. Singh, K., Marchand, B., Kirby, K. A., Michailidis, E., Sarafianos, S. G. *Structural Aspects of Drug Resistance and Inhibition of HIV-1 Reverse Transcriptase.* Viruses. 2010. 2(2), 606-638.
30. Craigie, R., Bushman, F. D. *DNA Integration.* Cold Spring Harb. Perspectives in med. 2012. 2(7): a006890.
31. De Clercq, E. *Anti-HIV drugs: 25 compounds approved within 25 years after the discovery of HIV.* Int. J. Antimicrob. Agents. 2009. 33:307-320.
32. Martinez-Cajas, J. L., Wainberg, M. A. *Antiretroviral therapy: optimal sequencing of therapy to avoid resistance.* Drugs. 2008. 68, 43-72.

33. Johnson, J. A. and Geretti, A. M. *Low-frequency HIV-1 drug resistance mutations can be clinically significant but must be interpreted with caution.* J. Antimicrob. Chemother. 2010. 65, 1322-6.
34. Meintjes, G., Moorhouse, M., Carmona, S. *Adult antiretroviral therapy guidelines.* S. Afr J HIV Med. 2017. 18(1), a776.
35. Strengthening Pharmaceutical Systems (SPS) Program. *Safety of Medicines in Sub-Saharan Africa: Assessment of Pharmacovigilance Systems and their Performance.* Arlington, VA: Management Sciences for Health. 2011' <http://apps.who.int/medicinedocs/documents/s19152en/s19152en.pdf>. (Accessed 6/01/2020).
36. Tang, W., He, P. L., Zhang, R. J. *Anti-hepatitis B virus activity of chlorogenic acid, quinic acid and caffeic acid in vivo and in vitro.* Antiviral Res. 2009. 83(2):186-190.
37. Shafer, R. W. *Genotypic testing for human immunodeficiency virus type 1 drug resistance.* Clin. Microbiol. Rev. 2002. 15, 247-77.
38. Ruud, K. W., Toverud, E. L., Radloff, S., Srinivas, S. C. *Antiretroviral treatment and follow-up of HIV-infected patients by healthcare providers in South African public primary healthcare.* J. Assoc. Nurses AIDS Care. 2010. 21(5): 417-428.
39. Brik, A., Wong, C. H. *HIV-1 protease: mechanism and drug discovery.* Organic & Biomol. Chem. 2003. 1 (1): 5–14.
40. Levy, Y., Caffisch, A. *Flexibility of monomeric and dimeric HIV-1 protease.* J. Phys. Chem. B. 2003. 107 (13), 3068–3079.

41. Wondrak, E. M., Nashed, N. T., Haber, M. T., Jerina, D. M., Louis, J. M. *A transient precursor of the HIV-1 protease. Isolation, characterization, and kinetics of maturation.* The J. of Biol. Chem. 1996. 271 (8): 4477–81.
42. Clavel, F., Mammano, F. *Role of Gag in HIV Resistance to Protease Inhibitors.* Viruses. 2010. 2, 1411-1426.
43. Rang, H. P. *Rang and Dale's pharmacology (6th ed.). Philadelphia, Pa., U.S.A.* Churchill Livingstone/Elsevier. (2007. ISBN 9780808923541.
44. Bhargava, S. N., Adhikari, S. A., Amin, K. Das, S. Gayen, and Jha, T. *Hydroxyethylamine derivatives as HIV-1 protease inhibitors: a predictive QSAR modelling study based on Monte Carlo optimization, SAR and QSAR.* J. Environ. Res. 2017. 28:12, 973-990.
45. Lynch, T., Price, A. *The Effect of Cytochrome P450 Metabolism on Drug Response, Interactions, and Adverse Effects.* Am. Fam. Physician. 2007. 1; 76 (3):391-396.
46. Griffin, L, Annaert, P, Brouwer, K. L. *Influence of drug transport proteins on the pharmacokinetics and drug interactions of HIV protease inhibitors.* J. of Pharmaceutical Sci. 2011. 100 (9): 3636–54.
47. Hartkoorn, R. C., Kwan, W. S., Shallcross, V., Chaikan, A., Liptrott, N., Egan, D., Sora, E. S., James, C. E., Gibbons, S., Bray, P. G., Back, D. J, Khoo, S. H., Owen, A. *HIV protease inhibitors are substrates for OATP1A2, OATP1B1 and OATP1B3 and lopinavir plasma concentrations are influenced by SLCO1B1 polymorphisms.* Pharmacogenomics. 2010. 20(2):112–120.

48. Shitara, Y. *Clinical importance of OATP1B1 and OATP1B3 in drug-drug interactions.* Drug Metab. Pharmacok. 2011. 26(3):220-7.
49. Weiss, J., Haefeli, W. E. *Impact of ATP-binding cassette transporters on human immunodeficiency virus therapy.* Int. Rev. Cell Mol. Biol. 2010. 280:219–279.
50. Van Waterschoot, R., Ter Heine, R., Wagenaar, E., Van Der Kruijssen, C., Rooswinkel, R., Huitema, A., Beijnen, J., Schinkel, A. *Effects of cytochrome P450 3A (CYP3A) and the drug transporters Pglycoprotein (MDR1/ABCB1) and MRP2 (ABCC2) on the pharmacokinetics of lopinavir.* Br. J. Pharmacol. 2010. 160(5):1224–1233.
51. Konig, S. K., Herzog, M., Theile, D., Zembruski, N., Haefeli, W. E., Weiss, J. *Impact of drug transporters on cellular resistance towards saquinavir and darunavir.* J. Antimicrob. Chemother. 2010. 65(11): 2319–2328.
52. Dewanjee, S., Tarun, K. D., Niloy, B., Anup, D., Moumita, G., Ritu, K., Swarnalata J, Muhammad R., De Feo, V., and Zia-Ul-Haq, M. *Natural Products as Alternative Choices for P-Glycoprotein (P-gp) Inhibition.* Molecules. 2017. 22(6), 871-895.
53. Gonzalez, F. J. *The 2006 Bernard B. Brodie Award Lecture. Cyp2E1.* Drug Metab. Dispos. 2007. 35, 1–8.
54. Guengerich, F.P. *Cytochrome p450 and chemical toxicology.* Chem. Res. in Toxicology. 2008. 21 (1): 70–83.

55. Berka, K., Hendrychová, T., Anzenbacher, P., Otyepka, M. *Membrane position of ibuprofen agrees with suggested access path entrance to cytochrome P450 2C9 active site. The J. of Physical Chemistry A.* 2011. 115 (41): 11248–55.
56. Nebert, D.W., Kjell, W., Walter L. M. *Human cytochromes P450 in health and disease.* Philos. Trans. R. Soc. Lond. B. Biol. Sci. 2013. 368(1612): 20120431.
57. Walubo, A. *The role of cytochrome p450 in antiretroviral drug interactions.* Expert Opin. Drug Metab. Toxicol. 2007. 3: 583-598.
58. Fabbiani, M., Bracciale, L., Ragazzoni, E., Santangelo, R., Cattani, P., Di Giambenedetto, S., Fadda, G., Navarra, P., Cauda, R., De Luca, A. *Relationship between antiretroviral plasma concentration and emergence of HIV-1 resistance mutations at treatment failure.* Infection. 2011. 39:563–569.
59. Gunda, D., W., Kasang, C., Kidenya, B., R., Kabangila, R., Mshana, S., E. *Plasma Concentrations of Efavirenz and Nevirapine among HIV-Infected Patients with Immunological Failure Attending a Tertiary Hospital in North-Western Tanzania.* PLoS ONE. 2013. 8(9).
60. Fishelovitch, D., Shaik, S., Wolfson, H. J., Nussinov, R. *How does the reductase help to regulate the catalytic cycle of cytochrome P450 3A4 using the conserved water channel.* The j. of phys. chem. 2010. 114(17), 5964–5970.
61. Yuanchao, Z., Xisheng, G., Emil, T., Lin, Leslie, Z. B., *Overlapping Substrate Specificities of Cytochrome P450 3a and P-Glycoprotein for A Novel Cysteine Protease Inhibitor.* Drug. Metab. Dispos. 2000. 26; 4, 360-366).

62. Schuetz, E. G., Beck, W. T., Schuetz, J. D. *Modulators and substrates of P-glycoprotein and cytochrome P4503A coordinately up-regulated these proteins in human colon carcinoma cells*. Mol. Pharmacol. 1996. 49:311–318.
63. Fromm, M.F. *Importance of P-glycoprotein at blood-tissue barriers*. Trends Pharmacol. Sci. 2004. 25:424-9.
64. Meyer, Z., Schwabedissen H., Kim, R., *Hepatic OATP1B transporters and nuclear receptors PXR and CAR: interplay, regulation of drug disposition genes, and single nucleotide polymorphisms*. Mol. Pharm. 2009. 6(6):1644–1661.
65. Pal, D., Mitra, A. *MDR- and CYP3A4-mediated drug-drug interactions*. J. Neuroimmune Pharmacol. 2006. 1(3):323–339.
66. World Health Organisation. *Scaling up antiretroviral therapy in resource limited settings*. 2002. http://www.who.int/HIV_AIDS/first.html. (Accessed 06/10/2020).
67. Wondrak, E. M., Nashed, N. T., Haber, M. T., Jerina, D. M., Louis, J. M. *A transient precursor of the HIV-1 protease. Isolation, characterization, and kinetics of maturation*. The J. of Biol. Chem. 1996. 271 (8): 4477–81.
68. World Health Organization. *Traditional medicine*. 2008. <http://www.who.int/mediacentre/factsheets/fs134/en/>. (Accessed 10/01/2020).
69. Evans, A., Duncan, B., Mchugh, P., Shaw, J., Wilson, C. *Inpatients' use, understanding, and attitudes towards traditional, complementary and alternative therapies at a provincial New Zealand hospital*. New Zeal. Med. J. 2008. 121:21-34.

70. Broom, A., Wijewardena, K., Sibbritt, D., Adams, J., Nayar, K. R. *The use of traditional, complementary and alternative medicine in Sri Lankan cancer care: Results from a survey of 500 cancer patients*. Pub. Health. 2010. 124:232-237.
71. World Health Organisation. *Severe acute respiratory syndrome: Clinical Trials on Treatment Using A Combination of Traditional Chinese Medicine and Western Medicine*. 2003. pp. 53-61. ISBN 92 4 154643 3.
72. Tilburt, J. C., Kaptchuk, T. J. *Herbal medicine research and global health: an ethical analysis*. Bull W.H.O Organ. 2008. 86(8):594–599.
73. Natako, L. *Honouring the African Traditional Herbalist*. Afri. Traditional Herbal Res.; Clinic Newsletter. Special Edition—HIV/AIDS. 2006. 1(10).
74. Kofi-Tsekpo, M. *Institutionalization of African traditional medicine in health care systems in Africa*. Afr. J. of Health Sci. 2004. 11(1-2).
75. Traditional Medicine Fact sheet. 2008. <http://www.who.int/mediacentre/factsheets/fs134/en/>. no. 134. (Accessed 10/01/2020).
76. Tabuti, J., Kukunda, R. S., Kaweesi D, C., Kasilo, O. M. J. *Herbal medicine use in the districts of Nakapiripirit, Pallisa, Kanungu, and Mukono in Uganda*. 2012. J. of Ethnobiol. and Ethnomed. 2012. 8:35-49.
77. Oreagba, I. A., Oshikoya, K. A., Amachree, M. *Herbal medicine use among urban residents in Lagos, Nigeria*. BMC Compl. and Altern. Med. 2011.11: 117.

78. Puoane, T., Hughes, G., Uwimana, L., Johnson, Q., Folk, W. *Why HIV positive patients on antiretroviral treatment and / or Cotrimoxazole prophylaxis use traditional medicine: A study in two provinces of South Africa.* Afr. J. Trad., Compl. and Altern. Med. 2012. 9(4): 495 – 502.
79. Peltzer, K., Friend-Du, P. N., Ramlagan, S., Fomundam, H. *Use of traditional complementary and alternative medicine for HIV patients in KwaZulu-Natal, South Africa.* BMC Pub. Health. 2008. 8:255.
80. Van Staden, J. *Ethnobotany in South Africa.* J. of Ethnopharm.. 2008. 119:329330.
81. Stafford, G. I., Peddersen, M. E., Van Staden, J., Jäger, A. K. *Review on plants with CNS-effects used in traditional South African medicine against mental diseases.* J. of Ethnopharm. 2008. 119:513-537.
82. Muller, A., Kanfer, I. *Potential pharmacokinetic interactions between antiretrovirals and medicinal plants used as complementary and African traditional medicines.* Biopharm. and Drug Disp. 32: 458-470.
83. Mills, E., Cooper, C., Kanfer, I. *Traditional African medicine in the treatment of HIV.* The Lancet Infect. Dis. 2005. 5:465-467.
84. Mudzviti, T., Maponga, C. C., Khoza, S., Ma, Q., Morse, G. D. *The Impact of Herbal Drug Use on Adverse Drug Reaction Profiles of Patients on Antiretroviral Therapy in Zimbabwe.* AIDS Res. Treat. 2012. 434171, pp1-5.

85. Namuddu, B., Kalyango, J. N., Karamagi, C., Mudiope, P., Sumba, S., Kalende, H., Wobudeya, E., Kigozi, B. K., Waako, P. *Prevalence and factors associated with traditional herbal medicine use among patients on highly active antiretroviral therapy in Uganda.* 2011. BMC Pub. Health. 11: 855.
86. Langlois-Klassen, D., Kipp, W., Jhangri, G. S., Rubaale, T. *Use of traditional herbal medicine by AIDS patients in Kabarole District, western Uganda.* Am. J. Trop. Med. Hyg. 2007.77:757–763.
87. Tamuno, I. *Traditional medicine for HIV infected patients in antiretroviral therapy in a tertiary hospital in Kano, Northwest Nigeria.* Asian Pacific J. of Trop. Med. 2011. 4:152-155.
88. Owen-Smith, Diclemente, R., Wingood, G. *Complementary and alternative medicine use decreases adherence to HAART in HIV-positive women.* AIDS Care. 2007. 19 (5) 589-593.
89. Gallicano, K., Foster, B., Choudhri, S. *Effect of short-term administration of garlic supplements on single-dose ritonavir pharmacokinetics in healthy volunteers.* Br. J. Clin Pharmacol. 2003. 55:199–202.
90. Yong, E.L., Loh, Y.S. *Herbal medicine: criteria for use in health and disease, Herbal Traditional Medicine: Molecular Aspects.* Marcel Dekker, New York. 2004. 223-232.
91. Yeh, P., Kishony, R. *Networks from drug–drug surfaces.* Mol. Syst. Biol. 2007. 3:85.
92. Rosenblatt, M., Mindel, J. *Spontaneous hyphema associated with ingestion of ginkgo biloba extract.* N. Engl. J. Med. 1997. 336; 1108.

93. Matthews, M. K. *Association of Ginkgo biloba with intracerebral haemorrhage.* Neurology. 1998. 50(6):1933-4.
94. Bon S, Hartmann K, Kuhn M. *JohanniskrauteinEnzyminduktor?Schweitzer Apothekerzeitung.* 1999. 16: 535–36.
95. Demott, K. *St John's wort tied to serotonin syndrome.* Clin. Psychiatry News. 1998 26, p. 28.
96. Lantz, M. S., Buchalter, E., Giambanco, V. *St John's Wort and antidepressant drug interactions in the elderly.* J. Geriatr.Psychiatr. Neurol.1999. 12, 7-10.
97. De Smet, P.A.G.M., D'arcy, P. F. *Drug interactions with herbal and other non-toxic remedies.* Springer-Verlag, Berlin. 1996. ISBN 978-3-642-61015-8.
98. Tomlinson, B., Hu, M., Lee, V. W. *In vivo assessment of herb-drug interactions: possible utility of a pharmacogenetic approach.* Mol. Nutr. Food Res. 2008. 52:799–809.
99. Zhou, S. F., Zhou, Z. W., Li, C. G., Chen, X., Yu, X., Xue, C. C., Herington, A. *Identification of drugs that interact with herbs in drug development.* Drug Discov. Today. 2007. 12:664–673.
100. Hajda, J., Rentsch, K. M., Gubler, C., Steinert, H., Stieger, B., Fattinger, K. *Garlic extract induces intestinal P-glycoprotein but exhibits no effect on intestinal and hepatic CYP3A4 in humans.* Eur. J. Pharm. Sci. 2010. 41:729–735.

101. Gallicano, K., Foster, B., Choudhri, S. *Effect of short-term administration of garlic supplements on single-dose ritonavir pharmacokinetics in healthy volunteers.* Br. J. Clin. Pharmacol. 2003. 55:199–202.
102. Ndhhlala, A. R., Stafford, G. I., Finnie, J. F., Van Staden, J. *Commercial herbal preparations in KwaZulu-Natal, South Africa: The urban face of traditional medicine.* South African J. of Botany. 2011. 77; 830–843
103. Ndhhlala, A.R., Stafford, G.I., Finnie, J.F., Van Staden, J. *In vitro pharmacological effects of manufactured herbal concoctions used in KwaZuluNatal South Africa.* J. of Ethnopharm. 2009. 122, 117–122.
104. Sumba, S., Waako, P., Mudiope, P., *Prevalence and factors associated with traditional herbal medicine use among patients on highly active antiretroviral therapy in Uganda.* BMC Pub. Health. 2012. 11(1), 1232-1241.
105. Babb, D.A., Pemba, L., Seatlanyane, P., Charalambous, S., Churchyard, G.J., Grant, A.D. *Use of traditional medicine by HIV-infected individuals in South Africa in the era of antiretroviral therapy.* Psychol. Heal Med. 2007. 12(3):314-320.
106. Peltzer, K., Preez, N.F., Ramlagan, S., Fomundam, H., Anderson, J., Chanetsa, L. *Antiretrovirals and the Use of Traditional, Complementary and Alternative Medicine by HIV Patients in Kwazulu-Natal, South Africa: A Longitudinal Study.* Afr. J. Tradit. Complement Altern. Med. 2011. 8(4):337-345.
107. Centre of Awareness. *COA®-Food Suppliments herbal medicine.* <https://www.coadrugs.org/coafs/>. Accessed on 20/01/2020.

108. Tang, W., He, P.L., Zhang, R.J. *Anti-hepatitis B virus activity of chlorogenic acid, quinic acid and caffeic acid in vivo and in vitro*. Antiviral Res. 2009. 83(2):186-190.
109. Notka, F., Meier, G.R., Wagner, R. *Inhibition of wild-type human immunodeficiency virus and reverse transcriptase inhibitor-resistant variants by Phyllanthus amarus*. Antiviral Res. 2003. 58(2):175-186.
110. Liu, Z., Bin, Yang, J.P., Xu, L.R. *Effectiveness and safety of traditional Chinese medicine in treating acquired immune deficiency syndrome: 2004-2014*. Infect. Dis. Poverty. 2015. 4(1):1-6.
111. Notka, F., Meier, G., Wagner, R. *Concerted inhibitory activities of Phyllanthus amarus on HIV replication in vitro and ex vivo*. Antiviral Res. 2004. 64(2):93-102.
112. Huang, R., Huang, Y., Ou, J., Chen, C., Hsu, F. *Screening of 25 Compounds Isolated from Phyllanthus Species for Anti-Human Hepatitis B Virus In Vitro*. Phytother. Res. 2003. 453:449-453.
113. Petretera, E., Nittolo, A.G., Alché, L.E. *Antiviral Action of Synthetic Stigmasterol Derivatives on Herpes Simplex Virus Replication in Nervous Cells In Vitro*. J. Antiviral. 2014. 1014-1023.
114. Souza, S., José, C., Ramos, B. *Antiviral activity of 7-keto-stigmasterol obtained from green Antarctic algae Prasiolacrispa against equine herpesvirus 1*. J. Appl. Phycol. 2016. 2, 323-351.

115. Uozaki, M., Yamasaki, H., Katsuyama, Y., Higuchi, M. *Antiviral effect of octyl gallate against DNA and RNA viruses*. J. antiviral. 2007.73:85-91.
116. Kratz, J.M., Nunes, R.J, Bergström, T. *Evaluation of Anti-HSV-2 Activity of Gallic Acid and Pentyl Gallate*. Biol. Pharm. Bull. 2008 31(5):903-907.
117. Kim, T.G., Lee C-K, Kim, C.Y. *Inhibition of HIV-1 Integrase by Galloyl Glucoses from Terminalia chebula and Flavonol Glycoside Gallates from Euphorbia pekinensis*. Planta Med. 2002. 68(5):457-459.
118. Yadav, M., Jain, S., Bhardwaj, A. *Review Biological and Medicinal Properties of Grapes and Their Bioactive Constituents: AnUpdate*. J. Med. food. 2009. 12(3):473-484.
119. Govea-Salas, M., Rivas-Estilla, A.M., Rodríguez-Herrera, R., *Gallic acid decreases hepatitis C virus expression through its antioxidant capacity*. Exp. Ther. Med. 2016. 11(2):619-624.
120. Yang, Z.F., Bai, L.P., Huang, W.B. *Comparison of in vitro antiviral activity of tea polyphenols against influenza A and B viruses and structure-activity relationship analysis*. Fitoterapia. 2014. 93:47-53.
121. Meneses, M. E., Martínez-carrera, D., Torres, N., Sánchez-tapia, M. *Hypocholesterolemic Properties and Prebiotic Effects of Mexican Ganoderma lucidum*. J. pon. 2016. 1-20.
122. Mukhtar, M., Arshad, M., Ahmad, M., Pomerantz, R.J., Wigdahl, B., Parveen, Z. *Antiviral potentials of medicinal plants*. Antiviral res. 2008. 131:111-120.

123. Gyotoku T, Aurelian L, Neurath A.R., *Cellulose acetate phthalate (CAP): an 'inactive pharmaceutical excipient with antiviral activity in the mouse model of genital herpesvirus infection.* Antiviral. 1999. 327-332.
124. Manson, K. H., Wyand, M. S., Miller, C., Neurath, A. R. *Effect of a Cellulose Acetate Phthalate Topical Cream on Vaginal Transmission of Simian Immunodeficiency Virus in Rhesus Monkeys.* J. mol. 2000. 44(11):3199-3202.
125. Boadu, A.A., Nlooto, M. comparative Chemistry of COA Herbal Medicine and Herbal Extracts of *Veronia mygdalina* (Bitter leaf) and *Persea americana* (Avocado)' unpublished thesis, University of KwaZulu-Natal, Durban, South Africa. 2019.
126. Nwabuife, J. C 'A comparative chemistry of COA-FS herbal medicine and herbal extracts of *Azadirachta indica* and *Carica papaya*' unpublished thesis, University of KwaZulu-Natal, Durban, South Africa. 2019.
127. Mukhtar, M., Arshad, M., Ahmad, M., Pomerantz, R.J., Wigdahl, B., Parveen, Z. *Antiviral potentials of medicinal plants.* Antiviral res. 2008. 131:111-120.
128. Daniel, R., Marusich, E., Argyris, E., Zhao, R.Y., Skalka, A.M., Pomerantz, R.J. *Caffeine inhibits human immunodeficiency virus type 1 transduction of nondividing cells.* J. Virol. 2005. 79(4):2058-2065.
129. Koul, O., Multani, J.S, Singh, G., Daniewski, W.M., Berlozecki, S. *6 β -hydroxygedunin from Azadirachta indica. Its potentiation effects with some non-azadirachtin limonoids in neem against lepidopteran larvae.* J. Agric. Food Chem. 2003. 51(10):2937-2942.

130. Dehart, J.L., Andersen, J.L., Zimmerman, E.S. *The Ataxia Telangiectasia-Mutated and Rad3-Related Protein Is Dispensable for Retroviral Integration*. J. Virol. 2005. 79(3):1389-1396.
131. Ho, J., Kang, E., Yoon, H., Jeon, H., Jun, W., Watson, R. R., Lee, J. *Inhibition of Premature Death by Isothiocyanates through Immune Restoration in LP-BM5 Leukemia Retrovira-infected C57BL/6 Mice*. Biosci. Biotechnol. Biochem. 2011. 75 (7), 1234-1239.
132. Nunnari, G., Argyris, E., Fang, J., Mehlman, K.E., T., Daniel, T. *Inhibition of HIV-1 replication by caffeine and caffeine-related methylxanthines*. Virology. 2005. 335:177-184.
133. Pang, R., Tao, J., Zhang, S. *In Vitro Antiviral Activity of Lutein against Hepatitis B Virus*. Phytother. Res. 2010. 24(11): 1627-1630.
134. Yu, C., Yan, Y., Wu, X., Zhang, B., Wang, W., Wu, Q. *Anti-influenza virus effects of the aqueous extract from Moslascabra*. J. Ethnopharmacol. 2010. 3; 127(2):280-5.
135. Shen, J., Wang, G., Zuo, J. *Caffeic acid inhibits HCV replication via induction of IFN α antiviral response through p62-mediated Keap1/Nrf2 signaling pathway*. Antiviral Res. 2018. 154:166-173.
136. De Paiva, L.B., Goldbeck, R., dos Santos, W.D, Squina, F.M. *Ferulic acid and derivatives: Molecules with potential application in the pharmaceutical field*. Brazilian J. Pharm. Sci. 2013. 49(3):395-411.

137. Lee, K.S., Lin, C., Oyugi, D.A., Izevbigie, E.B., Luo, X. *Isolation and characterization of the antibreast carcinoma cell growth components of Vernonia amygdalina extracts*. Exp. Biol. Med. 2011. 235(12):1472-1478.
138. Verde, S., McDougall, B., Junior, C. *Synthesis and HIV-1 Inhibitory Activities of Dicafeoyl and Digalloyl Esters of Quinic Acid Derivatives*. Curr. Med. Chem. 2013. 20(5):724-733.
139. Hayashi, K., Yoshida, I., Mori, M., *Anti Influenza Virus Activity of a Red-Fleshed Potato Anthocyanin*. Food Sci. Technol. Res. 2003. 9(3):242-244.
140. King, P.J., Ma, G., Miao, W. *Structure - Activity Relationships: Analogues of the Dicafeoylquinic and Dicafeoyltartaric Acids as Potent Inhibitors of Human Immunodeficiency Virus Type 1 Integrase and Replication*. J. Med. Chem. 1999. 42(3): 497-509.
141. Miranda, M.M., Costa, S.S., Wigg, M.D., Simoni, I.C., de Almeida, A.P., Lagrota, M.H.C. *Flavonolmonoglycosides isolated from the antiviral fractions of Persea americana (Lauraceae) leaf infusion*. Phyther. Res. 2002. 12(8):562-567.
142. Ding, Y., Cao, Z., Cao, L., Ding, G., Wang, Z., Xiao, W. *Antiviral activity of chlorogenic acid against influenza A (H1N1/H3N2) virus and its inhibition of neuraminidase*. Sci. Rep. 2017. 7:1-11.
143. Tang, W., He, P. L., Zhang, R. J. *Anti-hepatitis B virus activity of chlorogenic acid, quinic acid and caffeic acid in vivo and in vitro*. Antiviral Res. 2009. 83(2):186-190.

144. Tanida, I., Fukasawa, M., Wakita, T. *Inhibitory Effects of Caffeic Acid, a Coffee-Related Organic Acid, on the Propagation of Hepatitis C Virus*. Jpn. J. Infect. Dis. 2015. 68(4):268-275.
145. Wang, S.Y., Lee, J.C., Wu, Y.H. *Limonoids from the Seeds of Swietenia macrophylla with Inhibitory Activity against Dengue Virus 2*. J. Nat. Prod. 2014. 77(11):2367-2374.
146. Orhan, D. D., Özçelik, B., Özgen, S., Ergun, F. *Antibacterial, antifungal, and antiviral activities of some flavonoids*. Microbiol. Res. 2010. 165(6):496-504.
147. Lin, Y.J., Chang, Y.C., Hsiao, N.W. *Fisetin and rutin as 3C protease inhibitors of enterovirus A71*. J. Virol. Methods. 2012. 182(1-2):93-98.
148. Zandi, K., Teoh, B.T., Sam, S.S., Wong, P.F., Mustafa, M., Abubakar, S. *Antiviral activity of four types of bioflavonoid against dengue virus type-2*. Virol. J. 2011. 8:1-11.
149. Lyu, S.Y., Rhim, J.Y., Park, W.B. *Antiherpetic activities of flavonoids against herpes simplex virus type 1 (HSV-1) and type 2 (HSV-2) in vitro*. Arch. Pharm. Res. 2005. 28(11):1293-1301.
150. Choi, H.J., Kim, J.H., Lee, C.H. *Antiviral activity of quercetin 7-rhamnoside against porcine epidemic diarrhea virus*. Antiviral Res. 2009. 81(1):77-81.
151. Silva, A.R.A., Morais, S.M., Marques, M.M. *Antiviral activities of extracts and phenolic components of two Spondias species against dengue virus*. J. Venom Anim. Toxins Incl. Trop. Dis. 2011. 17(4):406-413.

152. Kaul, T. N., Middleton, E. Jr, Ogra, P. L. *Antiviral effect of flavonoids on human viruses*. J. Med. Virol. 1985. 15(1):71-9.
153. Ghazal, S. A., Abuzarqua, M., Mahansneh, A. M. *Effect of plant flavonoids on immune and inflammatory cell function*. Phytother. Res. 1992. 6,265-71.
154. Mahmood, N., Piacente, S., Pizza, C., Burke, A., Khan, A.I., Hayt, A.J. *The anti-HIV activity and mechanisms of action of pure compounds isolated from Rosa damascena*. Biochem. Biophys Res. Commun. 1996. 229(1):73-79.
155. Tateo, F., Pagani, L. *Effects of propolis flavonoids on virus infectivity and replication*. Microbiologica. 1990. 13(3):207-13
156. Lv, X., Qiu, M., Chen, D., Zheng, N., Jin, Y., Wu, Z. *Apigenin inhibits enterovirus 71 replication through suppressing viral IRES activity and modulating cellular JNK pathway*. Antiviral Res. 2014. 109(1):30-41.
157. Kang, E.H., Kown, T.Y., Oh, G.T. *The flavonoid ellagic acid from a medicinal herb inhibits host immune tolerance induced by the hepatitis B virus-e antigen*. Antiviral Res. 72(2):100-106.
158. Shin, M.S., Kang, E.H., Lee, Y.I. *A flavonoid from medicinal plants blocks hepatitis B virus-e antigen secretion in HBV-infected hepatocytes*. Antiviral Res. 2005. 67(3):163-168.
159. Tripoli, E., Guardia, M. La, Giammanco, S., Majo, D., Di, Giammanco, M. *Citrus flavonoids: Molecular structure, biological activity and nutritional properties: A review*. Food Chem. 2007. 104:466-479.

160. Esquenazi, D., Wigg, M.D., Miranda, M.F.S. *Antimicrobial and antiviral activities of polyphenolics from Cocos nucifera Linn. (Palmae) husk fiber extract*. Res. Microbiol. 2002. 153(10):647-652.
161. Zhou, S. F., Zhou, Z. W., Li, C. G., Chen, X., Yu, X., Xue, C. C., Herington, A. *Identification of drugs that interact with herbs in drug development*. Drug Discov. Today. 2007. 12:664-673.
162. Khan, A.K., Rashid, R., Fatima, N. *Pharmacological Activities of Protocatechuic Acid*. Acta Pol. Pharm. 2015. 72(4):643-650.
163. Yamaguchi, K., Honda, M., Ikigai, H., Hara, Y., Shimamura, T. *Inhibitory effects of (-)-epigallocatechin gallate on the life cycle of human immunodeficiency virus type 1 (HIV-1)*. Antiviral Res. 2002. 53(1):19-34.
164. Carneiro, B. M., Batista, M.N., Cláudia, A., Braga, S., Nogueira, M.L., Rahal, P. *The green tea molecule EGCG inhibits Zika virus entry*. 2016. Virology. 496:215-218.
165. Lani, R., Hassandarvish, P., Shu, M.H. *Antiviral activity of selected flavonoids against Chikungunya virus*. Antiviral Res. 2016. 133:50-61.
166. Lin, Y.J., Chang, Y.C., Hsiao, N.W. *Fisetin and rutin as 3C protease inhibitors of enterovirus A71*. J. Virol. Methods. 2012. 182(1-2):93-98.
167. Quéré, L., Wenger, T., Schramm, H.J. *Triterpenes as potential dimerization inhibitors of HIV-1 protease*. Biochem. Biophys. Res. Commun. 1996. 227, 484-488.

168. Mounce, B.C., Cesaro, T., Carrau, L., Vallet, T., Vignuzzi, M. *Curcumin inhibits Zika and chikungunya virus infection by inhibiting cell binding*. Antiviral Res. 2017. 142:148-157.

CHAPTER THREE

In this chapter, the pharmacokinetic properties and inhibitory activities of selected PCs found in THMs against South African HIV-1 Sub-type C protease enzyme (PR) were described. Four FDA-approved protease inhibitor drugs LPV, DRV, ATV, and SQV were used as standard. In order to achieve this, computational tools were employed to predict both the pharmacokinetic and inhibitory properties of the PCs.

An article titled ‘The pharmacokinetic properties of HIV-1 protease inhibitors: A computational perspective on herbal phytochemicals’ was published in an Elsevier Journal (Heliyon, 5; e02565, Appendix E).

The Pharmacokinetic Properties of HIV-1 Protease Inhibitors: A Computational Perspective on Herbal Phytochemicals

Abstract

Recent studies have isolated phytochemicals from plants to repress HIV, but few studies have focused on the effects of these phytochemicals on the activities of enzymes/transporters involved in the metabolism of antiretroviral drugs. Centre of Awareness-Food Supplement (COA[®]-FS) herbal medicine is one of the herbal medicines reported to have potential anti-HIV features. The aim of this study was to examine the activity of selected phytochemical compounds present in this supplement using computational tools. SWISSTARGETPREDICTION and SWISSADME servers were used to determine the effects of selected phytochemicals on the enzymes/transporters involved in the metabolism of protease inhibitor drugs, (PIs) (Atazanavir, Lopinavir, Darunavir, Saquinavir). Potential structural inhibitory activities of these phytochemicals were explored. Six phytochemicals (Geranin, Apigenin, Fisetin, Luteolin, Phthalic acid and Gallic acid) were predicted to be inhibitors of CYP3A4, which may slowdown elimination of PIs thereby maintaining optimal PI concentrations. Free binding energy analysis for antiviral activities identified four phytochemicals with favourable binding landscapes with HIV-1 protease, with Epigallocatechin gallate and Kaempferol-7-glucoside being the best of the four. Computational methods are useful tools for predicting the interactions of phytochemicals found in herbal medicines with ARVs.

Introduction

The World Health Organization (WHO) reported that approximately 72 million people had already been infected with the Human Immunodeficiency Virus (HIV) worldwide in 2017 (WHO, 2018). Of these, sub-Saharan Africa was the most heavily affected region, accounting for over 69% of all infected cases. The Joint United Nations (UNAIDS report) (2018) states that although there is a steady decline in Acquired Immune Deficiency Syndrome (AIDS) related illnesses over the past decade, the global rate of new HIV infections is not falling fast enough to reach the 2020 targets (WHO, 2018).

In the replication cycle of HIV in human immune cells, the HIV protease enzyme is required to produce mature and infectious HIV virions. This has allowed the enzyme to be a focus for anti-HIV inhibitors (Scholar, 2011). The protease enzyme is a C2-symmetric active homodimer, consisting of a non-covalently connected dimer of 99 amino acid residues each. The two monomeric chains assemble to form an enclosed tunnel covered by two flaps that characteristically “open and close” upon substrate binding (Levy and Caflich, 2003). Viral replication by HIV is inhibited by protease inhibitor drugs (PIs) by binding to the HIV proteases and subsequently obstructing the proteolytic cleavage of the protein precursors which results in the development of immature non-infectious viral particles (Soontornniyomkij et al., 2014; Geretti and Easterbrook, 2001). In South Africa, there are currently four FDA-approved PIs in use: atazanavir, darunavir, lopinavir and saquinavir, with ritonavir being used as boosters with the PIs (Carmona and Nash, 2017).

The use of traditional herbal medicine is gaining more popularity in the treatment of diseases such as HIV, not only in developing countries but also in developed countries, which has caused great public health concern among scientists and physicians who are sometimes not sure about the safety of herbal preparations especially when used concurrently with regular

orthodox medications (WHO, 2018). In South Africa, many patients undergoing antiretroviral therapy also consume traditional herbal medicine (Nlotoo and Naidoo, 2014). One of the most consumed herbal medicine by HIV positive patients in South Africa is COA[®]-FS (Centre of Awareness) herbal medicine (Nlotoo and Naidoo, 2014). Other herbal medicines include Imbiza Herbal Tonic, Ngoma herbal tonic, Ingungumbane Mahlabizifo and many more (Ndhlala et al. 2011).

In a previous study in our lab, one of the herbal medicines and its component plants (COA[®]-FS herbal medicine) were subjected to Gas Chromatography-Mass Spectrometry (GC-MS) to identify the phytochemical compounds present in them (Boadu et al., 2019; Nwabuike, et al, 2019). COA[®]-FS herbal medicine comprised of six plants, namely; *A. indica*, *P. americana*, *C. papaya*, *S. mombin*, *O. viride* and *V. amygdalina* (<https://www.coadrugs.org/coafs/>). Over fifty compounds were identified from the crude, methanol, hexane, dichloromethane, ethylacetate and ethanol extracts of the different plants, fifteen of which were structurally related and have been reported in some of the other herbal medicines or their component plants and, also reported to possess antiviral activities against different viral infections were chosen for this study.

While previous studies have reported on antiviral activity of herbal medicine, few studies have looked at the effect of the chemical constituents of the herbal medicines on the enzymes and transporters involved in the metabolism of drugs such as PI drugs, and the possibility of serious side effects. This study examines the pharmacokinetic effect of fifteen phytochemical compounds potentially found in some of the herbal medicine on the activities of major enzymes and transporters involved in the metabolism of FDA-approved protease inhibitor drugs commonly used in South Africa, and to determine if they are potential inhibitors of HIV-1 protease using *in silico* pharmacodynamics and pharmacokinetic analysis.

Figure 1 illustrates the 2-D structures of the selected fifteen phytochemical compounds, 2-D structures of the four FDA-approved protease inhibitor drugs and the crystalline structure of HIV protease enzyme indicating the active site amino acid residues of the enzyme. Three letter codes were assigned for the phytochemical compounds and the four FDA-approved drugs.

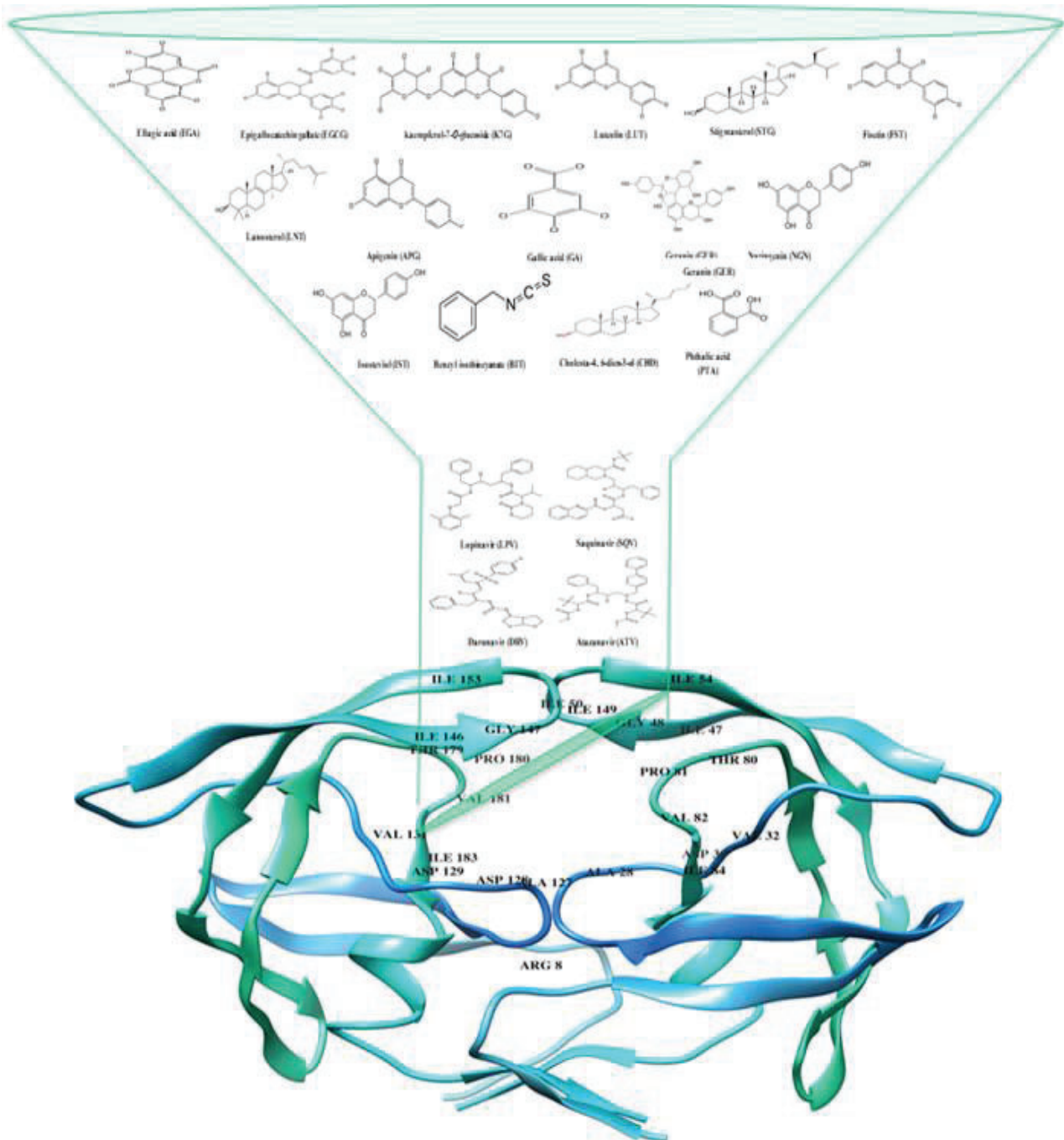


Figure 1: 2D Structures of the fifteen selected phytochemical compounds and 2D structures of the Four FDA approved drugs and Crystal structure of South African HIV-1 sub-type C (PDB code 3U71)

Table 1: Selected Phytochemicals with antiviral activities present COA®-FS herbal medicine and its component plants

Compounds Name	Plant name	Extracts	Plant parts	Literature Reference	COA-FS herbal medicine		
					GC-MS	Extracts	Reference
EGA	<i>Spondias mombin</i> , <i>Carica papaya</i>	Hydroethanolic,	Leaf	Shin et al, 2005; Nwabuife, et al, 2019	+	Ethanollic, Hexane,	Boadu et al., 2019; Nwabuife, et al, 2019
CHD	<i>Azadirachta indica</i> , <i>Vernonia amygdalina</i> , <i>Carica papaya</i>	Methanolic, Hexane, Ethanol, Ethylacetate, Dichloromethane	Leaf	Dineshkumar and Rajakumar, 2017; Boadu et al., 2019; Nwabuife, et al, 2019	+	Ethanol, Hexane	Boadu et al., 2019; Nwabuife, et al, 2019
LNT	<i>Azadirachta indica</i> , <i>Vernonia amygdalina</i>	Chloroform, Dichloromethane	Leaf	Siddiqui et l., 2006; Boadu et al., 2019	+	Dichloromethane	Boadu et al., 2019
BIT	<i>Carica papaya</i>	Hydroethanolic	Seed, leaf	Kermanshai et al., 2001	+	Ethanollic	Boadu et al., 2019
GA (methyl salicylate)	<i>Persea Americana</i>	Methanolic	Pulp, Leaf	(Hurtado-Fernández et al., 2014)	+	Standard	Boadu et al., 2019
IST	<i>Vernonia amygdalina</i>	Chloroform, Dichloromethane, Ethanol,	Leaf	(Adewole et al., 2018) Boadu et al., 2019	+	Dichloromethane	Boadu et al., 2019
STG	<i>Carica papaya</i> , <i>Persea Americana</i> , <i>Vernonia amygdalina</i> , <i>Azadirachta indica</i>	Petroleum ether, Hydroethanolic, Hexane, Dichloromethane, Ethylacetate, Ethanol	Leaf	Rashed et al., 2013; Monika and Geetha, 2015; Boadu et al., 2019; Nwabuife, et al, 2019	+	Hexane, Dichloromethane, Ethylacetate	Boadu et al., 2019; Nwabuife, et al, 2019
PTA	<i>Carica papaya</i> , <i>Azadirachta indica</i>	Methanolic, Crude oil, Hexane, Dichloromethane, Ethylacetate, Ethanol	Leaf	Sajin et eal., 2015; Boadu et al., 2019; Babatunde et al., 2019	+	Hexane, Ethylacetate	Boadu et al., 2019; Nwabuife, et al, 2019

NGN	<i>Persea Americana</i> , <i>Carica papaya</i>	Methanolic, Ethylacetate	Leaf	Hurtado-Fernández et al., 2014; Nwabuike, et al, 2019	-	Methanolic, Ethylacetate	
K7G	<i>Carica papaya</i>	Ethanollic, Aqueous	Fruit/pulp, dry leaf	Kongkachuichai and Charoensiri, 2010; Lako, 2007	-		ND
EGCG	<i>Persea Americana</i>	Hydromethanolic	Seed	Calderón-Oliver et al., 2015	-		ND
LUT	<i>Vernonia amygdalina</i> , <i>Carica papaya</i>	Ethanollic, Methanolic	Leaf, Fruit/pulp	Igile et al., 1995	-		ND
GER	<i>Spondias mombin</i>	Hydroalcoholic	Leaf	Mukhtar et al., 2008	-		ND
APG	<i>Carica papaya</i>	Hydrothanolic	Fruit/pulp	Franke et al., 2004	-		ND
FST	<i>Carica papaya</i>	Hydrothanolic	Fruit/pulp	Lako et al., 2007	-		ND

Key: + means present, - means not present, ND means not detected.

Methods

Table 1 shows the fifteen selected phytochemical compounds investigated. Nine of the selected phytochemical compounds (EGA, CHD, LNT, BIT, GA, IST, STG, PTA and NGN) were present in the COA[®]-FS herbal medicine and the remaining 6 (six) compounds were reported in literature to be present in the component plants of the herbal medicine.

Computational Methods

Prediction of Enzymes and Transporters Targets

SwissTargetPrediction and SwissADME servers were used for the prediction of proteins (enzymes and transporters) involved in the metabolism of the four FDA approved drugs and the selected phytochemical compounds from the supplement and its component plants and their pharmacokinetic effects (Gaffer et al., 2013). The server predicts the target of small molecules.

Measurement of Pharmacokinetics Properties and Drug Likelihood of the Phytochemical compounds

SWISSADME server was used for the determination of the physicochemical descriptors and defines the pharmacokinetic properties and drug-like nature of each phytochemical compound. The “Brain Or Intestinal Estimated permeation, (BOILED-Egg)” method was utilized as it computes the lipophilicity and polarity of small molecules (Daina et al, 2017).

HIV-1 Enzyme and ligand Acquisition and Preparation

The X-ray crystal structures of the HIV-1 Protease enzyme (PDB codes: 3U71) was obtained from the RSCB Protein Data Bank (Burley et al., 2018). The structures of HIV-1 protease

was then prepared on the UCSF Chimera software package (Yang et al., 2012) where the monomeric protein was converted to a dimeric structure. The four FDA-approved drugs Atazanavir, Darunavir, Lopinavir, and Saquinavir, as well as the fifteen phytochemical compounds, were accessed from PubChem (Kim et al., 2016) and the 3-D structures prepared on the Avogadro software package (Hanwell et al., 2012).

Molecular Docking

The Molecular docking software utilized in this study was the Autodock Vina Plugin available on Chimera (Yang et al., 2012), with default docking parameters. Prior to docking, Gasteiger charges were added to the compounds and the non-polar hydrogen atoms were merged to carbon atoms. The phytochemical compounds were then docked into the binding pocket of Protease (by defining the grid box with a spacing of 1 Å and size of 24 × 22 × 22 pointing in x, y and z directions). The four FDA-approved drug systems, as well as the four best-docked phytochemical compounds systems, were then subjected to molecular dynamics simulations.

Molecular Dynamic (MD) Simulations

The MD simulations were performed using the CPU version of the SANDER engine provided with the AMBER package, in which the FF14SB variant of the AMBER force field (Nair and Miners, 2014) was used to describe the protein.

ANTECHAMBER was used to generate atomic partial charges for the ligand by utilizing the Restrained Electrostatic Potential (RESP) and the General Amber Force Field (GAFF) procedures. The Leap module of AMBER 14 allowed for the addition of hydrogen atoms, as well as Na⁺ and Cl⁻ counter ions for neutralization of all systems. The amino acids were renumbered based on the dimeric form of the enzyme, thus numbering residues 1-198.

The eight systems were then suspended implicitly within an orthorhombic box of TIP3P water molecules such that all atoms were within 8Å of any box edge.

An initial minimization of 2000 steps were carried out with an applied restraint potential of 500 kcal/mol for both solutes, were performed for 1000 steps using the steepest descent method followed by 1000 steps of conjugate gradients. An additional full minimization of 1000 steps was further carried out by conjugate gradient algorithm without restraint.

A gradual heating MD simulation from 0K to 300K was executed for 50ps, such that the systems maintained a fixed number of atoms and fixed volume. The solutes within the systems were imposed with a potential harmonic restraint of 10kcal/mol and collision frequency of 1.0ps. Following heating, an equilibration estimating 500ps of each system was conducted; the operating temperature was kept constant at 300K. Additional features such as several atoms and pressure were also kept constant mimicking an isobaric-isothermal ensemble (NPT). The system's pressure was maintained at 1 bar using the Berendsen barostat.

The total time for the MD simulations conducted were 100ns. In each simulation, the SHAKE algorithm was employed to constrict the bonds of hydrogen atoms. The step size of each simulation was 2fs and an SPFP precision model was used. The simulations coincided with the isobaric-isothermal ensemble (NPT), with randomized seeding, the constant pressure of 1 bar maintained by the Berendsen barostat, a pressure-coupling constant of 2ps, a temperature of 300K and Langevin thermostat with collision frequency of 1.0ps.

Post-Dynamic Analysis

The coordinates of the eight systems were then saved and the trajectories were analyzed every 1ps using PTRAJ, followed by analysis of RMSD, RMSF and Radius of Gyration using the CPPTRAJ module employed in AMBER 14 suit.

Binding Free Energy Calculations

To estimate and compare the binding affinity of the systems, the free binding energy was calculated using the Molecular Mechanics/GB Surface Area method (MM/GBSA) (Ylilauri & Pentikäinen, 2013). Binding free energy was averaged over 100000 snapshots extracted from the 100 ns trajectory. The free binding energy (ΔG) computed by this method for each molecular species (complex, ligand, and receptor) can be represented as (Hayes and Archontis, 2011):

$$\Delta G_{\text{bind}} = G_{\text{complex}} - G_{\text{receptor}} - G_{\text{ligand}} \quad (1)$$

$$\Delta G_{\text{bind}} = E_{\text{gas}} + G_{\text{sol}} - TS \quad (2)$$

$$E_{\text{gas}} = E_{\text{int}} + E_{\text{vdw}} + E_{\text{ele}} \quad (3)$$

$$G_{\text{sol}} = G_{\text{GB}} + G_{\text{SA}} \quad (4)$$

$$G_{\text{SA}} = \gamma \text{SASA} \quad (5)$$

The term E_{gas} denotes the gas-phase energy, which consists of the internal energy E_{int} ; Coulomb energy E_{ele} and the van der Waals energies E_{vdw} . The E_{gas} was directly estimated from the FF14SB force field terms. Solvation free energy, G_{sol} , was estimated from the energy contribution from the polar states, G_{GB} , and non-polar states, G . The non-polar solvation energy, SA. G_{SA} , was determined from the solvent accessible surface area (SASA), using a water probe radius of 1.4 Å, whereas the polar solvation, G_{GB} , contribution was estimated by solving the GB equation. S and T denote the total entropy of the solute and temperature respectively.

Data analysis

All raw data plots were generated using the Origin data analysis software (Seifert, 2014).

Results

Assessing the predicted targets for the drugs and phytochemicals

Using two different methods, the SWISSPREDICTION and SWISSADME servers, the enzymes and transporters involved in the metabolism of the four FDA-approved drugs and the fifteen selected phytochemical compounds were predicted. The SWISSPREDICTION server predicted all possible enzymes and transporters that are likely to be targets of the phytochemical compounds. On the other hand, the SWISSADME predicted the possibility of the phytochemicals compounds having pharmacokinetic effect on some cytochrome P450 enzymes (CYP450) such as CYP1A2, CYP2C19, CYP2C9, CYP2D9, CYP2D6 and CYP3A4 and their possibility to be substrates (inducers) of Permeability glycoprotein (P-gp). Although, the probability of DRV and SQV binding to Renin as a target was predicted to be low, Renin is the only enzyme predicted by the SWISSPREDICTION server to be a target for the four conventional drugs. CYP3A4 (with higher probability) and cathepsin D (lower probability) were predicted to be targets for DRV, ATV and LPV. CYP2C19 was predicted only for LPV. For the selected phytochemical compounds, CYP3A4 was predicted to be a target for Geranin (GER), Apigenin (APG), Fisetin (FST), Garlic acid (GA), Luteolin (LUT), and Naringenin (NGN). Isosteviol (IST) and NGN were only predicted substrates of P-gp. CYPY1A2, CYP2D6, CYP2C9 and CYP2C19 are other sub-families of cytochrome P450 enzymes predicted by the SWISSADME server to be targets for EGA, APG, LNT, BIT, GA, IST, STG, PTA and NGN and IST.

Table 2: Predicted targets involved in the metabolism of the four FDA-approved PI drugs and selected phytochemical compounds

Compound Name	SWISSPREDICTION			SWISSADME	
	Enzymes	Transporters	Enzymes	Transporters	
ATV	Renin, Cathepsin D, Pepsin A-5, Cathepsin E, Napsin-A, CYP3A4, Gastricsin	NP	CYP3A4	P-glycoprotein	
SQV	Thromboxane-A synthase, Renin, CYP3A4	D (2), D(4) dopamine receptors, Substance-K receptor, Substance-P receptor, Neuromedin-K receptor, Oxytocin receptor, Mu-type opioid receptor	CYP3A4	P-glycoprotein	
LPV	Renin, Cathepsin D, Napsin-A, Beta-secretase 1, Beta-secretase 2, Gastricsin	Potassium voltage-gated (ion channel),	CYP3A4, CYP2C19	P-glycoprotein	
DRV	CYP3A4, Thromboxane-A synthase, CYP3A5, CYP3A7, CYP3A43, Renin, Cathepsin D	C-C chemokine receptor type 1-8, CX3C chemokine receptor 1,	CYP3A4	P-glycoprotein	
EGCG	PEX, 67 kDa matrix metalloproteinase-9, 14, 15, Beta-secretase 1, 2, Tyrosyl-DNA phosphodiesterase 1, 6-phosphogluconate dehydrogenase, decarboxylating, Telomerase reverse transcriptase, Dihydrofolate reductase, Dihydrofolate reductase	Potassium voltage-gated channel subfamily H member 2	NP	NP	
K7G	Tyrosyl-DNA phosphodiesterase 1, Xanthine dehydrogenase/oxidase, Aldehyde oxidase, Aldo-keto reductase family 1, Aldose reductase, Lysine-specific demethylase 4A, Lysine-specific demethylase 4A, 4B, 4C	Adenosine receptor A1, Alpha-2A, 2C, 2B, Muscle blind-like protein 1	NP	NP	
EGA	Cytidine deaminase, Thymidine kinase, Adenosine deaminase, Thymidine phosphorylase, Histone deacetylase 1-3, Adenosyl homocysteinease, Putative adenosyl homocysteinease 2, Carbonic anhydrase 1, 2, 3, 12	NP	CYP1A2	NP	
LUT	22 kDa interstitial collagenase, CYP1A2, PEX, Stromelysin-1, 67 kDa matrix metalloproteinase-9, Aldose reductase	NP	CYP1A2, CYP2D6,	NP	

					CYP3A4	
GER	Squalene monooxygenase, Tyrosyl-DNA phosphodiesterase 1, Muscle blind-like protein 1, Muscle blind-like protein 2 and 3, DNA topoisomerase 1, Tyrosine-protein phosphatase non-receptor type 2	Androgen receptor, CYP19A1, Estrogen receptor, Estrogen receptor beta, Oxysterols receptor LXR-beta, Oxysterols receptor LXR-alpha, Tyrosyl-DNA phosphodiesterase 1, Tyrosine-protein phosphatase non-receptor type 1 and 2, M-phase inducer phosphatase 1, Lanosterol 14-alpha demethylase, 3-oxo-5-alpha-steroid 4-dehydrogenase 2	Multidrug resistance protein 1 (P-glycoprotein)		CYP3A4, CYP2C9	NP
CHD			Sodium-dependent noradrenaline transporter		CYP2C9	NP
APG	Aldo-keto reductase family 1, CYP1A2, Cyclin-dependent kinase 1, Microtubule-associated protein tau, CYP19A1, Cyclin-dependent kinase 4, Estradiol 17-beta-dehydrogenase 1, Aldose reductase, Casein kinase II subunit alpha		Estrogen receptor, Adenosine receptor A2a		CYP1A2, CYP2D6, CYP3A4	NP
FST	Cyclin-dependent kinase 1, Arachidonate 5-lipoxygenase, Microtubule-associated protein tau, Cyclin-dependent kinase 4, Arachidonate 15-lipoxygenase, Xanthine dehydrogenase/oxidase		NP		CYP1A2, CYP2D6, CYP3A4	NP
NGN	CYP450 1A2, CYP450 19A1, Estradiol 17-beta-dehydrogenase 1, Carbonyl reductase [NADPH] 1, Cytochrome P450 1B1, Tyrosyl-DNA phosphodiesterase 1, CYP1A1, Retinol dehydrogenase 8, Carbonyl reductase [NADPH] 3, Adenosine receptor A1		Multidrug resistance-associated protein 1 (P-glycoprotein), Estrogen receptor		CYP1A2, CYP3A4	P-glycoprotein
BIT	Tyrosyl-DNA phosphodiesterase 1, Microtubule-associated protein tau, Carbonic anhydrase 1-9, Indoleamine 2,3-dioxygenase 1 and 2, Quinone oxidoreductase, Carbonic anhydrase 5B (mitochondrial), Indoleamine 2,3-dioxygenase 1		Transient receptor potential cation channel subfamily A member 1, Sodium-dependent serotonin transporter		NP	NP
GA	Carbonic anhydrase 12, Carbonic anhydrase 1-9, Tyrosyl-DNA phosphodiesterase 1, Carbonic anhydrase 5B and 5A, FAD-		NP		CYP3A4	NP

	linked sulphhydryl oxidase ALR				
STG	Androgen receptor, Tyrosyl-DNA phosphodiesterase 1, CYP19A1, 3-hydroxy-3-methylglutaryl-coenzyme A reductase, Lanosterol 14-alpha demethylase, Oxysterols receptor LXR-beta, Oxysterols receptor LXR-alpha	Low-density lipoprotein receptor, Very low-density lipoprotein receptor, Estrogen receptor, Estrogen receptor beta, Sodium-dependent noradrenaline transporter	CYP2C9	NP	
IST	Aldo-keto reductase family 1 member B10, Aldose reductase, Corticosteroid 11-beta-dehydrogenase isozyme 1, Hydroxysteroid 11-beta-dehydrogenase 1-like protein, M-phase inducer phosphatase 1, M-phase inducer phosphatase 2, Alcohol dehydrogenase [NADP (+)], 1,5-anhydro-D-fructose reductase, UDP-glucuronosyltransferase	NP	CYP2C9	P-glycoprotein	
LNT	3-hydroxy-3-methylglutaryl-coenzyme A reductase, Lanosterol 14-alpha demethylase, Cytochrome P450 19A1, Tyrosyl-DNA phosphodiesterase 1	Androgen receptor, Oxysterols receptor LXR-beta, Sodium-dependent noradrenaline transporter, Sodium-dependent serotonin transporter, Sodium-dependent dopamine transporter, Estrogen receptor, Sodium-chloride-dependent neutral and basic amino acid transporter B(0+)	NP	NP	
PTA	Tyrosyl-DNA phosphodiesterase 1, Dual specificity tyrosine phosphorylation-regulated kinase 1A, Microtubule-associated protein tau, Carbonic anhydrase 1, 2, 3, 4, 5A, 5B, 6, 7, 9, 13, Carbonic anhydrase 12,	Gamma-secretase C-terminal fragment 59	NP	NP	

KEY:

NP

means

Nonpredicted

Pharmacokinetic effects of the phytochemical compounds on the predicted targets involved in the metabolism of the four PI drugs

The SWISSADME server was employed to predict the pharmacokinetic effects of the selected phytochemical compounds on the cytochrome P450 enzymes and P-glycoprotein

Table 3: Pharmacokinetic effects of phytochemical compounds on the enzymes and transporter involved in the metabolism of the four FDA-approved PIs.

Compound Name	Enzymes		Transporter
	CYP3A4 Inhibitor	CYP2C19 Inhibitor	P-gp Substrate/inducers
<i>FDA-Approved Drugs</i>			
DRV	Yes	No	Yes
LPV	Yes	Yes	Yes
ATV	Yes	No	Yes
SQV	Yes	No	Yes
<i>Phytochemical compounds</i>			
IST	No	No	Yes
EGA	No	No	No
K7G	No	No	No
EGCG	No	No	No
NGN	Yes	No	Yes
GER	Yes	No	No
LNT	No	No	No
FST	Yes	No	No
LUT	Yes	No	No
APG	Yes	No	No
PTA	Yes	No	No
STG	No	No	No
CHD	No	No	No
BIT	No	No	No
GA	Yes	No	No

transporter involved in the metabolism of the four FDA-approved drugs. LPV was also predicted to inhibit CYP2C19. The four drugs were predicted inducers of P-gp, while only IST and NGN were predicted inducers of P-gp. Seven of the phytochemical compounds were predicted to possess inhibitory activity on CYP3A4 and none of the phytochemical compound was predicted to inhibit CYP2C19. The inhibition of CYP3A4 and P-gp by the phytochemical compound could decrease the elimination and clearance of the four PI drugs from the systemic circulation and the cells, respectively.

Assessing the Drug-likeness of phytochemical compounds

As shown in Table 4, three of the selected phytochemical compounds (CHD, STG and NGN) are poorly soluble in water. However, three of the FDA-approved drugs (ATV, SQV and LPV) were also poorly soluble. Table 4 also shows the drug likeness of the fifteen selected phytochemical compounds compared to the four FDA-approved drugs. Nine of the phytochemical compounds (K7G, EGA, LUT, APG, FST, BIT, GA, IST and NGN) pass the test. Interestingly, only two of the four conventional drugs pass the drug likeness test (DRV and LPV).

Table 4: Predicted ADME parameters, drug-likeness, pharmacokinetic and physicochemical properties of phytochemical and four FDA-approved drugs using SWISSADME server.

Compound Name	Molecular Formula	Molecular Weight(g/mol)	Lipophilicity (iLOGP)	Water Solubility	GIT Absorption	BBB Permeability	Bioavailability Score	Synthetic Accessibility	Drug likeness (Lipinski)
ATV	C ₃₈ H ₅₂ N ₆ O ₇	704.869	3.56	Poor	Low	No	0.17	6.24	No (2)
SQV	C ₃₈ H ₅₀ N ₆ O ₅	670.855	3.66	Poor	Low	No	0.17	5.94	No (2)
LPV	C ₃₇ H ₄₈ N ₄ O ₅	1349.762	3.44	Poor	High	No	0.55	5.67	Yes
DRV	C ₂₇ H ₃₇ N ₃ O ₇ S	547.667	3.20	Moderate	Low	No	0.55	5.67	Yes
EGCG	C ₂₂ H ₁₈ O ₁₁	458.37	1.83	High	Low	No	0.17	4.20	No (2)
K7G	C ₂₁ H ₂₀ O ₁₁	448.38	1.55	High	Low	No	0.17	5.24	No (2)
EGA	C ₁₄ H ₆ O ₈	302.19	0.79	High	High	No	0.55	3.17	Yes
LUT	C ₁₅ H ₁₀ O ₆	286.24	1.86	High	High	No	0.55	3.02	Yes
GER	C ₃₀ H ₂₄ O ₁₀	544.51	2.14	Moderate	Low	No	0.17	5.73	No (2)
CHD	C ₂₇ H ₄₄ O	384.64	4.81	Poor	Low	No	0.55	6.29	No (3)
APG	C ₁₅ H ₁₀ O ₅	270.24	1.89	Moderate	High	No	0.55	2.96	Yes
FST	C ₁₅ H ₁₀ O ₆	286.24	1.50	High	High	No	0.55	3.16	Yes
LNT	C ₃₀ H ₅₀ O	426.72	5.09	Poor	Low	No	0.55	6.07	No (3)
BIT	C ₈ H ₇ NS	149.21	2.19	High	High	Yes	0.55	1.59	Yes
GA	C ₇ H ₆ O ₅	170.12	0.21	High	High	No	0.56	1.22	Yes
IST	C ₂₀ H ₃₀ O ₃	318.45	2.27	Moderate	High	Yes	0.56	4.83	Yes
STG	C ₂₉ H ₄₈ O	412.69	4.96	Poor	Low	No	0.55	6.21	No (3)
NGN	C ₁₅ H ₁₂ O ₅	272.25	1.75	Soluble	High	No	0.55	3.01	Yes
PTA	C ₈ H ₆ O ₄	166.13	0.60	Soluble	High	No	0.56	1.00	No (2)

Binding affinity of the phytochemical compounds to HIV-1 protease Enzyme (HIVpro)

Fifteen phytochemicals and its component plants and four FDA-approved protease inhibitor drugs (PIs) were docked with HIVpro to estimate the affinity of the drugs to the enzyme in comparison to the four known PIs (Table 5). The docking score showed the fit of the ligands into the active site pocket of the enzyme; the more the negative the value the better the fitness of the ligand. All PIs had better docking scores (range: -8.1 to -9.2kcal/mol) than the phytochemical compounds, except EGA and K7G which were better than LPV. The binding conformation of the fifteen phytochemical compounds (ligands) and the four FDA-approved drugs were taken for further molecular dynamics and binding energy calculations.

Table 5: Docking scores for the four FDA-approved PI drugs and phytochemical compounds.

Compounds Name	Docking score (kcal/mol)
<i>FDA Approved Drugs</i>	
SQV	-9.8
DRV	-9.2
ATV	-8.7
LPV	-8.1
<i>Phytochemical compounds</i>	
EGA	-8.3
K7G	-8.1
EGCG	-7.5
STG	-7.5
GER	-7.5
NGN	-7.5
CHD	-7.4
LNT	-7.4
FST	-7.3
LUT	-7.3
APG	-7.2
IST	-7.1
PTA	-4.8
BIT	-4.6
GA	-4.5

Thermodynamic binding free energy of Phytochemical compounds to HIVpro

As molecular docking only measures the geometric fit of ligands at the active site of a protein, molecular dynamics simulations were run for 100ns to assess the binding free energy of each system. The more negative the values, the better the binding free energy between the enzyme (*HIVpro*) and the ligands. The binding free energy of the four FDA-approved drugs and the fifteen phytochemical compounds were determined using the MMGBSA method to estimate the interaction strength between the FDA-approved inhibitors in comparison to the phytochemical compounds (Table 6). ATV showed the highest binding energy out of all the PIs and the fifteen selected phytochemical compounds. However, EGCG had better binding energy than three conventional PIs (DRV, LPV and SQV). In addition, K7G was better than LPV and DRV.

Table 6. Thermodynamic binding free energy for Phytochemical compounds and FDA-approved drugs to *HIVpro*

Energy Components (kcal/mol)					
Complex	ΔE_{vdw}	ΔE_{elec}	ΔG_{gas}	ΔG_{solv}	ΔG_{bind}
FDA-Approved Drugs					
SQV	-59.300±5.140	6.139±4.847	-53.161±19.400	-0.514±1.35	-53.979±4.874
DRV	-43.805 ±6.108	-25.424 ±8.120	-69.223 ±10.871	29.235 ±4.206	-35.311 ± 4.943
ATV	-65.905±4.965	-28.758±5.760	-94.664±8.314	37.824±4.796	-56.839±5.292
LPV	-51.973±5.433	-27.534±6.605	-79.507±7.958	38.291±3.540	-44.571±3.952
Phytochemical compounds					
EGCG	-36.589±4.054	-76.679±10.634	-113.26±10.265	61.364±3.586	-55.954 ± 2.705
K7G	-45.850±4.123	-44.778±9.576	-90.628±8.503	48.269±5.467	-45.740 ± 4.288
EGA	-25.883±3.400	-57.201±6.132	-83.084±5.446	46.585±3.653	-38.500 ± 2.101
LUT	-26.604±3.702	-48.553±7.929	-75.157±6.895	41.611±4.879	-37.487 ± 1.223
GER	-46.385±4.820	-17.375±5.847	-63.759±7.842	29.458±4.423	-35.532 ± 2.510
LNT	-34.047±5.941	-11.624±2.458	-45.669±6.293	18.170±3.523	-27.486 ± 3.599
APG	-31.671±8.375	-16.449±2.766	-48.112±11.223	22.104±4.239	-26.017 ± 2.966
NGN	-21.952±3.673	-36.188±8.717	-58.140±9.018	35.379±5.518	-22.761 ± 4.494
STG	-20.604±4.023	20.222±4.907	-0.373±1.485	-19.216±4.776	-19.584 ± 5.041
BIT	-18.433±3.600	-264.05±22.483	-225.00±14.578	206.99±17.374	-18.014 ± 3.083
GA	-18.545±6.221	-252.39±13.425	-213.60±20.032	195.98±19.394	-17.622 ±2.094
IST	-18.825±3.748	-254.24±4.827	-215.62±12.739	198.31±9.202	-17.315 ± 2.650
CHD	-18.52±3.777	-245.58±10.393	-206.69±11.342	189.51±9.342	-17.184 ±2.417
FST	-17.65±4.034	-254.16±14.288	-213.67±8.384	198.16±7.323	-15.516 ± 3.993
PTA	-21.145±2.327	-17.168±3.602	-38.312±3.942	23.679±2.555	-14.633 ± 2.248

Structural Analysis of the Most Optimal Phytochemical-HIVpro Complexes

To further establish the mechanistic inhibitory characteristics of these four selected phytochemical compounds (EGCG, K7G, EGA and LUT) with antiviral activity against *HIVpro*, Root mean square deviation (RMSD), Root mean square fluctuation (RMSF), Radius of gyration (RoG) and ligand interaction plots were assessed. Figure 2 depicts the RMSD plot for the four phytochemical compounds and the four FDA-approved drugs. RMSD measures protein stability as the simulation progresses. The RMSD plots of K7G, EGA and EGCG with average values of 1.432Å, 1.442Å and 1.465Å respectively are similar to the RMSD of ATV (1.511 Å), DRV (1.451Å), SQV (1.402Å), apoenzyme, 1.342Å (protease enzyme without ligand). The RMSD of EGCG seems to be close to LPV

(1.9189Å). The RMSD of K7G (1.351Å) was very similar to SQV (1.345 Å). The RMSD of the four compounds deviated from the RMSD of LPV with the highest average value of 2.187Å. The first 40ns of simulation of LPV showed the instability of the enzyme, but from 40 to 100ns of simulation the enzyme was stable.

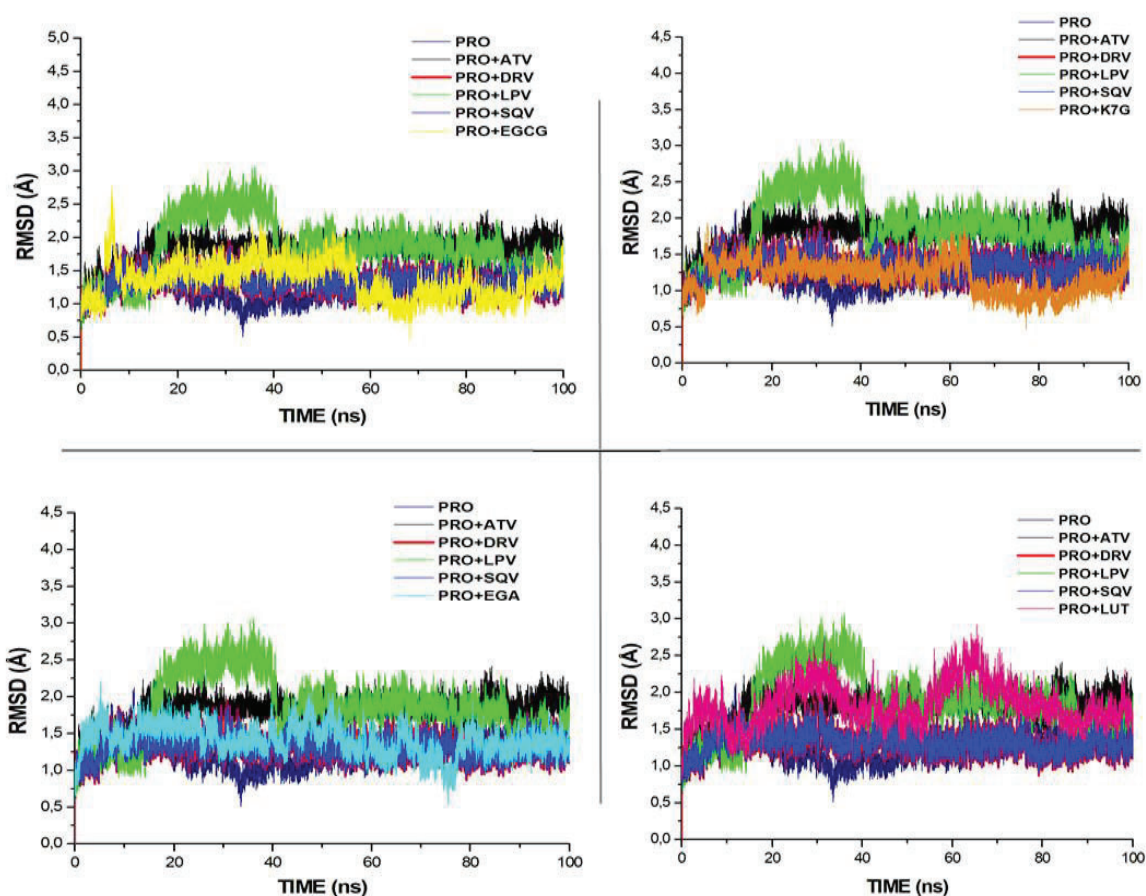


Figure 2: RMSD profile of protein backbone atoms calculated over the course of 100 ns molecular dynamics of *HIVpro* bound to the four different ligands and FDA-approved PI drugs.

Figure 3 and 4 showed the Radius of Gyration (RoG) and Root mean square fluctuations values over the course of 100ns of simulations of the HIV-1 protease enzymes bound to different ligands. RoG is a measure of the compactness of the protein structure. The RoG values of each of the compound were compared to the RoG of the four FDA approved drugs (Figure 3). RoG of EGCG (17.544 Å), LUT (17.431Å), EGA (17.354Å) and K7G (17.455 Å) shows similarity with the RoG of LPV (17.411 Å), ATV (17.327 Å) and SQV (17.423 Å) but deviated from the RoG of DRV (18.345 Å). None of the four compounds showed the same trend and values with RoG of DRV (18.345 Å).

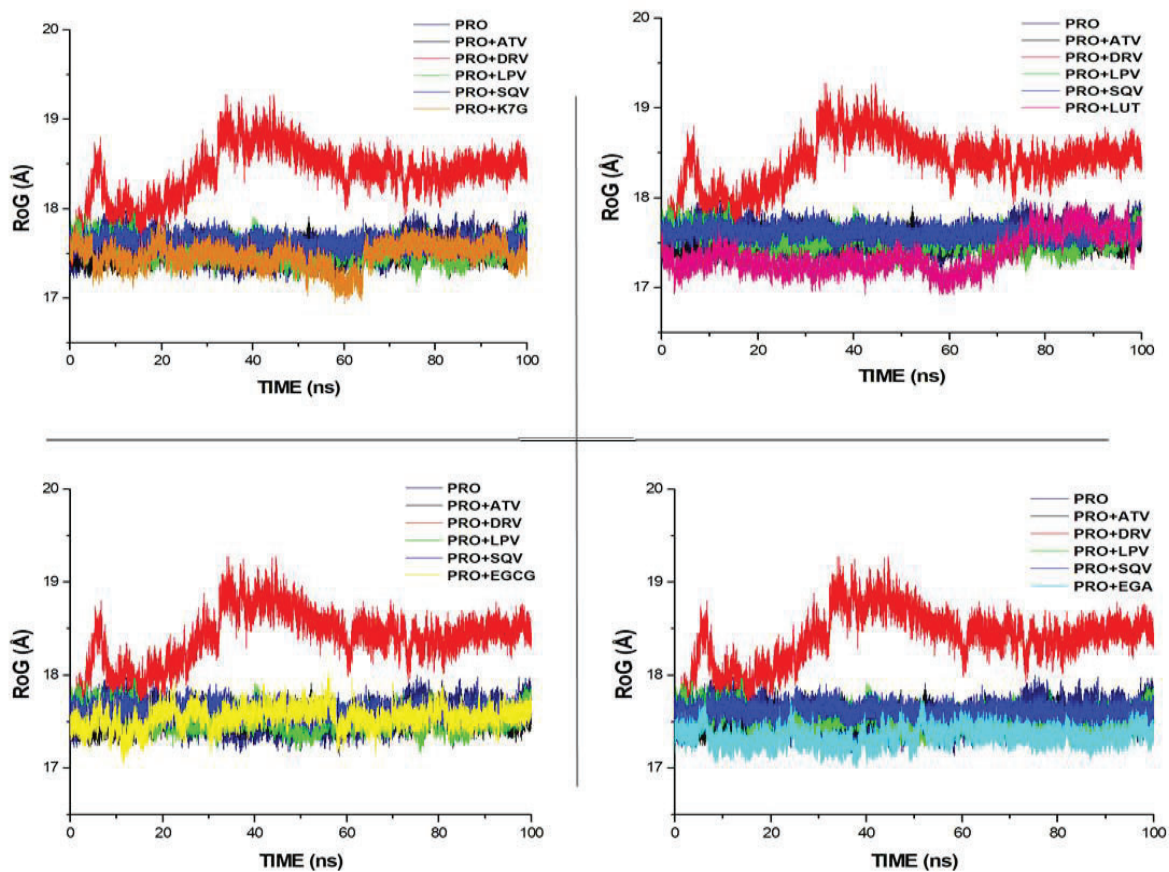


Figure 3: RoG profile of protein backbone atoms calculated over the course of 100 ns molecular dynamics of *HIVpro* bound to different ligands and drugs.

RMSF values monitor the fluctuation of each amino residue as they interact with the ligand throughout a trajectory. The RMSF values of each of the four phytochemical compounds were compared to the RMSF of the four FDA-approved drugs (Figure 4).

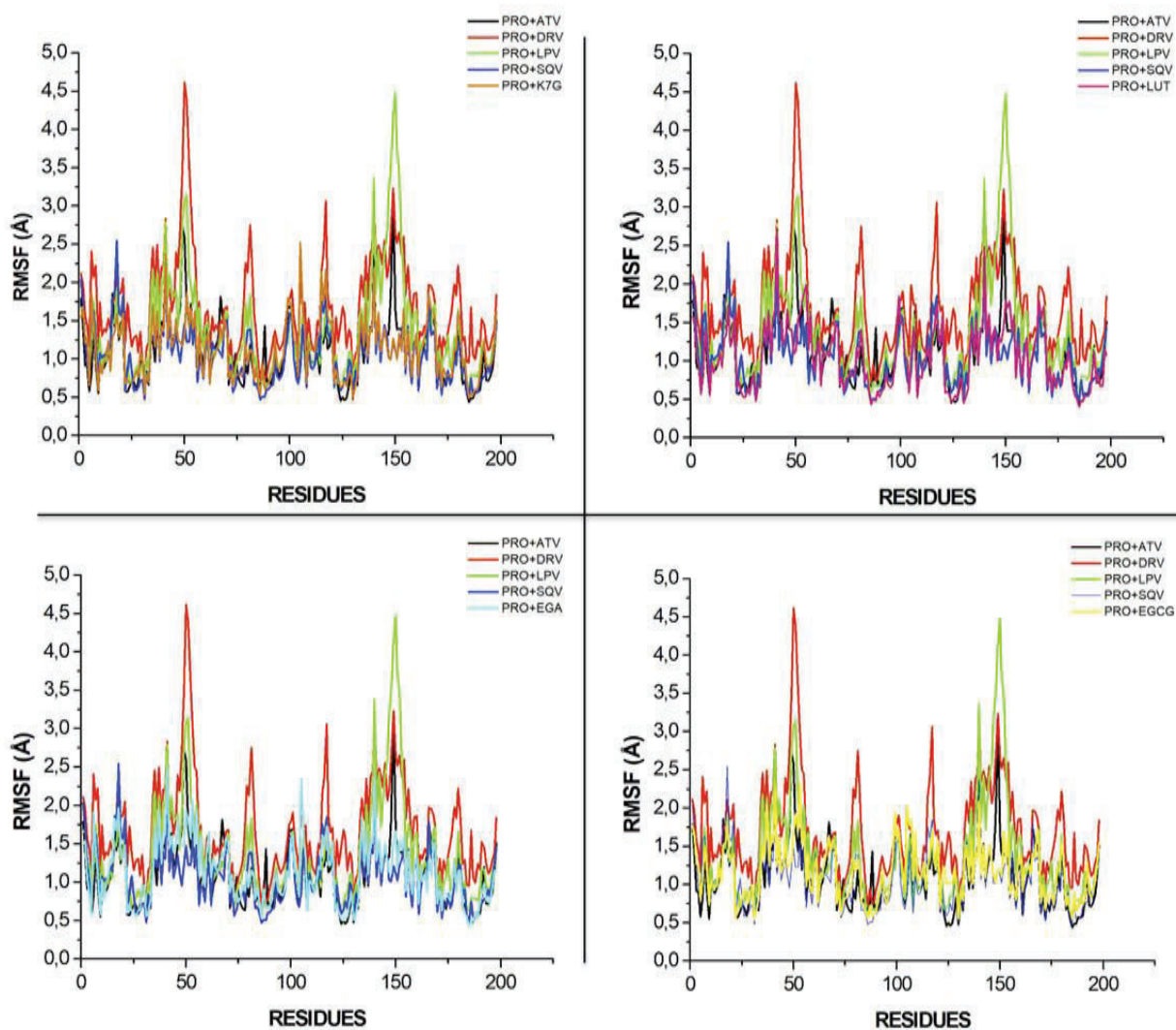


Figure 4: RMSF profile of protein backbone atoms calculated over the course of 100 ns molecular dynamics of *HIVpro* bound to four different ligands and FDA-approved drugs.

Figure 5 illustrates the ligand-interaction plots of the above-mentioned systems following the 100 ns trajectory. The type and number of interactions between proteins and ligands are the major determinants of the overall binding free energy.

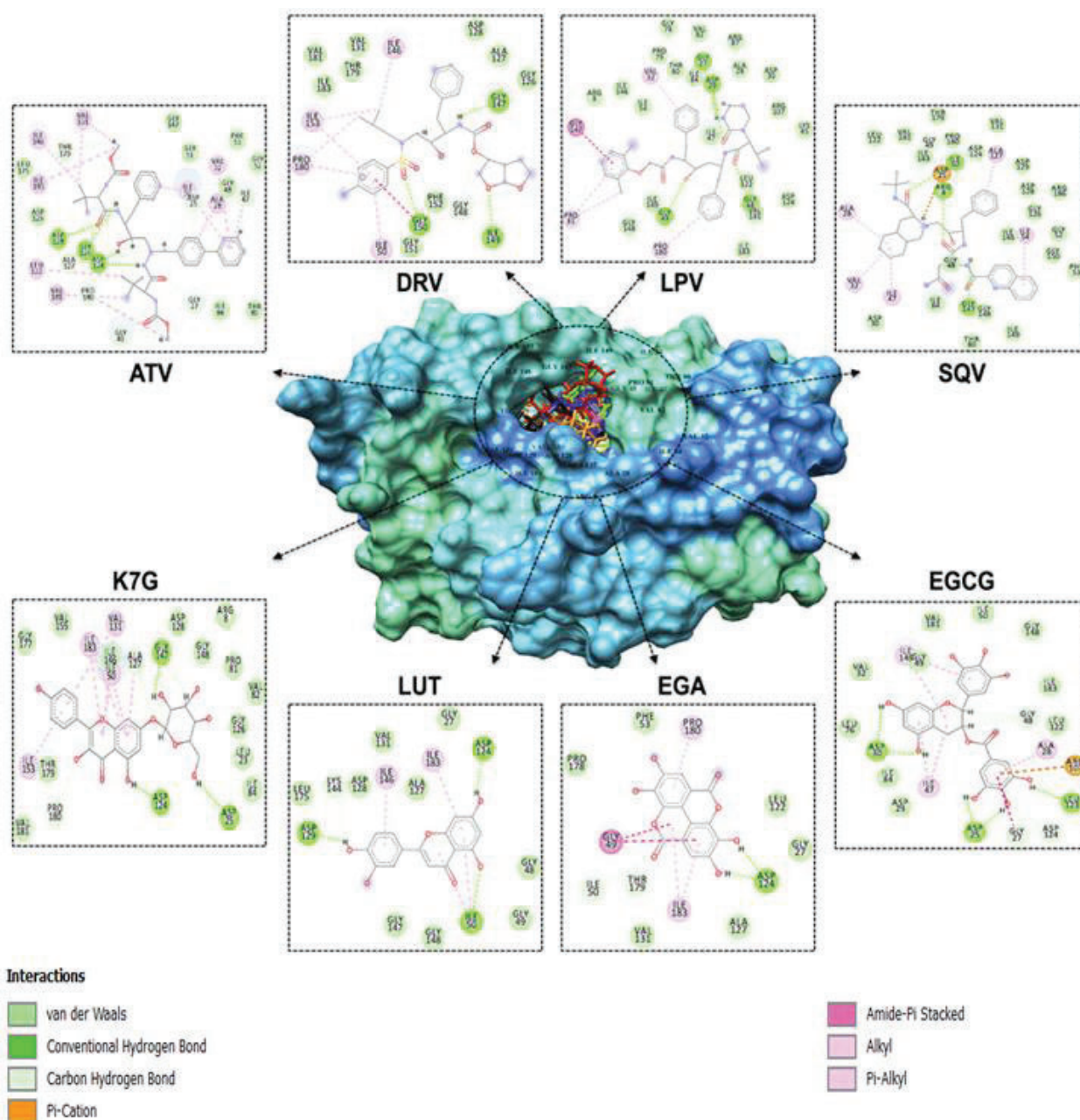


Figure 5: Representation of ligand-HIVpro interactions with different amino acid residues.

Discussion

Assessing the predicted targets for the drugs and phytochemical compounds

The result of this study showed that the phytochemical compounds also target the predicted targets for the four conventional PIs. CYP3A4 and CYP2C19, two sub families of cytochrome P450 enzymes were predicted to be involved in the metabolism of the four FDA-approved drugs. CYP3A4 was the predicted common target for the four conventional drugs,

in addition was predicted to be target of LPV. This prediction agrees with the reports of Brian et al and Bierman et al that reported CYP3A4 is the major form of cytochrome P450 enzymes involved in the metabolism of HIV protease inhibitor drugs (Brian et al., 2011; Bierman et al., 2009). All the four FDA-approved drugs were also predicted to be substrates of P-gp, which is in accordance to the report of Griffin et al. that reported that P-gp was actively involved in the metabolism of PI drugs (Griffin et al., 2010). A different sub type of cytochrome P450 was predicted as targets for the some of the phytochemical compounds.

Pharmacokinetic effects of the phytochemical compounds on the predicted targets involved in the metabolism of the four PI drugs

Several studies have also shown that both CYP3A4 and P-gp have a wide and overlapping substrate specificity (Konig et al., 2013; Fromm, 2004), as this explained why the four PI drugs are both inhibitors and inducers of CYP3A4 and P-gp respectively. The pharmacokinetic effect of the phytochemicals on CYP3A4 and P-gp revealed that NGN, GER, FST, LUT, APG, PTA and GA are inhibitors of CYP 3A4. Inhibition of CYP3A4 has been reported to decrease the rate of elimination of drugs from the systemic circulation thereby increasing bioavailability of drugs (Liyue et al., 2001). NGN and IST were predicted inducers of P-gp and could increase the rate of elimination of the four drugs thereby lowering PI drugs bioavailability (Richard et al., 2014). Other phytochemical compounds were predicted to be non-inducers of P-gp and could possibly inhibit the activity of P-gp to increase PI drugs bioavailability. Infection of cells by HIV has been reported to increase P-gp expressing and reduction in CD4 count (Andreana et al., 1996) therefore, inhibitors of P-gp and *HIVpro* could eventually lead to increase in CD4 count. The result of this study revealed phytochemical compounds are predicted inhibitors of CYP3A4 and P-gp, and they could

increase the bioavailability of PI drugs in the plasma drug, and also lower the elimination of PIs from the systemic circulation and thereby exerting their therapeutic antiviral effects.

Assessing the Drug-likeness of Phytochemical compounds

One of the important rules in drug design is Lipinski's rule, which is a set of five rules use to assess the drug-likeness of a compound with pharmacological or biological activities with the aim of examining if it possesses both physical and chemical properties to act as an orally active drug in humans (Lipinski, 2004; Lipinski, 2012). The rule centres on the number of hydrogen bond donors in the compound (not more than 5), the number of hydrogen bond acceptors (not more than 10), molecular mass less than 500 daltons and partition coefficient ($\log P$) not greater than 5. The results showed that eight of the phytochemical compounds (EGA, LUT, APG, FST, BIT, GA, IST and NGN) were predicted to pass the rules and would be suitable for oral administration. Interestingly, ATV and DRV, together with the remaining seven compounds failed up to three of the rules.

Gastrointestinal (GIT) absorption is significant for the maintenance of optimal drug levels in the systemic circulation. For drugs or potential compounds to reach their target, they must be absorbed from the GIT and enter the systemic circulation in sufficient quantities (Kremers, 2002). Highly absorbed drugs from the GIT will easily attain optimal concentration and exert a pharmacological effect at its target site. Nine of the fifteen phytochemical compounds were predicted to be highly absorbed from the GIT (EGA, LUT, APG, FST, BIT, GA, IST, NGN, and PTA), Again, it was interesting to note that LPV was the only drug out of the four conventional drugs that had a predicted high GIT absorption rate.

The blood-brain barrier (BBB) is a protection developed by the endothelial cells that line cerebral microvessels (Abbott, 2002; Begley and Brightman, 2011) and drugs or compounds that are not soluble in lipid with molecular weight greater than 400 Dalton cannot go across

the BBB; smaller and lipophilic molecules can go across the BBB (Begley and Brightman, 2011). Therefore, the BBB permeability parameter is always considered in the development of a drug for neuro-degenerated and related diseases. None of the four FDA-approved conventional drugs was predicted to permeate the BBB and only two of the phytochemical compounds (BIT and IST) were predicted to go across the BBB. These compounds are of significant advantage in targeting viral reservoirs inaccessible by other antiviral agents.

Drug bioavailability is a measurement of the degree of absorption and fraction of a given amount of unchanged drug that goes to the systemic circulation (Heaney, 2018). Orally and intravenously administered drugs have different bioavailabilities as a result of some factors like first pass-drug metabolism. It is a significant pharmacokinetic property of the drug that must be carefully thought of when calculating drug dosages. A higher bioavailability score is required for a drug to reach a higher and optimal concentration in the systemic circulation and to exert notable pharmacological response. When compared with the four conventional drugs, EGCG, GER and K7G shared the same bioavailability scores of 0.17 with ATV and SQV. Drugs with lower bioavailability score will not reach optimal concentration in the systemic circulation and will exert little or no pharmacological response.

Thermodynamic binding free energy of Phytochemical compounds to HIVpro

The binding free energy calculated for the four conventional drugs ranges from -35.311±4.943 to -56.056 ± 4.978 kcal/mol, with Atazanavir (ATV) and Darunavir having the highest and the lowest values respectively. Epigallocatechin gallate (EGCG), Kaempferol-7-O-glucoside (K7G), Ellagic acid (EGA) and Luteolin (LUT) indicated the most optimal binding when compared to the FDA approved drugs. It was also interesting to note that although compounds FST, APG and NGN demonstrated relatively high docking scores, binding free energy calculations for these systems indicated dissimilar results. This validates

the need for molecular dynamics simulations, which may allow for a compound to become “comfortable” within an enzyme’s binding site.

Structural Analysis of the Most Optimal Phytochemical compound-HIVpro Complexes

The structural stability of the protein was measured following experimental simulation of the phytochemical compounds together with the protein. Root mean square deviation (RMSD) and root mean square fluctuation (RMSF) were studied in several molecular dynamics studies to study conformational stability of ligands and proteins (Agoni et al., 2018; McGillemie and Soliman, 2015; Munsamy et al., 2018; Ramharack et al., 2017). The deviation produced by a protein during stimulation is a factor determining its stability, and the lower the deviation produced the more stable the protein. Therefore, RMSD, which measures protein stability as the simulation progresses, can be used to determine protein stability. In this study, RMSD values for the C-alpha atoms of the amino acid residues of the protein were determined.

The RMSD of each phytochemical compound was compared to the RMSD values of the four FDA approved drugs. The RMSD plots of three phytochemical compounds (EGCG, EGA and K7G) were similar to the FDA-approved drugs (ATV, SQV and DRV) and apo-enzyme (positive control), showing good enzyme stability. The RMSD value of the LUT (1.843Å) is slightly like that of LPV (2.187), as this mean similar enzyme stability after ligand binding.

The values of the radius of gyration (RoG) were also plotted for each system. RoG is a measure of the compactness of the protein structure. The RoG values of each of the phytochemical compounds were compared to the RoG of the four FDA approved drugs and the apo-enzyme (Figure 3). The four phytochemical compounds shows similarity with the RoG of three of the FDA-approved protease inhibitor drugs (LPV, SQV and ATV) and the apo-enzyme but deviated from the RoG value of DRV. This means similar protein compartment was observe between the three FDA-approved drugs and four compounds and

they could confer the same stability on the protein structure and affect the protein function in a similar way with the three FDA-approved drugs (LPV, SQV and ATV).

The RMSF values monitor the fluctuation of each amino residue as they interact with the ligand throughout the trajectory. The RMSF values of each of the compounds were compared to the RMSF of the four FDA approved drugs (Figure 4). The K7G (1.130) system showed the greatest similarity to the four FDA-approved drugs, with fluctuations occurring at similar residues at 45-55 and 145-155 (mirror residues in the dimeric form). This substantiates the necessity of the dimeric activity of the HIV-protease (Hayashi et al., 2014).

Ligand-HIVpro interactions with different amino acid residues.

As mentioned above, ATV showed the highest free binding energy of the 19 systems. This could possibly be due to the greater number of hydrogen bond interactions produced between the drug and HIVpro amino acid residues (ASP128, GLY126, ASP124, THR179, ALA127, PRO180, GLY49, GLY27, ASP25, and ILE47). The hydrogen bond interactions for SQV, LPV, and DRV are 4, 5 and 4 respectively. A Salt-bridge interaction at amino residue ASP25, together with numerous van der Waals, alkyl, and Pi-alkyl interactions contributed to the SQV-system gaining second highest binding energy. With 20 van der Waals interactions and 5 hydrogen bond interactions, LPV showed higher binding energy than DRV. Of the phytochemical compounds, EGCG demonstrated the highest binding energy. This may have been the result of a salt-bridge interaction at ARG107, 6 hydrogen bond interactions, 13 van der Waals and 3 Pi-alkyl interactions. It was interesting to note that the “two-component” salt-bridges, made up of a hydrogen bond and electrostatic interaction, were only recorded within the EGCG and SQV systems. This could have led to the overall binding energy of EGCG being higher than K7G, despite K7G having a higher overall number of interactions. These similar bond interactions observed and their binding energies that fall within the range

of the binding energies for the FDA-approved drug also make EGA and LUT to be suitable potential inhibitors of *HIVpro*.

Conclusion

The analysis predicted both inhibitors and inducers of CYP3A4 and P-gp among the selected phytochemical compounds. The phytochemical compounds predicted to be inhibitors of CYP3A4 and P-gp could increase the bioavailability of the four FDA-approved drugs in the systemic circulation thereby enhancing the four drugs to exert maximum pharmacological effects. Of all the docked selected phytochemical compounds, EGCG, K7G, EGA, NGN, STG, GER, and LUT gave the best binding score when compared to the four conventional PIs. The results of the MD simulations and MMGBSA showed that only EGCG, K7G, EGA and LUT fit well into the *HIVpro* active site pocket with better binding free energy. The study implied that the ligands interacted hydrophobically with the active amino residues. This study also identified some of the key residues that are helpful in dual inhibitor design. The EGCG and K7G compounds proved to be more potent inhibitors of *HIVpro*. Therefore, this study showed that some of the phytochemical compounds could be utilised to enhance the therapeutic effect of PIs by inhibiting both P-gp and CYP3A4. These phytochemical compounds could as well serve as natural inhibitors of *HIVpro*.

References

- Adewole, E., Ojo, A., Ogunmodede, O. T., Adewumi, D. F., Omoaghe, A. O., & Jamshed, I. 2018. Characterization and Evaluation of *Vernonia amygdalina* Extracts for its Antidiabetic Potentials. *International Journal of Sciences* 4(01):31-38.
- Agoni, C., Ramharack, P., & Soliman, M. E. S. 2018. Co-inhibition as a strategic therapeutic approach to overcome rifampin resistance in tuberculosis therapy: Atomistic insights. *Future Medicinal Chemistry*, 10(14), 1665–1675.
- Babatunde, D. E., Otusemade, G. O., Efevbokhan, V. E., Ojewumi, M. E., Bolade, O. P., & Owoeye, T. F. 2019. PT. *Chemical Data Collections*, 100208.
- Begley, D. J., & Brightman, M. W. 2011. Structural and functional aspects of the blood-brain barrier. *Peptide Transport and Delivery into the Central Nervous System*, 61(5), 39–78.
- Boadu, A.A., Nlooto, M. comparative Chemistry of COA Herbal Medicine and Herbal Extracts of *Veronia mygdalina* (Bitter leaf) and *Persea americana* (Avocado)' unpublished thesis, University of KwaZulu-Natal, Durban, South Africa. 2019.
- Brian, J., Kirby, A.C., Collie, E.D., Kharasch, V., Dixit, P.D., Whittington, K.T., Jashvant, D.U., 2011. Complex drug interactions of HIV protease inhibitors 2 in vivo induction and in vitro correlation of induction of cytochrome P450 1A2, 2B6, and 2C by ritonavir. *Drug Metabolism Disposition*. 3 (12), 2329-2337.
- Brik, A., Wong, C. H. 2003. HIV-1 protease: Mechanism and drug discovery. *Organic and Biomolecular Chemistry*, 1(1), 5–14.
- Burley, S. K., Berman, H. M., Christie, C., Duarte, J. M., Feng, Z., Westbrook, J., ... Zardecki, C. 2018. RCSB Protein Data Bank: Sustaining a living digital data resource that enables breakthroughs in scientific research and biomedical education. *Protein Science*, 27(1), 316–330.
- Calderón-Oliver, M., Medina-Campos, O. N., Ponce-Alquicira, E., Pedroza-Islas, R.,

- Pedraza-Chaverri, J., & Escalona-Buendía, H. B. 2015. Optimization of the antioxidant and antimicrobial response of the combined effect of nisin and avocado byproducts. *LWT - Food Science and Technology*, 65, 46–52.
- Carmona, S., Nash, J. 2017. *Adult antiretroviral therapy guidelines 2017 as per HIV Medicine SAJ*. 18(1), 1–24.
- Daina, A., Michielin, O., Zoete, V. 2017. SwissADME: A free web tool to evaluate pharmacokinetics, drug-likeness and medicinal chemistry friendliness of small molecules. *Scientific Reports*, 7(1), 1–13.
- Dineshkumar, I. A., G., Rajakumar, R. 2017. Gc-MS Evaluation Of Bioactive Molecules From The Methanolic Leaf Extract Of *Azadirachta Indica* (A . Juss). *Asian Journal of Pharmaceutical Science & Technology*.2, 1023-1033.
- Fromm, M.F., 2004. Importance of P-glycoprotein at blood-tissue barriers. *Trends Pharmacology Science*. 2004 (25), 424-429.
- Geretti, A. M., Easterbrook, P. 2001. Antiretroviral resistance in clinical practice. *International Journal of STD and AIDS*, 12(3), 15–153.
- Gfeller, D., et al., 2014. Swiss target prediction a web server for target prediction of bioactive small molecules. *Nucleic Acids Residues*. 42, W32-W38.
- Griffin, L, Annaert, P, Brouwer, K. L. 2011. Influence of drug transport proteins on the pharmacokinetics and drug interactions of HIV protease inhibitors. *Journal. of Pharmaceutical Sciences*. 100 (9): 3636–54.
- Hanwell, M. D., Curtis, D. E., Lonie, D. C., Vandermeersch, T., Zurek, E., & Hutchison, G. R. 2012. Avogadro: An advanced semantic chemical editor, visualization, and analysis platform. *Journal of Cheminformatics*, 4(8), 1–17.
- Hayashi, H., Takamune, N., Nirasawa, T., Aoki, M., Morishita, Y., Das, D., Mitsuya, H. 2014. Dimerization of HIV-1 protease occurs through two steps relating to the

- mechanism of protease dimerization inhibition by darunavir. *Proceedings of the National Academy of Sciences*, *111*(33), 12234–12239.
- Hayes, J.M and Archontis G. 2011. Molecular Dynamic-Studies of Synthetic and Biological Molecules. IntechOpen. Chapter 9.
- Heaney, R. P. 2018. Factors Influencing the Measurement of Bioavailability, Taking Calcium as a Model. *The Journal of Nutrition*, *131*(4), 1344S–1348S.
- Huisman, M.T., Smit, H.R, Wiltshire, R.M., Hoetelmans, J.H., Beijnen, Schinkel, A.H., 2001. P-glycoprotein limits oral availability, brain, and fetal penetration of saquinavir even with high doses of ritonavir. *Molecular Pharmacology*. *59*, 806-813.
- Hurtado-Fernández, E., Pacchiarotta, T., Mayboroda, O. A., Fernández-Gutiérrez, A., & Carrasco-Pancorbo, A. 2014. Quantitative characterization of important metabolites of avocado fruit by gas chromatography coupled to different detectors (APCI-TOF MS and FID). *Food Research International*, *62*, 801–811.
- Igile, G. O., Oleszek, W., Burda, S., & Jurzysta, M. 1995. Nutritional Assessment of Vernonia amygdalina Leaves in Growing Mice. *Journal of Agricultural and Food Chemistry*, *43*(8), 2162–2166.
- Kermanshai, R., McCarry, B. E., Rosenfeld, J., Summers, P. S., Weretilnyk, E. A., & Sorger, G. J. 2001. Benzyl isothiocyanate is the chief or sole anthelmintic in papaya seed extracts. *Phytochemistry*, *57*(3), 427–435.
- Kim, S., Thiessen, P. A., Bolton, E. E., Chen, J., Fu, G., Gindulyte, A., Bryant, S. H. 2016. PubChem substance and compound databases. *Nucleic Acids Research*, *44*(1), 1202–1213.
- Kongkachuichai, R., & Charoensiri, R. I. N. (2010). Carotenoid, flavonoid profiles and dietary fiber contents of fruits commonly consumed in Thailand. *International Journal of Food Science and Nutrition*. 2010. *61*(5):536-48.

- Konig, S. K., Herzog, M., Theile, D., Zembruski, N., Haefeli, W. E., Weiss, J. 2010. Impact of drug transporters on cellular resistance towards saquinavir and darunavir. *J. Antimicrobial Chemotherapy*. 65(11): 2319–2328.
- Kremers, P. 2002. In vitro tests for predicting drug-drug interactions: The need for validated procedures. *Pharmacology and Toxicology*, 91(5), 209–217.
- Lako, J. 2007. Phytochemical flavonols , carotenoids and the antioxidant properties of a wide selection of Fijian fruit , vegetables and other readily available foods. *Food Chemistry*. 101, 1727–1741.
- Levy, Y., Caflisch, A. 2003. Flexibility of monomeric and dimeric HIV-1 protease. *Journal of Physical Chemistry B*, 107(13), 3068–3079.
- Lipinski, C. A. 2004. Lead- and drug-like compounds: The rule-of-five revolution. *Drug Discovery Today: Technologies*, 1(4), 337–341.
- Lipinski, C. A., Lombardo, F., Dominy, B. W., & Feeney, P. J. 2012. Experimental and computational approaches to estimate solubility and permeability in drug discovery and development settings. In *Advanced Drug Delivery Reviews*. 64:4-17.
- Liyue, H., Stephen, A., Wring, J. L., Woolley, K.R., Brouwer, C., Serabjit-Singh, Joseph, W.P. 2001. Induction Of P-Glycoprotein and Cytochrome P450 3A by HIVProtease inhibitors. *Drug Metabolism and Disposition*. Vol. 29, No. 5.p755-760.
- Mcgillewie, L., Soliman, M. E. 2015. Flap flexibility amongst I, II, III, IV, and V: Sequence, structural, and molecular dynamic analyses. *PROTEINS: Structure, Function and Genetics*, 83(9), 1693–1705.
- Monika P, Geetha A. 2015. Effect of hydroalcoholic fruit extract of *Persea americana* Mill. on high fat diet induced obesity: a dose response study in rats. *Indian Journal of Experimental Biology* 54: 370–378.
- Mukhtar, M., Arshad, M., Ahmad, M., Pomerantz, R. J., Wigdahl, B., Parveen, Z. 2008.

- Antiviral potentials of medicinal plants. *Virus Research*. 131, 111–120.
- Munsamy, G., Ramharack, P., & Soliman, M. E. S. 2018. Egress and invasion machinery of malaria: an in depth look into the structural and functional features of the fl ap dynamics of plasmepsin IX and X. *RSC Advances*, 8, 21829–21840.
- Nair, P. C., & Miners, J. O. 2014. Molecular dynamics simulations: from structure function relationships to drug discovery. *In Silico Pharmacology*, 2(4), 1–4.
- Ndhlala, A. R., Stafford, G. I., Finnie, J. F., Van Staden, J. 2011 Commercial herbal preparations in KwaZulu-Natal, South Africa: The urban face of traditional medicine. *South African Journal of Botany*. 77; 830–843
- Nlooto, M., Naidoo, P. 2014. Clinical relevance and use of traditional , complementary and alternative medicines for the management of HIV infection in local African communities, 1989 - 2014 : A review of selected literature. *Botswana Journal of African Studies*. 28(1), 105–116.
- Nwabuife, J. C ‘A comparative chemistry of COA-FS herbal medicine and herbal extracts of *Azadirachta indica* and *Carica papaya*’unpublished thesis, University of KwaZulu-Natal, Durban, South Africa. 2019.
- Ramharack, P., Oguntade, S., & Soliman, M. E. S. 2017. Delving into Zika virus structural dynamics – a closer look at NS3 helicase loop flexibility and its role in drug discovery. *RSC Advances*, 7(36), 22133–22144.
- Rashed, K., Luo, M.-T., Zhang, L. T., Zheng, Y.-T. 2013. Phytochemical Screening of the Polar Extracts of *Carica papaya* Linn . and the Evaluation of their anti-HIV-1 activity. *Journal of Applied and Industrial Sciences*, 1(3), 49–53.
- Richard, C., Frederick, L., Mary, B., 2014. Inhibition of the multidrug resistance P-glycoprotein Time for a change o strategy. *Drug Metabolism Disposition*. 42, 623-631.
- Sajin, A. K., Rathnan, R. K., & Mechoor, A. 2015. Molecular Docking studies on

- phytocompounds from the methanol leaf extract of *Carica papaya* against Envelope protein of dengue virus (type-2). *Journal of Computational Methods in Molecular Design*. 5(2), 1–7.
- Sanjay, U.C., Sankatsing, J.H., Beijnan, A.H., Schinkel, Joep, M.A.L., Jan, M.p., 2004. P-glycoprotein in human immunodeficiency virus type 1 infection and therapy. *Antimicrobial Agents Chemotherapy*. 48 (4), 1073-1081.
- Scholar, E. 2011. HIV protease inhibitors. *The Comprehensive Pharmacology Reference*, pp. 1–4.
- Seifert, E. 2014. OriginPro 9.1: scientific data analysis and graphing software-software review. *Journal of Chemical Information and Modeling*, 54(5), 1552–1552.
- Shin, M. S., Kang, E. H., Lee, Y. I. 2005. A flavonoid from medicinal plants blocks hepatitis B virus-e antigen secretion in HBV-infected hepatocytes. *Antiviral Research*, 67(3), 163–168.
- Siddiqui, B. S., Afshan, F., Arfeen, S. S., Gulzar, T. 2006. A new tetracyclic triterpenoid from the leaves of *Azadirachta indica*. *Natural Product Research*, 20(12), 1036–1040.
- Soontornniyomkij, V., Umlauf, A., Chung, S. A., Cochran, M. L., Soontornniyomkij, B., Gouaux, B., Achim, C. L. 2014. HIV protease inhibitor exposure predicts cerebral small vessel disease. *AIDS*, 28(9), 1297–1306.
- Vaishali, D., Niresh, H., Fang, L.I.P., Desai, K., Thummel, E., Jashvant, D.U., 2007. Cytochrome P450 Enzymes and transporters induced by anti-human immunodeficiency virus protease inhibitors in human hepatocytes Implications on predicting clinical drug interactions. *Drug Metabolism Disposition*. 35 (10), 1473-1477.
- Walubo, A. 2007. The role of cytochrome p450 in antiretroviral drug interactions' *Expert Opin. Drug Metabolism Toxicology*. 3: 583-598.
- WHO, UNAIDS, UNFPA, UNICEF, UNWomen, and The World Bank Group. 2018.

Survive, Thrive, Transform. Global Strategy for Women's, Children's and Adolescents' Health: 2018 report on progress towards 2030 targets. *Geneva: World Health Organization.*

Yang, Z., Lasker, K., Schneidman-Duhovny, D., Webb, B., Huang, C. C., Pettersen, E. F., ... Ferrin, T. E. (2012). UCSF Chimera, MODELLER, and IMP: An integrated modeling system. *Journal of Structural Biology*, *179*(3), 269–278.

Ylilauri, M., Pentikäinen, O. T. 2013. MMGBSA as a tool to understand the binding affinities of filamin-peptide interactions. *Journal of Chemistry, Information and Modeling*, *53*(10), 2626–2633.

CHAPTER FOUR

The published article in chapter three described the pharmacokinetic properties and potential antiviral activities of the selected PCs. The study showed that similar to the PIs (used as standard), some PCs were predicted to be inhibitors and substrates of P-gp and CYP3A4 (drug-metabolizing proteins involved in the metabolism of PIs), and four PCs (epigallocatechin gallate (EGCG), kaempferol-7-glucoside (K7G), luteolin (LUT) and ellagic acid (EGA)) were predicted to be potential inhibitors of South African HIV-1 Sub-type C protease enzyme. In this chapter, the inhibitory potentials of these four PCs, and their molecular mechanisms of inhibiting the two drug-metabolizing proteins, using computational tools were described. The ability of these four PCs to act as inhibitors of drug-metabolism proteins will be beneficial in enhancing the bioavailability and therapeutic effects of PIs.

A manuscript titled 'Molecular Dynamic Mechanism(s) of inhibition of Bioactive Antiviral Phytochemical Compounds targeting Cytochrome P450 3A4 and P-glycoprotein' and has been published by the Journal Biomolecular structure and dynamics (Appendix F).

Molecular Dynamic Mechanism(s) of inhibition of Bioactive Antiviral Phytochemical Compounds targeting Cytochrome P450 3A4 and P-glycoprotein

Abstract

P-glycoprotein (ABCB1) and cytochrome P450 3A4 (CYP3A4) metabolize almost all known human immunodeficiency virus' protease inhibitor drugs (PIs). Over induction of these proteins' activities has been linked to rapid metabolism of PIs which are then pumped out of the circulatory system, eventually leading to drug-resistance in HIV-positive patients. This study aims to determine, with the use of computational tools, the inhibitory potential of four phytochemical compounds (PCs) (epigallocatechin gallate (EGCG), kaempferol-7-glucoside (K7G), luteolin (LUT) and ellagic acid (EGA)) in inhibiting the activities of these drug-metabolizing proteins. The comparative analysis of the MM/GBSA results revealed that the binding affinity (ΔG_{bind}) of EGCG and K7G for CYP3A4 and ABCB1 are higher than LUT and EGA and fall between the ΔG_{bind} of the inhibitors of CYP3A4 and ABCB1 (Ritonavir (strong inhibitor) and Lopinavir (moderate inhibitor)). The structural analysis (RMSD, RMSF, RoG and protein-ligand interaction plots) also confirmed that EGCG and K7G showed similar inhibitory activities with the inhibitors. The study has shown that EGCG and K7G have inhibitory activities against the two proteins and assumes they could decrease intracellular efflux of PIs, consequently increasing the optimal concentration of PIs in the systemic circulation.

Keywords: P-glycoprotein, Cytochrome P450 3A4, protease inhibitor drugs, Computational tools

Introduction

P-glycoprotein (ABCB1) and cytochrome P450 3A4 (CYP3A4) have been reported to play significant roles in the metabolism of many protease inhibitors drugs (PIs). Over induction of ABCB1 and CYP3A4 has been reported to lead to rapid metabolism and elimination of PIs from the systemic circulation, and alter PIs' pharmacokinetics by reducing bioavailability which can result in patients developing resistance to PIs [1, 2].

P-glycoprotein is an essential member of the ATP-binding cassette (ABC) superfamily and is referred to as multidrug resistance proteins 1 (MDR1) as it is the most significant drug transporter in the central nervous system and other tissues. It is essential proteins present in the cell membrane, encoded in humans by the ABCB1 gene [3, 4]. As an ATP-dependent efflux pump, ATP-binding cassette transporters have broad substrate specificity, and their primary role is to pump many potentially toxic substances out of the cells and influence the bioavailability of drugs and other compounds. Evidence suggests that ABC transport proteins caused drug resistance and alter PI pharmacokinetics by reducing bioavailability and decreasing accumulation in organs and tissues [5]. Van Waterschoot *et al.* (2010) reported that all known PIs are substrates of P-glycoprotein [3], and over-expression of P-glycoprotein reduces the concentration of PIs [6]. PIs such as Atazanavir (ATV), Lopinavir (LPV), Amprenavir (AMP) and Ritonavir (RTV) have been reported to be inhibitors of ABCB1 [7-9].

Cytochrome P450 belongs to a superfamily of 25 closely related, membrane bound CYP450 enzymes containing heme as a cofactor. The enzymes can deactivate drugs, either directly or by facilitated elimination from the system, as well as bioactivating several substances to form their active compounds. [10]. CYP3A4 is a subtype of CYP450 and is known to metabolize many of the PIs [11]. Ritonavir was reported to be a strong inhibitors of CYP3A4, decrease

hepatic metabolism and eventually increase the concentration of drugs metabolized by CYP3A4 [11]. Studies have reported substrates overlapping between the two proteins; for example cyclosporin and ritonavir inhibits both proteins), many drug-drug interactions are attributed to either inhibition or induction of both P-glycoprotein and CYP3A4 [6, 7]. This substrate overlapping has prompted many to hypothesize that inhibition of CYP3A4 may be a fundamental characteristic of inhibitors of ABCB1 [6, 12].

In silico determination of potential antiviral activities of phytochemical compounds (PCs) from our laboratory reported that four PCs (epigallocatechin gallate (EGCG), kaempferol-7-glucoside (K7G), luteolin (LUT) and ellagic acid (EGA)) possess inhibitory activities against the HIV-1 protease enzyme similar to the control FDA-approved PIs [13]. Several *in vitro* studies have also reported the inhibitory activities of these four compounds against HIV-1 reverse transcriptase, integrase and protease enzymes' activities [14-17].

One of the limitations of the current antiretroviral therapy (ARV), is the inability of ARVs to reach sanctuary sites of HIV or suboptimal antiretroviral concentrations at these sites in the body (sites such as central nervous system, gut-associated lymphoid tissue, lymph nodes, and tissue macrophages) [18, 19]. This is because many ARVs are substrates of efflux transporters and metabolic enzymes (such as P-glycoprotein and CYP3A4) [19, 20]. Inhibiting the activities of efflux transporters and the metabolism of ARV is an important strategy in increasing the concentrations of ARV. Studies have shown that EGCG and EGA inhibit the activities of ABCB1 and CYP3A4 [21, 22] but, no study has reported on K7G and LUT. Athukuri *et al.* reported in an *in vitro* study that the bioavailability of diltiazem was significantly raised when treated with ellagic acid as a result of inhibition of CYP3A4-mediated drug metabolism and ABCB1-mediated efflux in the intestine, ileum and liver [21]. The study further reported that both the peak plasma concentration (C_{max}) and area under

plasma concentration-time curve (AUC) were improved by the EGA treatment [21]. In a separate study by Shaik and Vanapatla, 2019, EGA through the inhibition of ABCB1 was reported to significantly improve the C_{max} , AUC and increase the bioavailability of oral linagliptin in rats [22]. EGCG at both 3 and 10 mg/kg significantly increase the bioavailability of tamoxifen [23]. The bioavailability of tamoxifen was approximately twice greater than that of the control group and the AUC was significantly increased in the presence of EGCG. The study suggested that the increase in bioavailability of tamoxifen is due to the decrease in first-pass metabolism in the intestine and liver by the inhibition of ABCB1 and CYP3A4 [23].

It is therefore essential to source for natural compounds that can inhibit the activities of these drug-metabolism proteins to boost the bioavailability of PIs in the plasma and sanctuary sites. This study, therefore, investigated the inhibitory potentials of these PCs and their mechanism of inhibiting these PIs-metabolizing proteins (CYP3A4 and ABCB1) using computational tools.

METHODS

P-Glycoprotein Transporter and CYP3A4 Enzyme, Ligand Acquisition and Preparation

The X-ray crystal structures of the P-glycoprotein 1 (PDB code: 6C0V) [24] and CYP3A4 (PDB code: 4NY4 [25]) were obtained from publicly available RSCB Protein Data Bank. The structures of the proteins were then prepared on the UCSF Chimera software package. Two drugs reported to be inhibitors of CYP3A4 and ABCB1, Lopinavir [27, 28], and Ritonavir [28, 29], as well as the four antiviral PCs, were accessed from PubChem [30] and the 3-D structures prepared on the Avogadro software package [31]. The two FDA-approved drugs were used as positive controls.

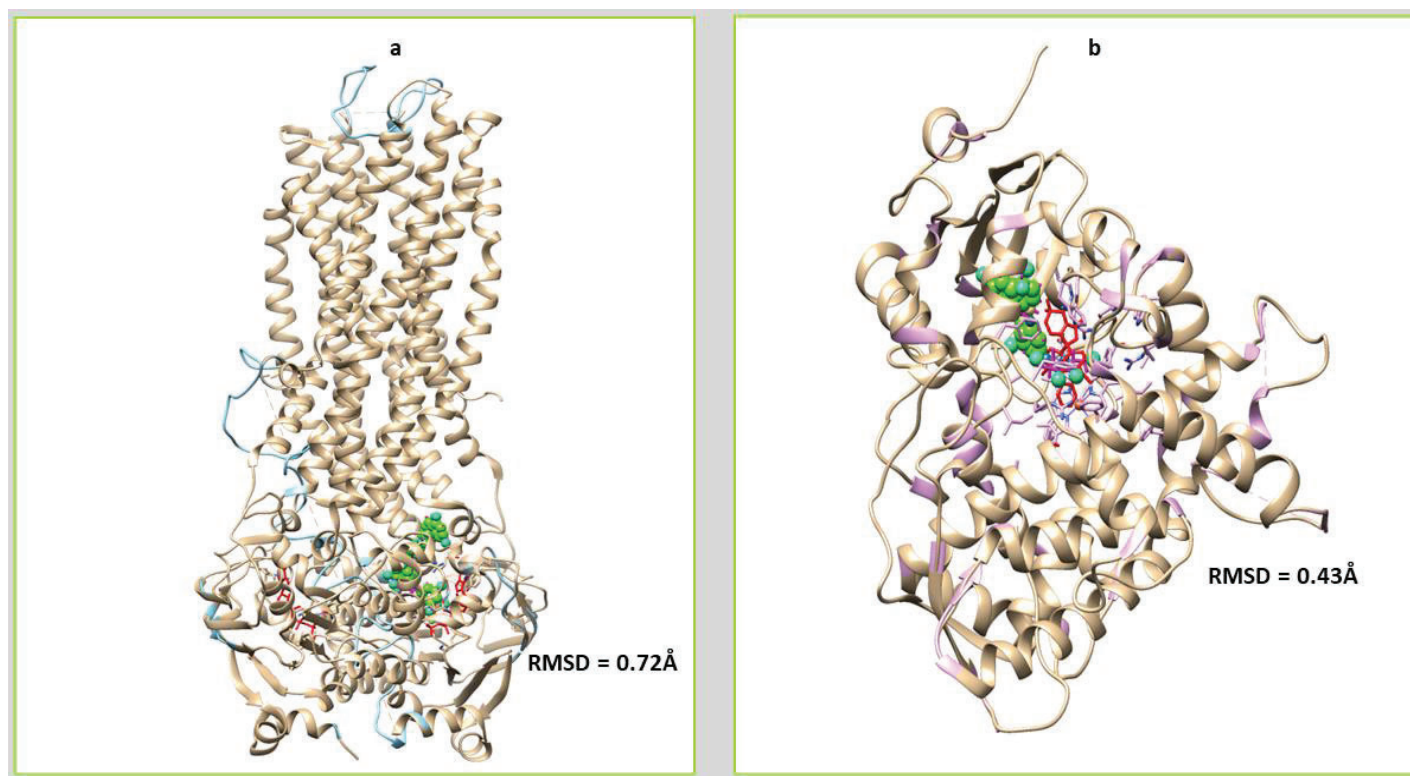


Figure 1. Superpositions of the crystalized structures of the natural substrates (in red) of the proteins and the ligand-complexes (in green). a) ABCB1 b) CYP3A4 and their respective RMSD values.

Molecular Docking

The Molecular docking software utilized in this study was the Autodock Vina Plugin available on Chimera [32], with default docking parameters. The structure of the proteins were prepared removing water molecules, nonstandard naming, protein residue connectivity, missing side-chain or backbone atoms. Gasteiger charges were added to the compounds, and the non-polar hydrogen atoms were merged to carbon atoms. The PCs were then docked into the nucleotide-binding domain pocket of ABCB1 and the active site of CYP3A4 (by defining the grid box with a spacing of 1 Å and size of 106 × 112 × 64 and 52 x 38 x 52 pointing in x, y and z directions respectively). The two FDA-approved drugs (Lopinavir and Ritonavir) systems, as well as the four PCs systems, were then subjected to molecular dynamics simulations. Studies have reported both Lopinavir and Ritonavir to be inhibitors of CYP3A4 and ABCB1 [27-29].

Molecular Dynamic (MD) Simulations

The MD simulation was performed as described by Idowu *et al.*, 2019 [13]. The simulation were performed using the GPU version provided with the AMBER package (AMBER 18), in which the FF18SB variant of the AMBER force field [33] was used to describe the systems.

ANTECHAMBER was used to generate atomic partial charges for the compounds by utilizing the Restrained Electrostatic Potential (RESP) and the General Amber Force Field (GAFF) procedures. The Leap module of AMBER 18 allowed for the addition of hydrogen atoms, as well as Cl⁻ counter ions for neutralization all (both ABCB1 and CYP3A4) systems. The amino acids were numbered, numbering residues 1-1242 for ABCB1 and 1-484 for CYP3A4. The systems were then suspended implicitly within an orthorhombic box of TIP3P water molecules such that all atoms were within 8Å of any box edge [34].

An initial minimization of 2000 steps were carried out with an applied restraint potential of 500 kcal/mol for both solutes, were performed for 1000 steps using the steepest descent method followed by 1000 steps of conjugate gradients. An additional full minimization of 1000 steps were further carried out using the conjugate gradient algorithm without restraint. A gradual heating MD simulation from 0K to 300K was executed for 50ps, such that the systems maintained a fixed number of atoms and fixed volume. The solutes within the systems were imposed with a potential harmonic restraint of 10 kcal/mol and collision frequency of 1.0ps. Following heating, an equilibration estimating 500 ps of each system was conducted; the operating temperature was kept constant at 300K. Additional features such as several atoms and pressure were also kept constant mimicking an isobaric-isothermal ensemble. The system's pressure was maintained at 1 bar using the Berendsen barostat [35, 36].

The total time for the MD simulations conducted were 100ns. In each simulation, the SHAKE algorithm was employed to constrict the bonds of hydrogen atoms [37]. The step size of each simulation was 2fs, and an SPFP precision model was used. The simulations coincided with the isobaric-isothermal ensemble (NPT), with randomized seeding, the constant pressure of 1 bar maintained by the Berendsen barostat [36], a pressure-coupling constant of 2ps, a temperature of 300K and Langevin thermostat [38] with a collision frequency of 1.0ps.

Post-Dynamic Analysis

Analysis of Root mean square deviation (RMSD), Root Means Square Fluctuation (RMSF), Solvent accessible surface area (SASA) and Radius of Gyration (RoG) was done using the CPPTRAJ module employed in the AMBER 18 suit [39]. All raw data plots were generated using the Origin data analysis software [40].

Binding Free Energy Calculations

To estimate and compare the binding affinity of the systems, the free binding energy was calculated using the Molecular Mechanics/GB Surface Area method (MM/GBSA) [41]. Binding free energy was averaged over 100000 snapshots extracted from the 100ns trajectory. The free binding energy (ΔG) computed by this method for each molecular species (complex, ligand, and receptor) can be represented as:

$$\Delta G_{\text{bind}} = G_{\text{complex}} - G_{\text{receptor}} - G_{\text{ligand}} \quad (1)$$

$$\Delta G_{\text{bind}} = E_{\text{gas}} + G_{\text{sol}} - TS \quad (2)$$

$$E_{\text{gas}} = E_{\text{int}} + E_{\text{vdw}} + E_{\text{ele}} \quad (3)$$

$$G_{\text{sol}} = G_{\text{GB}} + G_{\text{SA}} \quad (4)$$

$$G_{\text{SA}} = \gamma \text{SASA} \quad (5)$$

The term E_{gas} denotes the gas-phase energy, which consists of the internal energy E_{int} ; Coulomb energy E_{ele} and the van der Waals energies E_{vdw} . The E_{gas} was directly estimated

from the FF14SB force field terms. Solvation free energy, G_{sol} , was estimated from the energy contribution from the polar states, GGB, and non-polar states, G. The non-polar solvation energy, SA. GSA, was determined from the solvent-accessible surface area (SASA), using a water probe radius of 1.4 Å. In contrast, the polar solvation, GGB, the contribution was estimated by solving the GB equation. S and T denote the total entropy of the solute and temperature, respectively.

Results and Discussions

Stability and Flexibility of proteins apo and bound systems

To discover the dynamic stability of the systems and to evaluate the MD simulations, root-mean-square deviation (RMSD) values of alpha carbon ($C\alpha$) atoms were monitored along the entire MD trajectory for both the apo and the bound systems (Figure 2). RMSD is a measure of system convergence and stability [42] and the deviation produced by a protein during MD simulation is a factor determining its stability; the lower the deviation produced the more stable the protein. As shown in figure 1a-d, the overall RMSD values of the complexes of the four PCs and the two drugs are lower than the RMSD value of the ABCB1 apoenzyme implying that the binding of the ligand brings more stability to the enzyme. The result showed that the binding of inhibitors drastically influences the dynamic of P-glycoprotein, which can be reflected in the function of the protein [43]. Unlike the RMSD pattern observed in the apo and bound systems of ABCB1, the binding of the four ligands raised the RMSD values higher than the value of the apo for CYP3A4, while the values of the two FDA-approved drugs are lower than that of the apo. However, the higher RMSD values observed in the four PCs complexes showed that the binding of ligands does not disrupt the stability of the enzymes (CYP3A4), and the functions of the proteins were not altered.

The radius of gyration (RoG)

Graphical plots of the radius of gyration were plotted for the systems after 100 ns MD simulation. The RoG was carried out to evaluate the overall structural compactness of the systems [44-46]. The plots of RoG for the apoenzymes and the bound ligands for both CYP3A4 and ABCB1 are shown in Figure 3. For the P-glycoprotein complexes, the average values for the RoG of the PCs were compared to the average values of the two FDA-approved inhibitors of the two enzymes. The result showed that the apo has an average value

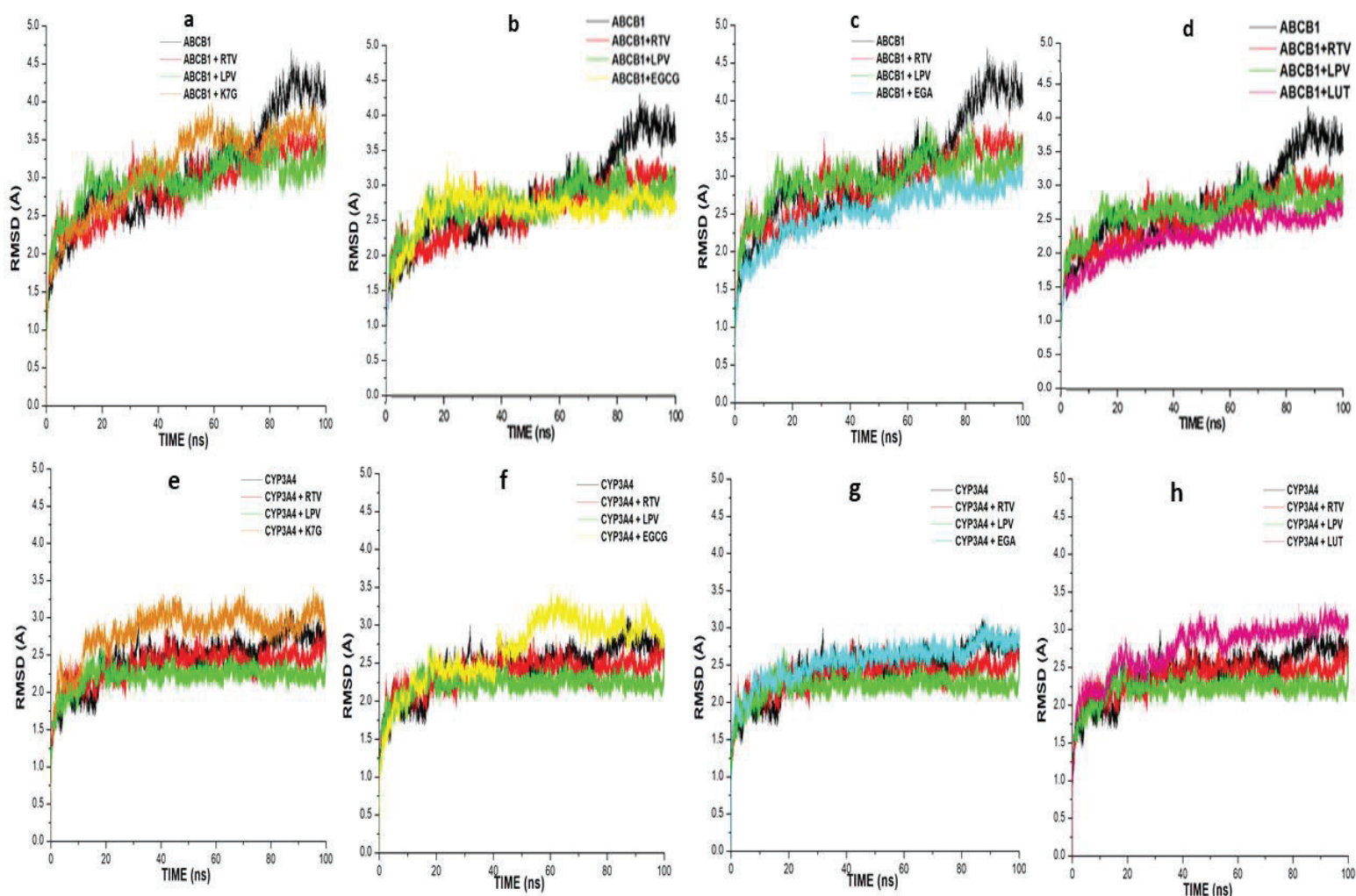


Figure 2: Comparative RMSD profile plots of C-a atoms of the ABCB1, RTV and LPV with ligands, a) K7G, b) EGCG, c) EGA and d) LUT systems and CYP3A4, RTV and LPV with e) K7G, f) EGCG, g) EGA and h) LUT calculated throughout 100 ns molecular dynamics.

of 38.467 Å. Values of 38.012 Å, 38.253, 38.398 Å, 38.501 Å, 38.689 Å and 38.872 Å were recorded for LUT, EGA, EGCG, K7G, LPV and RTV, respectively. K7G showed RoG

values that are most similar to the average values recorded for LPV and RTV. These results suggested that the binding of the three compounds induced conformational changes similar to both LPV and RTV. In complex with the CYP3A4 enzyme, the average RoG values for EGA, apo, RTV, LUT, K7G, EGCG and LPV are 22.862 Å, 23.013 Å, 23.113 Å, 23.232 Å, 23.254 Å, 23.223 Å and 23.652 Å respectively. Similar degrees of structural compactness were observed between RTV and LUT and K7G. The study therefore suggests that conformational changes that occurred in K7G, EGCG and LUT induced a more favourable structural compactness that enhances the stability of the protein in a similar way with RTV.

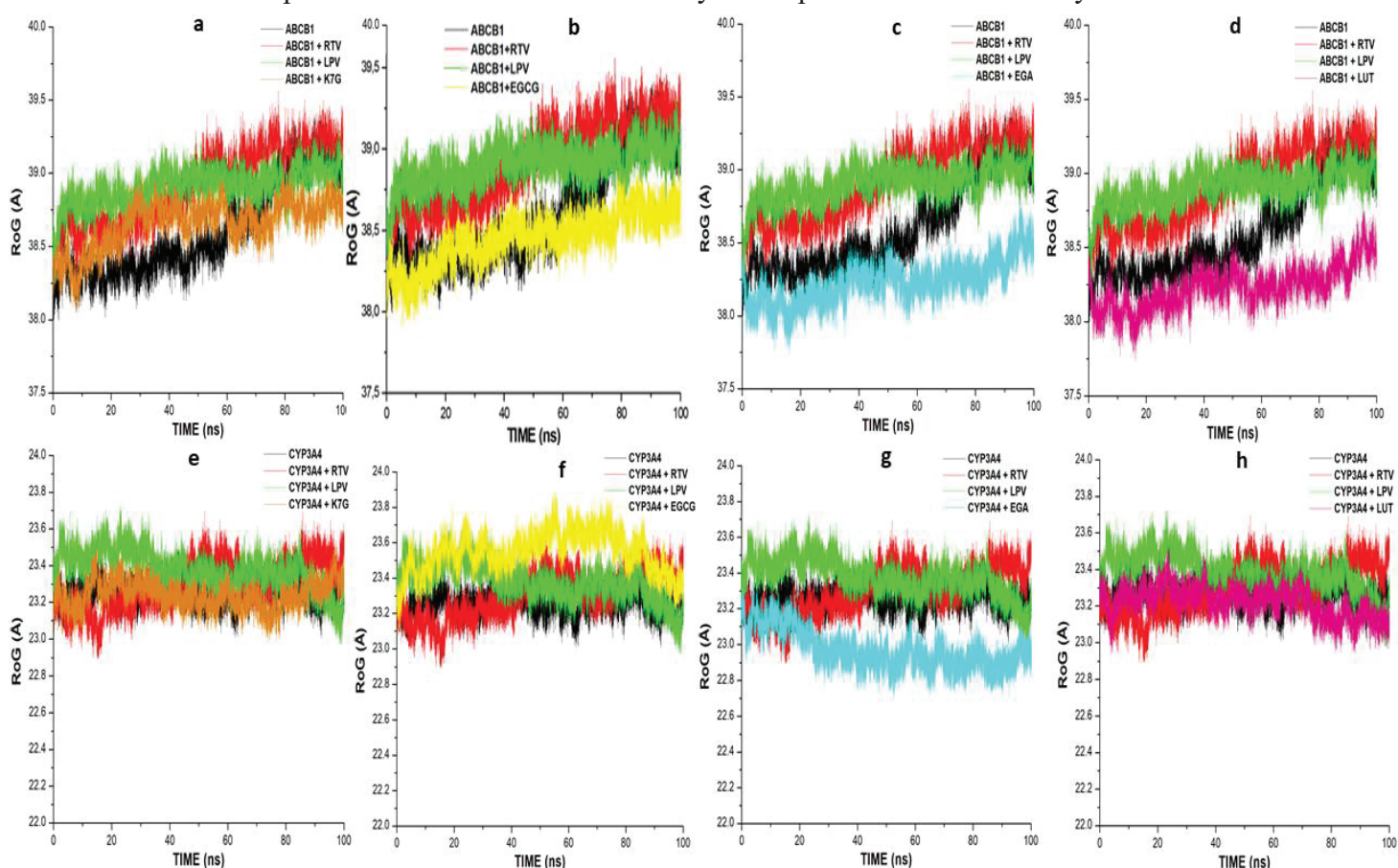


Figure 3: RoG profile of protein backbone atoms calculated throughout 100 ns molecular dynamics of ABCB1 bound RTV, LPV and ligands, a) K7G, b) EGCG, c) EGA and d) LUT and CYP3A4 bound to RTV, LPV and ligands, e) K7G, f) EGCG, g) EGA and h) LUT systems calculated throughout 100 ns molecular dynamics.

RMSF plots (Figure 4) showed the effect of the binding of the ligands on the behaviour of the active residue. Higher fluctuation values indicated more flexible movements, and in contrast, reduced values expressed restricted fluctuations during the simulation [47]. From the RMSF

plots, the apo (ABCB1) showed the overall highest fluctuation value of 5.53 Å. However, the binding of ligands at the active sites of the protein lowered the overall fluctuation values for the respective ligands. This agrees with the study of Pan and Stephen, 2015 that also reported decreased in the RMSF values after ligand binding to ABCB1 [48]. RTV and LPV showed average values of 4.52 Å and 5.11 Å respectively. K7G (4.301 Å) and EGCG (4.33 Å) showed average RMSF values of similar to RTV (4.52 Å). EGA (3.51 Å) and LUT (3.07 Å) showed RMSF values lower than that the recorded values for the two inhibitors (Figure 4a-d). The decrease in fluctuation observed in all the compounds strongly indicated that their binding lowered dynamic residual fluctuations of the enzyme, thus inducing stability of the complex state [39, 47].

Figure 4e-h showed the RMSF plots of both the apo and the bound systems of CYP3A4. Similar protein fluctuation and flexibility were observed in the CYP3A4 system when compared to the P-gp. Generally, higher fluctuation and flexibility in the amino acid residues 140 – 240 was observed in all the PCs and the two drugs bound systems of CYP3A4, and the average fluctuation values for all the ligands (RTV 4.43 Å, LPV 3.4 Å, K7G 4.5 Å, EGCG 4.34 Å, EGA 4.43 Å and LUT 4.23 Å) are lower than the Apo values (5.77 Å). When compared with the two inhibitors, K7G, EGCG, LUT and EGA showed similar RMSF values with RTV.

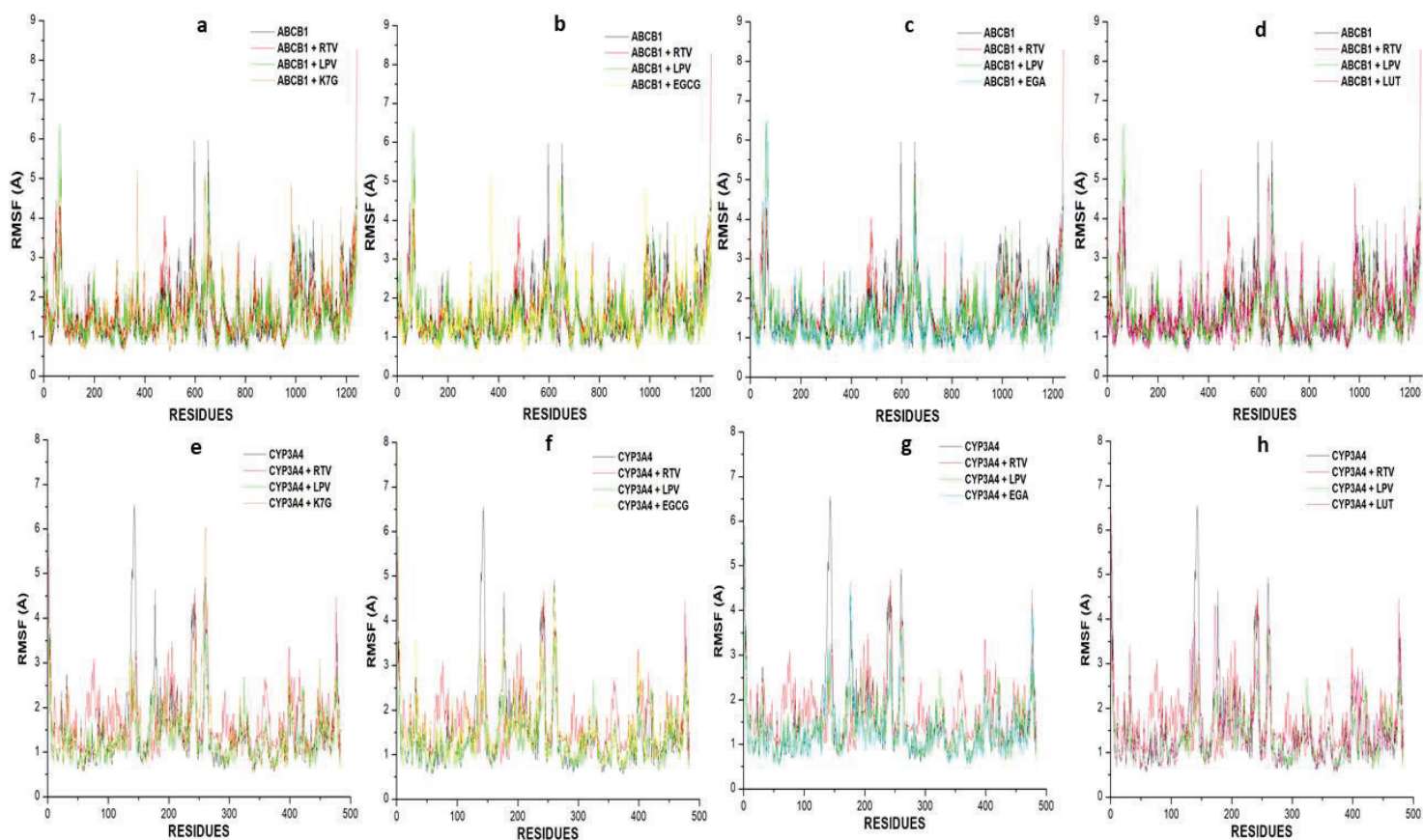


Figure 4: Comparative RMSF plots of Residue-based average C-a fluctuations of the apo (ABCB1), and bound with RTV, LPV and ligands, a) K7G, b) EGCG, c) EGA and d) LUT and CYP3A4 bound to RTV, LPV and ligands, e) K7G, f) EGCG, g) EGA and h) LUT systems calculated throughout 100 ns molecular dynamics.

Solvent Accessible Surface Area (SASA)

In addition to the RMSD, RoG and RMSF plots, SASA is also a vital parameter to examine the impact of the binding of the different ligands to the two enzymes (CYP3A4 and ABCB1). The SASA quantifies the enzyme exposure to solvent molecules [49].

In the ABCB1 system (Figure 5a-d), the average SASA values for EGA, LUT, APO, LPV, RTV, K7G and EGCG were $45,333.53 \text{ \AA}^2$, $45,8212 \text{ \AA}^2$, $46,333.63 \text{ \AA}^2$, $47,500.00 \text{ \AA}^2$, $47,8333.33 \text{ \AA}^2$, $48,166.67 \text{ \AA}^2$ and $48,723.73 \text{ \AA}^2$ respectively. Decline in the exposure of LPV (at approximately 20 ns), and both EGCG and K7G (at approximately 60 ns) was observed, followed by consistent exposure to the solvent molecules. This is an indication that the structural integrity of the protein was altered after 20 ns for LPV and 60 ns for both EGCG and K7G respectively. However, the progressive increase in the SASA plots after 20 ns for

LPV and stable plots for EGCG and K7G, indicated that the enzyme structural integrity is not altered [49]. When compared to the inhibitors, EGCG and K7G showed more similarity in

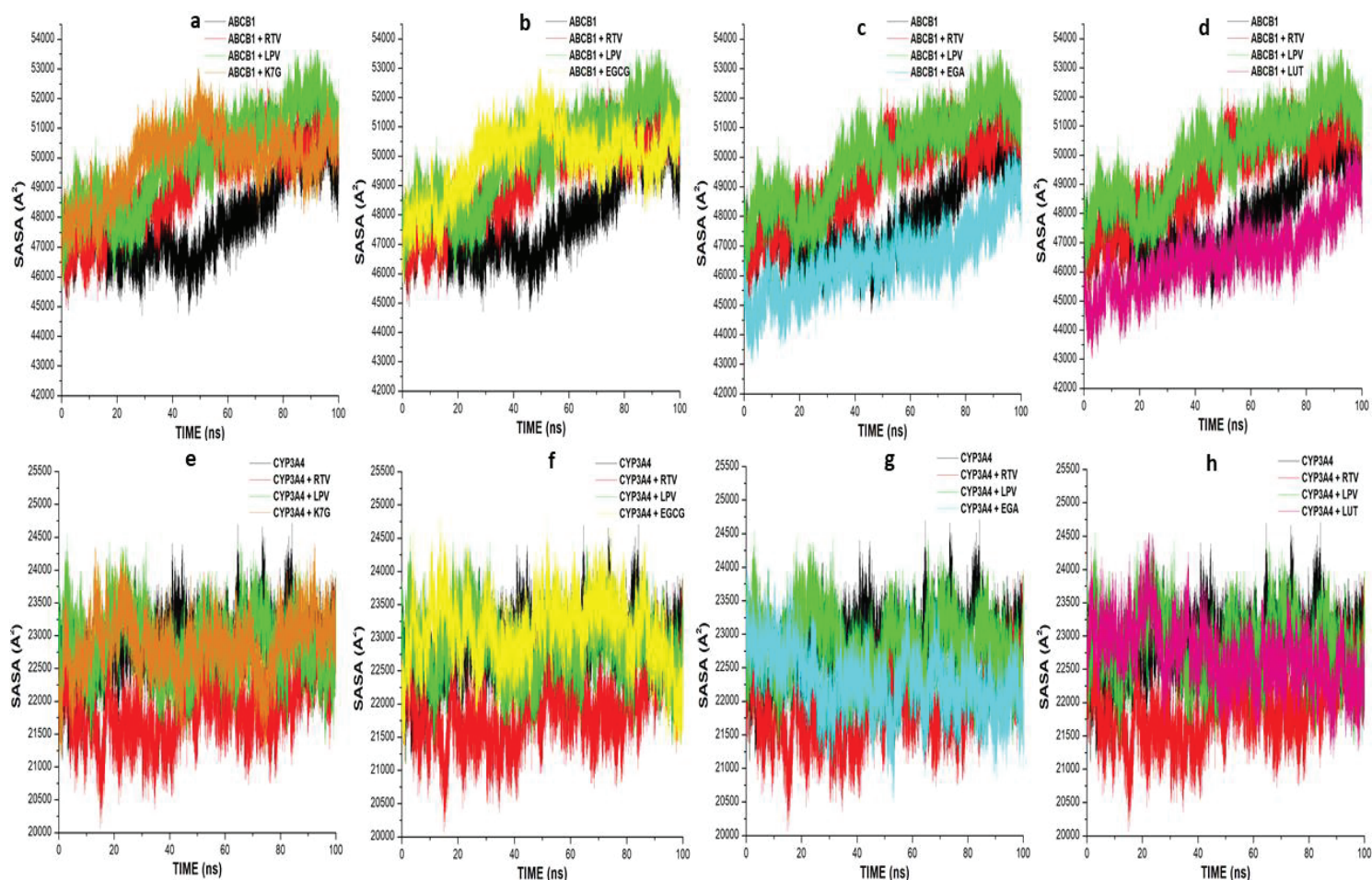


Figure 5: Solvent accessible surface area of apo (ABCB1) RTV, LPV and ligands, a) K7G, b) EGCG, c) EGA and d) LUT, and CYP3A4 bound to RTV, LPV and ligands, e) K7G, f) EGCG, g) EGA and h) LUT systems calculated throughout 100 ns molecular dynamics.

SASA values with both RTV and LPV. In the CYP3A4 systems (Figure 5e-h), EGA ($22,000.00 \text{ \AA}^2$) shows the average SASA values similar to RTV ($21,833.33 \text{ \AA}^2$), while EGCG ($22,821.33 \text{ \AA}^2$), K7G ($22,333.33 \text{ \AA}^2$) and LUT ($22,166.62 \text{ \AA}^2$) showed similar values with LPV ($22,333.33 \text{ \AA}^2$).

Table 1. Thermodynamic Binding Free Energy for PCs and Inhibitors of ABCB1 and CYP3A4

Energy Components (kcal/mol)					
P-gp (ABCB1)					
Complex	ΔE_{vdw}	ΔE_{elec}	ΔG_{gas}	ΔG_{solv}	ΔG_{bind}
Inhibitors					
RTV	-64.77±5.04	-31.62±9.99	-71.39±13.32	36.07±9.21	-60.33±5.52
LPV	-65.42±4.74	-40.37±5.98	-105.79±6.73	60.92±5.87	-44.87±4.02
Phytochemical Compounds					
EGCG	-51.36±4.60	-84.47±9.55	-135.83±8.56	72.89±5.41	-52.94±5.73
K7G	-58.39±5.63	-47.27±12.30	-100.66±14.85	62.66 ±8.36	-42.01±3.86
EGA	-38.61±4.84	-31.32±18.94	-69.93±15.81	40.19±8.93	-29.73 ± 8.02
LUT	-35.66±3.37	-18.26±9.16	-53.92±10.34	29.01±5.40	-24.92±5.85
CYP3A4					
Inhibitors					
RTV	-81.94±4.98	-36.21±8.22	-122.15±10.89	47.97±4.38	-70.188±5.28
LPV	-66.94±4.31	-23.15±8.69	-90.09±9.88	44.79±6.14	-43.299±5.80
Phytochemical Compounds					
EGCG	-53.21±4.09	-73.97±11.42	-126.18±10.84	73.97±5.66	-54.21±4.42
K7G	-50.32±4.39	-57.43±11.76	-105.75±11.01	60.98±7.65	-48.77 ± 4.23
EGA	-39.54±3.31	-38.63±11.53	-76.16±10.28	33.95±5.72	-46.21± 3.32
LUT	-36.97±3.19	-25.85±5.30	-62.82±5.71	26.34±4.32	-36.47± 3.03

Thermodynamic binding free energy of the inhibitor drugs and PCs to CYP3A4 and ABCB1

After the 100 ns MD simulation, the binding free energy (ΔG_{bind}) was calculated using the MM/GBSA method. The MM/GBSA calculations have been widely used to evaluate the total binding energy of compounds to protein [41, 50-54]. From the MD trajectory analysis, the affinity of a ligand to a protein is computed. The binding energies of all the ligands (both the conventional drugs and compounds) were calculated, to understand the inhibitory potentials of the ligands (Table 1).

RTV, a potent inhibitor of both CYP3A4 and ABCB1 showed the highest ΔG_{bind} of -60.326 kcal/mol and -70.188 kcal/mol ABCB1 and CYP3A4, respectively. This was expected as RTV has been reported to be a potent inhibitor of both proteins and is currently used in combination with HIV PIs [55]. EGCG has the second highest ΔG_{bind} of -52.941 kcal/mol and -54.207 kcal/mol in ABCB1 and CYP3A4, respectively. The two ΔG_{bind} values recorded in both CYP3A4 and ABCB1 are higher than the binding energies calculated for LPV in both CYP3A4 and ABCB1, which is an indication that EGCG might be useful as an inhibitor of the two drug-metabolising proteins. There is little difference in the ΔG_{bind} of LPV (-44.874) and K7G (-42.001) in ABCB1 complex; however, in CYP3A4 K7G (-48.769) binding energy was higher than LPV (-43.299). EGA and LUT have ΔG_{bind} values far lower than RTV and LPV in ABCB1 complexes. These binding energy values might suggest that EGCG and K7G could inhibit the activities of both CYP3A4 and ABCB1 at levels better than LPV. RTV was reported to be a stronger inhibitor of ABCB1 and CYP3A4 than LPV (moderate inhibitor); None of the PCs showed binding energies as high as RTV, however since they display qualities of a moderate inhibitor, their use in ARV therapy to increase plasma concentrations warrants further investigation.

Protein-Ligand interaction with ABCB1 and CYP450 3A4

To further establish the mechanistic inhibitory characteristics of the four phytochemical compounds, protein-ligand interaction plots were assessed. Figure 6 showed the amino acid residues at the nucleotide binding domain (NBD) of ABCB1 (figure 6A) and the catalytic site of CYP3A4 (figure 6B).

Protein-ligand interaction has been used widely to examine the molecular interactions between residues at the active sites of a protein and bound ligands [13, 56-58]. The effect of the binding of the different ligands on ABCB1 and CYP3A4 was analysed and the

interactions between the critical residues at the binding sites in the presence of the two known inhibitors (RTV and LPV) and the four tested PCs was plotted. Figures 7 and 8 not only shows a 2D visualisation of the interactions between the ligands and the proteins, but also showed different types of interactions observed in the protein-ligand plots. Interactions such as hydrogen bond, ionic interaction, π -Sulfur, π -cation interaction, and Van der Waals (vdW) overlaps can be observed.

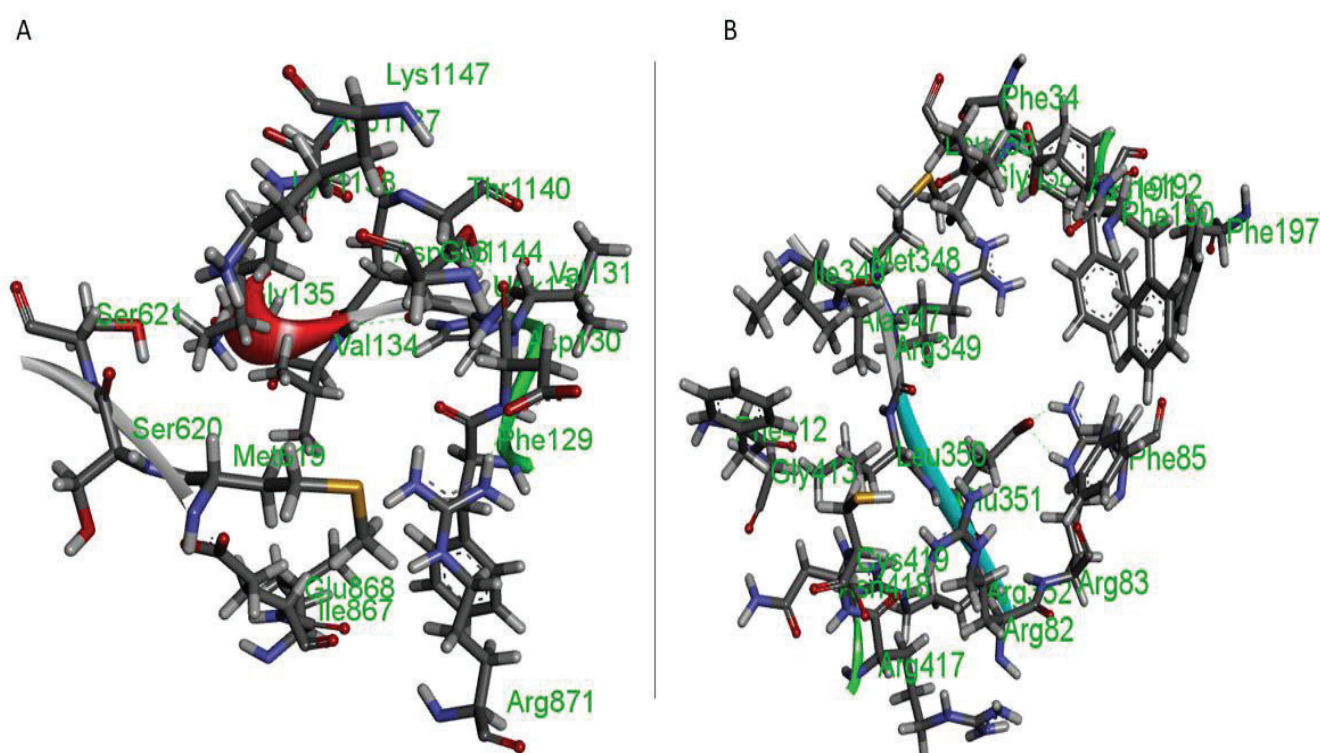


Figure 6: Amino acid Residues at the NBD of ABCB1 (A) and catalytic site of CYP3A4 (B).

In P-glycoprotein (ABCB1) apo and bound systems (Figure 7), more interactions were observed in RTV (24) than LPV (22) and the tested PCs (EGA 12, LUT 13, K7G 18 and EGCG 20). This correlates with the highest binding free binding energy recorded for RTV (Table 1). LPV only showed similar types of interactions with RTV at amino residues Leu1141, Val1135 and Lys1134, however there were less number of interactions in total amino residues in LPV when compare with RTV, which also correlates with the lower binding energy recorded for LPV when compared with RTV.

K7G and LUT showed similar type of interactions with LPV at amino residues Glu868, Val134, Thr1140, Asp130, Ile867, Phe870, Phe129, Hie132 and Asp1137. At residues Cys397, Leu1142, Ser1143, Gly396, Ile375 and Tyr367, EGA showed similar interactions with RTV. EGCG showed no similarity in protein-ligand interactions with LPV, however, it showed some similarity with RTV at amino acid residues Thr367, Gln1141 and Leu1142, suggesting that EGCG and EGA inhibit ABCB1 in a related mechanism to RTV.

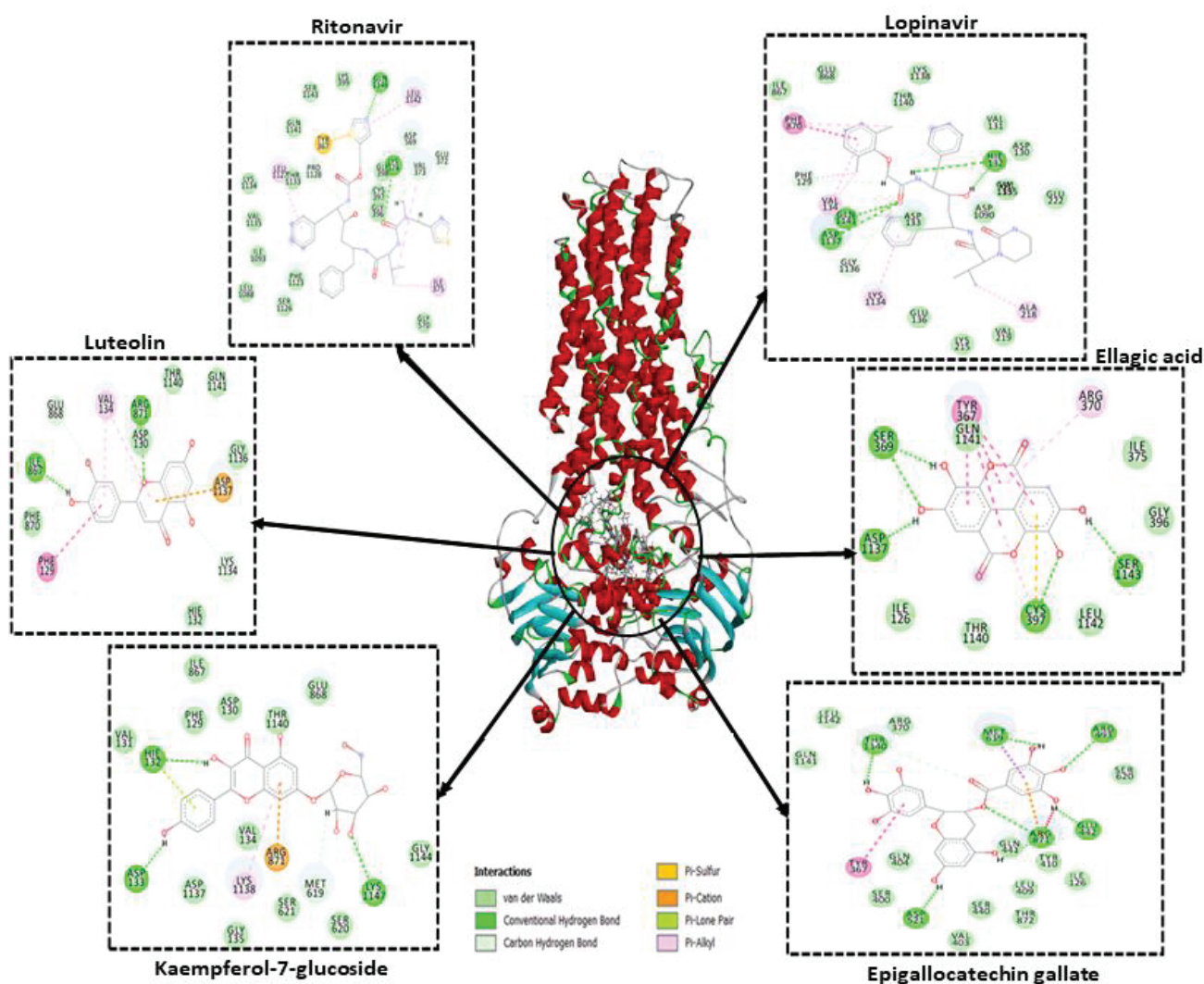


Figure 7: Representation of Protein (ABCB1)-ligand interactions plots with different amino acid residues.

As shown in Table 1, RTV has the highest free binding energy, higher than LPV and the four PCs complexes. This is due to the number and type of interactions between the individual RTV and the active site amino acids of the CYP3A4 (Figure 8). As shown in the ligand-

protein interaction plots, there is a total of 28 interactive bonds (19 hydrogen and Van der Waal bonds, 2 Pi-cation bonds, 6 Pi-alkyl bonds and 1 Pi-Pi bond) between RTV and the active site amino residues of CYP3A4. These bonds significantly contributed to its over-all binding energy.

RTV has the highest number of interactions, higher than EGCG (22 bonds), K7G (18 bonds), LUT (18 bonds) and EGA (12 bonds). While K7G and LUT showed the same number of bonds (18 bonds) they showed different binding affinity (-48.769 kcal/mol and -46.214 kcal/mol, respectively). This can be attributed to two pi-cation bonds in K7G compared to one Pi-cation bond in LUT. Similar interactions were observed at amino acid residues Phe34, Arg82, Phe85, Arg189, Phe192, Phe281, Ala282, Ile346, Met348, Arg349, Leu350, Glu351, Gly413, Asn418 and Gly458 between LPV and RTV. The four PCs showed some similarity in term of interactions with both inhibitors: K7G (Phe34, Arg82, Phe85, Arg189, Phe192 and Phe281 for LPV and Arg83, Phe190, Phe218 and Thr286 for RTV), EGCG (Arg82, Phe192, Ile346, Phe34, Phe85, Met348, Arg349, Leu350, Glu351, Gly413, Asn418 and Gly458 for LPV and Phe34, Arg82, Arg83, Phe85, Phe192, Ile346, Ala347, Met348, Arg349, Leu350, Glu351, Arg352, Phe412, Gly413, Arg417, Asn418, Cys419 and Gly458 for RTV). The interaction plot showed that EGCG has similar type of interactions with RTV than LPV. This therefore suggests that it could inhibit CYP3A4 in similar way with RTV. The numbers of interactions of LUT and EGA with CYP3A4 are lower than that of RTV and LPV, however, the they showed some similar interactions (Phe34, Arg82, Arg83, Phe85, Ser96, Ile97, Phe190, Phe192, Arg349 and Glu351) with the two inhibitors, indicating they could be moderate inhibitors of CYP3A4.

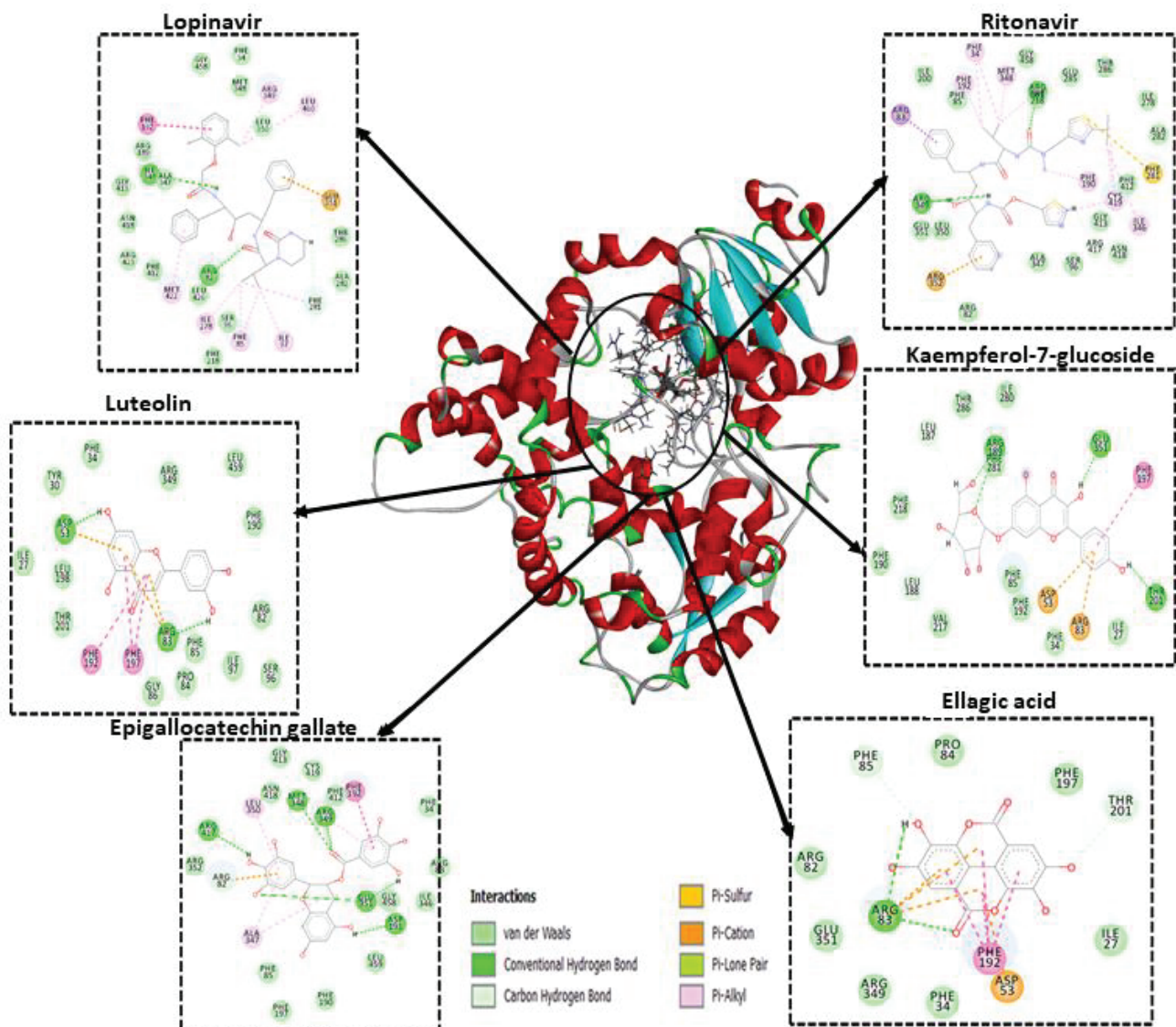


Figure 8: Representation of Protein (CYP3A4)-ligand interaction plots with different amino acid residues.

Conclusion

P-glycoprotein and CYP3A4 have been reported to play essential roles in controlling plasma concentrations of drugs, and their absorption and excretion. The inhibitory potentials of four phytochemical compounds and their mechanism(s) of inhibiting ABCB1 and CYP3A4 enzymes were examined using a combination of MD simulation and MM/GBSA free energy calculations. The MM/GBSA binding free energies showed that the binding energies (ΔG_{bind}) of both EGCG and K7G for the two proteins (ABCB1 and CYP3A4) are higher than LUT and EGA and fall between the ΔG_{bind} of the standard inhibitors (RTV and LPV) of both

proteins. Structural analysis of the bound systems and the apo of the two proteins also confirmed that the binding of the compounds (EGCG and K7G) at the active sites of the two proteins does not alter the structural integrity of the proteins. The results further showed that there are similar interactions between the drugs and the compounds, suggesting potential inhibitory similarities between the drugs and compounds. This study suggests that EGCG, EGA and K7G showed more similarity with RTV in their interaction with CYP3A4. While similar interactions were observed between K7G and LPV, and EGCG and RTV respectively in P-glycoprotein systems. This result suggests that EGCG and K7G might be a suitable substitute for RTV in its use as a booster for HIV protease drugs. And eventually increase the optimal concentration of PIs in the systemic circulation by inhibiting the clearance and the rate of metabolism of PIs from the circulating system thereby, enhancing the therapeutic effect of the PI drugs.

References

1. Weiss, J., Rose, J., Storch, Ch., Ketabi-Kiyanvash, N., Sauer, A., Haefeli, W. *Modulation of human BCRP (ABCG2) activity by anti-HIV drugs*. J. Antimicrob. Chemother., 2007. 59(2): p. 238-45.
2. Liyue, H., Stephen, A., Wring, J. L., Woolley, K. R., Brouwer, C., Serabjit-Singh, Joseph, W. P. *Induction of P-glycoprotein and Cytochrome P450 3A by HIV proteaseinhibitors*. Drug Metab. Dispos., 2001. 29(5):754-60.
3. Van Waterschoot, R., Ter Heine, R., Wagenaar, E., Van Der Kruijssen, C., Rooswinkel, R., Huitema, A., Beijnen, J., Schinkel, A. *Effects of cytochrome P450 3A (CYP3A) and the drug transporters Pglycoprotein (MDR1/ABCB1) and MRP2 (ABCC2) on the pharmacokinetics of lopinavir*. Br. J. Pharmacol., 2010. 160(5):1224–1233.

4. Dhananjay, P., Deep, K., Mukul, M., Durga, K., Paturi, B., and Ashim, K. M. *Efflux transporters and cytochrome P-450-mediated interactions between drugs of abuse and antiretrovirals*. 2011. *Life Sci.*, 2011; 88(21-22): 959–971.
5. Weiss, J. and Haefeli, W.E. *Impact of ATP-Binding Cassette Transporters on Human Immunodeficiency Virus Therapy*. 2010. 219-279.
6. Konig, J., Muller, F., Fromm, M. F. *Transporters and drug-drug interactions: Important determinants of drug disposition and effects*. *Pharmacol. Rev.* 2013. 65:944-66.
7. Fromm, M. F., *Importance of P-glycoprotein at blood-tissue barriers*. *Trends Pharmacol. Sci.*, 2004. 25(8): p. 423-9.
8. Janneh, O., Jones, E., Chandler, B., Owen, A., Khoo, S. H. *Inhibition of P-glycoprotein and multidrug resistance-associated proteins modulates the intracellular concentration of lopinavir in cultured CD4 T cells and primary human lymphocytes*. *J. Antimicrob. Chemother.*, 2007. 60(5): p. 987-93.
9. Bierman, W., George, L., Scheffer, A. S., Gerrit, J., Michiel, A. A., Sven, A. D., Rik, J. S. *Protease inhibitors atazanavir, lopinavir and ritonavir are potent blockers, but poor substrates, of ABC transporters in a broad panel of ABC transporter-overexpressing cell lines*. *Antimicrob. Chemother.*, 2010. 65: 1672 –1680.
10. Danielson, P. B. *The Cytochrome P450 Superfamily: Biochemistry, Evolution and Drug Metabolism in Humans*. *Curr. Drug Metab.*, 2002, 3, 561-597.
11. Walubo, A. *The role of cytochrome p450 in antiretroviral drug interactions*. *Expert Opin. Drug Metab. Toxicol.*, 2007. 3: 583-598.
12. Pan, L., Aller, S. G. *Equilibrated Atomic Models of Outward-Facing P-glycoprotein and Effect of ATP Binding on Structural Dynamics*. *Sci. Reports*. 2015.5(1), 343-355.
13. Idowu, K., Ramharack, P., Nlooto, M., Gordon, M. *The pharmacokinetic properties of HIV-1 protease inhibitors: A computational perspective on herbal phytochemicals*. *Heliyon*, 2019. 5(10): p. e02565.

14. Mahmood, N., Sonia, P., Cosimo, P., Andrew, B., Adil, I. K., and Alan, J. H. *The Anti-HIV Activity and Mechanisms of Action of Pure Compounds Isolated from Rosa Damascena*. *Biochem. and Biophys. Res. Comm.*, 1996. 229 (1): 73–79.
15. Yamaguchi, K., Mitsuo, Honda, H. I., Yukihiro, H. and Tadakatsu, S. *Inhibitory Effects of (-)-Epigallocatechin Gallate on the Life Cycle of Human Immunodeficiency Virus Type 1 (HIV-1)*. *Antiviral Res.* 2002. 53 (1): 19–34.
16. Tripoli, E., Maurizio, L., Santo, G., Danila, D., and Marco, G. *Food Chemistry Citrus Flavonoids : Molecular Structure , Biological Activity and Nutritional Properties: A Review*. *Food chem.* 2007. 104: 466–79.
17. Yang, Z. F., Bai, L., Wen, B. H., Xu, Z. L., Sui, S. Z., Nan, S. Z. and Zhi, H. J. *Comparison of in Vitro Antiviral Activity of Tea Polyphenols against Influenza A and B Viruses and Structure-Activity Relationship Analysis*. *Fitoterapia.* 2014. 93: 47–53.
18. Varatharajan, L., Thomas, S. A. *The transport of anti-HIV drugs across blood–CNS interfaces: Summary of current knowledge and recommendations for further research*. *Antiviral Res.*, 2009.82(2), A99–A109.
19. Cory, T. J., Schacker, T. W., Stevenson, M., Fletcher, C. V. *Overcoming pharmacologic sanctuaries*. *Curr. Opin. HIV/AIDS.* 2013. 8(3):190–195.
20. Loscher, W., Potschka, H. *Role of drug efflux transporters in the brain for drug disposition and treatment of brain diseases*. *Prog. Neurobiol.*, 2005. 76, 22–76.
21. Athukuri, B. L., and Neerati, P. *Enhanced Oral Bioavailability of Diltiazem by the Influence of Gallic Acid and Ellagic Acid in Male Wistar Rats: Involvement of CYP3A and P-gp Inhibition*. *Phytotherapy.* 2017. 31:1441–8.
22. Shaik, M., and Vanapatla, S. R. *Enhanced oral bioavailability of linagliptin by the influence of gallic acid and ellagic acid in male Wistar albino rats: involvement of p-glycoprotein inhibition*. *Drug Metab. and Personalized Ther.* 2019. 34(2).
23. Shin, S. C., Choi, J. S. *Effects of epigallocatechin gallate on the oral bioavailability and pharmacokinetics of tamoxifen and its main metabolite, 4-hydroxytamoxifen, in rats*. *Anti-Cancer Drugs*, 2009. 20(7), 584–588.

24. Kim, Y., Chen, J. *Molecular structure of human P-glycoprotein in the ATP-bound, outward-facing conformation*. *Sci.*, 2018. 359: 915-919.
25. Branden, G., Sjogren, T., Schnecke, V., Xue, Y. *Structure-based ligand design to overcome CYP inhibition in drug discovery projects*. *Drug Discov. Today*. 2014. 19: 905-911.
27. Weemhoff, J. L., von Moltke, L. L., Richert, C., Hesse, L. M., Harmatz, J. S., Greenblatt, D. J. *Apparent mechanism-based inhibition of human CYP3A in-vitro by lopinavir*. *J. Pharm. Pharmacol.*, 2003. 55(3): p. 381-6.
28. Storch, C. H., Theile, D., Lindenmaier, H. *Comparison of the inhibitory activity of anti-HIV drugs on P-glycoprotein*. *Biochem. Pharmacol.*, 2007. 73(10): p. 1573-81.
29. Drewe, J., Gutmann, H., Fricker, G. *HIV protease inhibitor ritonavir: a more potent inhibitor of P-glycoprotein than the cyclosporin analog SDZ PSC 833*. *Biochem. Pharmacol.*, 1999. 57; 1147–52.
30. Kim, S., Thiessen, P. A., Bolton, E. E., Chen, J., Fu, G., Gindulyte, A., Bryant, S. H. *PubChem substance and compound databases*. *Nucleic Acids Res.*, 2016. 44(1), 1202–1213.
31. Hanwell, M. D., Curtis, D. E., Lonie, D. C., Vandermeersch, T., Zurek, E., and Hutchison, G. R. *Avogadro: An advanced semantic chemical editor, visualization, and analysis platform*. *J. of Chem.*, 2012. 4(8), 1–17.
32. Yang, Z., Lasker, K., Schneidman-Duhovny, D., Webb, B., Huang, C. C., Pettersen, E. F., Ferrin, T. E. *UCSF Chimera, MODELLER, and IMP: An integrated modeling system*. *J. of Struct. Biol.*, 2012. 179(3), 269–278.
33. Nair, P. C., Miners, J. O. *Molecular dynamics simulations: from structure function relationships to drug discovery*. *In Silico Pharmacol.*, 2014. 2(4), 1–4.
34. Jorgensen, W. L., Chandrasekhar, J., Madura, J. D., Impey, R. W., and Klein, M. L. (1983). *Comparison of simple potential functions for simulating liquid water*. *The J. of Chem. Phys.*, 79(2), 926–935.

35. Gonnet, P., *P-SHAKE: A quadratically convergent SHAKE* in. *J. of Comp. Phy.*, 2007. 220(2): p. 740-750.
36. Basconi, J. E., & Shirts, M. R. (2013). *Effects of Temperature Control Algorithms on Transport Properties and Kinetics in Molecular Dynamics Simulations*. *J. of Chem. Theory and Comput.*, 9(7), 2887–2899.
37. Ryckaert, J.-P., Ciccotti, G., & Berendsen, H. J. . (1977). *Numerical integration of the cartesian equations of motion of a system with constraints: molecular dynamics of n-alkanes*. *J. of Comput. Phy.*, 23(3), 327–341.
38. Izaguirre, J. A., Catarello, D. P., Wozniak, J. M., & Skeel, R. D. (2001). *Langevin stabilization of molecular dynamics*. *The J. of Chem. Phy.*, 114(5), 2090–2098.
39. Shunmugam, L. and Soliman, M. E. *Targeting HCV polymerase: a structural and dynamic perspective into the mechanism of selective covalent inhibition*. *RSC Advances*, 2018. 8(73): p. 42210-42222.
40. Seifert, E. *OriginPro 9.1: scientific data analysis and graphing software-software review*. *J. of Chem. Inform. and Modeling*. 2014. 54(5), 1552–1552.
41. Ylilauri, M., Pentikäinen, O. T. *MMGBSA as a tool to understand the binding affinities of filamin-peptide interactions*. *J. of Chem. Info. and Modeling*, 2013. 53(10), 2626–2633.
42. Hess, B. *Convergence of sampling in protein simulations*. *Phys. Review*. 2002.65(3).
43. Shekari, F., Sadeghpour, H., Javidnia, K., Saso, L., Nazari, F., Firuzi, O., Miri, R. *Cytotoxic and multidrug resistance reversal activities of novel 1, 4-dihydropyridines against human cancer cells*. *Euro. J of pharmacol.*, 2015. 746, 233-244.
44. McGillewie, L., M. Ramesh, and Soliman, M. E. *Sequence, Structural Analysis and Metrics to Define the Unique Dynamic Features of the Flap Regions Among Aspartic Proteases*. *Protein J.*, 2017. 36(5): p. 385-396.
45. Salleh, A. B., Rahim, A. S., Rahman, R. N. *The role of Arg157Ser in improving the compactness and stability of ARM lipase* *J. Comput. Sci. Syst. Biol.* 2012. 5:38–46.

46. Sindhu, T., Srinivasan, P. *Exploring the binding properties of agonists interacting with human TGR5 using structural modeling, molecular docking and dynamics simulations. RSC Advances.* 2015. 5(19):14202-14213.
47. Kumar, C. V., Swetha, R. G., Anbarasu, A. Ramaiah, S. *Computational Analysis Reveals the Association of Threonine 118 Methionine Mutation in PMP22 Resulting in CMT-1A.* Adv. Bioinf., 2014, 1–10.
48. Pan, L. and S. G. Aller, *Equilibrated atomic models of outward-facing P-glycoprotein and effect of ATP binding on structural dynamics.* Sci. Rep, 2015. 5: p. 7880.
49. Boyce, S. E., Tirunagari, N., Niedziela-Majka, A., Perry, J., Wong, M., Kan, E., Sakowicz, R. *Structural and Regulatory Elements of HCV NS5B Polymerase – β -Loop and C-Terminal Tail – Are Required for Activity of Allosteric Thumb Site II Inhibitors.* 2014. PLoS ONE, 9(1), e84808.
50. Ramharack, P. and Soliman, M. E. S. *Zika virus NS5 protein potential inhibitors: an enhanced in silico approach in drug discovery.* J. Biomol. Struct. Dyn. 2018. 36(5): p. 1118-1133.
51. Farrokhzadeh, A., Akher, F. B. and Soliman, M. E. S. *Probing the Dynamic Mechanism of Uncommon Allosteric Inhibitors Optimized to Enhance Drug Selectivity of SHP2 with Therapeutic Potential for Cancer Treatment.* Appl. Biochem. Biotechnol. 2019. 188(1): p. 260-281.
52. Massova, I., Kollman, P. A. *Combined molecular mechanical and continuum solvent approach (MM-PBSA/GBSA) to predict ligand binding.* Perspectives Drug Discov. and Des., 2000. 18, 113–135.
53. Osterberg, F., et al., *Automated docking to multiple target structures: incorporation of protein mobility and structural water heterogeneity in AutoDock.* Proteins, 2002. 46(1): p. 34-40.
54. Pang, X., Baoyue Z., Guangyan, M., Jie, X., Qian, X., Xia, Z., Ailin, L., Guanhua, D. and Yimin, C. (2018). 'Screening of cytochrome P450 3A4 inhibitors via in silico and in vitro approaches' RSC Adv., 2018, 8, 34783.

55. Meintjes, G., Moorhouse, M. A, Carmona S. *Adult antiretroviral therapy guidelines*. S. Afr. J. HIV Med., 2017. 18(1), a776.
56. Moonsamy, S., Dash, R. C. and Soliman, M. E. *Integrated computational tools for identification of CCR5 antagonists as potential HIV-1 entry inhibitors: homology modeling, virtual screening, molecular dynamics simulations and 3D QSAR analysis*. Molecules, 2014. 19(4): p. 5243-65.
57. Chetty, S., et al., *Multi-drug resistance profile of PR20 HIV-1 protease is attributed to distorted conformational and drug binding landscape: molecular dynamics insights*. J. Biomol. Struct. Dyn, 2016. 34(1): p. 135-51.
58. Ndagi, U., Mhlongo, N. N. and Soliman, M. E. *The impact of Thr91 mutation on c-Src resistance to UM-164: molecular dynamics study revealed a new opportunity for drug design*. Mol. Biosyst, 2017. 13(6): p. 1157-1171.

CHAPTER FIVE

The *in-silico* studies in chapter three and four have predicted the pharmacokinetic properties of the selected PCs and their effects on the activities of PIs drug-metabolising proteins (CYP3A4 and P-gp). These were predictive studies and their significant findings necessitated an *in vitro* study to evaluate the effects of the four promising antiviral PCs (EGCG, K7G, LUT and EGA) on cytotoxicity, cell viability profiles and regulatory influences on the mRNA and protein expressions of CYP3A4 and P-gp/ABCB1 in two human cell lines (liver (Hep-G2) and kidney (HEK-293)).

A manuscript titled ‘Evaluation of Cytotoxicity, Cell Viability and Modulatory Influences of Antiviral Bioactive Compounds on mRNA Expressions and Protein activities of Cytochrome P450 3A4 and P-glycoprotein in HepG2 and HEK293 cell lines’ is under review for publication.

Modulatory Influences of Antiviral Bioactive Compounds on Cell Viability, mRNA and Protein Expression of Cytochrome P450 3A4 and P-glycoprotein in HepG2 and HEK293 cells

Abstract

The induction of cytochrome P450 3A4 (CYP3A4) and P-glycoprotein (ABCB1) influences drug plasma concentrations, and eventually decreases the drugs' therapeutic effects. The effects of Plant-derived compounds (PCs) on drug-metabolising proteins are largely unknown. This study investigated the cytotoxicity, cell viability profiles and regulatory influences of four PCs (epigallocatechin gallate (EGCG), kaempferol-7-glucoside (K7G), luteolin (LUT) and ellagic acid (EGA)) on the mRNA and protein expression of CYP3A4 and ABCB1 in HepG2 and HEK293 cells. After treatment with the PCs (0-400 μ M) for 24 hours, 80% (IC₂₀) and 50% (IC₅₀) cell viability were determined. The PCs were not toxic to HepG2, ATP levels increased at IC₂₀, there was insignificant change in LDH (lactate dehydrogenase), with the exception of LUT, and ABCB1 protein expressions decreased. The PCs decreased CYP3A4 at IC₂₀ (except LUT), EGCG and K7G at IC₂₀ decreased mRNA expression. For HEK293 cells, no significant change in ATP was observed, except for EGCG IC₂₀ and K7G IC₅₀ which decreased and increased, respectively. LDH decreased at IC₂₀, but at IC₅₀ there was a significant increase in LDH following LUT treatment. ABCB1 protein expression increased at both IC₂₀ and IC₅₀, but LUT and EGA at IC₅₀ decreased mRNA expression. The PCs at IC₂₀, and IC₅₀ of LUT, K7G and of EGCG may enhance drug bioavailability.

Keywords: Cytochrome P450 3A4, P-glycoprotein, Cytotoxicity, Cell viability profile, Regulatory influence.

INTRODUCTION

Plants have been reported to be a good source of natural bioactive compounds that can be used as models for the development and synthesis of new potent drugs. Rates (2001) reported that about 25 % drugs prescribed in the world were derived from plants [1]. Several phytochemical compounds found in plants including flavonoids, tannins and phenols have been reported by several studies for the treatment of different diseases due to their inhibitory and antiproliferation activities against diseases [2]. The use of these plant-derived compounds is gaining popularity in the treatment of various diseases like cancer [3], human immunodeficiency virus (HIV) [4, 5] and in the discovery of many potential drugs.

In silico studies by Idowu *et al.* (2019 and 2020) reported four plant-derived compounds; (epigallocatechin gallate (EGCG), kaempferol-7-glucoside (K7G), luteolin (LUT) and ellagic acid (EGA)) (Figure 1) to be potential inhibitors of cytochrome P450 3A4 enzyme (CYP3A4) and P-glycoprotein transporter (ABCB1) [6, 7]. These two proteins have been reported to mediate or restrict pharmacokinetic properties such as absorption, distribution, metabolism and excretion of drugs [8]. Indeed, the significant roles of CYP3A4 and ABCB1 in the metabolism of drugs like antiretroviral protease inhibitor drugs (PIs) have been widely studied and established. The induction of their proteins or overexpression of their genes in response to drugs or compounds that can modulate their activities can cause dangerous adverse interactions and compromised therapeutic consequences [9]. Marchetti *et al.* (2007) suggested that the alteration of their expressions and activities might be a beneficial strategy to improve the effectiveness and safety of drugs like the PIs [9].

This study therefore evaluated the modulatory influences of four phytochemical compounds (EGCG, K7G, LUT and EGA) present in some of the herbal medicines (COA-herbal medicine, Imbiza Herbal, Ingungumbane Mahlabizifo, Ngoma herbal and many more) [10]

used by HIV positive patients in South Africa on the protein activities and gene expressions of CYP3A4 and ABCB1 in conjunction with their cytotoxicity and cell viability profiles in two human cell lines (HEK293 and HepG2).

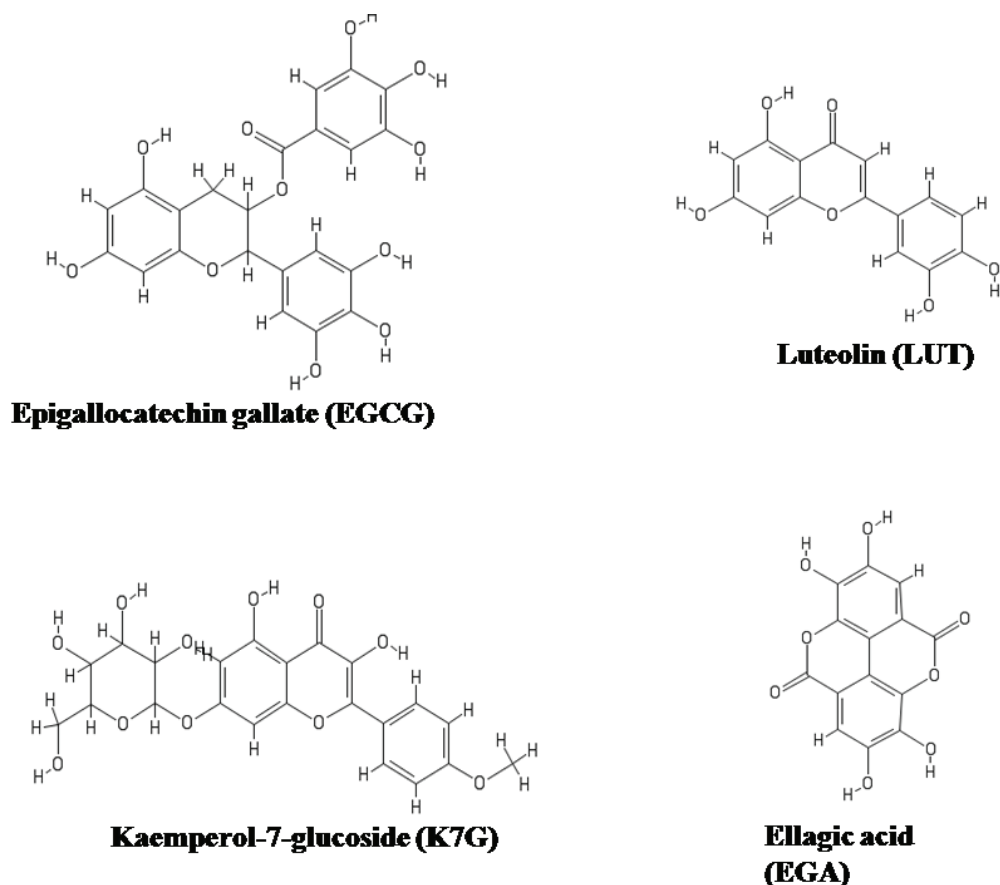


Figure 1. Molecular structures of Luteolin, Ellagic acid, Kaempferol-7-glucoside and Epigallocatechin gallate[11]

2. METHODS

2.1. Cell Culture:

Cells were obtained from the laboratory of Medical Biochemistry department, College of Health Science, University of KwaZulu-Natal. HepG2 and HEK293 cells were cultured at 37°C, in 5% CO₂ in complete culture media (CCM): minimum essential medium supplemented with 1% L-glutamine, 1% penstrep-fungizone and 10% foetal bovine serum.

According to their requirements, Eagles minimum essential medium (EMEM) and Dulbecco's Modified Eagle's Medium (DMEM) were used for HepG2 and HEK293 cells, respectively.

2.2. Preparation of Compounds:

The four compounds were purchase from Sigma-aldrich, Johannesburg 1645 South Africa. Stock solutions (400 μ M) for the MTT assay were prepared for each of the compounds by dissolving 1mg in the respective CCM for the cells. Subsequent treatments were diluted from the stock solution.

2.3. Cell Viability Assay:

Cells were seeded in a 96-well microtitre plate at a concentration of 20,000 cells/well (200 μ l CCM), and allowed to attach overnight (37°C, 5% CO₂). Cells were then subject to treatment in triplicate with each compound (0-400 μ M). Following a 24h incubation, the MTT assay was performed, where the cells were incubated (37°C, 4h) with MTT substrate (3-(4,5-dimethylthiazol-2-yl)-2,5-diphenyltetrazolium bromide) (1 : 5 5mg/ml in 0.1M PBS : CCM). After that, supernatants were aspirated, and cells were incubated in dimethyl sulphoxide (DMSO; 100 μ l/well) for 1h. Optical density (OD) was then measured at 570nm, with a reference wavelength of 690nm by an enzyme-linked immunosorbent assay (ELISA) plate reader (BioTek μ Quant, USA). The percentage cell viability was calculated, and the log concentration-response curves were plotted using GraphPad Prism version 5.0 software (USA) to extrapolate the half maximum inhibitory concentration (IC₅₀) and concentration that produced 20% inhibition of cell viability (IC₂₀). For subsequent assays, the cells were treated at 80% confluency with both IC₅₀ and IC₂₀ concentrations of the respective compounds for 24h.

2.4. Adenosine Triphosphate (ATP) Assay:

Adenosine triphosphate (in relative light units, RLU) was evaluated by the luminometric Cell Titer-Glo® assay (G775A, Promega, Madison, Wisconsin, USA) [12]). Treated cells were seeded in triplicate in a white microtitre plate (20,000 cells per well in 50µl PBS) and 50µl ATP Cell Titer-Glo Reagent was added to each well. The plate was incubated for 30 minutes (30min) at room temperature (RT). Luminescence was measured on a Modulus™ microplate luminometer (Turner BioSystems, Sunnyvale, California, USA). Luminescence is proportional to ATP concentration and was expressed as relative light units (RLU).

2.5. Lactate Dehydrogenase (LDH) Assay:

The LDH cytotoxicity detection kit (Roche, Mannheim, Germany) was used to measure cell death/damage [13]. The cell culture medium was aspirated following treatment with the respective compounds and used to measure extracellular LDH activity. The cell culture supernatant (100µl) was transferred into a microtitre plate in triplicate. Subsequently, substrate mixture (100µl) containing catalyst (diaphorase/NAD⁺) and dye solution (INT/sodium lactate) was added to the supernatant and allowed to react at ambient temperature for 25min as per the manufacturer's instructions. The optical density of the resulting formazan product was measured at 500nm with an ELISA plate reader (BioTekµQuant), USA). Results are represented as mean optical density.

2.6. Western Blot (WB):

Cytobuster™ reagent (Novagen) supplemented with protease and phosphatase inhibitor was used for protein isolation. Cytobuster (200µl) was added to the treated cells (4°C, 15min) and centrifuged (180xg; 4°C, 10min) to obtain a crude protein extract. Protein samples were quantified using the Bicinchoninic Acid (BCA) assay and standardised to 1mg/ml. Samples

were then denatured by boiling for 5min with a 4:1 dilution of 5 x Laemmli sample buffer [0.375 Tris-HCL pH 6.8;10% w/v SDS; 3% v/v glycerol; 2% w/v bromophenol blue; 12% β -mercaptoethanol in dH₂O].

Samples were electrophoresed on 10% SDS-PAGE gels, run at 150V. Transfer to nitrocellulose membranes was conducted using the Bio-Rad Trans-Blot Turbo Transfer System (25V, 2.5A, 30min). Membranes were blocked with 5% bovine serum albumin (BSA) in Tris buffer saline containing Tween 20 (20mM Tris-HCl (pH 7.4), 500mM NaCl and 0,5% Tween 20 (TTBS)) for 1h, and probed overnight at 4°C with anti-CYP3A4 (13384S, Cell Signalling) and anti- ABCB1 (13342S, Cell Signalling) diluted to 1:1000 in 5% BSA in TTBS.

Membranes were then washed four times (10ml TTBS, 15min) and treated with horseradish peroxidase (HRP)-conjugated secondary antibody (goat anti-rabbit; rabbit anti-mouse: 1:2500 in 5% BSA:TTBS, 1h, RT). Membranes were washed four times (TTBS, 15min) and immunoreactivity was detected by Clarity ECL substrate (Bio-Rad). Images were captured and analysed with the Bio-Rad imaging system (Molecular Imager® Chemidoc XRS and Bio-Rad ImageLab software; Bio-Rad, Hercules, CA). Membranes were stripped with 30% hydrogen peroxide (H₂O₂), rinsed thrice in TTBS, blocked in 5% BSA:TTBS (1 h; RT) and probed with HRP-conjugated anti- β -actin (Sigma, St Louis, Missouri, USA). The results were expressed as mean relative band density (RBD), which is relative to the loading control and housekeeping protein β -actin.

2.7. Quantitative Polymerase Chain Reaction (PCR)

2.7.1. Ribonucleic Acid (RNA) Isolation

The control and compounds treated cells were washed with phosphate buffer saline (PBS), then 500µl Qiazol reagent (Qiagen) diluted in 500µl 0.1M PBS was added to each flask. The contents were scraped and transferred to an eppendorf for overnight storage at -80°C. Chloroform (100µl) was added to thawed samples and centrifuged (12,000xg, 15min, 4°C). The aqueous upper phase was transferred to a new eppendorf followed by the addition of 250µl propan-2-ol and stored overnight at -80°C. The thawed samples were centrifuged (12,000xg, 20min, 4°C). The resulting sample pellet was washed with 75% cold ethanol and centrifuged (7,400xg, 15min, 4°C). The ethanol was aspirated, and the RNA pellet was resuspended in 15µl nuclease-free water. The RNA was quantified (Nanodrop 2000) and standardised to 1000ng/µl.

2.7.2 Complementary Deoxyribonucleic Acid (cDNA) synthesis

A 20µl reaction volume containing 1µl RNA template, 4µl 5X iScript™ reaction mix, 1µl iScript reverse transcriptase and nuclease-free water was used to synthesise cDNA (iScript™ cDNA Synthesis kit (BioRad; catalogue no 107-8890). Thermocycler conditions were 25°C for 5min, 42°C for 30min, 85°C for 5min and a final hold at 4°C.

2.7.3. Quantitative (PCR)

The mRNA expression of CYP3A4 (forward: 5'-CATCCCAATTCTTGAAGTATTAAATATCT-3', reverse: 5'-TTGTGGGACTCAGTTTCTTTTGAA-3'), and ABCB1 (forward: 5'-AAGGCCTAATGCCGAACACA-3', reverse: 5'-TTTGCCATCAAGCAGCACTTT-3') were investigated using quantitative PCR (qPCR). Amplification proceeded in triplicate, in a

25µl reaction consisting of 12.5µl 5X iScript reaction mix, 2µl of cDNA, 1µl of the primer set and 9.5µl of RNase-free water. Thermocycler conditions were initial denaturation (95°C, 4min), 37 cycles of denaturation (95°C, 15s), annealing (57°C, 40s) and extension (72°C, 30s). The plate was read at the end of every cycle (CFX96 Touch™ Real-Time PCR Detection System (BioRad)). The housekeeping gene, glyceraldehyde-3-phosphate dehydrogenase (GAPDH) was run under the same conditions. Analysis of results was conducted as per the method described by Livak and Schmittgen, (2001) [14]. Results are expressed as fold change ($2^{-\Delta\Delta Ct}$) relative to the housekeeping gene, GAPDH (forward: 5'-TCCCTGAGCTGAACGGGAAG -3', reverse: 5'- GGAGGAGTGGGTGTCGCTGT -3') and control [10].

2.8. Statistical Analysis:

Statistical analyses were performed using GraphPad Prism version 5.0 software package (GraphPad PRISM®) and Microsoft excel 2010. Data are expressed as mean \pm standard error of the mean (SEM). Dose-response-Inhibition (Log(inhibitor) vs. normalized response) was used for the MTT assay. Comparisons were made using the unpaired Student *t*-tests using Welch correction. Statistical significance was set at 0.05.

3. RESULTS

3.1. MTT Assay:

The dose-response was determined using concentrations in the range 0 to 400 µM for 24h (Figures 2 and 3). Analysis of the dose-dependent cell viability curves show that HepG2 (IC₅₀ = 140 µM) are more sensitive to the effects of EGCG, compared to HEK293 cells (IC₅₀ = 1075 µM). Table 1 showed the summary of the calculated IC₂₀ and IC₅₀ concentrations. Figure 2 shows that the treatment of HepG2 cells with the compounds yielded cell viability

above 75% at the highest concentrations tested, with only EGCG decreasing cell viability below 50%. HEK293 cells demonstrated greater sensitivity to the effects of K7G (56 μM), LUT (353 μM) and EGA (207 μM) (Figure 3, Table 1) compared to HepG2 cells (842.60 μM , 1466.00 μM and 1187.00 μM respectively) (Figure 2, Table 1). The dose-response curves further revealed that the compounds are less toxic to the two cell lines at their IC_{20} concentrations (Table 1).

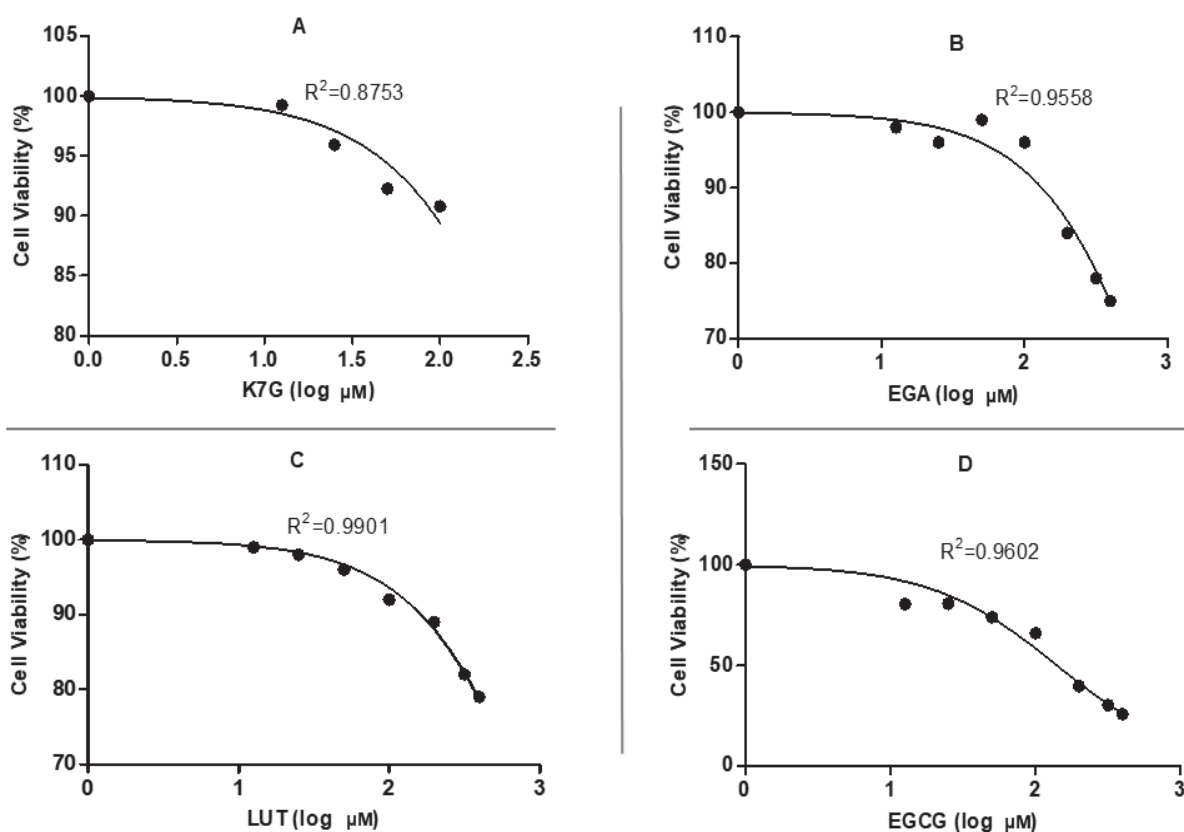


Figure 2: Cell viability (MTT assay) of HepG2 cells treated with (A) K7G, (B) EGA, (C) LUT and (D) EGCG. Data is represented as a percentage relative to the untreated control (0 μM). A concentration-dependent reduction in HepG2 cell viability after treatment with the different compounds.

HEK293 cells are more sensitive than HepG2 cells to the cytotoxic effects of the compounds, as cell viability reached 50% and lower for all treatments (Figure 3). The HEK293 IC_{50} concentrations are significantly lower than those extrapolated for HepG2, further demonstrating their sensitivity (Figure 3, Table 1). However, HEK293 cells demonstrated tolerance to EGCG over a wide concentration range, and a high IC_{50} was calculated (1075 μM) compared to HepG2 cells (140.8 μM).

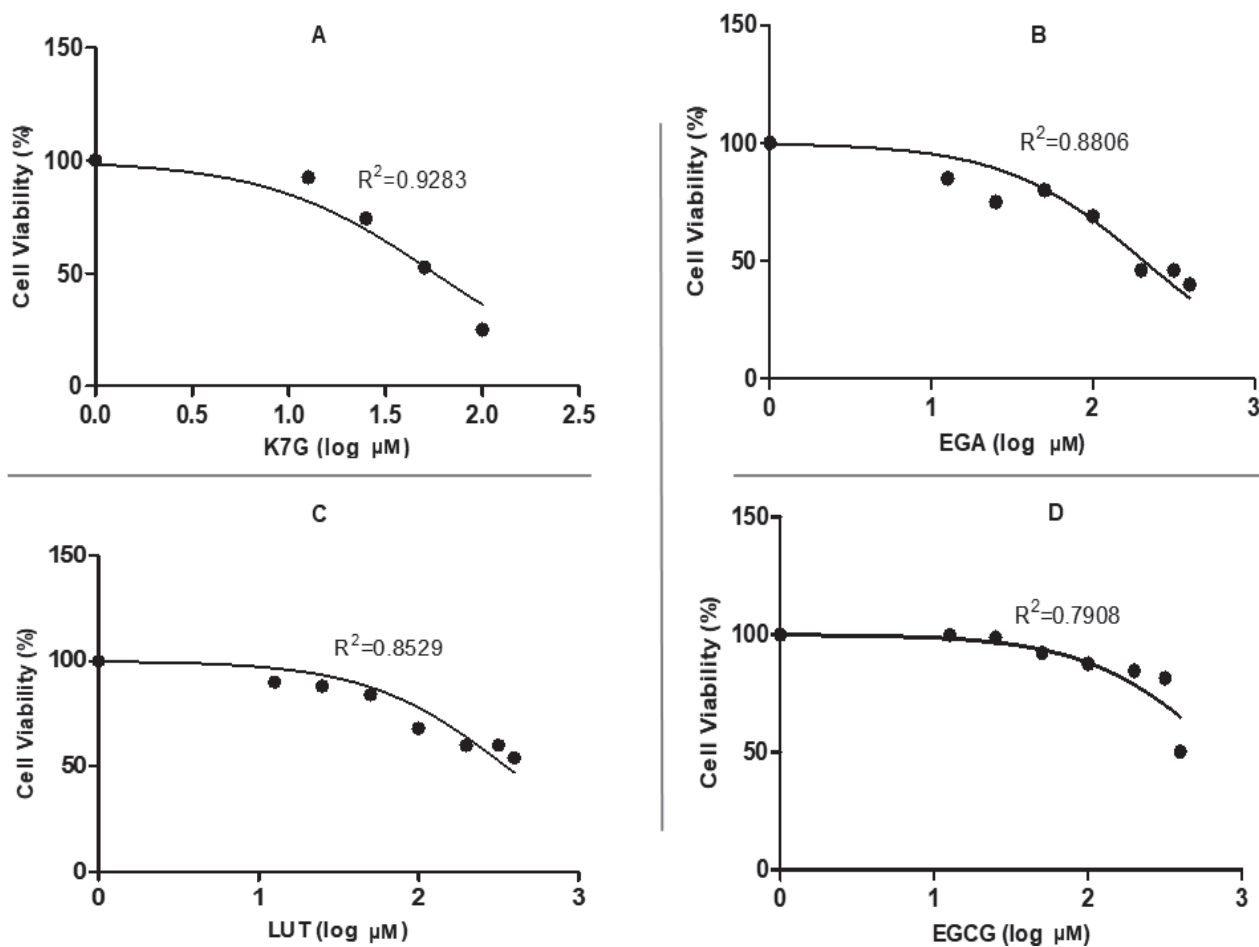


Figure 3: Cell viability (MTT assay) of HEK-293 cells treated with (A) **K7G**, (B) **EGA**, (C) **LUT** and (D) **EGCG**. Data is represented as a percentage relative to the untreated control (0 μM). A concentration-dependent reduction in HEK-293 cell viability after treatment with the different compounds.

Table 1. Result of analysis of the dose dependent curve showing IC₂₀ and IC₅₀ of the compounds on HepG2 and HEK293 cells.

Compounds	HepG2		HEK293	
	IC ₂₀ (μM)	IC ₅₀ (μM)	IC ₂₀ (μM)	IC ₅₀ (μM)
EGCG	25.12 ± 2.37	140.80 ± 4.58	218.78 ± 5.34	1075.00 ± 8.77
K7G	7.76 ± 1.23	842.60 ± 8.38	31.62 ± 3.89	56.00 ± 2.33
LUT	26.30 ± 3.11	1466.00 ± 9.78	9.55 ± 0.74	353.20 ± 6.29
EGA	14.79 ± 0.62	1187.00 ± 12.41	10.96 ± 1.40	207.10 ± 7.17

3.2. ATP Assay:

The effect of both IC₂₀ and IC₅₀ concentrations of the compounds on cellular ATP concentration in HepG2 and HEK293 cells was investigated to examine the mitochondrial activity and cell viability. The IC₅₀ treatments of HepG2 cells-maintained ATP concentration similar to the control (Figure 4A), while significant increase in ATP concentration was recorded for all IC₂₀ treatments (Figure 4A). For EGCG IC₂₀ (14.8 x 10⁶ RLU), 2.85 fold increase was observed when compared to the control (5.2 x 10⁶ RLU); a 3.5-fold increase was noted for K7G IC₂₀ (18 x 10⁶ RLU, p < 0.05), while LUT IC₂₀ and EGA IC₂₀ recorded 2.3-fold (p < 0.05) and 3.7-fold (p < 0.05) increases in ATP concentration respectively compared to the control. In HEK293 cells, the IC₅₀ concentration of EGCG reduced ATP levels, with a significant 13.1-fold decrease (0.8 x 10⁶ RLU) compared to the control (10.05 x 10⁶ RLU; p < 0.05) (Figure 4B). A non-significant decrease in ATP was also noted for the IC₅₀ treatment of LUT and EGA. However, IC₅₀ treatment with K7G significantly increased ATP level by 2.5-fold compared to the control (Figure 4B). While the IC₂₀ treatment of HEK293 cells with EGCG reduced cellular ATP levels, all other IC₂₀ treatments-maintained ATP concentration similar to the control (Figure 4B).

3.3. LDH Assay:

Results of the LDH assay are presented as mean optical density (OD)/relative viability to investigate the effects of the compounds on the membrane integrity of the cells. In HepG2 cells, only the IC₅₀ of LUT significantly increased the extracellular level of LDH (Figure 4C) by 0.5-fold (0.532 OD) compared to that of the control supernatant (0.311 OD); all other IC₅₀ treatments maintained extracellular LDH similar to the control (Figure 4C). The IC₂₀ treatments of HepG2 cells decreased (EGCG, K7G), maintained (LUT) or increased (EGA) extracellular LDH relative to the control (Figure 5A), but these differences were not

significant. In HEK293 cells, the IC₅₀ of EGCG decreased extracellular LDH, K7G maintained these levels relative to the control. Increases in LDH concentrations were noted for LUT ($p < 0.05$) and EGA (Figure 4D). The extracellular LDH levels were reduced at all IC₂₀ treatments of HEK293 cells, with significant ($p < 0.05$) 3.14-fold, 1.91-fold and 2.19-fold decrease for EGCG, K7G and LUT respectively (Figure 4D).

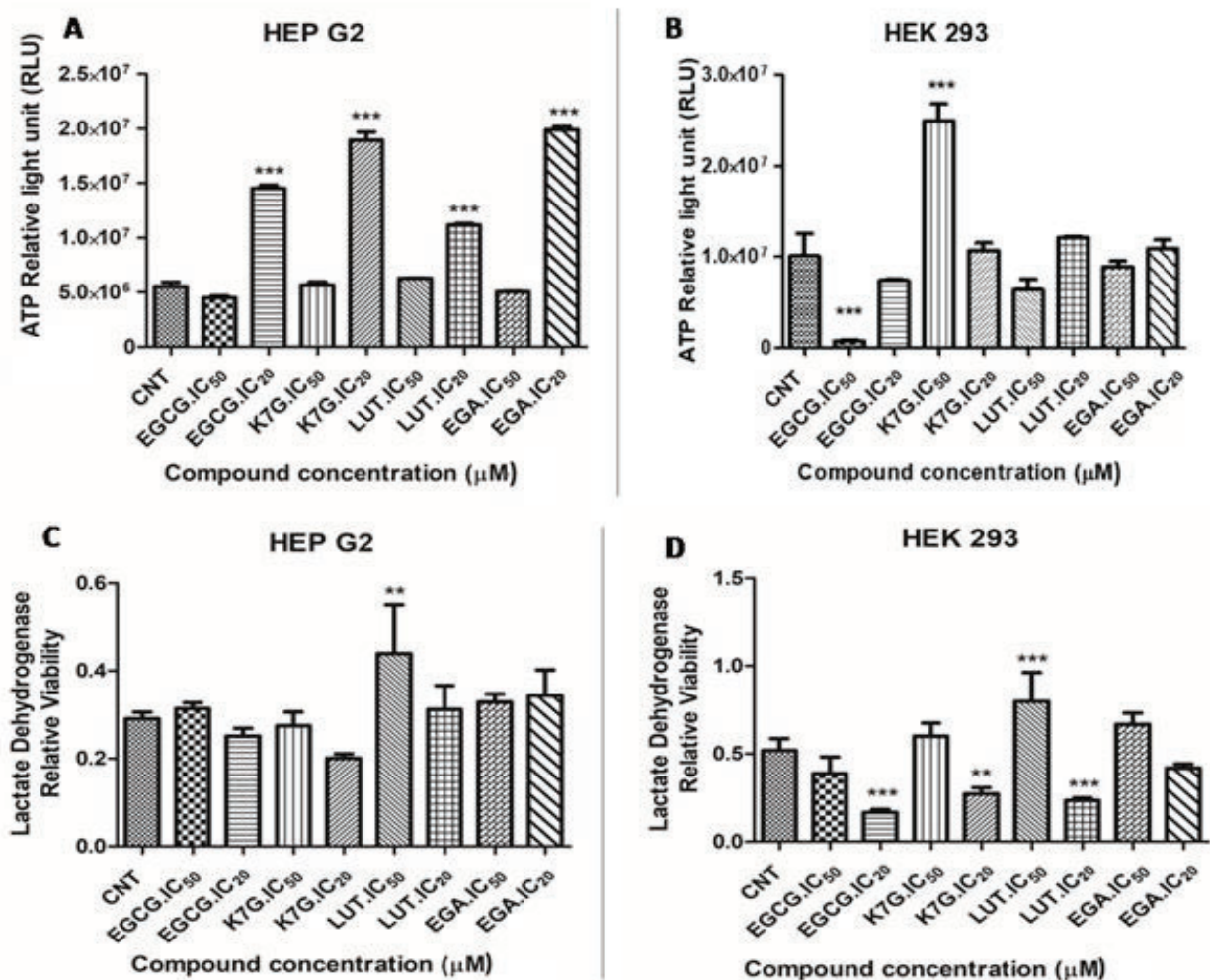


Figure 4. Intracellular ATP levels (A and B) and Extracellular LDH levels (C and D) in HepG2 and HEK293 cells treated with both IC₂₀ and IC₅₀ of EGCG, K7G, LUT and EGA.

Protein and mRNA expression of ABCB1

All treatments induced a significant decrease ($p < 0.05$) in ABCB1 protein activity in HepG2 cells (Figure 5A). Both IC₅₀ and IC₂₀ concentrations of EGCG (0.061 RBD for IC₅₀, 0.06 RBD for IC₂₀) and EGA (0.042 RBD for IC₅₀, 0.41 RBD for IC₂₀) induced similar changes in

ABCB1 protein concentration when compared to the control. However, the IC₂₀ concentration of K7G decreased ABCB1 protein concentration to lower levels than the IC₅₀ concentration (0.058 for IC₅₀, 0.04 RBD for IC₂₀), while the IC₅₀ concentration of LUT was more effective at reducing ABCB1 protein activity than the IC₂₀ concentration (0.04 RBD for IC₅₀, 0.06 RBD for IC₂₀) relative to the control. The IC₂₀ treatment of all the compounds significantly increased ($p < 0.05$) the mRNA expression of ABCB1 (Figure 5B), which was decreased at IC₅₀ of EGCG (0.34-fold change), LUT (0.52-fold change) and EGA (0.63-fold change) compared to the control.

All treatments induced an increase in ABCB1 protein expression in HEK293 cells (Figure 5C). Treatment with the IC₂₀ concentration of EGCG, K7G and EGA induced a concentration dependent decrease in ABCB1 protein expression towards control levels (0.05 RBD). EGA at both IC₂₀ showed increase in the ABCB1 protein quantity in HEK293 cell. In contrast, the IC₅₀ concentration (1466.00 μ M) of LUT was more effective at reducing ABCB1 protein quantity than the IC₂₀ concentration (26.30 μ M) relative to the control in HEK293 cells. In Figure 5D, treatment with IC₂₀ concentration of EGCG induced a significant 8.87-fold increase in the ABCB1 mRNA expression compared to the control. No significant difference was recorded after treatment IC₂₀ concentrations of K7G (1.87-fold change), EGA (1.15-fold change), LUT (1.15-fold change), and IC₅₀ concentrations of EGCG (2.01-fold change) and K7G (2.00-fold change). EGA (0.06-fold change) and LUT (0.03-fold change) reduced mRNA expression of ABCB1 at IC₅₀ concentrations.

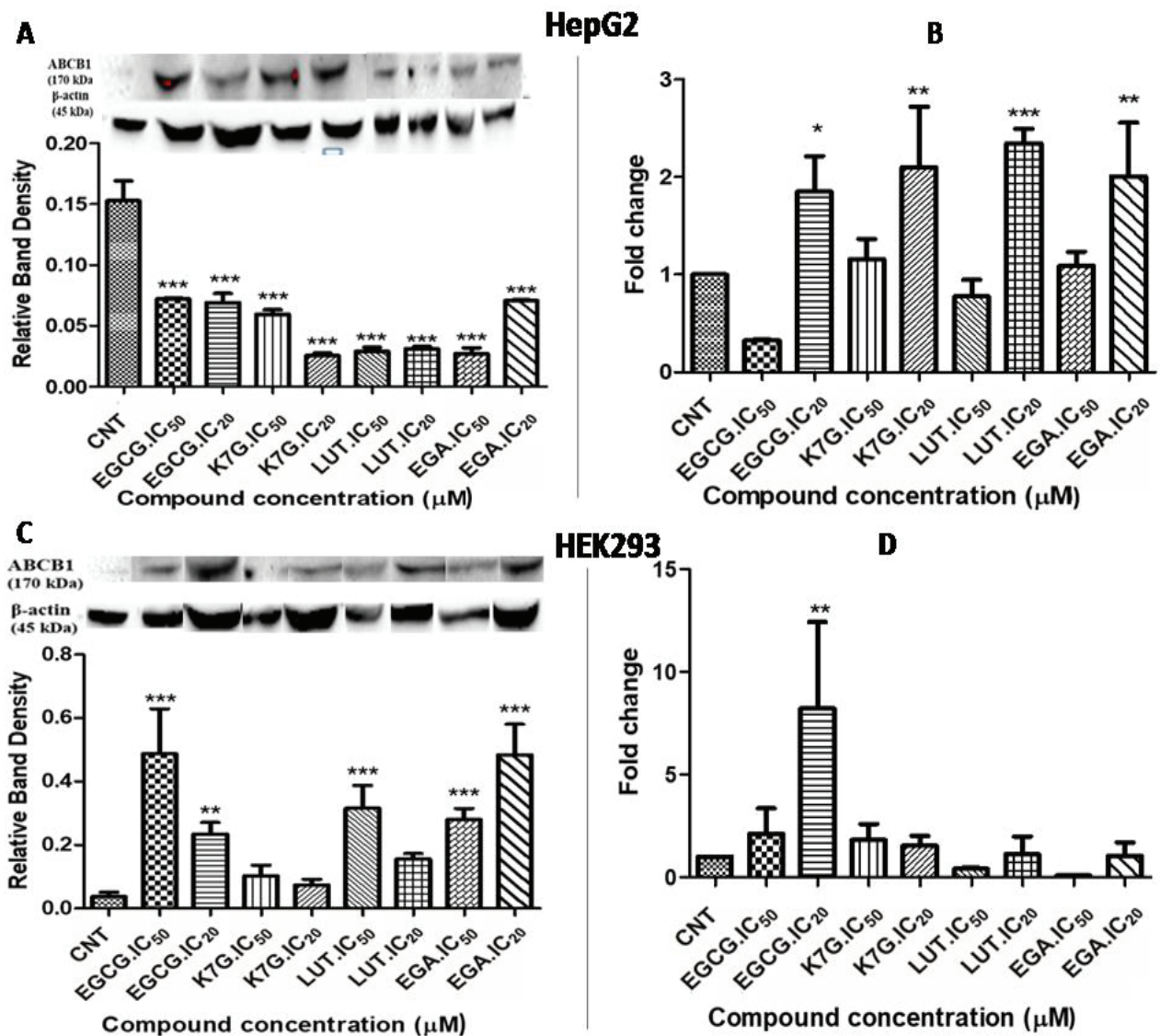


Figure 5: Effects of the compounds at IC₂₀ and IC₅₀ concentrations on ABCB1 protein and mRNA expression in HepG2 cells (A and B) and in HEK293 cells (C and D). (A) The representative western blot (WB) and relative densitometry illustrating differences in the concentration of crude ABCB1 protein in HepG2 cells cultured for 24 h in the presence of IC₂₀ and IC₅₀ concentrations of the compounds. (B) Representation of RT-PCR analysis demonstrating changes in ABCB1 mRNA levels in HepG2 cells. (C) The representative WB and relative densitometry illustrating differences in the level of crude ABCB1 protein in HEK293 cells cultured for 24 h in the presence of IC₂₀ and IC₅₀ concentrations of the compounds. (D) Representation of RT-PCR analysis demonstrating changes in ABCB1 mRNA levels in HEK293 cells. In the densitometric analysis, bars represent the means ± S.D of four independent experiments. *Significantly distinct from the value of the control ($p < 0.05$).

3.4. Protein and mRNA expression of CYP3A4

All IC₅₀ treatments induced a significant increase in CYP3A4 protein expression in HepG2 cells (Figure 6A). With the exception of the IC₂₀ of LUT and EGA that increased CYP3A4 protein expression relative to the control, all other IC₂₀ treatments significantly reduced CYP3A4 protein expression. When compared to the control, the IC₂₀ concentrations of EGA (57.222-fold change), LUT (37.32-fold change) and IC₅₀ of EGA (18.2-fold change) showed significant increase in CYP3A4 mRNA expressions in HepG2 cells (Figure 6B). No significant increase in CYP3A4 mRNA expressions was observed in IC₂₀ concentrations of EGCG (4.72-fold change), K7G (6.56-fold change) and IC₅₀ concentrations of EGCG (0.23-fold change), K7G (0.3-fold change) and LUT (0.43-fold).

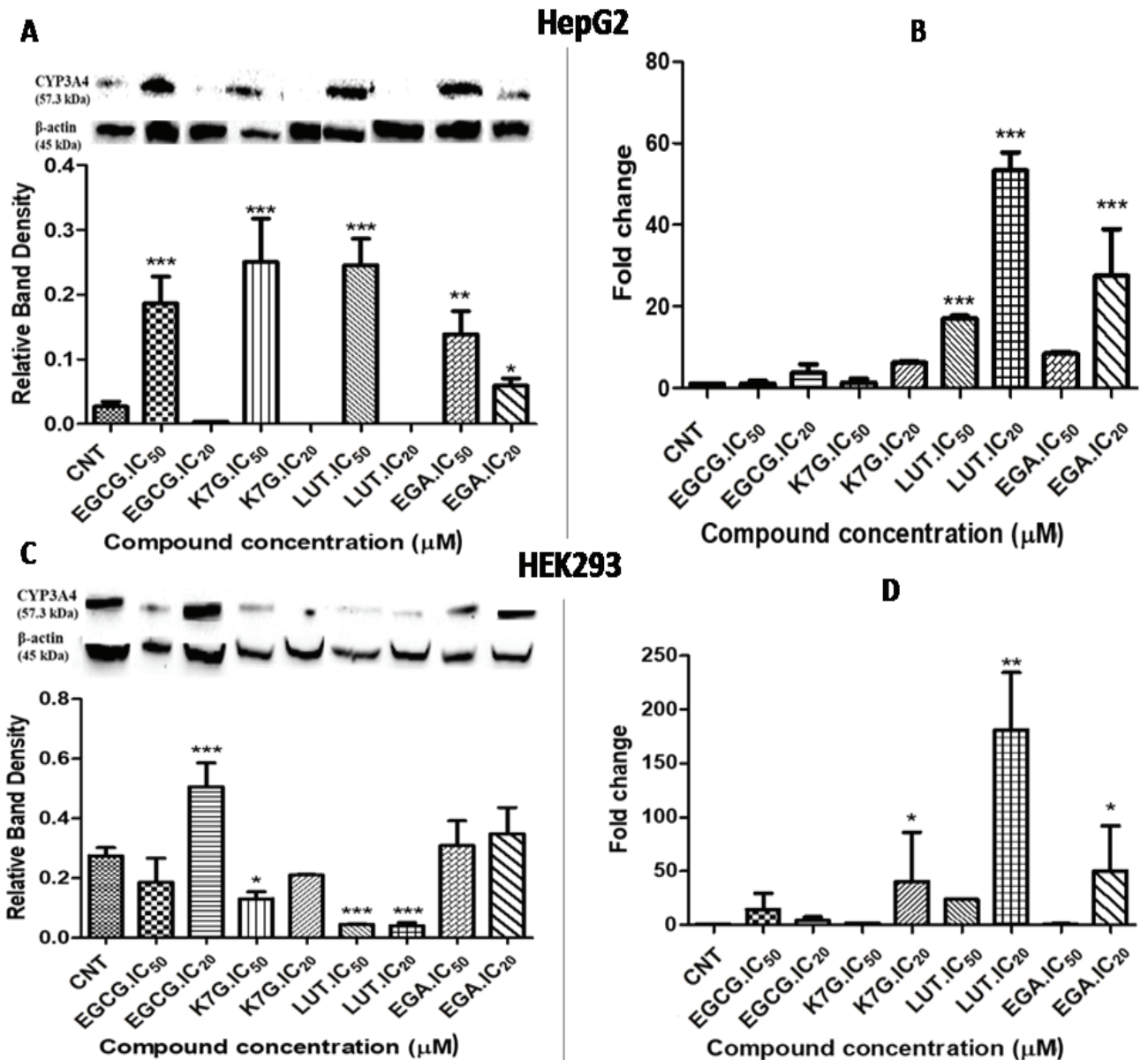


Figure 6: Effects of the compounds at IC₂₀ and IC₅₀ concentrations on CYP3A4 mRNA and protein expression in HepG2 cells (A and B) and in HEK293 cells (C and D). (A) The representative of WB and relative densitometry illustrating differences in the level of crude CYP3A4 protein in HepG2 cells cultured for 24h in the presence of IC₂₀ and IC₅₀ concentrations of the compounds. (B) Representation of RT-PCR analysis demonstrating changes in CYP3A4 mRNA levels in HepG2 cells. (C) The representative WB and relative densitometry illustrating differences in the level of crude CYP3A4 protein in HEK293 cells cultured for 24h in the presence of IC₂₀ and IC₅₀ concentrations of the compounds. (D) Representation of RT-PCR analysis demonstrating changes in CYP3A4 gene levels in HEK293 cells. In the densitometric analysis, bars represent the means ± S.D of four independent experiments. *Significantly distinct from the value of the control (p < 0.05).

Treatment with 218.78 μ M EGCG (IC₂₀) induced significant increase in CYP3A4 protein activity in HEK293 cells, while protein expression was slightly decreased after treatment with EGCG at the IC₅₀ concentration (Figure 6C). No significant difference in CYP3A4 protein quantity was also observed after treatment with IC₂₀ concentrations of K7G (0.195 RBD), EGA (0.341 RBD) and IC₅₀ concentration of EGA (0.322 RBD) compared to the control (0.280 RBD). Treatment with IC₂₀ concentration of LUT (0.04 RBD), IC₅₀ concentrations of LUT (0.05 RBD) and K7G (0.14 RBD) induced significant decrease in CYP3A4 protein quantity. EGA (40.34-fold change for IC₂₀ and 24.67-fold change for IC₅₀), K7G (12.35-fold change for IC₂₀) and LUT (29.65-fold change for IC₂₀) induced significant increase in CYP3A4 gene expression. EGA at an IC₅₀ is more efficient in decreasing gene expression of CYP3A4 than EGA at an IC₂₀ concentration in HEK293 cells (Figure 6D).

4. DISCUSSION

P-glycoprotein is an ATP-dependent efflux pump encoded by the ABCB1 gene [15]. This important drug transporter is associated with rapid uptake and elimination of drugs such as HIV protease inhibitors (PIs) [16]. The enzyme CYP3A4 is responsible for metabolism of approximately 30-55% of all drugs [17], including PIs [16]. P-glycoprotein and CYP3A4 genes are expressed in various healthy and tumour tissues with excretory functions including the kidney, liver, small intestine, blood-brain barrier and placenta [18]. Over-expression of both ABCB1 and CYP3A4 limits the bioavailability, increases the toxicity and reduces the therapeutic effect of PIs [16, 18, 20]. Therefore, inhibition or down-regulation of their protein activities and gene expression will enhance the maintenance of optimal plasma drug concentrations and ultimately improve the drug's therapeutic effects. Plant-derived phytochemical compounds like flavonoids, phenols, polyphenols and tannins may prove effective in this regard. In this study, the modulatory effect of four plant-derived

phytochemical compounds (Epigallocatechin gallate (EGCG), Kaempferol-7-glucoside (K7G), Luteolin (LUT) and Ellagic acid (EGA)) on the protein activity and mRNA expression of CYP3A4 and ABCB1 were examined in human kidney (HEK293) and liver (HepG2) cells. These cells are involved in excretion and drug metabolism and are part of the bodies' detoxification system. A previous *in silico study* has reported that these compounds possess potential inhibitory activities against CYP3A4 and ABCB1 [6]. Examining their *invitro* modulatory influence on both CYP3A4 and ABCB1 may provide vital findings on their therapeutic usage in boosting drug bioavailability. Their cytotoxic effects and cell viability profiles were also investigated in the same cell lines.

Cell viability testing is necessary to assess the *in vitro* toxicity of potential therapeutic compounds. It evaluates the inherent ability of a compound or chemical substance to inhibit cell growth, kill cells or interfere with energy metabolism [21]. The dose-response curves obtained indicate that K7G, EGA and LUT are less toxic to HepG2 cells (Figure 2), and thus had high extrapolated IC_{50} concentrations. However, the relatively low IC_{50} obtained for EGCG in HepG2 cells demonstrates sensitivity to the effects of EGCG (Figure 2). On the other hand, HEK293 cells were sensitive to the effects of K7G, LUT and EGA, but tolerant of EGCG that yielded a high IC_{50} (Figure 3). Sato *et al.* (2015) and Selvendiran *et al.* (2006) reported in separate studies that human hepatoma (HepG2) and breast cancer (MCF-7) cells are sensitive to the effect of LUT [22, 23], similar to HEK293 cells but contrasting with HepG2 cells in this study. This contradiction in HepG2 cells data might be associated with difference in LUT concentrations used in the two experiments. This study suggests the safety of EGCG to healthy kidney cells and an anti-proliferating effect exerted in HepG2 cells, and is in agreement with other studies that reported the anti-proliferating effects of EGCG to carcinoma cells [2, 24, 25]. Importantly, all IC_{20} concentrations were low in both cell lines

(Table 1), an indication that these concentrations could be used to exploit the potential therapeutic effects of the compounds.

Cell viability assays are a measure of cellular metabolic activity that is proportional to cellular maintenance and survival. These activities are typically a measure of mitochondrial function; decreased mitochondrial function is implied by the decreased capacity of succinate dehydrogenase in HepG2 and HEK293 cells to reduce the tetrazolium salt to formazan [26]. Early effects of mitochondrial toxicity include decreased energy production and increased lactate production, due to the shift in pyruvate metabolism where it is reduced to lactate by LDH [27]. Therefore, measurement of metabolic biomarkers such as ATP concentration and LDH are routinely used methods to evaluate cell viability [28-30]. In this study, both ATP cell content and LDH activities were determined to evaluate the cell viability in HepG2 and HEK293 cells treated separately with compounds at different concentrations.

The role of ATP in energy exchanges cannot be over-emphasised, as it plays a crucial role in biological systems. Healthy cells contain closely regulated levels of ATP, while non-viable cells are not only unable to synthesize ATP, they also contain endogenous ATPases that rapidly exhaust the existing ATP [31]. Since all living cells need ATP to survive and carry out their specialised functions, a decrease in ATP concentrations is an indicator that such cells are undergoing cell death [32]. In the HepG2 cells, sufficient ATP is available to carry out vital cellular processes following IC₅₀ treatments (Figure 4A) [31, 32]. Interestingly, intracellular ATP was significantly increased in IC₂₀ treated HepG2 cells (Figure 4A), indicating that the compounds increase cell metabolism. The significant decrease of ATP levels in HEK293 cells (Figure 4B) treated with IC₅₀ concentrations of EGCG may be related to energy failure resulting from mitochondrial dysfunction [31]. However, no significant

difference was recorded for the compound at its IC₂₀, indicating ATP concentrations within homeostatic levels.

LDH is found in all living cells (including liver and kidney cells) and is an important enzyme required for metabolising glucose to energy for living cells. Damage to the cell membrane results in an increase in extracellular LDH, thus LDH is also an indicator of cell membrane integrity [28, 29, 33]. At IC₅₀ concentrations, in both HepG2 and HEK293 cells, LUT significantly ($p < 0.05$) increased extracellular LDH levels (Figures 4C and 4D) when compared to the control, a strong indication that LUT results in increased lactate production, indicating a shift to aerobic glycolysis and possibly mitochondrial dysfunction. LDH was kept within control levels for IC₅₀ and IC₂₀ concentrations of all other treatments (Figures 4C) and suggests that EGCG, K7G and EGA did not induce membrane damage in HepG2 cells and that pyruvate was shunted to oxidative metabolism and ATP production (Figure 4A). In the HEK293 cells, this study showed significant reduction in the activities of extracellular LDH after treatment with IC₂₀ concentrations corresponding to unchanged or increased ATP was observed when compared to the control, indicating that cell viability was retained.

The ABCB1 transporter requires ATP to mediate the translocation of diverse substrates [34]. This study demonstrated the downregulatory effects of the compounds on the ABCB1 protein level in the HepG2 cells and was accompanied by increased mRNA expression at the IC₂₀ concentrations (Figures 5A and 5B). The ABCB1 protein downregulation is associated with sufficient ATP (Figure 4) to maintain the function of the protein, and thus may increase drug bioavailability, decrease the toxicity of the exposures and indicate a beneficial effect in terms of drug metabolism [35]. This depletion that is concurrent with ABCB1 gene upregulation may occur because of the inducible characteristic of the transporter [35].

The increased protein quantity of ABCB1 to varying degrees in HEK293 cells treated with the respective compounds (Figure 5C) was associated with decreased ATP concentration (although only significant for EGCG IC₅₀) (Figure 4B), with the exception of K7G where the expression was associated with increased ATP concentration (Figure 4B). The increase in protein concentration of ABCB1 in kidney cells was not surprising in light of kidney function to excrete drugs and metabolic products, and since ATP hydrolysis must occur to facilitate the translocation of substances into the tubular lumen for excretion [31]. In addition, the increased protein concentration in EGCG-treated cells was concurrent with increased mRNA expression for the compound; this suggests a role for the inducible efflux pump in removal of EGCG [35]. EGCG is a polyphenol that has been reported by several studies to modulate ABCB1 [36-38]. In this study, EGCG produced a concentration-dependent increase in the protein quantity of ABCB1 when compared with the control (Figure 5C), and concentration-dependent decrease in the level of ABCB1 mRNA amplicons in the RT-PCR (Figure 5D). Chieli *et al.* (2010) reported EGCG to decrease both the quantity and the expression of ABCB1 in HEK-2 cells [39], which would be beneficial to maintaining PI concentration. In contrast, in this study, EGCG upregulated the protein amount and ABCB1 mRNA expression in HEK293 cells. It may be that embryonic cells are adept at increasing the capacity to translocate xenobiotic molecules. The increased protein activity of ABCB1 in HEK293 cells treated with LUT and EGA are also attributed with the insignificant decrease in ATP concentration recorded for the two compounds.

CYP3A4 activation is associated with oxidation of xenobiotics into water-soluble intermediates that can be excreted [40]. This energy-requiring process is associated with activation of the *electron transport chain* (ETC) in healthy mitochondria and inhibition of AMP-dependent protein kinase α (AMPK α) [41]. Inhibition or decreased levels of CYP3A4 has been reported to activate AMPK α , thereby resulting in increased cellular ATP levels [41].

In other words, the activation or increase in the CYP3A4 protein expression deactivates AMPK α and eventually leads to decrease in intracellular ATP level.

The four compounds significantly increased CYP3A4 protein level at their respective IC₅₀ concentrations in the liver cell (Figure 6A) which may be attributed to the inducibility of CYP3A4 [42] and correlated to the insignificant decrease in the level of intracellular ATP produced in the cells. The IC₂₀ concentrations of the test compounds EGCG, K7G and LUT meaningfully and effectively decreased CYP3A4 protein activity in HepG2 cells (Figure 6A). This decreased CYP3A4 protein expression correlated with increased ATP levels in the liver cell (Figure 4A) and suggests that AMPK α activation cause by the reduced level of CYP3A4 resulted in a favourable increase in cellular ATP. Studies have shown EGCG to be an inhibitor of CYP3A4 activity [43, 44]. Since the other compounds also inhibit the function, perhaps this downregulation would be beneficial in combination with PI treatment. Only EGA and LUT demonstrated upregulation of the CYP3A4 mRNA expression, which could present a problem if it translates into increase in protein expression [9].

In this study, K7G, LUT and IC₅₀ of EGCG decreased the protein quantity of CYP3A4 when compared to the control in HEK293 cells (Figure 6C). With the exception of the IC₅₀ concentrations of K7G and EGA, and IC₂₀ of EGCG, all other treatments upregulated the inducible CYP3A4 gene. For CYP3A4 in the HEK293 cells and ABCB1 in the HepG2 cells, there was no correlation observed between the mRNA expressions and the protein activities results. Although the central dogma in molecular biology is DNA \rightarrow RNA \rightarrow proteins, [44], some studies observed inverse correlations between the mRNA expression and protein activities [45, 46]. Greenbaum *et al.* (2003) presumed some reasons for this inverse correlation [47]. Firstly, there is substantial difference in the *in vivo* half-lives of proteins; and

secondly, there are complicated and varied post-transcriptional mechanisms involved in the translation of mRNA into protein that have not yet been well defined [47, 48].

In summary, the compounds were not toxic to HepG2 cells at the IC₅₀ and IC₂₀ (ATP levels increased at IC₂₀, no significant change at IC₅₀, and no significant change in LDH with the exception of LUT, and ABCB1 protein activities decreased). However, while the compounds decreased CYP3A4 at IC₂₀, LUT increased CYP3A4 protein expression. All the compounds increased CYP3A4 at IC₅₀ in HepG2. Gene expression was decreased for EGCG and K7G at IC₂₀. For HEK293 cells, ATP concentration was similar to the control except for EGCG which decreased at IC₂₀, and K7G which increased at IC₅₀. Also, LDH decreased at IC₂₀ with minimal cytotoxicity, but significant ($P < 0.05$) increase was recorded in LUT IC₅₀. ABCB1 activities increased at both IC₂₀ and IC₅₀ concentrations, but LUT and EGA at IC₅₀ decreased gene expression. The decreased protein level of CYP3A4 in K7G IC₅₀ and LUT IC₂₀ correlates with increased intracellular ATP. This may therefore offer increased bioavailability of drugs in the long term.

5. CONCLUSION

The findings from the study generally showed that the compounds at both concentrations exhibited significant down regulatory influence on ABCB1 in liver cells compared to the HEK293 cells. This may be attributed to the vital role of liver in drug metabolism and the abundance of the two proteins in the liver. The decreased protein expression of ABCB1 at both concentrations and CYP3A4 at the IC₂₀ concentrations in treated liver cells corresponds with increase ATP in all treatments. This is significant because ATP is required for the activity of these drug-metabolising molecules and would translate to increased drug bioavailability and be beneficial in terms of drug metabolism. However, the significant increase in LDH for LUT indicates a cytotoxic effect. For HEK293 cells, at both IC₂₀ and

IC₅₀ concentrations, an increase in ABCB1 level is not surprising in light of kidney function, but gene expression decreased. The decrease in intracellular ATP level corresponds with increase in protein expression of ABCB1 in the kidney, this could be attributed to the usage of ATP for ABCB1 function. Furthermore, the decrease in protein activity of CYP3A4 in LUT, K7G and IC₅₀ of EGCG, which corresponds to an increase in intracellular ATP level in kidney cells, means drugs are not bio-transformed. This may therefore offer increased bioavailability of drugs in the long term. The decrease extracellular LDH for the compounds in the kidney (except for LUT at IC₅₀ concentration) indicate they are not cytotoxic to the kidney cells.

REFERENCES

1. Rate, S. M. K. Plants as source of drugs. *Toxicon*. 2001. 39, 603–613.
2. Weisburg, J. H., Weissman, D. B., Harvey, T. S. Invitro Cytotoxicity of Epigallocatechin Gallate and Tea Extracts to Cancerous and Normal Cells from the Human Oral Cavity. *Basic and Clin. Pharmacol. and Toxicol.* 2004. 95, 191–200.
3. Gokbulut, A.A., E. Apohan, and Y. Baran, Resveratrol and quercetin-induced apoptosis of human 232B4 chronic lymphocytic leukemia cells by activation of caspase-3 and cell cycle arrest. *Hematology*, 2013. **18**(3): p. 144-50.
4. James, P.B., et al., Traditional, complementary and alternative medicine use in Sub-Saharan Africa: a systematic review. *B.M.J Glob. Health*, 2018. **3**(5): p. e000895.
5. Gyasi, R. M., Tagoe-Darko, E., Mensah, C. M. Use of Traditional Medicine by HIV/AIDS Patients in Kumasi Metropolis, Ghana: A Cross-sectional Survey' *Amer. Int. J. of Contemp. Res.*; 2013. 3:117–129..
6. Kehinde, I., et al. The pharmacokinetic properties of HIV-1 protease inhibitors: A computational perspective on herbal phytochemicals. *Heliyon*, 2019. **5**(10): p. e02565.

7. Idowu, K., Pritika, R., Nlooto, M. and Gordon, M. Molecular dynamic mechanism(s) of inhibition of bioactive antiviral phytochemical compounds targeting cytochrome P450 3A4 and P-glycoprotein, *J. of Biomol. Struct. and Dyn.*, 2020. 1-11.
8. Griffin, L., P. Annaert, and K.L. Brouwer, Influence of drug transport proteins on the pharmacokinetics and drug interactions of HIV protease inhibitors. *J. Pharm. Sci*, 2011. **100**(9): p. 3636-54.
9. Marchetti, S., et al., Concise review: Clinical relevance of drug drug and herb drug interactions mediated by the ABC transporter ABCB1 (MDR1, P-glycoprotein). *Oncologist*, 2007. **12**(8): p. 927-41.
10. Ndhlala, A. R., Stafford, G. I., Finnie, J. F., Van Staden, J. Commercial herbal preparations in KwaZulu-Natal, South Africa: The urban face of traditional medicine. *South African J. of Botany*. 2011. 77; 830–843
11. Kim, S., Thiessen, P. A., Bolton, E. E., Chen, J., Fu, G., Gindulyte, A., Bryant, S. H. (2016). PubChem substance and compound databases. *Nucleic Acids Res.*, 44(1), 1202–1213.
12. Crouch, S.P. et al. The use of ATP bioluminescence as a measure of cell proliferation and cytotoxicity. *J. Immunol. Methods*. 1993. 160, 81–8.
13. Kumar P, Nagarajan A, Uchil PD. Analysis of Cell Viability by the Lactate Dehydrogenase Assay. *Cold Spring Harb. Protoc*. 2018. 1;2018(6).
14. Livak, K.J. and Schmittgen T.D. Analysis of relative gene expression data using real-time quantitative PCR and the 2^{(-Delta Delta C(T))} Method. *Methods*, 2001. **25**(4): p. 402-8.
15. Spiro, A.S., et al., Enhanced brain disposition and effects of Delta9-tetrahydrocannabinol in P-glycoprotein and breast cancer resistance protein knockout mice. *PLoS One*, 2012. **7**(4): p. e35937.

16. Fromm, M.F. Transporters and drug–drug interactions: Important determinants of drug disposition and effects. *Toxicol. Letters*, 2015. **238**(2).
17. Fleming, I. The pharmacology of the cytochrome P450 epoxygenase/soluble epoxide hydrolase axis in the vasculature and cardiovascular disease. *Pharmacol. Rev*, 2014. **66**(4): p. 1106-40.
18. Fromm, M.F. Importance of P-glycoprotein at blood-tissue barriers. *Trends Pharmacol. Sci.*, 2004. **25**(8): p. 423-9.
19. Walubo, A. The role of cytochrome P450 in antiretroviral drug interactions. *Expert Opin. Drug Metab. Toxicol.* 2007. **3**(4):583-598.
20. Weiss, J. and Haefeli W.E. Impact of ATP-Binding Cassette Transporters on Human Immunodeficiency Virus Therapy. *Intl. Rev. of Cell and Mol. Bio.*, 2010. p. 219-279.
21. Ferro, M., Doyle, A. Standardisation for In Vitro Toxicity Tests. *Cell Biol. Toxicol* **17**, 205–212 (2001).
22. Sato,Y.Sasaki, N., Saito, M., Endo, N., Kugawa, F., Ueno, A. Luteolin Attenuates Doxorubicin-Induced Cytotoxicity to MCF-7 Human Breast Cancer Cells. *Biol. Pharm. Bull.* 2015.38, 703–709.
23. Selvendiran, K., et al., Luteolin promotes degradation in signal transducer and activator of transcription 3 in human hepatoma cells: an implication for the antitumor potential of flavonoids. *Cancer Res.*, 2006. **66**(9): p. 4826-34.
24. Uesato, S., Kitagawa, Y., Kamishimoto, M., Kumagai, A., Hori, H., Nagasawa, H. Inhibition of green tea catechins against the growth of cancerous human colon and hepatic epithelial cells. *Cancer Lett.*, 2001. **170**, 41–44.
25. Takada, M., Nakamura, Y., Koizumi, T., Toyama, H., Kamigaki, T., Suzuki, Y., Takeyama, Y., Kuroda, Y. Suppression of human pancreatic carcinoma cell growth and invasion by epigallocatechin-3-gallate. *Pancreas*; 2002. **23**, 45–48.

26. Patravale, V., Dandekar, P. and Jain R., Nanotoxicology: evaluating toxicity potential of drug-nanoparticles, in Nanoparticulate Drug Delivery. 2012. p. 123-155. **ISBN: 9781908818195**
27. Gray, L.R., Tompkins S.C. and Taylor, E.B., Regulation of pyruvate metabolism and human disease. *Cell Mol. Life Sci.*, 2014. **71**(14): p. 2577-604.
28. Riss, T., Moravec, R. Introducing the CytoTox-ONE homogeneous membrane integrity assay. *CellNotes*. 2002. 4:6–9.
29. Huber, J.M., et al., Evaluation of assays for drug efficacy in a three-dimensional model of the lung. *J. Cancer Res. Clin. Oncol.*, 2016. **142**(9): p. 1955-66.
30. Requardt, H., et al. Surface defects reduce Carbon Nanotube toxicity in vitro. *Toxicol In Vitro*, 2019. **60**: p. 12-18.
31. Zhang, J., Han X., and Lin Y. Dissecting the regulation and function of ATP at the single-cell level. *PLoS Biol*, 2018. **16**(12): p. e3000095.
32. Pathak, D., et al., The role of mitochondrially derived ATP in synaptic vesicle recycling. *J. Biol Chem*, 2015. **290**(37): p. 22325-36.
33. Chan, F.K., Moriwaki, K., and De Rosa, M.J. Detection of necrosis by release of lactate dehydrogenase activity. *Methods Mol. Biol.*, 2013. **979**: p. 65-70.
34. Szollosi, D., et al., Comparison of mechanistic transport cycle models of ABC exporters. *Biochim. Biophys. Acta Biomembr.*, 2018. **1860**(4): p. 818-832.
35. Masereeuw, R. and Russel, F.G. Regulatory pathways for ATP-binding cassette transport proteins in kidney proximal tubules. *AAPS J.*, 2012. **14**(4): p. 883-94.
36. Mei, Y., et al., Reversal of cancer multidrug resistance by green tea polyphenols. *J. Pharm. Pharmacol.*, 2004. **56**(10): p. 1307-14.
37. Farabegoli, F., et al., (-)-Epigallocatechin-3-gallate downregulates Pg-P and BCRP in a tamoxifen resistant MCF-7 cell line. *Phytomedicine*, 2010. **17**(5): p. 356-62.

38. Yang, C. S., Pan, E. The effects of green teapolyphenols on drug metabolism. *Expert Opin. Drug Metab. Toxicol.* 2012 8(6):677-689.
39. Chieli, E., et al., In vitro modulation of ABCB1/P-glycoprotein expression by polyphenols from *Mangifera indica*. *Chem. Biol. Interact.*, 2010. **186**(3): p. 287-94.
40. Lynch, T., Price, M. The Effect of Cytochrome P450Metabolism on Drug Response,Interactions, and Adverse Effects. *Amer. Family Phys.n*, 2007. 76, 3. Pg 391-398.
41. Guo, Z., et al., Heme Binding Biguanides Target Cytochrome P450-Dependent Cancer Cell Mitochondria. *Cell Chem. Biol.*, 2017. **24**(10): p. 1314.
42. Kuang, Z., et al., Overexpression of CYP3A5 attenuates inducibility and activity of CYP3A4 in HepG2 cells. *Mol. Med. Rep.*, 2015. **11**(4): p. 2868-74.
43. Netsch, M.I., et al., Induction of CYP1A by green tea extract in human intestinal cell lines. *Planta Med.*, 2006. **72**(6): p. 514-20.
44. Wanwimolruk, S., Wong, K., Wanwimolruk, P. Variable inhibitory effect of different brands of commercial herbal supplements on human cytochrome P-450 CYP3A4. *Drug Metabol. Drug Interact.*, 2009. 24(1):17-35.
45. Gry, M., et al., Correlations between RNA and protein expression profiles in 23 human cell lines. *BMC Genomics*, 2009. **10**: p. 365.
46. Lichtinghagen, R., Musholt, P. B., Lein, M., Romer, A., Rudolph, B., Kristiansen, G.,Hauptmann, S, Schnorr, D., Leoning, S. A., Jung, K. Different mRNA and protein expression of matrix metalloproteinases 2 and 9 and tissue inhibitor of metalloproteinases 1 in benign and malignant prostate tissue. *Eur. Urol.* 2002. Oct;42(4):398-406.
47. Greenbaum, D., Colangelo, C., Williams, K., Gerstein, M. Comparing protein abundance and mRNA expression levels on a genomic scale. *Genome Biol.*, (2003), 4, Issue 9, pg 117-124

48. Baldi, P., Long, A. D. A Bayesian framework for the analysis of microarray expression data: regularized t-test and statistical inferences of gene changes. *Bioinformatics*. 2001. 17. 6. Pg 509–519.

CHAPTER SIX

This is the synthesis chapter of this thesis, the different findings from the study were highlighted, piece together and place the study in the broader context. And the summary of the research objectives and the main findings presented.

SYNTHESIS

Substantial evidence from the literature have established there is high prevalence of HIV in Africa, with Sub-Saharan Africa having the highest prevalence worldwide [1]. It has further been shown that a high percentage of African populations depend on THMs for primary healthcare, and there is an increase in the usage of THMs concomitantly with conventional ARVs among people living with HIV [2, 3]. The herb-drug interactions could adversely affect the concentration of the ARVs, while there is also the potential for beneficial effects of the THMs. These potential interactions prompted the investigation of the pharmacokinetic and modulatory influences of selected PCs from THMs on a drug-metabolising enzyme (CYP3A4) and transporter (P-gp/ABCB1) involved in the metabolism of commonly used HIV PIs. Likewise, the cytotoxicity and cell viability of these compounds in two human cell line models were evaluated. In addition, the inhibitory activities of these PCs against a South African subtype C HIV-1 protease enzyme were investigated by employing computational tools.

CYP3A4 and P-gp are crucial drug metabolising proteins involved in the metabolism of the HIV-1 PIs (DRV, LPV, ATV and SQV) [4-7]. Interestingly, many PIs such as ATV, LPV, AMP and RTV have also been reported to be inhibitors of P-gp and CYP3A4 [4, 8-10]. P-glycoprotein is an ATP-dependent efflux pump encoded by the ABCB1 mRNA [11]. This important drug transporter is associated with rapid uptake and elimination of drugs such as HIV protease inhibitors (PIs) [10]. CYP3A4 is responsible for metabolising of approximately 30-55% of all drugs [12], including PIs [10]. Inhibition or down-regulation of their protein activities and mRNA expression will enhance the maintenance of optimal plasma drug concentrations and ultimately improve the drug's therapeutic effects. From this study, it was shown that many of the selected PCs (NGN, GER, FST, LUT, PTA, APG, GA and IST) were

also metabolised by either CYP3A4 or P-gp, and were also predicted to be substrates, inducers or inhibitors of CYP3A4 and P-gp.

A Molecular dynamics study to investigate the potential inhibitory activities of the fifteen selected PCs against South African sub-type C HIV-1 protease enzyme (*HIVpro*) showed that four PCs (EGCG, K7G, LUT and EGA) possess similar binding energies to the FDA-approved PIs, with EGCG having better energy than three conventional PIs (DRV, LPV and SQV) as well as the other PCs. Both the results from the free binding energies and structural stability analyses (RMSD, RoG, RMSF and receptor-interaction plots) of these four PCs against *HIVpro* enzyme after 100 ns of simulations revealed they are capable of binding to South African sub-type C HIV-1 protease enzyme, and enhance the enzyme's stability. Its effect on protease inhibition warrants further investigation.

Further, the molecular dynamic mechanism(s) of inhibition of the four PCs (EGCG, K7G, LUT and EGA) targeting the catalytic site of CYP3A4 and nucleotide-binding domains of P-gp were investigated, The findings from the ligand-receptor interaction analysis showed that EGCG and K7G possessed better inhibitory activities against CYP3A4 and P-gp than EGA and LUT. While they were not better than ritonavir, they were only slightly lower and could potentially have a similar effect on inhibition. This finding is significant because the inhibition of the activities of efflux transporter and drug metabolising enzyme of ARVs are an important strategy in increasing the concentrations of ARVs in sanctuary sites.

The reported significant findings of the *in silico* studies necessitated the evaluation of the effects of the four promising antiviral plant-derived compounds (EGCG, K7G, LUT and EGA) on cytotoxicity (MTT and LDH assays), cell viability profiles (ATP) and regulatory influences on the mRNA expression and protein activities of CYP3A4 and ABCB1 (qPCR and western blotting) in two human cell lines (liver (HepG2) and kidney (HEK293)). The

effects of these potential anti-HIV PCs on organs (such as liver and kidney) and vital drug-metabolising proteins like CYP3A4 and ABCB1 are largely unknown. This study is the first to report the effects of K7G on these drug-metabolising proteins, while few studies have reported on LUT. The MTT assay was used to calculate optimum treatment concentrations at 80% (IC₂₀) and 50% (IC₅₀) cell viability for each compound after cells were treated with the compounds at different concentrations for 24 hours. From the MTT assay, the dose-response curves obtained indicate that K7G, EGA and LUT are less toxic to HepG2 cells at the highest concentration (400µM) tested and thus had high extrapolated IC₅₀ concentrations. However, the relatively low IC₅₀ obtained for EGCG in HepG2 cells demonstrates sensitivity to the effects of EGCG. On the other hand, HEK293 cells were sensitive to the effects of K7G, LUT and EGA, but tolerant of EGCG that yielded a high IC₅₀. However, the IC₂₀ concentrations for each of the PCs were low in both cell lines, an indication that these concentrations (IC₂₀) could be used to exploit the potential therapeutic effects of the compounds. Cell viability (ATP) assay showed the four PCs at their respective IC₅₀ and IC₂₀ are not toxic to Hep-G2 cells. Interestingly, in the liver cells except for LUT (IC₅₀), the LDH levels were not significantly altered when compared to the control, indicating no cell membrane damage. In HEK-293 cells, cell viability assay (ATP) also revealed that the PCs at both IC₂₀ and IC₅₀ (except EGCG at IC₅₀) concentrations are not cytotoxic to HEK-293. The LDH result further showed that the PCs are not toxic and safe at both IC₅₀ and IC₂₀ concentrations in HEK-293 and Hep-G2 cells, with the exception of LUT at IC₅₀, which significantly increase LDH level in both cells. This suggests increased lactate production, indicating a shift to anaerobic metabolism and possibly implies mitochondrial dysfunction in cells treated with LUT at IC₅₀. However, findings from this study showed that the four compounds are less cytotoxic at IC₂₀ concentrations and may thus prove safe to use.

The study generally showed that the compounds at both concentrations exhibited significant down-regulatory influence on ABCB1 in liver cells compared to the HEK293 cells, and the decrease in protein level of CYP3A4 in LUT, K7G and IC₅₀ of EGCG in the kidney cells, means drugs are not bio-transformed. This would translate to increased drug bioavailability and be beneficial in terms of drug metabolism. Our results showed that the PCs at their respective IC₂₀ significantly down-regulate protein activity of ABCB1 in the liver cells. And also, EGCG, K7G, LUT at their IC₂₀ concentrations down-regulate CYP3A4 protein level in the liver (the main organs involved in the metabolism of drugs) and increases ATP levels. These are significant findings, as the compounds at their IC₂₀ are not toxic to the liver cell and increase ATP level which is required for the activity of these drug-metabolising molecules. This might also translate to increased drug bioavailability (such as increasing the concentrations of ARVs in the sanctuary sites and in the plasma) and be beneficial in terms of drug metabolism. At IC₅₀ concentrations, the four PCs significantly increased CYP3A4 protein activity in the liver cell which could be attributed to the inducibility of CYP3A4 [13] and correlated to the insignificant change in the level of intracellular ATP produced in the cells. Inverse correlation between the mRNA expressions and the protein activities was observed for CYP3A4 in the HEK293 cells and ABCB1 in the HepG2 cells. Even though the general theory of molecular biology says mRNA contains information needed for the production of proteins through biological process of translation, however, inverse correlations between the two have been reported in studies [14, 15]. Certain factors such as post-transcription mechanisms involved in the translation of mRNA into protein could contribute to the inverse correlation [16]. The duration of the mRNA in the cytosol, initialisation of translation (which is regulated by eukaryotic initiation factor-2 (elf-2)), the readiness of the ribosome to attach the mRNA and the regulation by microRNAs are other factors that could contribute to the inverse correlation between mRNA expression and protein level [17-20]. In

this instance, the results of the protein activity are considered to be significant, being the final product of protein translation process.

Unlike in HepG2 cells, the PCs at both IC₂₀ and IC₅₀ concentrations increase ABCB1 quantity in HEK293 cells. These observations in the kidney cells are not surprising considering the function of the kidney cells as an excretory organ. LUT and EGA (at both concentrations), EGCG and K7G at IC₂₀ showed insignificant change (sufficient ATP is available to carry out vital cellular processes) in intracellular ATP level in the HEK293 cells treated with the PCs. This insignificant change in ATP level correlated with increase in protein expression of ABCB1 in the kidney, which might be attributed to the usage of ATP for ABCB1 function. The study further showed that K7G and LUT at lower concentrations, and LUT, K7G and EGCG at IC₅₀ could decrease protein level of CYP3A4 in HEK293 cells and would enhance increase bioavailability.

References

1. UNAIDS. AIDSinfo.unaids.org. 2019. https://www.avert.org/global-hiv-and-aids-statistics#footnote1_qlt481t. (Accessed 10/01//2020).
2. Gyasi, R. M., Tagoe-Darko, E., Mensah, C. M. *Use of Traditional Medicine by HIV/AIDS Patients in Kumasi Metropolis, Ghana: A Cross-sectional Survey*. American Int. J. of Contemp. Res. 2013. 3:117–129.
3. Nlooto, M. and Naidoo, P. *Types of Traditional , Complementary and Alternative Medicines and Reasons for Their Use by HIV-Infected Patients in KwaZulu-Natal Province : A Cross- Sectional Study*. BMC. 2017. 31 (1): 141–61.
4. Walubo, A. *The role of cytochrome p450 in antiretroviral drug interactions*. Expert Opin. Drug Metab. Toxicol. 2007. 3: 583-598.
5. Meyer, Zu Schwabedissen H., Kim, R., *Hepatic OATP1B transporters and nuclear receptors PXR and CAR: interplay, regulation of drug disposition genes, and single nucleotide polymorphisms*. Mol. Pharm. 2009. 6(6):1644–1661.
6. Pal, D, Mitra, A. *MDR- and CYP3A4-mediated drug-drug interactions*. J. Neuroimmune Pharmacol. 2006. 1(3):323–339.
7. Van Waterschoot, R., Ter Heine, R., Wagenaar, E., Van Der Kruijssen, C., Rooswinkel, R., Huitema, A., Beijnen, J., Schinkel, A. *Effects of cytochrome P450 3A (CYP3A) and the drug transporters Pglycoprotein (MDR1/ABCB1) and MRP2 (ABCC2) on the pharmacokinetics of lopinavir*. Br. J. Pharmacol. 2010. 160(5):1224–1233.

8. Janneh, O., Jones, E., Chandler, B., Owen, A., Khoo, S. H. *Inhibition of P-glycoprotein and multidrug resistance-associated proteins modulates the intracellular concentration of lopinavir in cultured CD4 T cells and primary human lymphocytes.* J Antimicrob. Chemother., 2007. 60(5): p. 987-93.
9. Bierman, W., George, L., Scheffer, A. S., Gerrit, J., Michiel, A. A., Sven, A. D., Rik, J. S. *Protease inhibitors atazanavir, lopinavir and ritonavir are potent blockers, but poor substrates, of ABC transporters in a broad panel of ABC transporter-overexpressing cell lines.* Antimicrob. Chemother., 2010. 65: 1672 –1680.
10. Fromm, M. F., *Importance of P-glycoprotein at blood-tissue barriers.* Trends Pharmacol. Sci., 2004. 25(8): p. 423-9.
11. Spiro, A.S. *Enhanced brain disposition and effects of Delta9-tetrahydrocannabinol in P-glycoprotein and breast cancer resistance protein knockout mice.* PLoS One. 2012.7(4): p. e35937.
12. Fleming, I., *The pharmacology of the cytochrome P450 epoxygenase/soluble epoxide hydrolase axis in the vasculature and cardiovascular disease.* Pharmacol. Rev., 2014. 66(4): p. 1106-40.
13. Kuang, Z., et al., *Overexpression of CYP3A5 attenuates inducibility and activity of CYP3A4 in HepG2 cells.* Mol. Med. Rep., 2015. 11(4): p. 2868-74.
14. Lichtinghagen, R., Musholt, P. B., Lein, M., Romer, A., Rudolph, B., Kristiansen, G., Hauptmann, S, Schnorr, D., Leoning, S. A., Jung, K. *Different mRNA and protein expression of matrix metalloproteinases 2 and 9 and tissue inhibitor of metalloproteinases 1 in benign and malignant prostate tissue.* Eur. Urol. 2002. Oct;42(4):398-406.

15. Baldi, P., Long, A. D. *A Bayesian framework for the analysis of microarray expression data: regularized t-test and statistical inferences of gene changes*. *Bioinformatics*. 2001. 17. 6. Pg 509–519.
16. Greenbaum, D., Colangelo, C., Williams, K., Gerstein, M. *Comparing protein abundance and mRNA expression levels on a genomic scale*. *Genome Biol.*, 2003. 4, 9, 117-124.
17. John W.B. Hershey, Nahum Sonenberg, Michael B. Mathews. *Principles of Translational Control: An Overview*. Cold Spring Harb. Perspect. Biol., 2012. 4(12): a011528.
18. Braun, J. E., Huntzinger, E., & Izaurralde, E. *A Molecular Link between miRISCs and Deadenylases Provides New Insight into the Mechanism of Gene Silencing by MicroRNAs*. Cold Spring Harb. Perspectives in Biol., 2012. 4(12), a012328–a012328.
19. Hinnebusch, A. G., & Lorsch, J. R. *The Mechanism of Eukaryotic Translation Initiation: New Insights and Challenges*. Cold Spring Harb. Persp. in Biol., 2012.4(10), a011544–a011544.
20. Pavitt, G. D., & Ron, D. *New Insights into Translational Regulation in the Endoplasmic Reticulum Unfolded Protein Response*. Cold Spring Harb. Persp. in Biol., 2012. 4(6), a012278–a012278.

CHAPTER SEVEN

This is the concluding chapter of this thesis, the study conclusion was presented and the recommendations for further research also presented.

CONCLUSION AND RECOMMENDATIONS

7.0 Conclusion

The concomitant use of THMs with orthodox medicine is gaining more acceptance and recognition in the treatment of numerous diseases which include HIV in several countries of the world. This study has described the pharmacokinetic and modulatory influences of some selected bioactive PCs present in THMs used by HIV-positive patients in South Africa on the drug-metabolising proteins involved in the metabolism of HIV-1 protease inhibitor drugs (PIs). The study corroborated existing studies that CYP3A4 and P-gp are actively involved in the metabolisms of commonly prescribed PIs, and further established that some of these PCs present in THMs are metabolised by either CYP3A4, or P-gp, or both. In addition, molecular dynamic study also showed that four of the selected PCs showed good binding affinity towards South African Sub-type C HIV-1 protease enzyme.

In another *in silico* study that examine the inhibitory activity of the four antiviral PCs, the results showed that three (EGCG, EGA and K7G) out of the four PCs showed more similarity with RTV in their interaction with CYP3A4, and two (K7G and EGCG) showed similar interactions with RTV in P-gp systems. The study, thereby, suggests that EGCG and K7G might be a suitable substitute for RTV in its use as a booster for HIV protease drugs where it is known to increase the optimal concentration of HIV PIs in the systemic circulation. RTV inhibits the pumping out and the rate of metabolism of HIV PIs from the circulating system thereby, enhancing the therapeutic effect of the PI drugs.

An *in vitro* study was performed to follow up the encouraging results of the *in silico* studies to evaluate the modulatory influences of four PCs (EGCG, K7G, LUT and EGA) present in some of the herbal medicines used by HIV positive patients in South Africa on the protein activities and mRNA expressions of CYP3A4 and ABCB1 in conjunction with their

cytotoxicity and cell viability profiles in two human cell lines (HEK293 and HepG2). Findings from the study showed that the four PCs are less cytotoxic at their respective IC₂₀ concentrations, decrease the biotransformation of drugs, could increase drug plasma concentrations in the systemic circulation and may thus prove safe to use. At IC₅₀ concentrations, K7G, LUT and EGA are sensitive to HEK-293, while EGCG is sensitive to Hep-G2 cells. The findings further revealed that elimination of drugs could be decreased, and bioavailability could be increased by IC₅₀ concentrations of LUT, K7G and EGCG.

This study is the first to report the effects of K7G on these drug-metabolising proteins. Our results showed that K7G at IC₂₀ concentrations significantly down-regulate protein activity of ABCB1 and CYP3A4 in the liver cells and increases ATP levels. The study further showed that K7G at IC₂₀ and IC₅₀ concentrations could decrease protein activity of CYP3A4 in HEK293 cells. These are significant findings, as the K7G at IC₂₀ is not toxic to the liver cell and enhance ATP level which is required for the activity of these drug-metabolising proteins, and would enhance increase bioavailability.

The study showed that some of the selected bioactive PCs possess potential dual inhibitory activities against both the two drug-metabolising proteins and South African subtype C HIV-1 protease enzyme, thereby making them promising lead agents in HIV treatments. These natural compounds can serve as inhibitors of the drug metabolizing proteins and eventually boost the bioavailability of HIV-1 PIs in the plasma and sanctuary sites.

7.1 Recommendations

This work has described the pharmacokinetic and modulatory influences of the PCs from THMs on drug-metabolising enzyme and transporter of HIV-1 PIs in both *in-silico* and *in vitro* studies. Therefore, further *in vitro* studies are needed to investigate and determine the antiviral and inhibitory activities of these PCs against HIV-1 protease enzyme and drug-

metabolism proteins. This work also recommends similar *in silico*, *in vitro* and clinical studies that involve other ARVs such as integrase inhibitors and Non-nucleoside reverse transcriptase inhibitors (NNRTIs) drugs to be carried out. Since these compounds showed good inhibitory activities against P-gp and CYP3A4, this work recommends that a similar study using these compounds should be done on multidrug resistance in cancer patients since over-expression of P-gp and over induction of CYP3A4 have been reported in cancer patients failing therapy. An additional investigation into the effects of these compounds on cell cycle arrest and their mechanism(s) of exerting cytotoxicity is recommended.

APPENDICES

Appendix A: Chapter 3 supporting information.

Appendix B: Chapter 4 supporting information.

Appendix C Input files for MD simulations for Chapter 3 and 4.

Appendix D: Chapter 5 supporting information.

Appendix E: Published manuscript (Chapter 3).

Appendix F: Published manuscript (Chapter 4).

Appendix G: Ethical Approval

Appendix A

Chapter 3 supporting information

A.2 Select docked complex structures of ligand-*HIVpro* used for molecular dynamic simulations

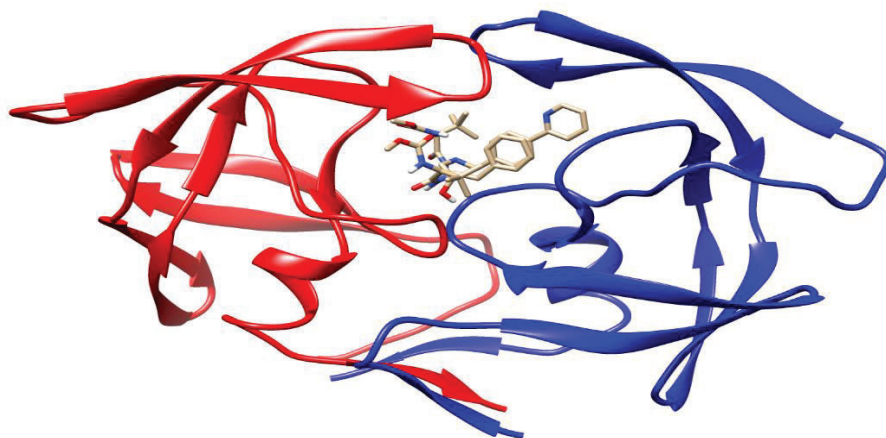


Figure 1: The selected docked structure for ATZ-*HIVpro*

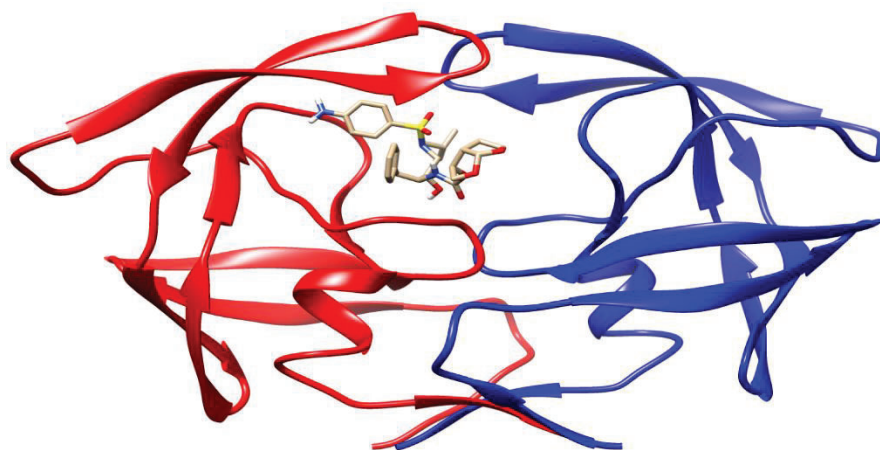


Figure 2: The selected docked structure for DRV-*HIVpro*

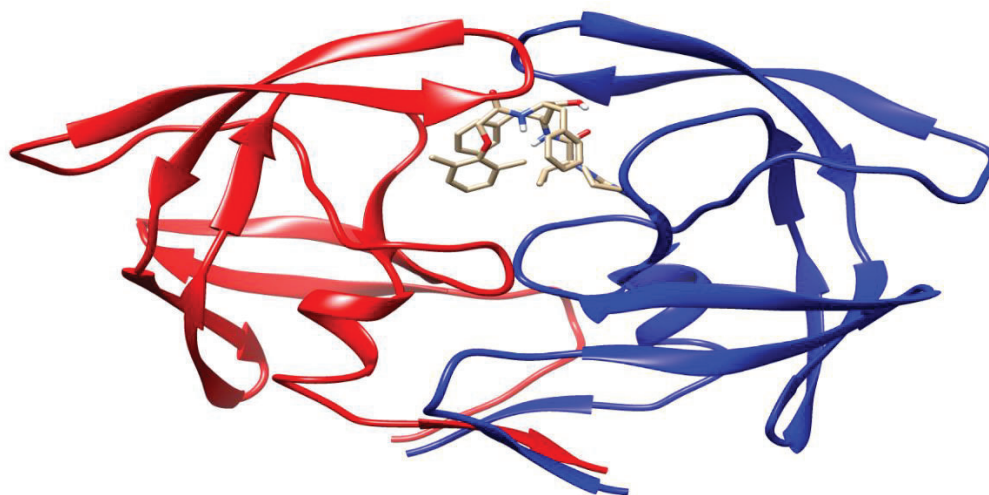


Figure 3: The selected docked structure for LPV-*HIVpro*

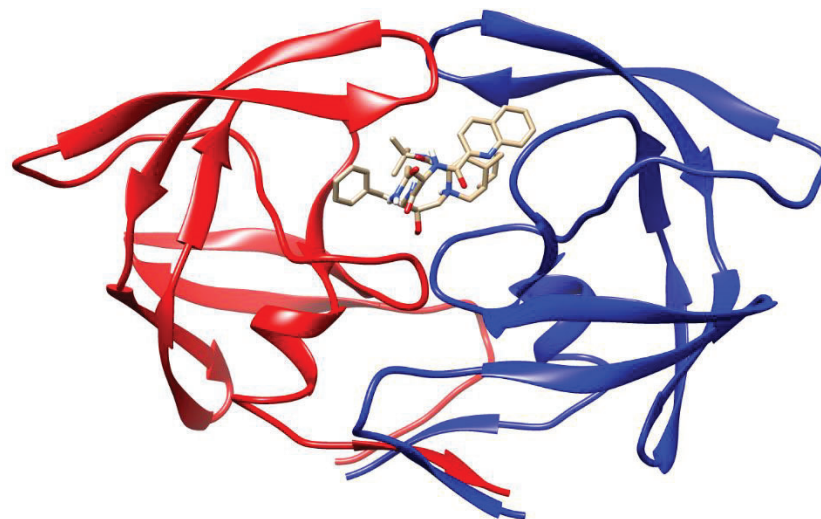


Figure 4: The selected docked structure for SQV-*HIVpro*

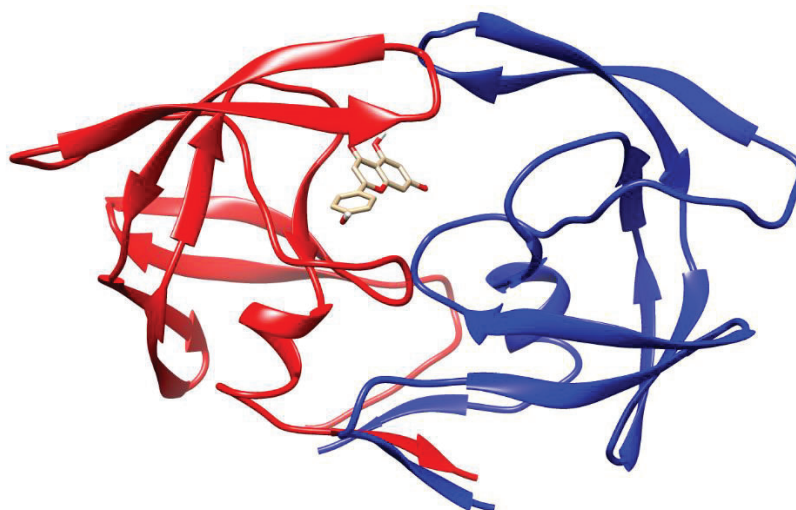


Figure 5: The selected docked structure for APG-*HIVpro*

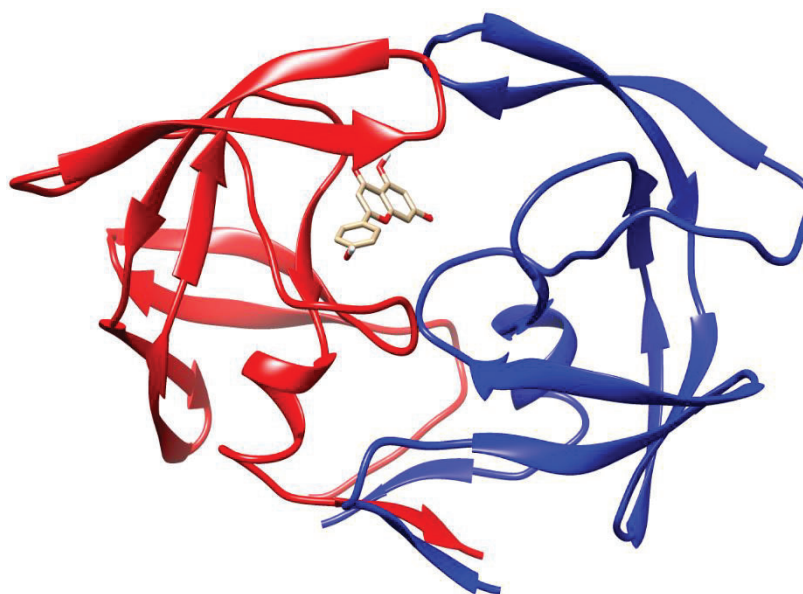


Figure 6. The selected docked structure for BIT-*HIVpro*

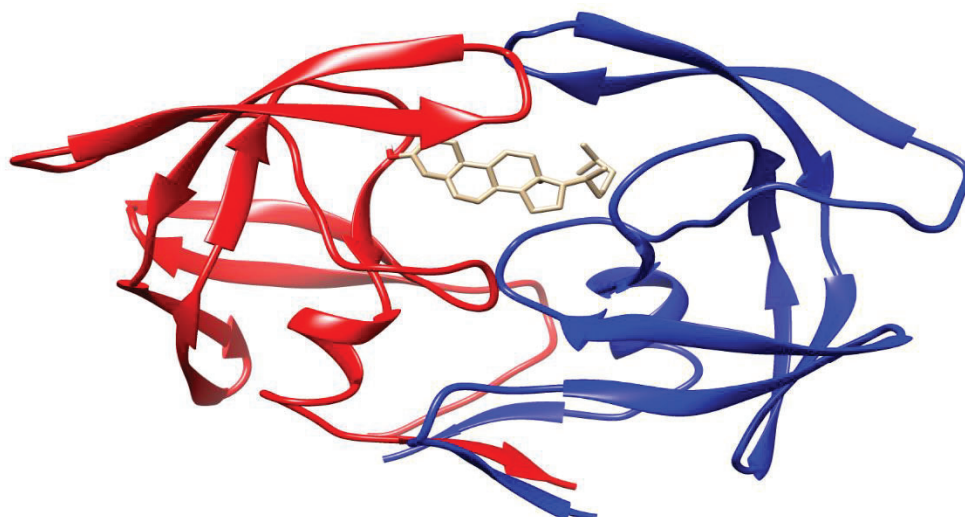


Figure 7. The selected docked structure for CHD-*HIVpro*

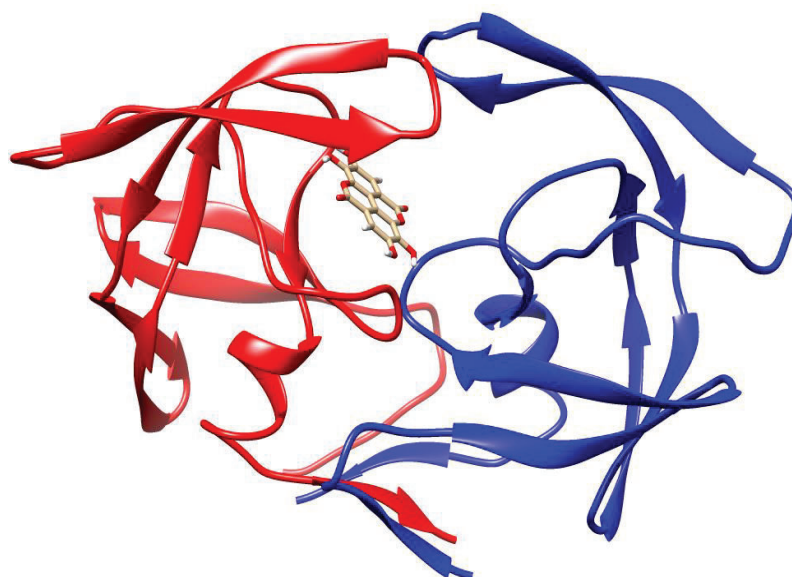


Figure 8. The selected docked structure for EGA-*HIVpro*

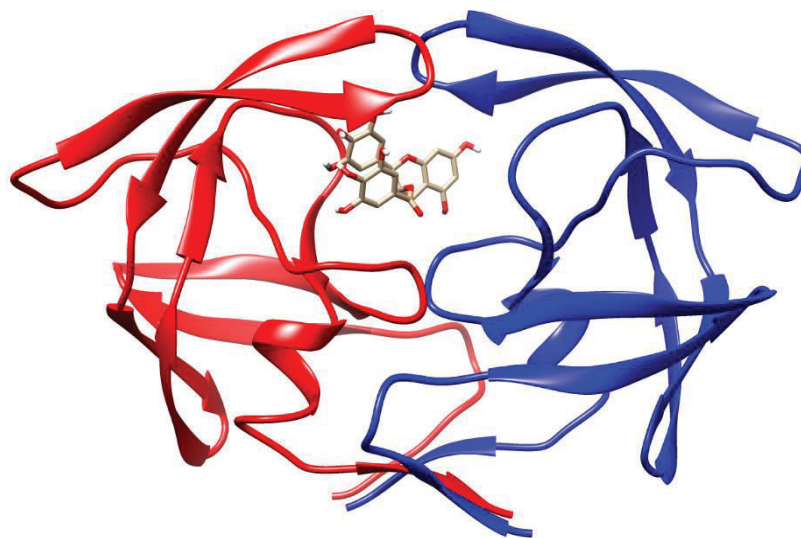


Figure 9. The selected docked structure for EGCG-*HIVpro*

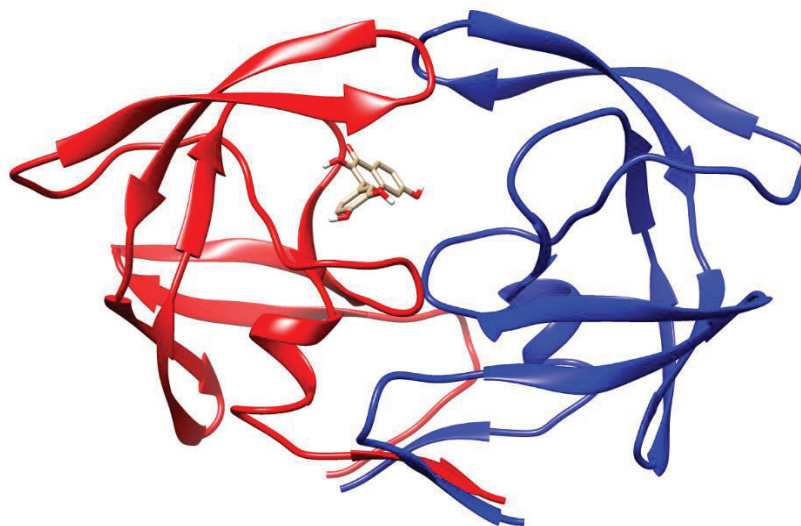


Figure 10. The selected docked structure for FST-*HIVpro*

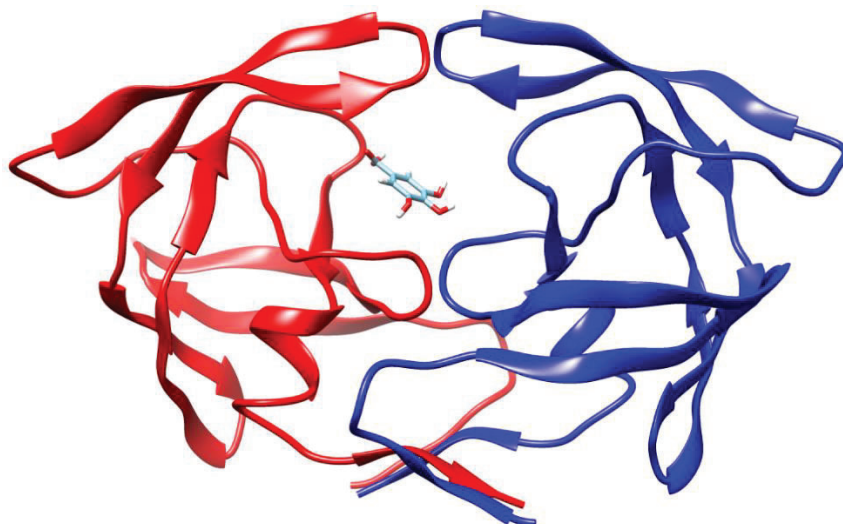


Figure 11. The selected docked structure for GA-*HIVpro*

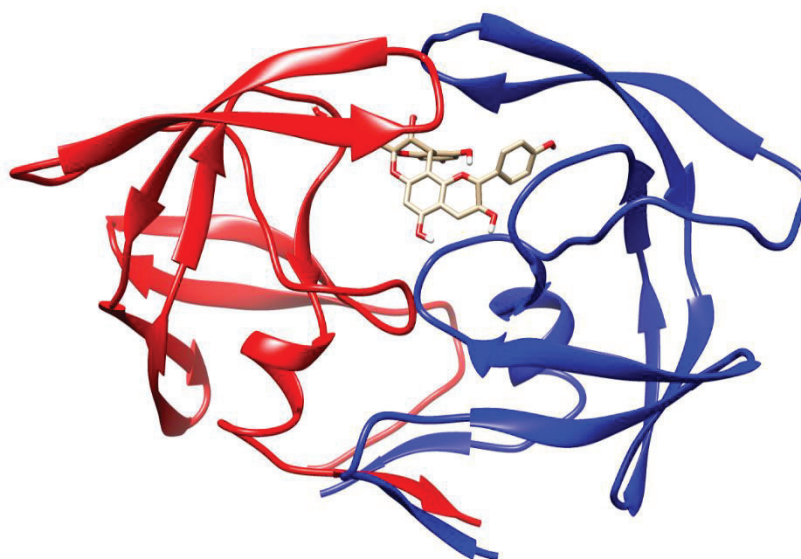


Figure 12. The selected docked structure for GER-*HIVpro*



Figure 13. The selected docked structure for K7G-*HIVpro*

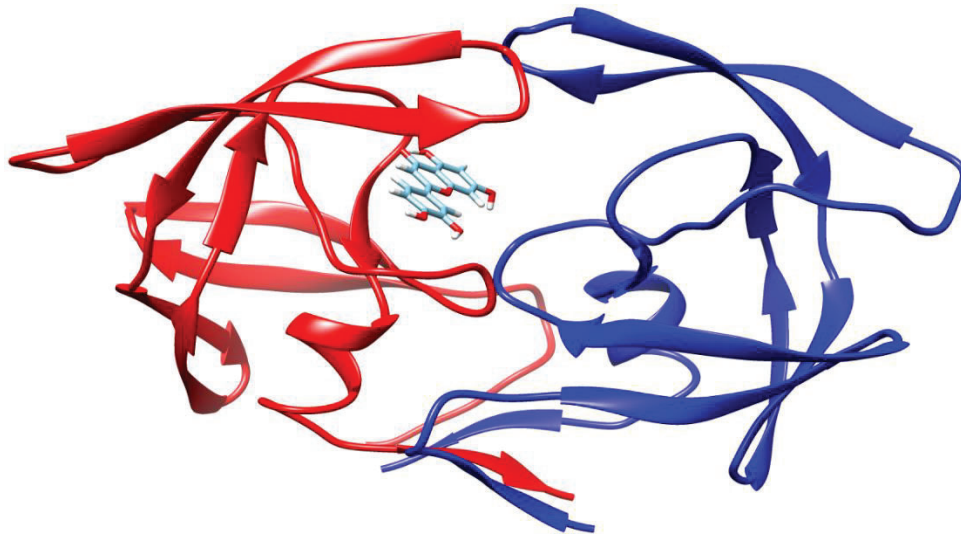


Figure 14. The selected docked structure for K7G-*HIVpro*



Figure 15. The selected docked structure for NGN-*HIVpro*

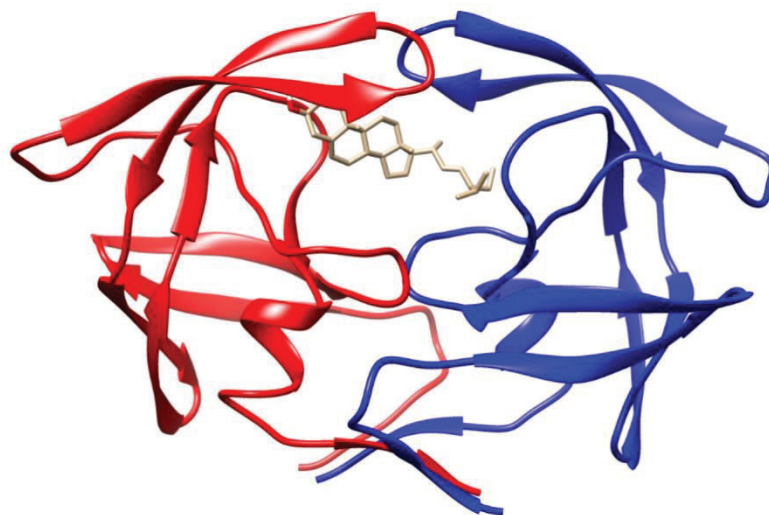


Figure 16. The selected docked structure for STG-*HIVpro*



Figure 17. The selected docked structure for PTA-*HIVpro*

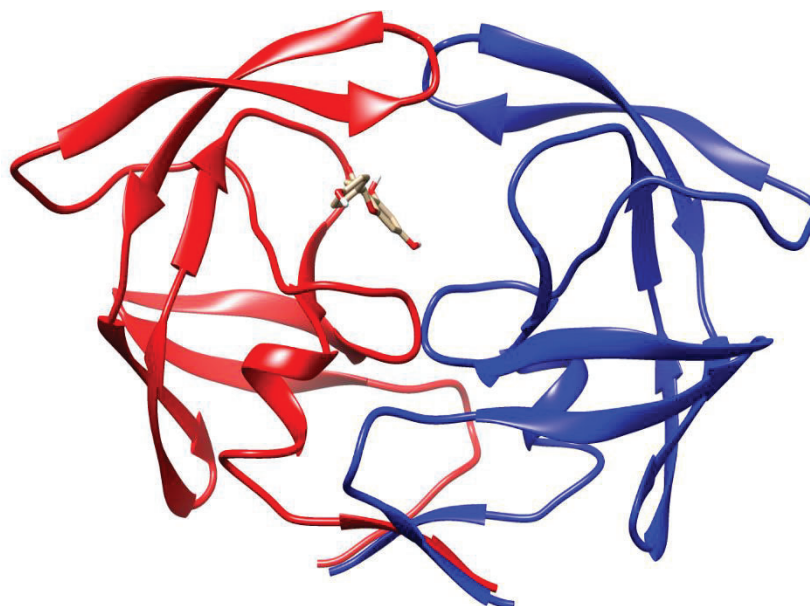


Figure 18. The selected docked structure for IST-*HIVpro*

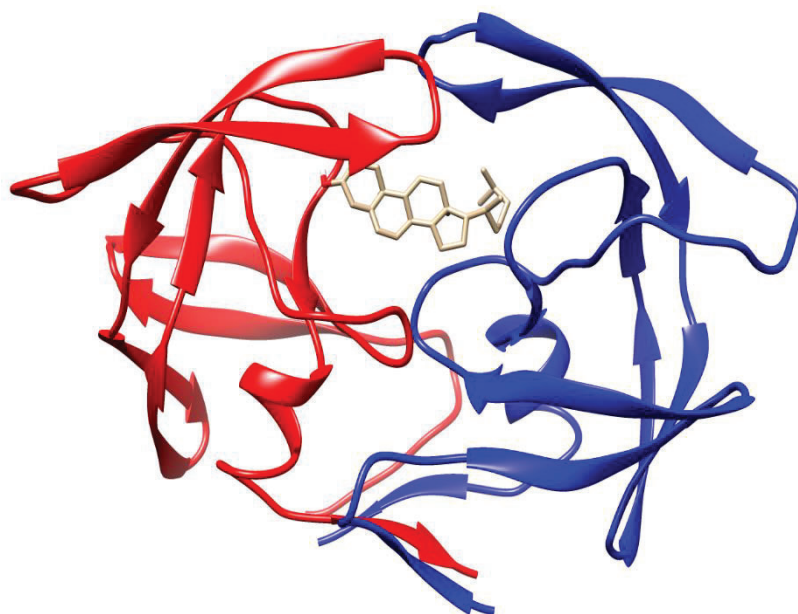


Figure 19. The selected docked structure for LNT-*HIVpro*

Appendix B

Chapter 4 supporting information

B.1 Select docked complex structures Ligand-CYP3A4 used for molecular dynamic simulations

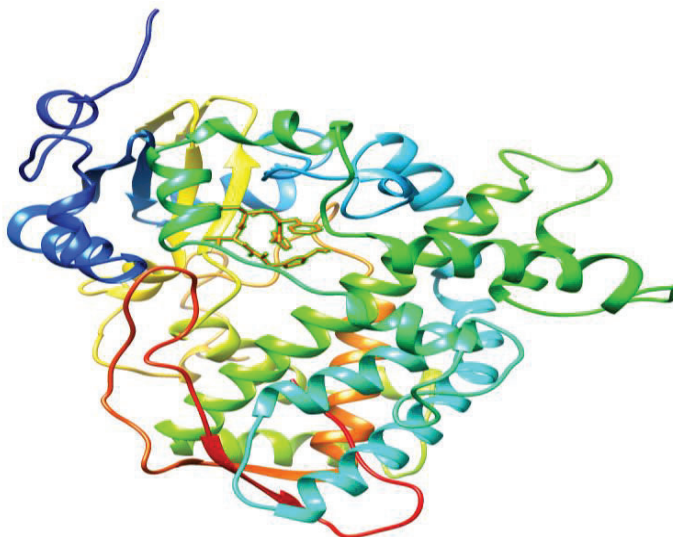


Figure 20. The selected docked structure for RTV-CYP3A4

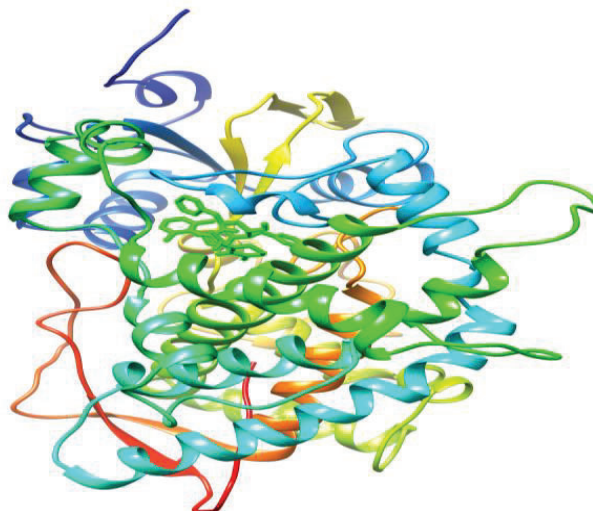


Figure 21. The selected docked structure for RTV-CYP3A4

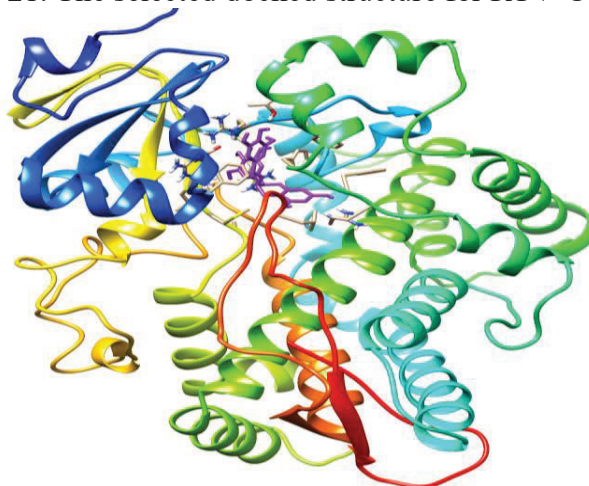


Figure 22. The selected docked structure for EGCG-CYP3A4

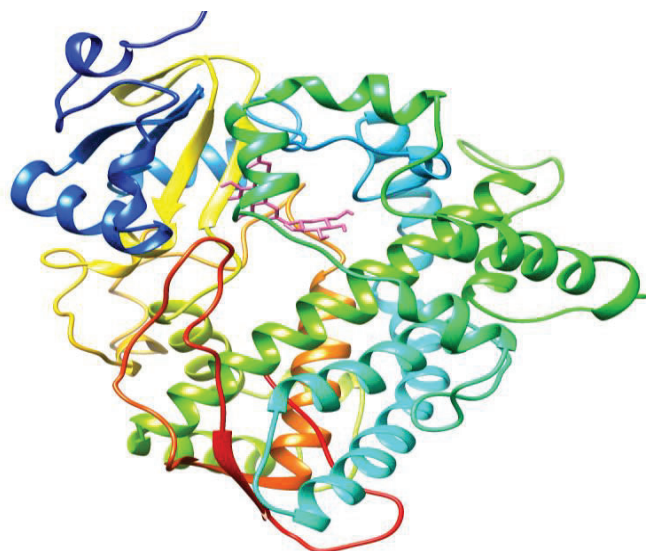


Figure 23. The selected docked structure for K7G-CYP3A4

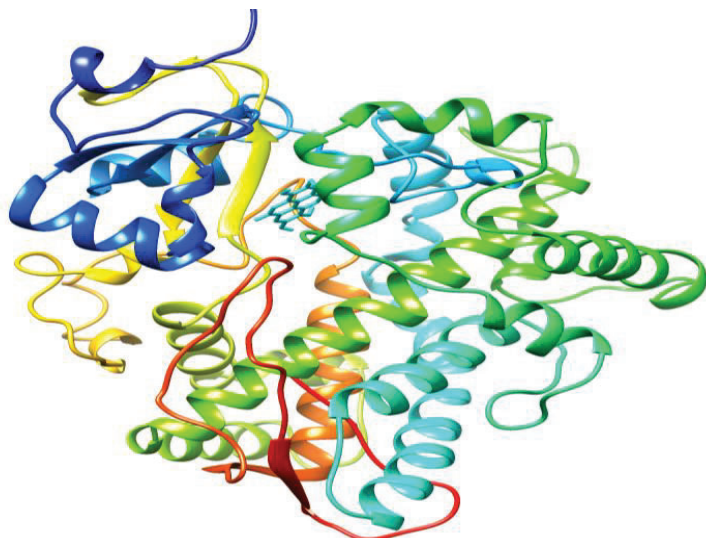


Figure 24. The selected docked structure for EGA-CYP3A4

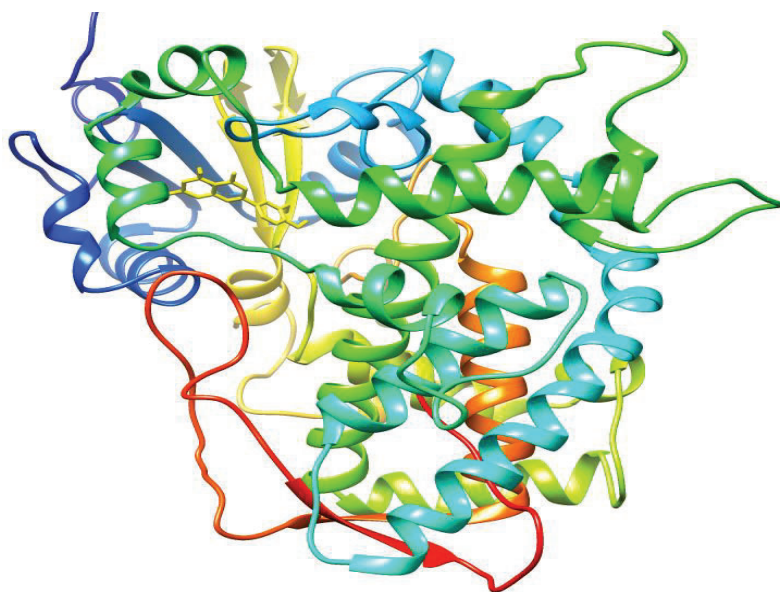


Figure 25. The selected docked structure for LUT-CYP3A4

B.2 Select docked complex structures Ligand-P-gp used for molecular dynamic simulation

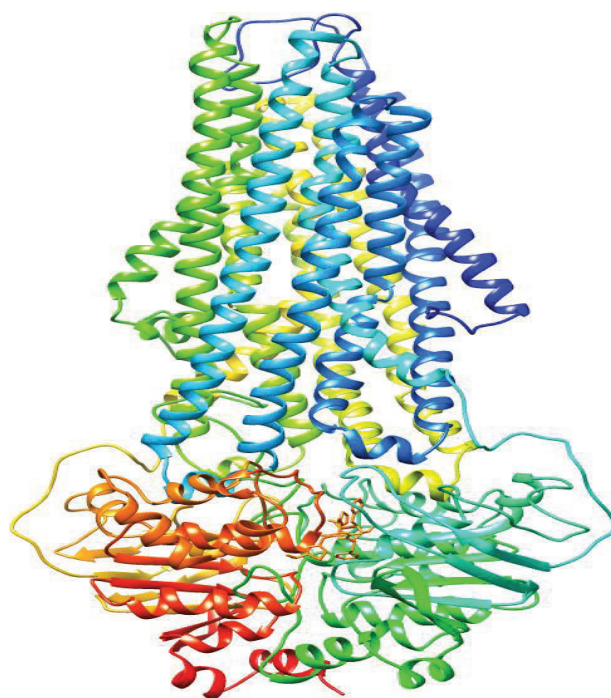


Figure 26. The selected docked structure for RTV-P-gp

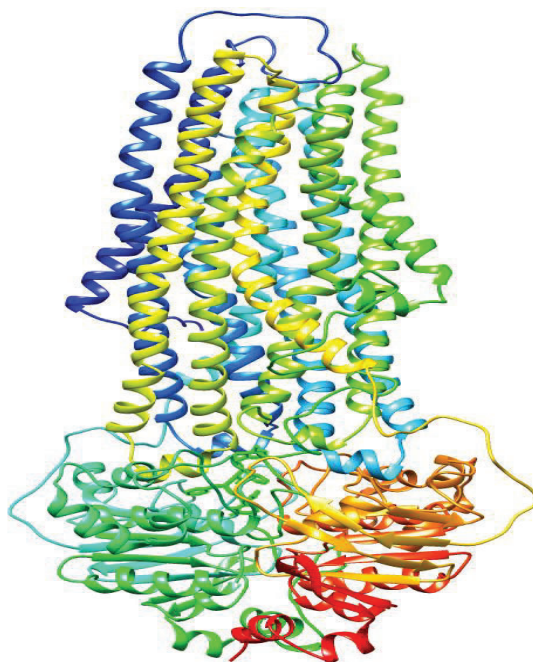


Figure 27. The selected docked structure for LPV-P-gp

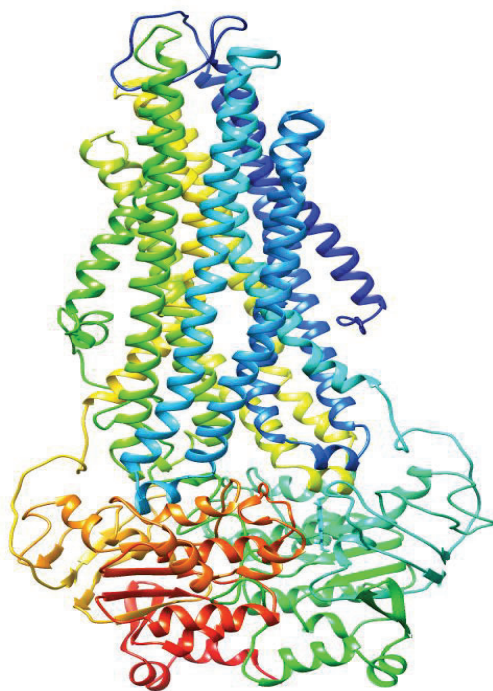


Figure 28. The selected docked structure for EGA-P-gp

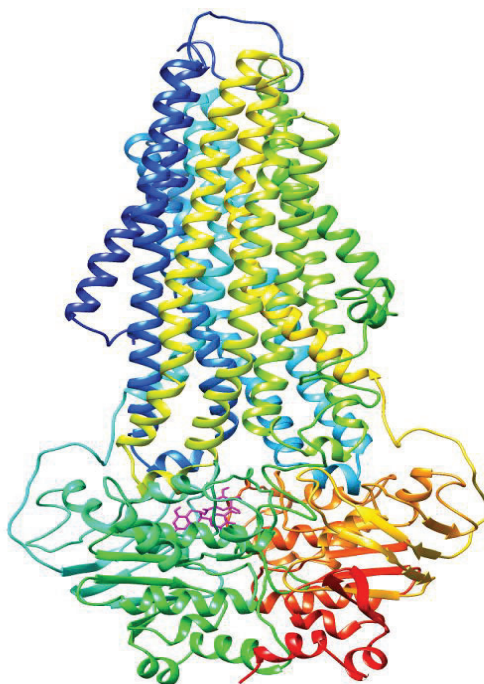


Figure 29. The selected docked structure for EGCG-P-gp

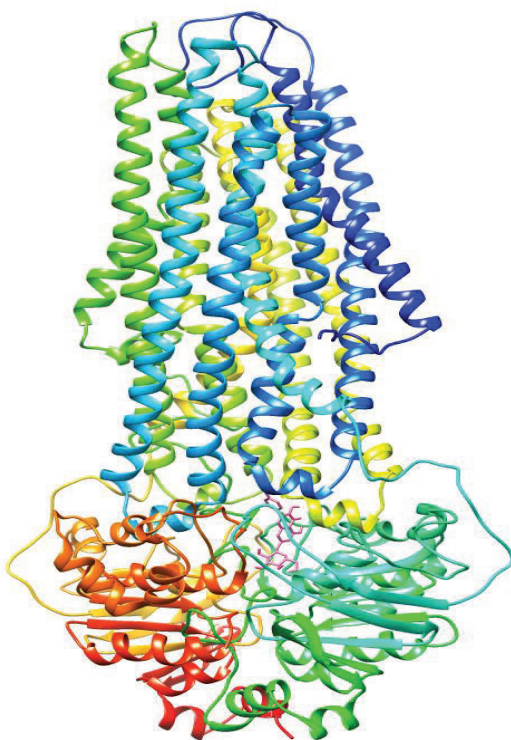


Figure 30. The selected docked structure for K7G-P-gp

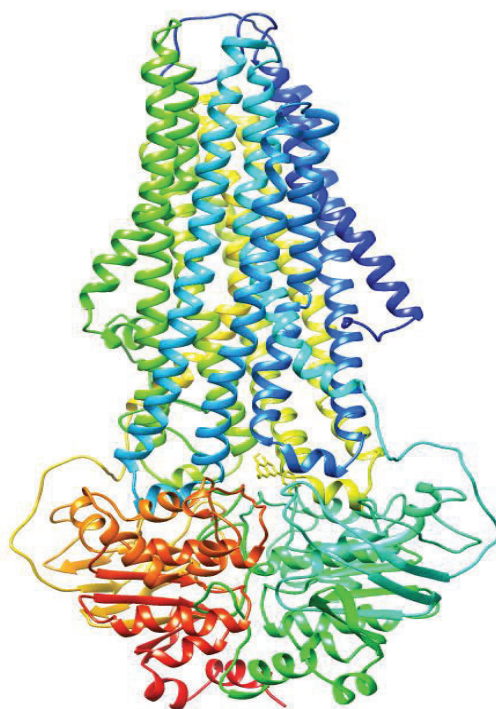


Figure 31. The selected docked structure for LUT-P-gp

Appendix C

Chapter 3 and 4 Input files for MD simulations

C.1 Input files for MD simulations in explicit solvation

The following input files were used in this thesis.

Partial minimization input file

Initial minimization of MMP3 (MMMM): solvent molecules and added ions

&cntrl

imin = 1,

maxcyc = 2500,

ncyc = 750,

ntb = 1,

ntr = 1,

cut = 12.0,

NTWR=500,

ntxo=1

ioutfm=0

/

Hold the Protein fixed

10.0

RES 1 198 (*HIVpro*), 1242 (P-gp) and 278 (CYP3A4)

END

END

Full minimization input file

full minimization of MMP3 (MMMM): protein, ligand, solvent molecules and added ions

&cntrl

imin = 1,

maxcyc = 200,

ncyc = 50,

ntb = 1,

ntr = 0,

cut = 12.0,

Drms = 0.0001,

ntxo=1

NTWR=500,

ntxo=1

ioutfm=0

/

END

Heating stage input file

Heating Step of MMP3 (MMMM): stage-5

&cntrl

imin= 0,

irest=0,

NTX=1,

ntb= 1,

NTPR=500,

NTWX=500,

NTWR=500,

ntr=1,

Tempi=0.0,

Temp0=300.0,

NTT=3,

gamma_ln=1.0,

NTC=2,

NTF=2,

cut= 12.0,

nstim=2500,

dt=0.002,

ntxo=1

ioutfm=0

/

Keep Protein and inhibitor fixed with weak restraints

10.0

RES 1 198 (HIVpro), 1242 (P-gp) and 278 (CYP3A4)

END

END

Equilibration Step Input file

Equilibration Step of MMP3 (MMMM): stage-1

&cntrl

imin= 0,

irest=1,

NTX=7,

ntb=2,

ntp=1,

PRES0=1.0,

TAUP=2.0,

NTPR=500,

NTWX=500,

NTWR=500,

ntr=0,

Tempi=300.0,

Temp0=300.0,

NTT=3,

gamma_ln=1.0,

NTC=2,

NTF=2,

cut=12.0,

nstlim=250000,

dt=0.002

ntxo=1,

ioutfm=0,

/

MD Input file

Equilibration Step of MMP3 (MMMM): stage-1

&cntrl

imin= 0,

iwrap=1,

irest=1,

NTX=5,

ntb=2,

ntp=1,

PRES0=1.0,

TAUP=2.0,

NTPR=500,

NTWX=500,

NTWR=500,

ntr=0,

Tempi=300.0,

Temp0=300.0,

NTT=3,

gamma_ln=1.0,

NTC=2,

NTF=2,

cut=12.0,

nstlim=10000000,

dt=0.002,

ntxo=1,

ioutfm=0,

/

Combining trajectories input file

trajinmd.mdcrd

trajin md2.mdcrd

trajin md3.mdcrd

trajin md4.mdcrd

trajin md5.mdcrd

autoimage

strip :WAT,Na+,Cl- outprefix stripped

trajoutcombined.mdcrd

C.2 Data analysis parameters

Calculating RMSD for the backbone

trajincombine.mdcrd

rms first out rmsd.dat @CA

Calculating the RMSF of the backbone

trajincombine.mdcrd

atomicfluct out rmsf.dat :1-198 (*HIVpro*), 1242 (P-gp) and 278 (CYP3A4) bytes

Calculating the RoG of the backbone

Trajincombine.mdcrd

radgyr out RoG.dat mass nomax

Calculating the Solvent accessible surface area

trajincombine.mdcrd

surf :1198 (*HIVpro*), 1242 (P-gp) and 278 (CYP3A4)out sasa.dat

Snapshots

trajincombine.mdcrd

outtraj snapshot.pdb onlyframes 100000

Appendix D

Chapter 5 supporting information

Table 1: Raw data for the determination of IC₅₀ and IC₂₀ using the cell viability (MTT) assay in HepG2 cell

Conc. (μ M)	EGCG			EGA			LUT		
	AVG	Log Conc	% cell viability	AVG	Log Conc	% cell viability	AVG	Log Conc	% cell viability
0	0.606		100	0.265	0	100	0.438	0	100
12.5	0.488	1.1	80.53	0.259	1,1	98	0.433	1,1	99
25	0.490	1.4	80.86	0.254	1,4	96	0.429	1,4	98
50	0.449	1.7	74.08	0.262	1,7	99	0.420	1,7	96
100	0.400	2.0	66.01	0.253	2	96	0.403	2	92
200	0.241	2.3	39.77	0.222	2,3	84	0.399	2,3	89
300	0.184	2.5	30.36	0.207	2,5	78	0.359	2,5	82
400	0.157	2.6	25.91	0.198	2,6	75	0.346	2,6	79

Table 2: Raw data for the determination of IC₅₀ and IC₂₀ using the cell viability (MTT) assay in HEK293 cell

Conc. (μ M)	EGCG			EGA			LUT		
	AVG	Log Conc.	% cell viability	AVG	Log Conc	% cell viability	AVG	Log Conc.	% cell viability
0	1.048		100,00	0.147		100	0.327		100
12.5	1.047	1.1	99.95	0.125	1,1	85	0.294	1,1	90
25	1.034	1.4	98.66	0.110	1,4	75	0.294	1,4	88
50	1.358	1.7	100.30	0.118	1,7	80	0.274	1,7	84
100	1.245	2.0	100.19	0.101	2	69	0.223	2	68
200	1.216	2.3	100.16	0.068	2,3	46	0.196	2,3	60
300	0.897	2.5	85.59	0.067	2,5	46	0.196	2,5	60
400	0.527	2.6	50.29	0.059	2,6	40	0.177	2,6	54

Table 3: Raw data for the determination of IC₅₀ and IC₂₀ using the cell viability (MTT) assay for K7G in HepG2 and HEK293 cells

Conc. (μ M)	HepG2			HEK293		
	AVG	Log Conc.	% cell viability	AVG	Log Conc	% cell viability
0	0.272		100	0.148		100
12.5	0.27	1.1	99.26	0.137	1.1	92.57
25	0.261	1.39	95.95	0.11	1.39	25
50	0.251	1.7	92.28	0.078	1.7	74.32
100	0.247	2	90.81	0.037	2	52.7

Table 4: Absorbance and concentrations of standards.

Abs1	Abs2	Ave Abs	BSA (mg/ml)	Abs
0.174	0.172	0.173	0	
0.427	0.303	0.365	0.2	0.192
0.467	0.456	0.461	0.4	0.289
0.632	0.678	0.655	0.6	0.482
0.829	0.843	0.836	0.8	0.655
0.974	1.017	0.995	1	0.823

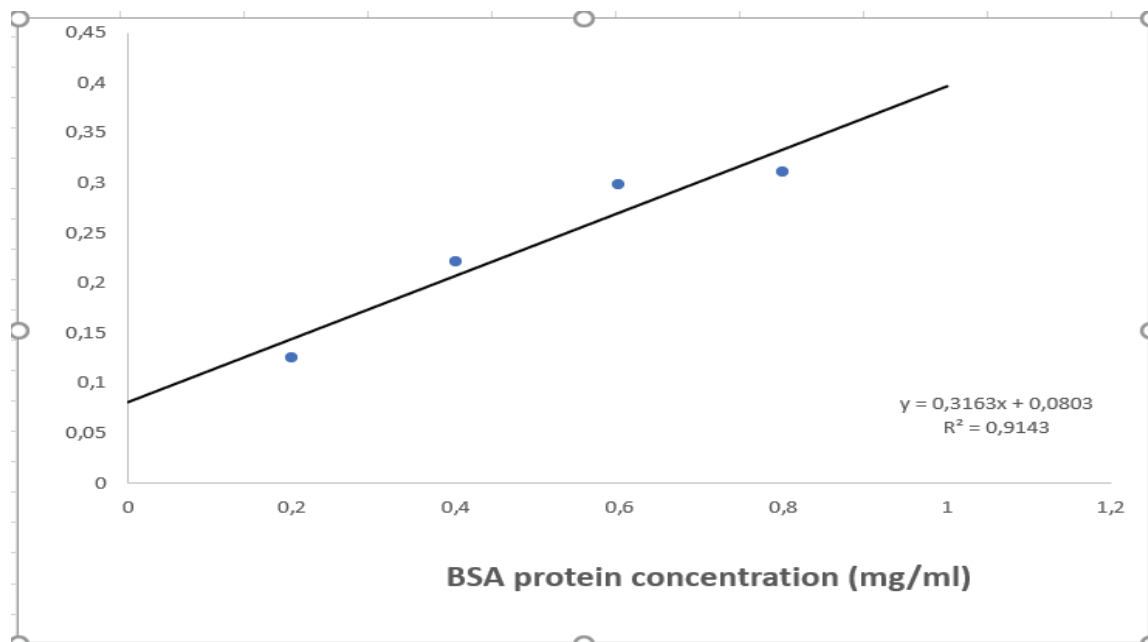


Figure 51: BSA protein concentration Vs average absorbance.

Figure was constructed as a standard curve. The equation defining the curve ($y = 0,3163x + 0,0803$) was used to determine the protein concentration of each sample.



Research article

The pharmacokinetic properties of HIV-1 protease inhibitors: A computational perspective on herbal phytochemicals

Idowu Kehinde^{a,*}, Pritika Ramharack^b, Manimbulu Nlooto^b, Michelle Gordon^a^a KwaZulu-Natal Research, Innovation and Sequencing Platform (KRISP)/Genomics Unit, School of Laboratory Medicine and Medical Sciences, College of Health Sciences, Nelson R Mandela School of Medicine, University of KwaZulu-Natal, Medical Campus, Durban, 4001, South Africa^b Department of Pharmacy, School of Health Sciences, University of KwaZulu-Natal, Westville Campus, Durban, 4001, South Africa

ARTICLE INFO

Keywords:

Pharmaceutical chemistry
 Pharmaceutical science
 HIV protease
 Phytochemical
 Enzymes
 Transporters
 Antiviral activities

ABSTRACT

Acquired Immune Deficiency Syndrome is the most severe phase of Human Immunodeficiency Virus (HIV) infection. Recent studies have seen an effort to isolate phytochemicals from plants to repress HIV, but less studies have focused on the effects of these phytochemicals on the activities of enzymes/transporters involved in the metabolism of these drugs, which is one of the aims of this study and, to examine the antiviral activity of these compounds against HIV-1 protease enzyme using computational tools. Centre of Awareness-Food Supplement (COA®-FS) herbal medicine, has been said to have potential anti-HIV features. SWISSTARGETPREDICTION and SWISSADME servers were used for determination of the enzymes/transporters involved in the metabolism of these protease inhibitor drugs, (PIs) (Atazanavir, Lopinavir, Darunavir, Saquinavir) and the effects of the selected phytochemicals on the enzymes/transporters involved in the metabolism of these PIs. Using Computational tools, potential structural inhibitory activities of these phytochemicals were explored. Two sub-families of Cytochrome P450 enzymes (CYP3A4 and CYP2C19) and Permeability glycoprotein (P-gp) were predicted to be involved in metabolism of the PIs. Six phytochemicals (Geranin, Apigenin, Fisetin, Luteolin, Phthalic acid and Gallic acid) were predicted to be inhibitors of CYP3A4 and, may slowdown elimination of PIs thereby maintain optimal PIs concentrations. Free binding energy analysis for antiviral activities identified four phytochemicals with favourable binding landscapes with HIV-1 protease enzyme. Epigallocatechin gallate and Kaempferol-7-glucoside exhibited pronounced structural evidence as potential HIV-1 protease enzyme inhibitors. This study acts as a steppingstone toward the use of natural products against diseases that are plagued with adverse drug-interactions.

1. Introduction

The World Health Organization (WHO) reported that approximately 72 million people had already been infected with the Human Immunodeficiency Virus (HIV) worldwide in 2017 (WHO, 2018). Of these records, the sub-Saharan Africa was the most heavily affected region, accounting for over 69% of all infected cases. The Joint United Nations (UNAIDS report) (2018) states that although there is a steady decline in Acquired Immune Deficiency Syndrome (AIDS) related illnesses over the past decade; however, the global rate of new HIV infections is not falling fast enough to reach the milestones set in place by 2020 (WHO, 2018).

Of the enzymes involved in the replication cycle of HIV in human immune cells, the HIV protease enzyme is one of the most significant enzymes required to produce mature and infectious HIV virions. This has allowed the enzyme to be the utmost protuberant focus for anti-HIV

inhibitors (Scholar, 2011). The protease enzyme is a C₂-symmetric active homodimer, consisting of a non-covalently connected dimer of 99 amino acid residues each to form an active homodimer. The two monomeric chains assemble to form an enclosed tunnel covered by two flaps that characteristically “open and close” upon substrate binding (Levy and Caflich, 2003). The effective activity of HIV protease in the viral cycle is crucial for the maturation of infectious HIV virions (Brik and Wong, 2003). Therefore, there is no doubt that inhibition or inactivation of the enzyme will result to the production of less viable and noninfectious virions and will eventually lead to a reduction in the spread of the infection to vulnerable hosts or cells.

Viral replication by HIV is inhibited by protease inhibitor drugs (PIs) by binding to the HIV proteases and subsequently obstructing the proteolytic cleavage of the protein precursors which are important for making of mature HIV virions (Soontornniyomkij et al., 2014). PIs are

* Corresponding author.

E-mail addresses: 218068180@stu.ukzn.ac.za (I. Kehinde), 218068180@stu.ukzn.ac.za (M. Nlooto).<https://doi.org/10.1016/j.heliyon.2019.e02565>

Received 15 August 2019; Received in revised form 9 September 2019; Accepted 30 September 2019

2405-8440/© 2019 The Author(s). Published by Elsevier Ltd. This is an open access article under the CC BY-NC-ND license (<http://creativecommons.org/licenses/by-nc-nd/4.0/>).

designed to look like the natural substrates of the viral protease. They prevent the HIV-1 protease from cleaving the precursor proteins by precisely binding the active site of the virus protease, which eventually results in the development of immature non-infectious viral particles (Geretti and Easterbrook, 2001). In South Africa, the current Adult antiretroviral therapy guidelines in use recommend four FDA-approved PIs, atazanavir, darunavir, lopinavir and saquinavir, with ritonavir being used as boosters with the drugs (Carmona and Nash, 2017).

The use of traditional herbal medicine is gaining more popularity in the treatment of diseases such as HIV in many countries, (WHO, 2018) despite the possibility of Herbal-drug interactions and toxicity that could occur as a result of co-administration of Herbs and antiretroviral drugs (ARVs). Nonetheless, there have been significant increases in the usage of herbal medicine not only in developing countries but also in developed countries, which has caused great public health concern among scientists and physicians who are sometimes not sure about the safety of herbal preparations especially when used concurrently with regular orthodox medications such as ARV (WHO, 2018). In South Africa, many patients undergoing antiretroviral therapy also consume traditional herbal medicine (Nlooto and Naidoo, 2014). One of the most consumed herbal medicine by HIV patients in South Africa is COA®-FS (Centre of Awareness) herbal medicine (COA®-FS) (Nlooto and Naidoo, 2014).

COA®-FS herbal medicine is produced by Centre of Awareness (COA), an organization, based in Cape Coast, Ghana. According to the producer, the COA®-FS herbal medicine contains six Africa plants namely; *Asadirachta indica*, *Persea americana*, *Carica papaya*, *Spondias mombin*, *Ocimum viride* and *Vernonia amygdalina* (FDA/DRID/HMD/HMU/16/0981, 2016). HIV patients purchase it as immune boosters against HIV/AIDS

and as treatments for other diseases (<https://www.coadrugs.org>).

Previous studies have showed that HIV positive patients use herbal medicine concurrently with prescribed protease inhibitor drugs. No or few studies on the effect of the chemical constituents of the herbal medicines on the enzymes and transporters involved in the metabolism of drugs such as PI drugs have been done, therefore there is paucity of evidence or information on the effectiveness and the possibility of serious side effects of phytochemical compounds from herbal medicine on prescribed protease inhibitor drugs. This has motivated this study to examine the pharmacokinetic effect of numerous phytochemical compounds from COA®-FS herbal medicine on the activities of major enzymes and transporters involved in the metabolism of FDA-approved protease inhibitor drugs used in South Africa (Atazanavir, Lopinavir, Darunavir, Saquinavir) commonly use in South Africa and to examine their antiviral activities as potent inhibitors of HIV-1 protease enzyme using *in silico* pharmacodynamics and pharmacokinetic analysis. These phytochemical compounds will then be compared with FDA approved drugs against the HIV-1 protease enzyme to identify the least toxic and most favourable compounds that may act as lead molecules for experimental analysis.

In a previous study in our lab, COA®-FS herbal medicine and its component plants were subjected to Gas Chromatography-Mass Spectrometry <https://www.sciencedirect.com/topics/biochemistry-genetics-and-molecular-biology/gas-chromatography-mass-spectrometry> (GC-MS) to identify the phytochemical compounds present in them (Boadu, 2019; Nwabuiife, 2019). A comprehensive literature search on the antiviral activities of phytochemical compounds from COA® and its component plants was as well done. Fifteen of the phytochemical

Table 1

Selected phytochemicals with antiviral activities present COA®-FS herbal medicine and its component plants.

Compounds Name	Plant name	Extracts	Plant parts	Literature Reference	COA-FS herbal medicine		
					GC-MS	Extracts	Reference
EGA	<i>Spondias mombin</i> , <i>Carica papaya</i>	Hydroethanolic,	Leaf	(Shin et al., 2005) Nwabuiife, 2019	+	Ethanolic, Hexane,	Boadu, 2019; Nwabuiife, 2019
CHD	<i>Asadirachta indica</i> , <i>Vernonia amygdalina</i> , <i>Carica papaya</i>	Methanolic, hexane, ethanol, ethylacetate, Dichloromethane	Leaf	(Dineshkumar and Rajakumar, 2017) Boadu, 2019; Nwabuiife, 2019	+	Ethanol, hexane	Boadu, 2019; Nwabuiife, 2019
LNT	<i>Asadirachta indica</i> , <i>Vernonia amygdalina</i>	Chloroform, Dichloromethane	Leaf	(Siddiqui et al., 2006) Boadu, 2019	+	Dichloromethane	Boadu, 2019
BIT	<i>Carica papaya</i>	Hydroethanolic	Seed, leaf	(Kermanshai et al., 2001)	+	Ethanolic	Boadu, 2019
GA (methyl salicylate)	<i>Persea Americana</i>	Methanolic	Pulp, Leaf	(Hurtado-Fernández et al., 2014)	+	Standard	Boadu, 2019
IST	<i>Vernonia amygdalina</i>	Chloroform, Dichloromethane, ethanol,	Leaf	(Adewole et al., 2018) Boadu, 2019	+	Dichloromethane	Boadu, 2019
STG	<i>Carica papaya</i> , <i>Persea Americana</i> , <i>Vernonia amygdalina</i> , <i>Asadirachta indica</i>	Petroleum ether, Hydroethanolic, hexane, Dichloromethane, ethylacetate, ethanol	Leaf	(Rashed et al., 2013; Monika and Geetha, 2015; Boadu, 2019; Nwabuiife, 2019)	+	Hexane, Dichloromethane, ethylacetate	Boadu, 2019; Nwabuiife, 2019
PTA	<i>Carica papaya</i> , <i>Asadirachta indica</i>	Methanolic, Crude oil, hexane, Dichloromethane, ethylacetate, ethanol	Leaf	(Sajin et al., 2015; Boadu, 2019; Babatunde et al., 2019)	+	Hexane, ethylacetate	Boadu, 2019; Nwabuiife, 2019
NGN	<i>Persea Americana</i> , <i>Carica papaya</i>	Methanolic, Ethylacetate	Leaf	(Hurtado-Fernández et al., 2014; Nwabuiife, 2019)	-	Methanolic, Ethylacetate	
K7G	<i>Carica papaya</i>	Ethanolic, aqueous	Fruit/pulp, dry leaf	(Kongkachuichai and Charoensiri, 2010; Lako, 2007)	-		ND
EGCG	<i>Persea Americana</i>	HydroMethanolic	seed	(Calderón-Oliver et al., 2015)	-		ND
LUT	<i>Vernonia amygdalina</i> , <i>Carica papaya</i>	Ethanolic, methanolic	Leaf, Fruit/pulp	(Igile et al., 1995)	-		ND
GER	<i>Spondias mombin</i>	Hydroalcoholic	Leaf	(Mukhtar et al., 2008)	-		ND
APG	<i>Carica papaya</i>	Ethanolic, aqueous	Fruit/pulp	Franke et al., 2004	-		ND
FST	<i>Carica papaya</i>	Ethanolic, aqueous	Fruit/pulp	Lako, 2007	-		ND

Key: + means present, - means not present, ND means not detected.

compounds from COA®-FS herbal medicine and its component plants were selected for this study, to examine the transporters and enzymes involved in the metabolisms of the selected phytochemical compounds and metabolism of four FDA-approved PIs (Atazanavir, Lopinavir, Darunavir, Saquinavir), and to evaluate the effects of these phytochemical compounds from COA®-FS herbal medicine and its component plants on the activities of enzymes and transporters involved in drug metabolism of the four PIs. In addition, the antiviral activity of these phytochemical compounds from COA®-FS herbal medicine and its constituent plants were examined using molecular docking and dynamics simulations.

Table 1 showed the fifteen selected phytochemical compounds present in the COA®-herbal medicine and its components plants. Nine of the selected phytochemical compounds (EGA, EPG, LNT, BIT, GA, IST, STG, PTA and NGN) were present in the COA®-FS herbal medicine and the remaining 6 compounds were reported in literature to be present in

different parts of the six plants.

Fig. 1 illustrates the 2-D structures of the selected fifteen phytochemical compounds from COA®-FS herbal medicine and its constituent plants, 2-D structures of the four FDA-approved protease inhibitor drugs and the crystalline structure of HIV protease enzyme indicating the active site amino acid residues of the enzyme. Three letters code were assigned for the phytochemical compounds and the four FDA-approved drugs.

2. Methods

2.1. Prediction of enzymes and transporters targets

SWISSTARGETPRIDITION and SWISSADME servers were used for the prediction of proteins (enzymes and transporters) involved in the metabolism of the Four FDA approved drugs and the selected phytochemical compounds from COA-Fs herbal medicine and its component

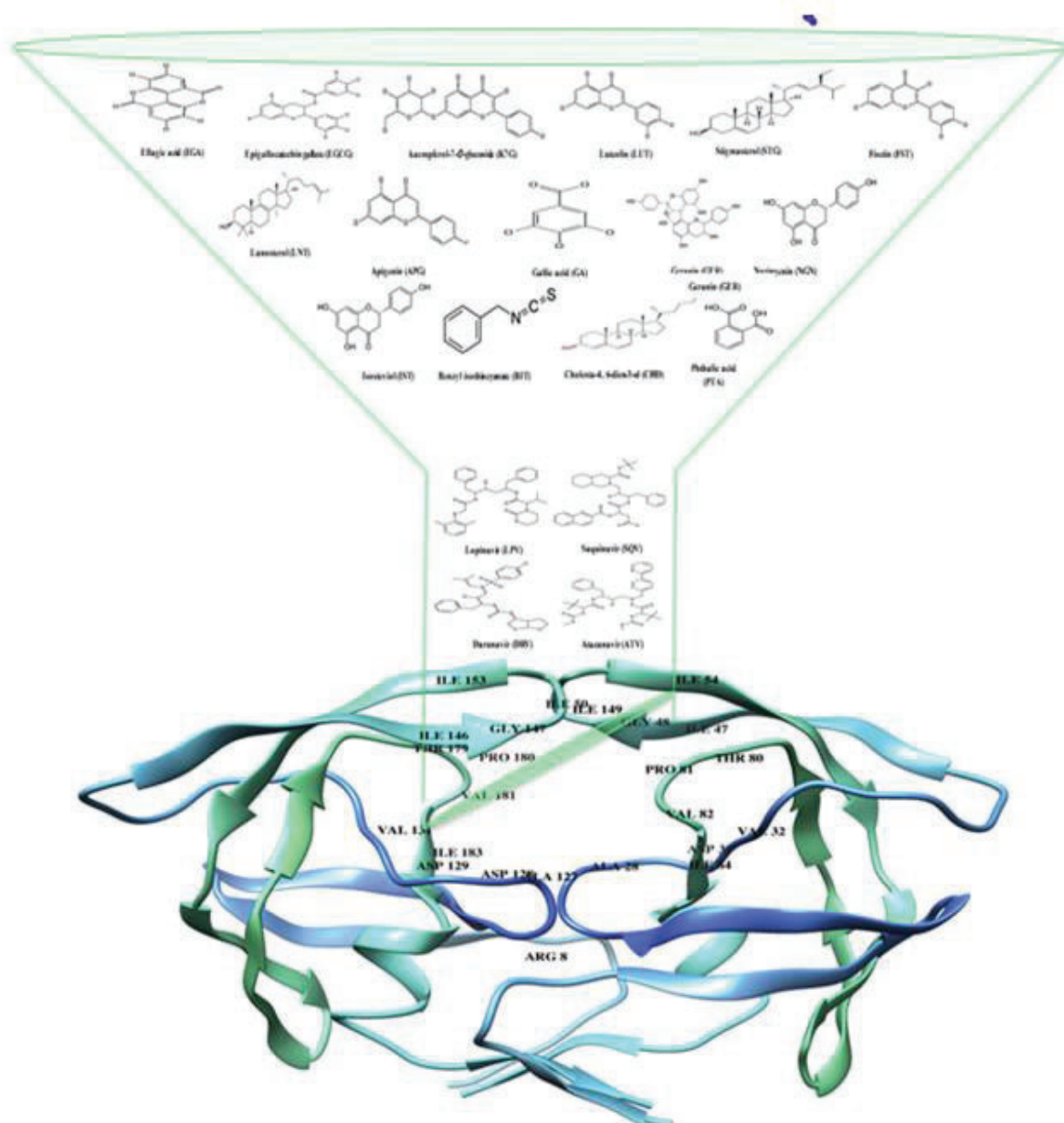


Fig. 1. 2D Structures of the fifteen selected phytochemical compounds from COA-Fs herbal medicine and its component plants and 2D structures of the Four FDA approved drugs.

plants and their pharmacokinetic effects (Gfeller et al., 2014). The server predicts the target of small molecules.

2.2. Measurement of pharmacokinetics properties and drug likeliness of the phytochemical compounds

SWISSADME server was used for the determination of the physico-chemical descriptors and define the pharmacokinetic properties and drug-like nature of each phytochemical compound. The "Brain Or Intestinal Estimated permeation, (BOILED-Egg)" method was utilized as it computes the lipophilicity and polarity of small molecules (Daina et al., 2017).

2.3. HIV-1 enzyme and ligand acquisition and preparation

The X-ray crystal structures of the HIV-1 Protease enzyme (PDB codes: 3U71) was obtained from the RSCB Protein Data Bank (Burley et al., 2018). The structures of HIV-1 protease was then prepared on the UCSF Chimera software package (Yang et al., 2012) where the monomeric protein was converted to a dimeric structure. The four FDA-approved drugs Atazanavir, Darunavir, Lopinavir, and Saquinavir, as well as the fifteen phytochemical compounds, were accessed from PubChem (Kim et al., 2016) and the 3-D structures prepared on the Avogadro software package (Hanwell et al., 2012).

2.4. Molecular docking

The Molecular docking software utilized in this study was the Auto-dock Vina Plugin available on Chimera (Yang et al., 2012), with default docking parameters. Prior to docking, Gasteiger charges were added to the compounds and the non-polar hydrogen atoms were merged to carbon atoms. The phytochemical compounds were then docked into the binding pocket of Protease (by defining the grid box with a spacing of 1 Å and size of 24 × 22 × 22 pointing in x, y and z directions). The four FDA-approved drug systems, as well as the four best-docked phytochemical compounds systems, were then subjected to molecular dynamics simulations.

2.5. Molecular dynamic (MD) simulations

The CPU version of the SANDER engine provided with the AMBER package was used for the MD simulations, and the FF14SB variant of the AMBER force field (Nair and Miners, 2014) was used to describe the protein.

To generate atomic partial charges for the ligand, ANTECHAMBER was used by utilizing the Restrained Electrostatic Potential (RESP) and the General Amber Force Field (GAFF) procedures. The Leap module of AMBER 14 allowed for the addition of hydrogen atoms, as well as Na⁺ and Cl counter ions for neutralization all systems. The amino acids were renumbered based on the dimeric form of the enzyme, thus numbering residues 1–198. The 8 systems were then suspended implicitly within an orthorhombic box of TIP3P water molecules such that all atoms were within 8 Å of any box edge.

An initial minimization of 2000 steps were carried out with an applied restraint potential of 500 kcal/mol for both solutes, were performed for 1000 steps using the steepest descent method followed by 1000 steps of conjugate gradients. An additional full minimization of 1000 steps were further carried out by conjugate gradient algorithm without restraint.

A gradual heating MD simulation from 0K to 300K was executed for 50ps, such that the systems maintained a fixed number of atoms and fixed volume. The solutes within the systems were imposed with a potential harmonic restraint of 10 kcal/mol and collision frequency of 1.0ps. Following heating, an equilibration estimating 500ps of each system was conducted; the operating temperature was kept constant at 300K. Additional features such as several atoms and pressure were also kept constant

mimicking an isobaric-isothermal ensemble (NPT). The system's pressure was maintained at 1 bar using the Berendsen barostat.

The MD simulations was conducted for 100ns. In each simulation, the SHAKE algorithm was employed to constrict the bonds of hydrogen atoms. The step size of each simulation was 2fs and an SPFP precision model was used. The simulations coincided with the isobaric-isothermal ensemble (NPT), with randomized seeding, the constant pressure of 1 bar maintained by the Berendsen barostat, a pressure-coupling constant of 2ps, a temperature of 300K and Langevin thermostat with collision frequency of 1.0ps.

2.6. Post-dynamic analysis

The coordinates of the 8 systems were then saved and the trajectories were analyzed every 1ps using PTRAJ, followed by analysis of RMSD, RMSF and Radius of Gyration using the CPPTRAJ module employed in AMBER 14 suit.

2.7. Binding free energy calculations

To estimate and compare the binding affinity of the systems, the free binding energy was calculated using the Molecular Mechanics/GB Surface Area method (MM/GBSA) (Ylilauri and Pentikäinen, 2013). Binding free energy was averaged over 100000 snapshots extracted from the 100ns trajectory. The free binding energy (ΔG) computed by this method for each molecular species (complex, ligand, and receptor) can be represented as (Hayes and Archontis, 2011):

$$\Delta G_{\text{bind}} = G_{\text{complex}} - G_{\text{receptor}} - G_{\text{ligand}} \quad (1)$$

$$\Delta G_{\text{bind}} = E_{\text{gas}} + G_{\text{sol}} - TS \quad (2)$$

$$E_{\text{gas}} = E_{\text{int}} + E_{\text{vdw}} + E_{\text{ele}} \quad (3)$$

$$G_{\text{sol}} = G_{\text{GB}} + G_{\text{SA}} \quad (4)$$

$$G_{\text{SA}} = \gamma \text{SASA} \quad (5)$$

The term E_{gas} denotes the gas-phase energy, which consists of the internal energy E_{int} ; Coulomb energy E_{ele} and the van der Waals energies E_{vdw} . The E_{gas} was directly estimated from the FF14SB force field terms. Solvation free energy, G_{sol} , was estimated from the energy contribution from the polar states, G_{GB} , and non-polar states, G . The non-polar solvation energy, SA, G_{SA} , was determined from the solvent accessible surface area (SASA), using a water probe radius of 1.4 Å, whereas the polar solvation, G_{GB} , contribution was estimated by solving the GB equation. S and T denote the total entropy of the solute and temperature respectively.

2.8. Data analysis

All raw data plots were generated using the Origin data analysis software (Seifert, 2014).

3. Results

3.1. Assessing the predicted targets for the drugs and phytochemicals

Using two different methods, the SWISSPREDICTION and SWISSADME servers the enzymes and transporters involved in the metabolism of the four FDA-approved drugs and the fifteen selected phytochemical compounds were predicted. The SWISSPREDICTION server predicted all possible enzymes and transporters that are likely to be targets of the phytochemical compounds. On the other hand, the SWISSADME predicted the possibility of the phytochemicals compounds having pharmacokinetic effect on some cytochrome P450

Table 2

Predicted targets involved in the metabolism of the four FDA-approved PI drugs and selected phytochemical compounds from COA®-Fs herbal medicine.

Compound Name	SWISSPREDICTION		SWISSADME	
	Enzymes	Transporters	Enzymes	Transporters
ATV	Renin, Cathepsin D, Pepsin A-5, Cathepsin E, Napsin-A, CYP3A4, Gastriclin	NP	CYP3A4	P-glycoprotein
SQV	Thromboxane-A synthase, Renin, CYP3A4	D (2), D (4) dopamine receptors, Substance-K receptor, Substance-P receptor, Neuromedin-K receptor, Oxytocin receptor, Mu-type opioid receptor	CYP3A4	P-glycoprotein
LPV	Renin, Cathepsin D, Napsin-A, Beta-secretase 1, Beta-secretase 2, Gastriclin	Potassium voltage-gated (ion channel),	CYP3A4, CYP2C19	P-glycoprotein
DRV	CYP3A4, Thromboxane-A synthase, CYP3A5, CYP3A7, CYP3A43, Renin, Cathepsin D	C-C chemokine receptor type 1-8, CX3C chemokine receptor 1,	CYP3A4	P-glycoprotein
EGCG	PEX, 67 kDa matrix metalloproteinase-9, 14, 15, Beta-secretase 1, 2, Tyrosyl-DNA phosphodiesterase 1, 6-phosphogluconate dehydrogenase, decarboxylating, Telomerase reverse transcriptase, Dihydrofolate reductase, Dihydrofolate reductase	Potassium voltage-gated channel subfamily H member 2	NP	NP
K7G	Tyrosyl-DNA phosphodiesterase 1, Xanthine dehydrogenase/oxidase, Aldehyde oxidase, Aldo-keto reductase family 1, Aldose reductase, Lysine-specific demethylase 4A, Lysine-specific demethylase 4A, 4B, 4C	Adenosine receptor A1, Alpha-2A, 2C, 2B, Muscle blind-like protein 1	NP	NP
EGA	Cytidine deaminase, Thymidine kinase, Adenosine deaminase, Thymidine phosphorylase, Histone deacetylase 1-3, Adenosyl homocysteinease, Putative adenosyl homocysteinease 2, Carbonic anhydrase 1, 2, 3, 12	NP	CYP1A2	NP
LUT	22 kDa interstitial collagenase, CYP1A2, PEX, Stromelysin-1, 67 kDa matrix metalloproteinase-9, Aldose reductase	NP	CYP1A2, CYP2D6, CYP3A4	NP
GER	Squalene monooxygenase, Tyrosyl-DNA phosphodiesterase 1, Muscle blind-like protein 1, Muscle blind-like protein 2 and 3, DNA topoisomerase 1, Tyrosine-protein phosphatase non-receptor type 2	Multidrug resistance protein 1 (P-glycoprotein)	CYP3A4, CYP2C9	NP
CHD	Androgen receptor, CYP19A1, Estrogen receptor, Estrogen receptor beta, Oxysterols receptor LXR-beta, Oxysterols receptor LXR-alpha, Tyrosyl-DNA phosphodiesterase 1, Tyrosine-protein phosphatase non-receptor type 1 and 2, M-phase inducer phosphatase 1, Lanosterol 14-alpha demethylase, 3-oxo-5-alpha-steroid 4-dehydrogenase 2	Sodium-dependent noradrenaline transporter	CYP2C9	NP
APG	Aldo-keto reductase family 1, CYP1A2, Cyclin-dependent kinase 1, Microtubule-associated protein tau, CYP19A1, Cyclin-dependent kinase 4, Estradiol 17-beta-dehydrogenase 1, Aldose reductase, Casein kinase II subunit alpha	Estrogen receptor, Adenosine receptor A2a	CYP1A2, CYP2D6, CYP3A4	NP
FST	Cyclin-dependent kinase 1, Arachidonate 5-lipoxygenase, Microtubule-associated protein tau, Cyclin-dependent kinase 4, Arachidonate 15-lipoxygenase, Xanthine dehydrogenase/oxidase	NP	CYP1A2, CYP2D6, CYP3A4	NP
NGN	CYP450 1A2, CYP450 19A1, Estradiol 17-beta-dehydrogenase 1, Carbonyl reductase [NADPH] 1, Cytochrome P450 1B1, Tyrosyl-DNA phosphodiesterase 1, CYP1A1, Retinol dehydrogenase 8, Carbonyl reductase [NADPH] 3, Adenosine receptor A1	Multidrug resistance-associated protein 1 (P-glycoprotein), Estrogen receptor	CYP1A2, CYP3A4	P-glycoprotein
BIT	Tyrosyl-DNA phosphodiesterase 1, Microtubule-associated protein tau, Carbonic anhydrase 1-9, Indoleamine 2,3-dioxygenase 1 and 2, Quinone oxidoreductase, Carbonic anhydrase 5B (mitochondrial), Indoleamine 2, 3-dioxygenase 1	Transient receptor potential cation channel subfamily A member 1, Sodium-dependent serotonin transporter	NP	NP
GA	Carbonic anhydrase 12, Carbonic anhydrase 1-9, Tyrosyl-DNA phosphodiesterase 1, Carbonic anhydrase 5B and 5A, FAD-linked sulfhydryl oxidase ALR	NP	CYP3A4	NP
STG	Androgen receptor, Tyrosyl-DNA phosphodiesterase 1, CYP19A1, 3-hydroxy-3-methylglutaryl-coenzyme A reductase, Lanosterol 14-alpha demethylase, Oxysterols receptor LXR-beta, Oxysterols receptor LXR-alpha	Low-density lipoprotein receptor, Very low-density lipoprotein receptor, Estrogen receptor, Estrogen receptor beta, Sodium-dependent noradrenaline transporter	CYP2C9	NP
IST	Aldo-keto reductase family 1 member B10, Aldose reductase, Corticosteroid 11-beta-dehydrogenase isozyme 1, Hydroxysteroid 11-beta-dehydrogenase 1-like protein, M-phase inducer phosphatase 1, M-phase inducer phosphatase 2, Alcohol dehydrogenase [NADP (+)], 1,5-anhydro-D-fructose reductase, UDP-glucuronosyltransferase	NP	CYP2C9	P-glycoprotein
LNT	3-hydroxy-3-methylglutaryl-coenzyme A reductase, Lanosterol 14-alpha demethylase, Cytochrome P450 19A1, Tyrosyl-DNA phosphodiesterase 1	Androgen receptor, Oxysterols receptor LXR-beta, Sodium-dependent noradrenaline transporter, Sodium-dependent serotonin transporter, Sodium-dependent dopamine transporter, Estrogen receptor, Sodium- and chloride-dependent neutral and basic amino acid transporter B (0+)	NP	NP
PTA	Tyrosyl-DNA phosphodiesterase 1, Dual specificity tyrosine-phosphorylation-regulated kinase 1A, Microtubule-associated protein tau, Carbonic anhydrase 1, 2, 3, 4, 5A, 5B, 6, 7, 9, 13, Carbonic anhydrase 12,	Gamma-secretase C-terminal fragment 59	NP	NP

KEY: NP means Non predicted.

Table 3

Pharmacokinetic effects of phytochemical compounds from COA®-FS herbal medicine on the enzymes and transporter involved in the metabolism of the four FDA-approved PIs.

Compound Name	Enzymes		Transporter
	CYP3A4 Inhibitor	CYP2C19 Inhibitor	P-gp Substrate/inducers
FDA-Approved Drugs			
DRV	Yes	No	Yes
LPV	Yes	Yes	Yes
ATV	Yes	No	Yes
SQV	Yes	No	Yes
COA®-FS Phytochemical compounds			
IST	No	No	Yes
EGA	No	No	No
K7G	No	No	No
EGCG	No	No	No
NGN	Yes	No	Yes
GER	Yes	No	No
LNT	No	No	No
FST	Yes	No	No
LUT	Yes	No	No
APG	Yes	No	No
PTA	Yes	No	No
STG	No	No	No
CHD	No	No	No
BIT	No	No	No
GA	Yes	No	No

enzymes (CYP450) such as CYP1A2, CYP2C19, CYP2C9, CYP2D9, CYP2D6 and CYP3A4 and their possibility to be substrates (inducers) of Permeability glycoprotein (P-gp). Although, the probability of DRV and SQV binding to Renin as a target was predicted to be low, Renin is the only enzyme predicted by the SWISSPREDICTION server to be target for the four conventional drugs. CYP3A4 with higher probability and cathepsin D (lower probability) were predicted to be targets for DRV, ATV and LPV. Apart from CYP3A4 and P-gp, CYP2C19 was predicted only for LPV. For the selected phytochemical compounds, CYP3A4 was predicted to be target for GER, APG, FST, GA, LUT, and NGN. IST and NGN were only predicted substrates of P-gp. CYP1A2, CYP2D6, CYP2C9 and CYP2C19 are other sub families of cytochrome P450 enzymes predicted by the SWISSADME server to be targets for EGA, LUT, GER, FST, APG, CHD, NGN, STG, and IST. P-gp and CYP3A4 are the common enzyme and transporter predicted for the four drugs and some of the phytochemical compounds (see Tables 2 and 3).

Table 4

Predicted ADME parameters, drug-likeness, pharmacokinetic and physicochemical properties of phytochemical compounds from COA®-FS herbal medicine and four FDA-approved drugs using SWISSADME server.

Compound Name	Molecular Formula	Molecular Weight (g/mol)	Lipophilicity (iLOGP)	Water Solubility	GIT Absorption	BBB Permeability	Bioavailability Score	Synthetic Accessibility	Drug likeness (Lipinski)
ATV	C ₃₈ H ₅₂ N ₆ O ₇	704.869	3.56	Poor	Low	No	0.17	6.24	No (2)
SQV	C ₃₈ H ₅₀ N ₆ O ₅	670.855	3.66	Poor	Low	No	0.17	5.94	No (2)
LPV	C ₇₄ H ₉₆ N ₁₀ O ₁₀ S ₂	1349.762	3.44	Poor	High	No	0.55	5.67	Yes
DRV	C ₂₇ H ₃₇ N ₃ O ₇ S	547.667	3.20	Moderate	Low	No	0.55	5.67	Yes
EGCG	C ₂₂ H ₁₈ O ₁₁	458.37	1.83	High	Low	No	0.17	4.20	No (2)
K7G	C ₂₁ H ₂₀ O ₁₁	448.38	1.55	High	Low	No	0.17	5.24	No (2)
EGA	C ₁₄ H ₆ O ₈	302.19	0.79	High	High	No	0.55	3.17	Yes
LUT	C ₁₅ H ₁₀ O ₆	286.24	1.86	High	High	No	0.55	3.02	Yes
GER	C ₃₀ H ₂₄ O ₁₀	544.51	2.14	Moderate	Low	No	0.17	5.73	No (2)
CHD	C ₂₇ H ₄₄ O	384.64	4.81	Poor	Low	No	0.55	6.29	No (3)
APG	C ₁₅ H ₁₀ O ₅	270.24	1.89	Moderate	High	No	0.55	2.96	Yes
FST	C ₁₅ H ₁₀ O ₆	286.24	1.50	High	High	No	0.55	3.16	Yes
LNT	C ₃₀ H ₅₀ O	426.72	5.09	Poor	Low	No	0.55	6.07	No (3)
BIT	C ₈ H ₇ NS	149.21	2.19	High	High	Yes	0.55	1.59	Yes
GA	C ₇ H ₆ O ₅	170.12	0.21	High	High	No	0.56	1.22	Yes
IST	C ₂₀ H ₃₀ O ₃	318.45	2.27	Moderate	High	Yes	0.56	4.83	Yes
STG	C ₂₉ H ₄₈ O	412.69	4.96	Poor	Low	No	0.55	6.21	No (3)
NGN	C ₁₅ H ₁₂ O ₅	272.25	1.75	Soluble	High	No	0.55	3.01	Yes
PTA	C ₈ H ₆ O ₄	166.13	0.60	Soluble	High	No	0.56	1.00	No (2)

3.2. Pharmacokinetic effects of the phytochemical compounds on the predicted targets involved in the metabolism of the four PI drugs

The SWISSADME server was employed to predict the pharmacokinetic effects of the selected phytochemical compounds from COA®-FS herbal medicine on the Cytochrome P450 enzymes and P-glycoprotein transporter involved in the metabolism of the four FDA-approved drugs. The result revealed that the PI drugs showed inhibitory activities on CYP3A4. LPV was also predicted to inhibit CYP2C19. The four drugs were predicted inducers of P-gp, as only IST and NGN were predicted inducers of P-gp. Seven of the phytochemical compounds were predicted to possess inhibitory activity on CYP3A4 and none of the phytochemical compound was predicted to inhibit CYP2C19. The inhibition of CYP3A4 and P-gp by the phytochemical compound could decrease the elimination and pumping out of the four PI drugs from the systemic circulation and the cells respectively.

3.3. Assessing the drug-likeness of phytochemical compounds from COA®-FS herbal medicine

As shown in Table 4, three of the FDA-approved drugs (ATV, SQV and LPV) with three of the selected phytochemical compounds from COA®-FS herbal medicine (CHD, STG and NGN) are poorly soluble in water. This may lower the bio availabilities of the three PI drugs and the three phytochemical compounds. The result also showed the drug likeness of the four FDA-approved drugs and the fifteen selected phytochemical compounds from COA®-FS herbal medicine, two of the four conventional drugs pass the drug likeness test (DRV and LPV) and Nine of the phytochemical compounds (K7G, EGA, LUT, APG, FST, BIT, GA, IST and NGN) pass the test. These showed that the nine phytochemical compounds have good drug properties as the two conventional drugs.

3.4. Binding affinity of the phytochemical compounds from COA®-FS herbal medicine to HIVpro

Fifteen phytochemicals from COA®-FS herbal medicine, its component plants and four FDA-approved protease inhibitor drugs (PIs) were docked with HIVpro to estimate the affinity of the drugs to the enzyme in comparison to the four known PIs (Table 5). The docking score showed the fitness of the ligands into the active site pocket of the enzyme and the more negative the value the better the fitness of the ligand. In term of the docking score, all the PIs are better than the phytochemical compounds except EGA and K7G which are better than LPV. The docking scores for

Table 5

Docking scores for the four FDA-approved PI drugs and phytochemical compounds from COA®-FS herbal medicine.

Compounds Name	Docking score (kcal/mol)
FDA Approved Drugs	
SQV	-9.8
DRV	-9.2
ATV	-8.7
LPV	-8.1
COA-FS Phytochemical compounds	
EGA	-8.3
K7G	-8.1
EGCG	-7.5
STG	-7.5
GER	-7.5
NGN	-7.5
CHD	-7.4
LNT	-7.4
FST	-7.3
LUT	-7.3
APG	-7.2
IST	-7.1
PTA	-4.8
BIT	-4.6
GA	-4.5

the four FDA-approved PIs range from -8.1 to -9.2 kcal/mol, while Ellagic acid and Kaempferol-7-O-glucoside showed the highest docking scores among the fifteen phytochemical compounds and the scores fall within the range of the docking score for the four FDA approved PI drugs. The binding conformation of the fifteen phytochemical compounds (ligands) and the four FDA-approved drugs were taken for further molecular dynamics and binding energy calculations.

3.5. Thermodynamic binding free energy of phytochemical compounds from COA®-FS herbal medicine to HIVpro

As molecular docking only measures the geometric fit of ligands at the active site of a protein, molecular dynamics simulations were run for 100ns to assess the binding free energy of each system. The more negative the values, the better the binding free energy between the enzyme (*HIVpro*) and the ligands. The binding free energy of the four FDA-approved drugs and the fifteen phytochemical compounds were determined using the MMGBSA method to estimate the interaction strength between the FDA-approved inhibitors in comparison to the COA®-FS

herbal medicine phytochemical compounds (Table 6). ATV showed the highest binding energy than the remaining three conventional PIs and the fifteen selected phytochemical compounds. However, EGCG had better energy than three conventional PIs (DRV, LPV and SQV). In addition, K7G is better than LPV and DRV.

3.6. Structural analysis of the most optimal Phytochemical-HIVpro complexes

To further establish the mechanistic inhibitory characteristics of these four selected phytochemical compounds (EGCG, K7G, EGA and LUT) with antiviral activity against *HIVpro*. Root mean square deviation (RMSD), Root mean square fluctuation (RMSF), Radius of gyration (RoG) and ligand interaction plots were assessed.

Fig. 2 depicts the RMSD plot for the four phytochemical compounds and the four FDA-approved drugs. RMSD measures protein stability as the simulation progresses. The RMSD plots of K7G, EGA and EGCG with average values of 1.432Å, 1.442Å and 1.465Å respectively are similar to the RMSD of ATV (1.511 Å), DRV (1.451Å), SQV (1.402Å), apo-enzyme, 1.342Å (protease enzyme without ligand). RMSD of EGCG seems to slightly close to the RMSD of LPV (1.9189Å). The RMSD of K7G (1.351Å) showed the same similarity with RMSD of SQV (1.345 Å). The RMSD of the four compounds deviates from the RMSD of LPV with the highest average value of 2.187Å. The first 40ns of simulation of LPV showed the instability of the enzyme, but from 40 to 100ns of simulation the enzyme was stable.

Figs. 3 and 4 showed the Radius of Gyration (RoG) and Root mean square fluctuations values over the course of 100ns of simulations of the HIV-1 protease enzymes bound to different ligands. RoG is a measure of the compactness of the protein structure. The RoG values of each of the compound were compared to the RoG of the four FDA approved drugs (Fig. 3). RoG of EGCG (17.544 Å), LUT (17.431Å), EGA (17.354Å) and K7G (17.455 Å) shows similarity with the RoG of LPV (17.411 Å), ATV (17.327 Å) and SQV (17.423 Å) but deviated from the RoG of DRV (18.345 Å). None of the four compounds showed the same trend and values with RoG of DRV (18.345 Å).

RMSF values monitor the fluctuation of each amino residue as they interact with the ligand throughout a trajectory. The RMSF values of each of the four phytochemical compounds were compared to the RMSF of the four FDA-approved drugs (Fig. 4).

Fig. 5 illustrates the ligand-interaction plots of the above-mentioned systems following the 100 ns trajectory. The type and number of

Table 6

Thermodynamic binding free energy for Phytochemical compounds from COA®-FS herbal medicine and FDA-approved drugs to *HIVpro*.

Complex	ΔE_{vdw}	ΔE_{elec}	ΔG_{gas}	ΔG_{solv}	ΔG_{bind}
FDA-Approved Drugs					
SQV	-59.300 ± 5.140	6.139 ± 4.847	-53.161 ± 19.400	-0.514 ± 1.35	-53.979 ± 4.874
DRV	-43.805 ± 6.108	-25.424 ± 8.120	-69.223 ± 10.871	29.235 ± 4.206	-35.311 ± 4.943
ATV	-65.905 ± 4.965	-28.758 ± 5.760	-94.664 ± 8.314	37.824 ± 4.796	-56.839 ± 5.292
LPV	-51.973 ± 5.433	-27.534 ± 6.605	-79.507 ± 7.958	38.291 ± 3.540	-44.571 ± 3.952
COA®-FS herbal medicine Phytochemical compounds					
EGCG	-36.589 ± 4.054	-76.679 ± 10.634	-113.26 ± 10.265	61.364 ± 3.586	-55.954 ± 2.705
K7G	-45.850 ± 4.123	-44.778 ± 9.576	-90.628 ± 8.503	48.269 ± 5.467	-45.740 ± 4.288
EGA	-25.883 ± 3.400	-57.201 ± 6.132	-83.084 ± 5.446	46.585 ± 3.653	-38.500 ± 2.101
LUT	-26.604 ± 3.702	-48.553 ± 7.929	-75.157 ± 6.895	41.611 ± 4.879	-37.487 ± 1.223
GER	-46.385 ± 4.820	-17.375 ± 5.847	-63.759 ± 7.842	29.458 ± 4.423	-35.532 ± 2.510
LNT	-34.047 ± 5.941	-11.624 ± 2.458	-45.669 ± 6.293	18.170 ± 3.523	-27.486 ± 3.599
APG	-31.671 ± 8.375	-16.449 ± 2.766	-48.112 ± 11.223	22.104 ± 4.239	-26.017 ± 2.966
NGN	-21.952 ± 3.673	-36.188 ± 8.717	-58.140 ± 9.018	35.379 ± 5.518	-22.761 ± 4.494
STG	-20.604 ± 4.023	20.222 ± 4.907	-0.373 ± 1.485	-19.216 ± 4.776	-19.584 ± 5.041
BIT	-18.433 ± 3.600	-264.05 ± 22.483	-225.00 ± 14.578	206.99 ± 17.374	-18.014 ± 3.083
GA	-18.545 ± 6.221	-252.39 ± 13.425	-213.60 ± 20.032	195.98 ± 19.394	-17.622 ± 2.094
IST	-18.825 ± 3.748	-254.24 ± 4.827	-215.62 ± 12.739	198.31 ± 9.202	-17.315 ± 2.650
CHD	-18.52 ± 3.777	-245.58 ± 10.393	-206.69 ± 11.342	189.51 ± 9.342	-17.184 ± 2.417
FST	-17.65 ± 4.034	-254.16 ± 14.288	-213.67 ± 8.384	198.16 ± 7.323	-15.516 ± 3.993
PTA	-21.145 ± 2.327	-17.168 ± 3.602	-38.312 ± 3.942	23.679 ± 2.555	-14.633 ± 2.248

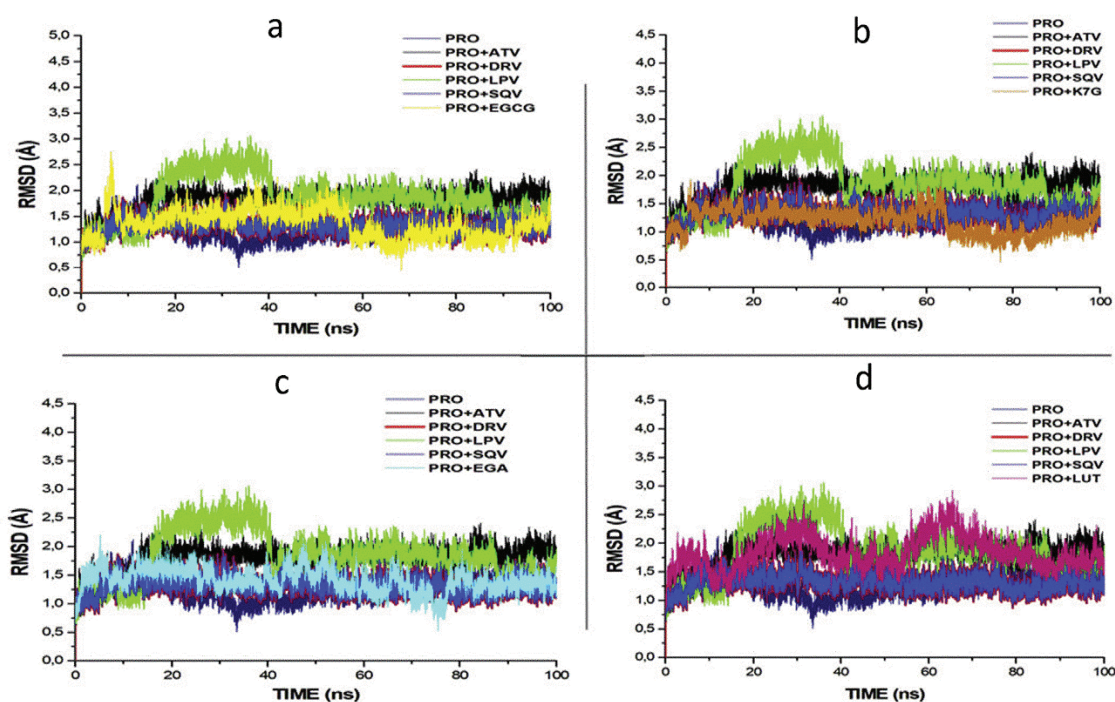


Fig. 2. RMSD profile of protein backbone atoms of PRO, ATV, DRV and SQV with (a) EGCG (b) K7G (c) EGA and (d) LUT calculated over the course of 100 ns molecular dynamics of HIVpro bound to the four different ligands and FDA-approved PI drugs.

interactions between proteins and ligands are the major determinants of the overall binding free energy.

4. Discussion

4.1. Assessing the predicted targets for the drugs and phytochemical compounds

The result of this study showed the predicted targets for the four conventional drugs and the phytochemical compounds from COA[®]-FS herbal medicine. Cytochrome P450 3A4 and CYP2C19, two sub families of cytochrome P450 enzymes were predicted to be involved in the metabolism of the four FDA-approved drugs. CYP3A4 was the predicted common target for the four conventional drugs, but LPV was additionally predicted to be inhibitor of CYP2C19. This prediction is in agreement with the report of Brian et al. and Vaishali et al. that reported CYP3A4 is the major form of cytochrome P450 enzymes involved in the metabolism of HIV protease inhibitor drugs (Brian et al., 2011; Vaishali et al., 2007). All the four FDA-approved drugs were as well predicted to be substrates of Permeability glycoprotein (P-gp), this validate the report of Griffin et al. that reported that P-gp was actively involved in the metabolism of PI drugs (Griffin et al., 2011). A different sub type of cytochrome P450 were predicted targets for the phytochemical compounds. Cytochrome P450 1A2 (CYP 450 1A2) was predicted for EGA, FST, NGN, LUT and APG, while CYP 450 2D6 was predicted target for FST, APG and LUT. CYP3A4 and multi-drug resistant protein (P-gp) are the commonly predicted targets for the FDA-approved drug and the phytochemicals.

4.2. Pharmacokinetic effects of the phytochemical compounds on the predicted targets involved in the metabolism of the four PI drugs

The SWISSTARGETPREDICTION and SWISSADME servers predicted many enzymes and transporters as targets for the four drugs based on structures of the drugs and physiological conditions. The SWISSADME server prediction for the four drugs validated studies that reported CYP3A4 and P-gp are the major enzyme and transporter involved in the

metabolism of the PI drugs (Huisman et al., 2001; Sanjay et al., 2004; Walubo, 2007). Several studies have also shown that both CYP3A4 and P-gp have a wide and overlapping substrate specificity (Konig et al., 2013; Fromm, 2004), as this explained why the four PI drugs are both inhibitors and inducers of CYP3A4 and P-gp respectively. The pharmacokinetic effect of the phytochemicals on CYP3A and P-gp revealed that NGN, GER, FST, LUT, APG, PTA and GA are inhibitors of CYP3A4. Inhibition of CYP3A4 has been reported to decrease the rate of elimination of drugs from the systemic circulation thereby increasing bioavailability of drugs (Liyue et al., 2001). The phytochemical compounds from COA[®]-FS herbal medicine predicted to be inhibitors of CYP3A4, when used concurrently with PI drugs could increase the bioavailability of the four FDA-approved PI drugs and enhance them to maximally exert their pharmacological effects. NGN and IST were predicted inducers of P-gp and could increase the rate of elimination of the four drugs thereby lowering PI drugs bioavailability (Richard et al., 2014). Other phytochemical compounds from COA[®]-FS herbal medicine were predicted to be non-inducers of P-gp and could inhibit the activity of P-gp to increase PI drugs bioavailability.

The result of this study revealed phytochemical compounds from COA[®]-FS herbal medicine and its constituent plants are predicted inhibitors of CYP3A and P-gp, and they could increase the bioavailability of PI drugs in the plasma drug, resulting to the drug being slowly eliminated from the systemic circulation and exerting their therapeutic antiviral effects.

4.3. Assessing the drug-likeness of phytochemical compounds from COA[®]-FS herbal medicine

One of the important rules in drug design is Lipinski's rule, it is a set of five rules use to assess the drug-likeness of a compound with pharmacological or biological activities with the aim of examining if it possess both physical and chemical properties to act as an orally active drug in humans (Lipinski, 2004; Lipinski et al., 2012). The rule centred on the number of hydrogen bond donors in the compound (not more than 5), a few hydrogen bond acceptor (not more than 10), molecular mass less

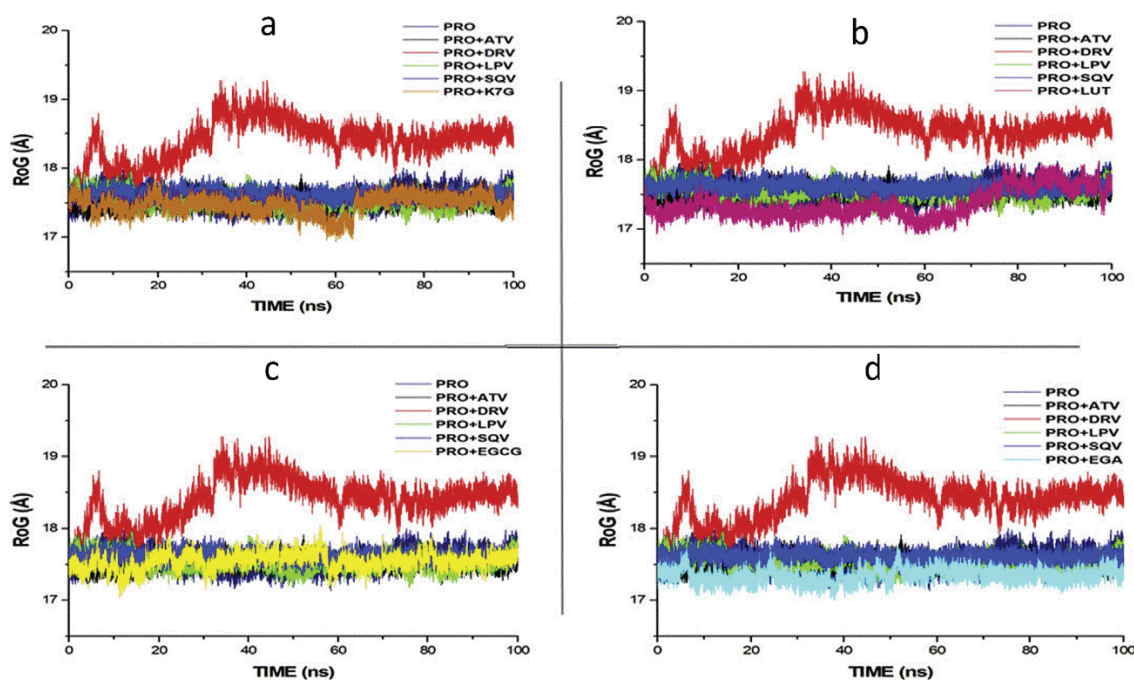


Fig. 3. RoG profile of protein backbone atoms of PRO, ATV, DRV and SQV with (a) K7G (b) LUT (c) EGCG and (d) EGA calculated over the course of 100 ns molecular dynamics of HIVpro bound to different ligands and drugs.

than 500 daltons and partition coefficient ($\log P$) not greater than 5. The result showed two of the conventional drugs (LPV and DRV) and eight of the phytochemical compounds from COA[®]-FS herbal medicine (EGA, LUT, APG, FST, BIT, GA, IST and NGN) were predicted to pass the rules. This indicates that the eight phytochemical compounds from COA[®]-FS herbal medicine possess the same chemical and physical properties with two of the FDA-approved drugs (LPV and DRV). ATV and DRV, the conventional drugs together with seven of the compounds failed a maximum of three out of the rules.

Gastrointestinal (GIT) absorption is significant for the maintenance of optimal drug levels in the systemic circulation. For drugs or potential compounds to reach their target, they must be absorbed from the GIT and enter the systemic circulation in enough amount or quantities (Kremers, 2002). Highly absorbed drugs from the GIT will easily attain optimal concentration and exert a pharmacological effect at its target site. LPV is the only drug out of the four conventional drugs that has high GIT absorption, while the remaining drugs' absorptions in GIT are low. Nine out of the fifteen phytochemical compounds from COA[®]-FS herbal medicine were predicted to be highly absorbed from the GIT (EGA, LUT, APG, FST, BIT, GA, IST, NGN, and PTA) and could eventually attain the required concentration needed for therapeutic effects.

The blood-brain barrier (BBB) is a protection developed by the endothelial cells that line cerebral microvessels (Abbott, 2002; Begley and Brightman, 2011) and drugs or compounds that are not soluble in lipid with molecular weight greater than 400 Dalton cannot go across the BBB but smaller and lipophilic molecules can go across the BBB (Begley and Brightman, 2011). Therefore, BBB permeability parameter is always considered in the development of a drug for neuro-degenerated and related diseases. None of the four FDA-approved conventional drugs was predicted to permeate the BBB and only two of the phytochemical compounds from COA[®]-FS herbal medicine (BIT and IST) were predicted to go across the BBB.

Drug bioavailability is a measurement of the degree of absorption and fraction of a given amount of unchanged drug that goes to the systemic circulation (Heaney, 2018). Orally and intravenously administered drug have different bioavailability as a result of some factors like first pass-drug metabolism. It is a significant pharmacokinetic property of the

drug that must be carefully thought of when calculating drug dosages. Higher bioavailability score is required for a drug to reach a higher and optimal concentration in the systemic circulation and to exert notable pharmacological response. When compared with the four conventional drugs, ATV and SQV have low and the same bioavailability scores of 0.17 with EGCG, GER and K7G. Slightly higher bioavailability scores of 0.55 were predicted for LPV and DRV, and the other phytochemical compounds from COA[®]-FS herbal medicine.

4.4. Thermodynamic binding free energy of phytochemical compounds to HIVpro

The binding free energy calculated for the four conventional drugs ranges from -35.311 ± 4.943 to -56.056 ± 4.978 kcal/mol, with Atazanavir (ATV) and Darunavir having the highest and the lowest values respectively. Epigallocatechin gallate (EGCG), Kaempferol-7-O-glucoside (K7G), Ellagic acid (EGA) and Luteolin (LUT) indicated the most optimal binding when compared to the FDA approved drugs. It was also interesting to note that although compounds FST, APG and NGN demonstrated relatively high docking scores, binding free energy calculations for these systems indicated dissimilar results. This validates the need for molecular dynamics simulations, which may allow for a compound to become "comfortable" within an enzyme's binding site. To further establish the mechanistic inhibitory characteristics of the best four phytochemical compounds (EGCG, K7G, EGA and LUT) with higher free binding energy, RMSD, RoG, RMSF, and ligand interaction plots were assessed.

4.5. Structural analysis of the most optimal phytochemical compound-HIVpro complexes

The structural stability of a protein complex was measured following experimental simulation of the phytochemical compounds together with the protein. Root mean square deviation (RMSD) and root mean square fluctuation (RMSF) were studied in several molecular dynamics simulations to study conformational stability of ligands and proteins (Agoni et al., 2018; McGillewie and Soliman, 2015; Munsamy et al., 2018; Ramharack

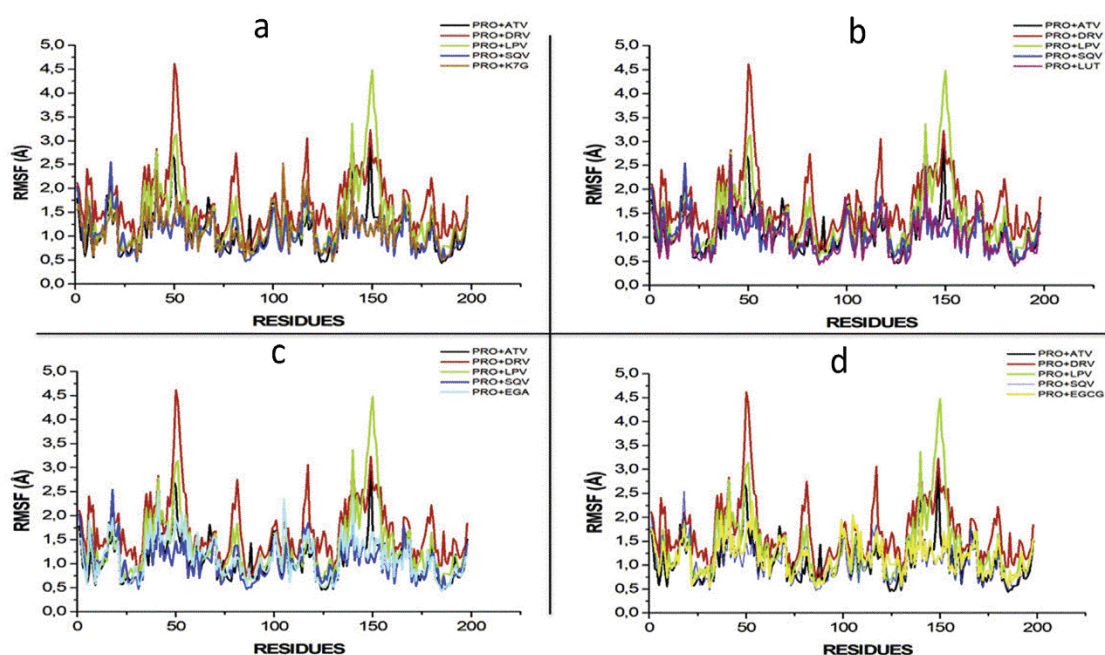


Fig. 4. RMSF profile of protein backbone atoms of PRO, ATV, DRV and SQV with (a) K7G (b) LUT (c) EGA and (d) EGCG calculated over the course of 100 ns molecular dynamics of *HIVpro* bound to four different ligands and FDA-approved drugs.

et al., 2017). The deviation produced by a protein during stimulation is a factor determining its stability, and the lower the deviation produced the more stable the protein. Therefore, RMSD, which measures protein stability as the simulation progresses, can be used to determine protein stability. In this study, RMSD values for the C-alpha atoms of the structures were determined. The RMSD values of the *HIVpro*-ligands (four FDA approved drugs and four compounds with highest binding energies) complexes are shown in Fig. 2.

The RMSD of each phytochemical compound was compared to the RMSD values of the four FDA approved drugs. The RMSD plots of three phytochemical compounds (EGCG, EGA and K7G) are like the RMSD values of the of the FDA-approved drugs (ATV, SQV and DRV) and apo-enzyme. This indicates the same enzyme stability was seen between the three phytochemical compounds and three of the FDA-approved drugs and the apo-enzyme (positive control). The RMSD value of the LUT (1.843Å) is slightly similar to that of LPV (2.187).

The values of the radius of gyration (RoG) were also plotted for each system. RoG is a measure of the compactness of the protein structure. The RoG values of each of the phytochemical compounds from COA®-FS herbal medicine were compared to the RoG of the four FDA approved drugs and the apo-enzyme (Fig. 3). The four phytochemical compounds shows similarity with the RoG of three of the FDA-approved protease inhibitor drugs (LPV, SQV and ATV) and the apo-enzyme but deviated from the RoG of value of DRV (18.345 Å). Like the RMSD values, none of the four phytochemical compounds from COA®-FS herbal medicine showed the same trend and values with RoG of DRV (18.345 Å).

The RMSF values monitor the fluctuation of each amino residue as they interact with the ligand throughout the trajectory. The RMSF values of each of the compound were compared to the RMSF of the four FDA approved drugs (Fig. 4). Based on the RMSF results, it was evident that the DRV (1.694) and LPV (1.380) systems demonstrated highest fluctuations, particularly at residues 50, 80, 115–120 and 130–155. The K7G (1.130) system showed the greatest similarity to the four FDA-approved drugs, with fluctuations occurring with similar residues. With this being said, fluctuations at 45–55 and 145–155 are mirror residues in dimeric form. This substantiates the necessity of the dimeric activity of the *HIV*-protease (Hayashi et al., 2014).

4.6. Ligand-*HIVpro* interactions with different amino acid residues

As mentioned above, ATV at the *HIVpro* binding led to the highest free binding energy of the 19 systems. These results may be attributed to the greater number of hydrogen bond interactions produced between the drug and *HIVpro* amino acid residues (ASP128, GLY126, ASP124, THR179, ALA127, PRO180, GLY49, GLY27, ASP25, and ILE47). The hydrogen bond interactions for SQV, LPV, and DRV are 4, 5 and 4 respectively. A Salt-bridge interaction at amino residue ASP25, together with numerous van der Waals, alkyl, and Pi-alkyl interactions contributed to the SQV-system gaining second highest binding energy. With 20 van der Waals interactions and 5 hydrogen bond interactions, LPV showed higher binding energy than DRV. Of the phytochemical compounds, EGCG demonstrated the highest binding energy. This may have been the result of salt-bridge interaction at ARG107, 6 hydrogen bond interactions, 13 van der Waals and 3 Pi-alkyl interactions. It was interesting to note that the “two-component” salt-bridges, made up of a hydrogen bond and electrostatic interaction, were only recorded within the EGCG and SQV systems. This could have led to the overall binding energy of EGCG higher than K7G, despite K7G having a higher overall number of interactions. EGA and LUT possess 3 and 4 hydrogen bond, 6 and 8 van der Waals, and 2 each of Pi-alkyl interactions respectively.

5. Conclusion

The predictive analysis predicted several enzymes and transporters as targets for the four FDA-approved drugs and the phytochemical compounds but CYP3A4 enzyme and P-gp transporters are majorly involved in the metabolism of PI drugs. The analysis also predicted both inhibitors and inducers of CYP3A4 and P-gp among the phytochemical compounds from COA®-FS herbal medicine and its component plants. The phytochemical compounds predicted to be inhibitors of CYP3A4 and P-gp could increase the bioavailability of the four FDA-approved drugs in the systemic circulation thereby enhancing the four drugs to exert maximum pharmacological effects. The Fifteen selected phytochemical compounds from COA-FS herbal medicine and its component plants were subjected to docking studies with *HIVpro* to recognize the best natural potential inhibitors as compared to the four FDA-approved *HIVpro* inhibitor drugs

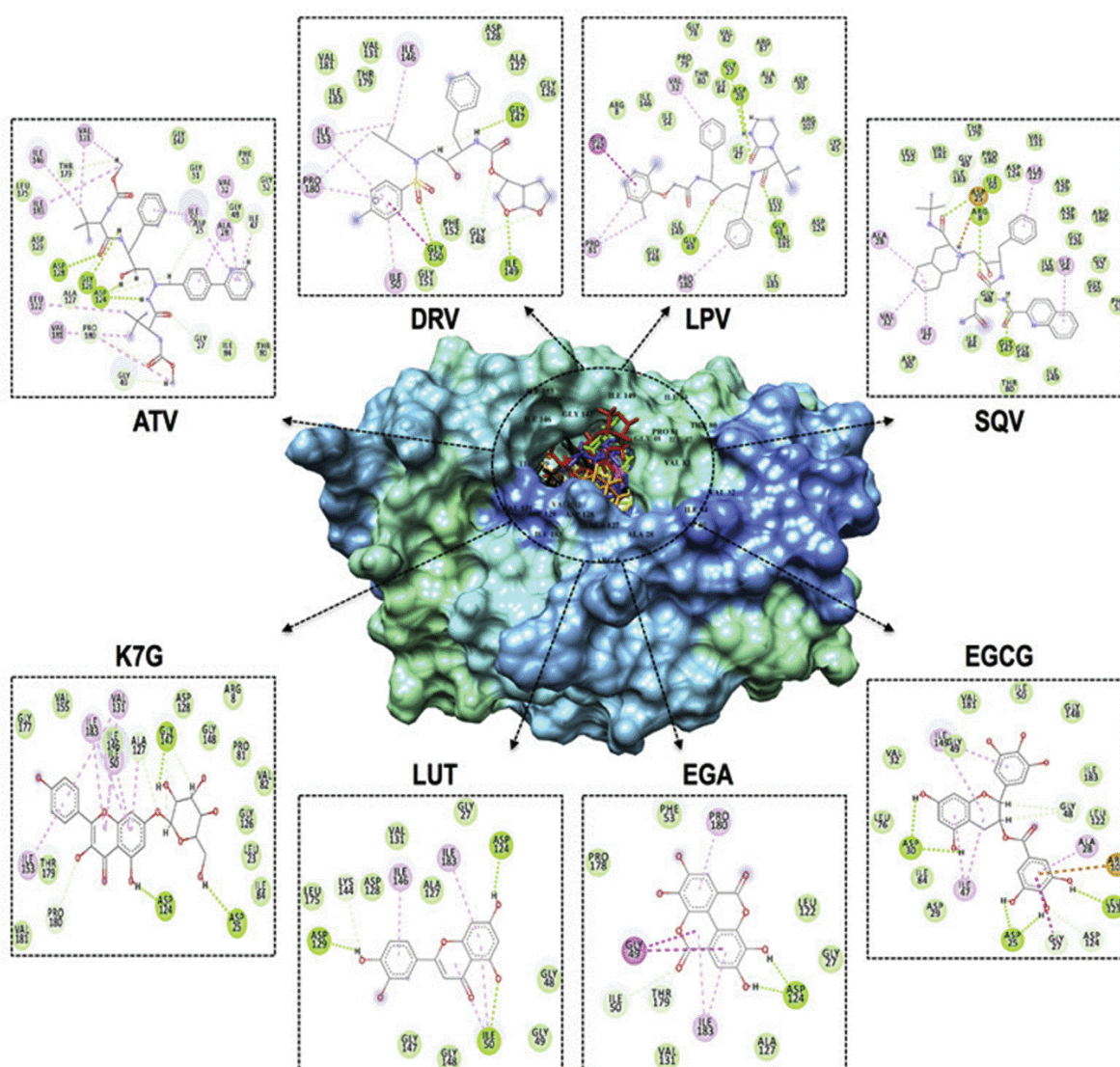


Fig. 5. Representation of ligand-HIVpro interactions with different amino acid residues.

in term of binding free energy/affinity. Of all the docked selected phytochemical compounds, EGCG, K7G, EGA, NGN, STG, GER, and LUT gave the best binding score when compared to the four conventional drugs. Molecular dynamics and MMGBSA analysis were done on all the fifteen compounds and the drugs. The results of the MD simulations and MMGBSA showed that only EGCG, K7G, EGA and LUT fit well into the HIVpro active site pocket with better binding free energy. The study implied that the ligands interacted hydrophobically with the active amino residues. This study also identified some of the key residues that are helpful in dual inhibitor design. The EGCG and k7G compounds proved to be more potent inhibitors of HIVpro. Therefore, this study showed that some of the phytochemical compounds could be utilised to enhance therapeutic effect of the four FDA-approved drugs and, could as well serve as natural inhibitors of HIVpro and be used as important standard in developing novel drugs to inhibit the activity of HIVpro.

Declarations

Author contribution statement

Idowu Kehinde, Pritika Ramharack: Conceived and designed the

experiments; Performed the experiments; Analyzed and interpreted the data; Wrote the paper.

Manimbulu Nlooto, Michelle Gordon: Conceived and designed the experiments; Analyzed and interpreted the data; Wrote the paper.

Funding statement

This work was supported by College of Health Sciences, University of KwaZulu-Natal Scholarship.

Competing interest statement

The authors declare no conflict of interest.

Additional information

No additional information is available for this paper.

References

Abbott, N.J., 2002. Astrocyte-endothelial interactions and blood-brain barrier permeability. *J. Anat.* 200 (6), 629–638.

- Adewole, E., Ojo, A., Ogunmodede, O.T., Adewumi, D.F., Omoaghe, A.O., Jamshed, I., 2018. Characterization and Evaluation of Vernonia Amygdalina Extracts for its Antidiabetic Potentials.
- Agoni, C., Ramharack, P., Soliman, M.E.S., 2018. Co-inhibition as a strategic therapeutic approach to overcome rifampin resistance in tuberculosis therapy: atomistic insights. *Future Med. Chem.* 10 (14), 1665–1675.
- Babatunde, D.E., Otusemade, G.O., Efevbokhan, V.E., Ojewumi, M.E., Bolade, O.P., Owoye, T.F., 2019. PT. Chemical Data Collections, 100208.
- Begley, D.J., Brightman, M.W., 2011. Structural and functional aspects of the blood-brain barrier. *Pept. Transp. Deliv. Cent. Nerv. Syst.* 61 (5), 39–78.
- Boadu, A., 2019. A Comparative Chemistry of COA Herbal Medicine and Herbal Extracts of *Veronia mygdalina* (Bitter Leaf) and *Persea americana* (Avocado). unpublished thesis. University of KwaZulu-Natal, Durban, South Africa.
- Brian, J., Kirby, A.C., Collier, E.D., Kharasch, V., Dixit, P.D., Whittington, K.T., Jashvant, D.U., 2011. Complex drug interactions of HIV Protease inhibitors 2: in vivo induction and in vitro to in vivo correlation of induction of cytochrome P450 1A2, 2B6, and 2C9 by ritonavir or nelfinavir. *Drug. Metab. Dispos.* 39 (12), 2329–2337.
- Brik, A., Wong, C.H., 2003. HIV-1 protease: mechanism and drug discovery. *Org. Biomol. Chem.* 1 (1), 5–14.
- Burley, S.K., Berman, H.M., Christie, C., Duarte, J.M., Feng, Z., Westbrook, J., et al., 2018. RCSB Protein Data Bank: sustaining a living digital data resource that enables breakthroughs in scientific research and biomedical education. *Protein Sci.* 27 (1), 316–330.
- Calderon-Oliver, M., Medina-Campos, O.N., Ponce-Alquicira, E., Pedroza-Islas, R., Pedraza-Chaverri, J., Escalona-Buendía, H.B., 2015. Optimization of the antioxidant and antimicrobial response of the combined effect of nisin and avocado byproducts. *LWT Food Sci. Technol.* 65, 46–52.
- Carmona, S., Nash, J., 2017. Adult antiretroviral therapy guidelines 2017 as per HIV Medicine. *SAJ* 18 (1), 1–24.
- Daina, A., Michielin, O., Zoete, V., 2017. SwissADME: a free web tool to evaluate pharmacokinetics, drug-likeness and medicinal chemistry friendliness of small molecules. *Sci. Rep.* 7 (1), 1–13.
- Dineshkumar, I.A.G., Rajakumar, R., 2017. GC-MS Evaluation of bioactive molecules from the methanolic leaf extract of *Azadirachta indica* (A. JUSS). *Asian J. Pharmaceut. Sci. Technol.*
- Fromm, M.F., 2004. Importance of P-glycoprotein at blood-tissue barriers. *Trends Pharmacol. Sci.* 25 (12), 424–429.
- Geretti, A.M., Easterbrook, P., 2001. Antiretroviral resistance in clinical practice. *Int. J. STD AIDS* 12 (3), 15–153.
- Gfeller, D., et al., 2014. Swiss target prediction: a web server for target prediction of bioactive small molecules. *Nucleic Acids Res.* 42, W32–W38.
- Hanwell, M.D., Curtis, D.E., Lonie, D.C., Vandermeersch, T., Zurek, E., Hutchison, G.R., 2012. Avogadro: an advanced semantic chemical editor, visualization, and analysis platform. *J. Cheminf.* 4 (8), 1–17.
- Hayashi, H., Takamune, N., Nirasawa, T., Aoki, M., Morishita, Y., Das, D., et al., 2014. Dimerization of HIV-1 protease occurs through two steps relating to the mechanism of protease dimerization inhibition by darunavir. *Proc. Natl. Acad. Sci.* 111 (33), 12234–12239.
- Hayes, J.M., Archontis, G., 2011. Molecular Dynamic-Studies of Synthetic and Biological Molecules, p. 2011.
- Heaney, R.P., 2018. Factors influencing the measurement of bioavailability, taking calcium as a model. *J. Nutr.* 131 (4), 1344S–1348S.
- Huisman, M.T., Smit, H.R., Wiltshire, R.M., Hoetelmans, J.H., Beijnen, Schinkel, A.H., 2001. P-glycoprotein limits oral availability, brain, and fetal penetration of saquinavir even with high doses of ritonavir. *Mol. Pharmacol.* 59, 806–813.
- Hurtado-Fernández, E., Pachiarotta, T., Mayboroda, O.A., Fernández-Gutiérrez, A., Carrasco-Pancorbo, A., 2014. Quantitative characterization of important metabolites of avocado fruit by gas chromatography coupled to different detectors (APCI-TOF MS and FID). *Food Res. Int.* 62, 801–811.
- Igile, G.O., Oleszek, W., Burda, S., Jurzysta, M., 1995. Nutritional assessment of Vernonia amygdalina leaves in growing mice. *J. Agric. Food Chem.* 43 (8), 2162–2166.
- Kermanshah, R., McCarty, B.E., Rosenfeld, J., Summers, P.S., Weretilnyk, E.A., Sorger, G.J., 2001. Benzyl isothiocyanate is the chief or sole anthelmintic in papaya seed extracts. *Phytochemistry* 57 (3), 427–435.
- Kim, S., Thiessen, P.A., Bolton, E.E., Chen, J., Fu, G., Gindulyte, A., et al., 2016. PubChem substance and compound databases. *Nucleic Acids Res.* 44 (1), 1202–1213.
- Kongkachuichai, R., Charoensiri, R.L.N., 2010. Carotenoid, flavonoid profiles and dietary fiber contents of fruits commonly consumed in Thailand. *Int. J. Food Sci. Nutr.* 61 (August), 536–548.
- Konig, J., Muller, F., Fromm, M.F., 2013. Transporters and drug-drug interactions: Important determinants of drug disposition and effects. *Pharmacol. Rev.* 65, 944–966.
- Kremers, P., 2002. In vitro tests for predicting drug-drug interactions: the need for validated procedures. *Pharmacol. Toxicol.* 91 (5), 209–217.
- Lako, J., 2007. Phytochemical flavonols, carotenoids and the antioxidant properties of a wide selection of Fijian fruit, vegetables and other readily available foods. *Food Chem.* 101, 1727–1741.
- Griffin, LaToya, Annaert, Pieter, Brouwer, Kim, 2011. Influence of drug transport proteins on pharmacokinetics and drug interactions of HIV protease inhibitors. *J. Pharm. Sci.* 100 (9), 3636–3654.
- Levy, Y., Caffisch, A., 2003. Flexibility of monomeric and dimeric HIV-1 protease. *J. Phys. Chem. B* 107 (13), 3068–3079.
- Lipinski, C.A., 2004. Lead- and drug-like compounds: the rule-of-five revolution. *Drug Discov. Today Technol.* 1 (4), 337–341.
- Lipinski, C.A., Lombardo, F., Dominy, B.W., Feeney, P.J., 2012. Experimental and computational approaches to estimate solubility and permeability in drug discovery and development settings. *Adv. Drug Deliv. Rev.* 64.
- Liyue, H., Stephen, A., Wring, J.L., Woolley, K.R., Brouwer, C., Serabjit-Singh, Joseph, W.P., 2001. Induction of p-glycoprotein and cytochrome p450 3a by hiv protease inhibitors. *Drug Metab. Dispos.* 29 (5), 755–760.
- Mcgillewie, L., Soliman, M.E., 2015. Flap flexibility amongst I, II, III, IV, and V: sequence, structural, and molecular dynamic analyses. *Proteins Struct. Funct. Genet.* 83 (9), 1693–1705.
- Monika, P., Geetha, A., 2015. PT US CR. Phytomedicine.
- Mukhtar, M., Arshad, M., Ahmad, M., Pomerantz, R.J., Wigdahl, B., Parveen, Z., 2008. Antiviral potentials of medicinal plants. *Virus Res.* 131, 111–120.
- Munsamy, G., Ramharack, P., Soliman, M.E.S., 2018. Egress and invasion machinery of malaria: an in depth look into the structural and functional features of the flap dynamics of plasmeprin IX and X. *RSC Adv.* 8, 21829–21840.
- Nair, P.C., Miners, J.O., 2014. Molecular dynamics simulations: from structure function relationships to drug discovery. *Silico Pharmacol.* 2 (4), 1–4.
- Nlooto, M., Naidoo, P., 2014. Clinical relevance and use of traditional, complementary and alternative medicines for the management of HIV infection in local African communities, 1989 - 2014: a review of selected literature. *Pula: Botsw. J. Afr. Stud.* 28 (1), 105–116.
- Nwabuife, J.C., 2019. A Comparative Chemistry of COA Herbal Medicine and Herbal Extracts of *Azadirachta indica* and *Carica papaya*. unpublished thesis. University of KwaZulu-Natal, Durban, South Africa.
- Ramharack, P., Oguntade, S., Soliman, M.E.S., 2017. Delving into Zika virus structural dynamics – a closer look at NS3 helicase loop flexibility and its role in drug discovery. *RSC Adv.* 7 (36), 22133–22144.
- Rashed, K., Luo, M.-T., Zhang, L.-T., Zheng, Y.-T., 2013. Phytochemical screening of the polar extracts of *Carica papaya* Linn. and the evaluation of their anti-Hiv-1 activity. *J. Appl. Ind. Sci.* 1 (3), 49–53. Retrieved from: <https://www.semanticscholar.org/paper/Phytochemical-Screening-of-the-Polar-Extracts-of-Rashed-Luo/445b4726079362a4960c3cedec7ae5904f7bc>.
- Richard, C., Frederick, L., Mary, B., 2014. Inhibition of the multidrug resistance P-glycoprotein: Time for a change of strategy. *Drug. Metab. Dispos.* 42, 623–631.
- Sajin, A.K., Rathnan, R.K., Mechoor, A., 2015. Molecular docking studies on phytochemicals from the methanol leaf extract of *Carica papaya* against Envelope protein of dengue virus (type-2). *J. Comput. Methods Mol. Des.* 5 (2), 1–7.
- Sanjay, U.C., Sankatsing, J.H., Beijnen, A.H., Schinkel, Joep M.A.L., Jan, M.P., 2004. P Glycoprotein in human immunodeficiency virus type 1 infection and therapy. *Antimicrob. Agents Chemother.* 48 (4), 1073–1081.
- Scholar, E., 2011. HIV Protease inhibitors. *XPharm: the Comprehensive Pharmacology Reference*, pp. 1–4.
- Seifert, E., 2014. OriginPro 9.1: scientific data analysis and graphing software-software review. *J. Chem. Inf. Model.* 54 (5), 1552–1552.
- Shin, M.S., Kang, E.H., Lee, Y.I., 2005. A flavonoid from medicinal plants blocks hepatitis B virus-e antigen secretion in HBV-infected hepatocytes. *Antivir. Res.* 67 (3), 163–168.
- Siddiqui, B.S., Afshan, F., Arfeen, S.S., Gulzar, T., 2006. A new tetracyclic triterpenoid from the leaves of *Azadirachta indica*. *Nat. Prod. Res.* 20 (12), 1036–1040.
- Soontornniyomkij, V., Umlauf, A., Chung, S.A., Cochran, M.L., Soontornniyomkij, B., Gouaux, B., et al., 2014. HIV protease inhibitor exposure predicts cerebral small vessel disease. *AIDS* 28 (9), 1297–1306.
- Vaishali, D., Niresh, H., Fang, L.I.P., Desai, K., Thummel, E., Jashvant, D.U., 2007. Cytochrome P450 Enzymes and transporters induced by anti-human immunodeficiency virus protease inhibitors in human hepatocytes: Implications for predicting clinical drug interactions. *Drug. Metab. Dispos.* 35 (10), 1473–1477.
- Walubo, A., 2007. The role of cytochrome p450 in antiretroviral drug interactions. *Expert Opin. Drug Metab. Toxicol.* 3, 583–598.
- WHO, UNAIDS, UNFPA, UNICEF, UNWomen, & The World Bank Group, 2018. *Survive, Thrive, Transform. Global Strategy for Women's, Children's and Adolescents' Health: 2018 Report on Progress towards 2030 Targets.* World Health Organization, Geneva.
- Yang, Z., Lasker, K., Schneidman-Duhovny, D., Webb, B., Huang, C.C., Pettersen, E.F., et al., 2012. UCSF Chimera, MODELLER, and IMP: an integrated modeling system. *J. Struct. Biol.* 179 (3), 269–278.
- Ylilauri, M., Pentikäinen, O.T., 2013. MMGBSA as a tool to understand the binding affinities of filament-peptide interactions. *J. Chem. Inf. Model.* 53 (10), 2626–2633.

Appendix F



Journal of Biomolecular Structure and Dynamics



ISSN: (Print) (Online) Journal homepage: <https://www.tandfonline.com/loi/tbsd20>

Molecular dynamic mechanism(s) of inhibition of bioactive antiviral phytochemical compounds targeting cytochrome P450 3A4 and P-glycoprotein

Idowu Kehinde , Pritika Ramharack , Manimbulu Nlooto & Michelle Gordon

To cite this article: Idowu Kehinde , Pritika Ramharack , Manimbulu Nlooto & Michelle Gordon (2020): Molecular dynamic mechanism(s) of inhibition of bioactive antiviral phytochemical compounds targeting cytochrome P450 3A4 and P-glycoprotein, Journal of Biomolecular Structure and Dynamics, DOI: [10.1080/07391102.2020.1821780](https://doi.org/10.1080/07391102.2020.1821780)

To link to this article: <https://doi.org/10.1080/07391102.2020.1821780>

 Published online: 16 Oct 2020.

 [Submit your article to this journal](#) 

 Article views: 5

 [View related articles](#) 

 [View Crossmark data](#) 

Full Terms & Conditions of access and use can be found at
<https://www.tandfonline.com/action/journalInformation?journalCode=tbsd20>



Molecular dynamic mechanism(s) of inhibition of bioactive antiviral phytochemical compounds targeting cytochrome P450 3A4 and P-glycoprotein

Idowu Kehinde^a, Pritika Ramharack^b, Manimbulu Nlooto^{b,c} and Michelle Gordon^a

^aKwaZulu-Natal Research, Innovation and Sequencing Platform (KRISP)/Genomics Unit, School of Laboratory Medicine and Medical Sciences, College of Health Sciences, Nelson R Mandela School of Medicine, University of KwaZulu-Natal, Durban, South Africa; ^bDiscipline of Pharmacy, School of Health Sciences, College of Health Sciences, University of KwaZulu-Natal, Durban, South Africa; ^cDepartment of Pharmaceutical Sciences, Healthcare Sciences, University of Limpopo, Durban, South Africa

Communicated by Ramaswamy H. Sama

ABSTRACT

P-glycoprotein (ABCB1) and cytochrome P450 3A4 (CYP3A4) metabolize almost all known human immunodeficiency virus' protease inhibitor drugs (PIs). Over induction of these proteins' activities has been linked to rapid metabolism of PIs which are then pumped out of the circulatory system, eventually leading to drug-resistance in HIV-positive patients. This study aims to determine, with the use of computational tools, the inhibitory potential of four phytochemical compounds (PCs) (epigallocatechin gallate (EGCG), kaempferol-7-glucoside (K7G), luteolin (LUT) and ellagic acid (EGA)) in inhibiting the activities of these drug-metabolizing proteins. The comparative analysis of the MM/GBSA results revealed that the binding affinity (ΔG_{bind}) of EGCG and K7G for CYP3A4 and ABCB1 are higher than LUT and EGA and fall between the ΔG_{bind} of the inhibitors of CYP3A4 and ABCB1 (Ritonavir (strong inhibitor) and Lopinavir (moderate inhibitor)). The structural analysis (RMSD, RMSF, RoG and protein-ligand interaction plots) also confirmed that EGCG and K7G showed similar inhibitory activities with the inhibitors. The study has shown that EGCG and K7G have inhibitory activities against the two proteins and assumes they could decrease intracellular efflux of PIs, consequently increasing the optimal concentration of PIs in the systemic circulation.

ARTICLE HISTORY

Received 10 July 2020
Accepted 6 September 2020

KEYWORDS

P-glycoprotein; cytochrome P450 3A4; protease inhibitor drugs; computational tools

Introduction

P-glycoprotein (ABCB1) and cytochrome P450 3A4 (CYP3A4) have been reported to play significant roles in the metabolism of many protease inhibitors drugs (PIs). Over induction of ABCB1 and CYP3A4 has been reported to lead to rapid metabolism and elimination of PIs from the systemic circulation, and alter PIs' pharmacokinetics by reducing bioavailability which can result in patients developing resistance to PIs (Liyue et al., 2001; Weiss et al., 2007).

P-glycoprotein are essential proteins present in the cell membrane, encoded in humans by the ABCB1 gene (Dhananjay et al., 2011; Van Waterschoot et al., 2010). As an ATP-dependent efflux pump they have a broad substrate specificity, and their primary role is to pump many potentially toxic substances out of the cells and influence the bio-availability of drugs and other compounds. Evidence suggests that ABC transport proteins caused drug resistance and alter PI pharmacokinetics by reducing bioavailability and decreasing accumulation in organs and tissues (Weiss & Haefeli, 2010). Van Waterschoot et al. reported that all known PIs are substrates of P-glycoprotein (Van Waterschoot et al., 2010), and over-expression of P-glycoprotein reduces the concentration of PIs (Konig et al., 2013). PIs such as

Atazanavir (ATV), Lopinavir (LPV), Amprenavir (AMP) and Ritonavir (RTV) have been reported to be inhibitors of ABCB1 (Bierman et al., 2010; Fromm, 2004; Janneh et al., 2007).

Cytochrome P450 can deactivate drugs, either directly or by facilitated elimination from the system, as well as to bio-activate several substances to form their active compounds. Cytochrome P450 are membrane bound CYP450 enzymes containing heme as a cofactor (Danielson, 2002). CYP3A4 is a subtype of CYP450 and is known to metabolize many of the PIs (Walubo, 2007). While a study have shown that some drugs can inhibit the activity of CYP3A4 enzyme, for example, was reported to be strong inhibitors of CYP3A4 (Walubo, 2007), which might result to decrease hepatic metabolism and an increase in the concentration of drugs metabolized by CYP3A4. Studies have reported substrates overlapping between the two proteins; for example cyclosporin and ritonavir inhibits both proteins), many drug-drug interactions are attributed to either inhibition or induction of both P-glycoprotein and CYP3A4 (Fromm, 2004; Konig et al., 2013). This substrate overlapping has prompted many to hypothesize that inhibition of CYP3A4 may be a fundamental characteristic of inhibitors of ABCB1 (Konig et al., 2013; Pan & Aller, 2015).

CONTACT Michelle Gordon  tarinm@ukzn.ac.za  KwaZulu-Natal Research, Innovation and Sequencing Platform (KRISP)/Genomics Unit, School of Laboratory Medicine and Medical Sciences, College of Health Sciences, Nelson R Mandela School of Medicine, University of KwaZulu-Natal, Medical Campus, Durban, 4001, South Africa

© 2020 Informa UK Limited, trading as Taylor & Francis Group

In silico determination of potential antiviral activities of phytochemical compounds (PCs) from our laboratory reported that four PCs (epigallocatechin gallate (EGCG), kaempferol-7-glucoside (K7G), luteolin (LUT) and ellagic acid (EGA)) possess inhibitory activities against the HIV-1 protease enzyme similar to the control FDA-approved PIs (Idowu et al., 2019). Several *in vitro* studies have also reported the inhibitory activities of these four compounds against HIV-1 reverse transcriptase, integrase and protease enzymes' activities (Mahmood et al., 1996; Tripoli et al., 2007; Yamaguchi et al., 2002; Yang et al., 2014).

One of the limitations of the current antiretroviral therapy (ARV), is the inability of ARVs to reach sanctuary sites of HIV or suboptimal antiretroviral concentrations at these sites in the body (sites such as central nervous system, gut-associated lymphoid tissue, lymph nodes, and tissue macrophages) (Cory et al., 2013; Varatharajan & Thomas, 2009). This is because many ARVs are substrates of efflux transporters and metabolic enzymes (such as P-glycoprotein and CYP3A4) (Cory et al., 2013; Loscher & Potschka, 2005). Inhibiting the activities of efflux transporters and the metabolism of ARV is an important strategy in increasing the concentrations of ARV. Studies have shown that EGCG and EGA inhibit the activities of ABCB1 and CYP3A4 (Athukuri & Neerati, 2017; Shaik & Vanapatla, 2019) but, no study has reported on K7G and LUT. Athukuri et al. reported in an *in vitro* study that the bioavailability of diltiazem was significantly raised when treated with ellagic acid as a result of inhibition of CYP3A4-mediated drug metabolism and ABCB1-mediated efflux in the intestine, ileum and liver (Athukuri & Neerati, 2017). The study further reported that both the peak plasma concentration (C_{max}) and area under plasma concentration-time curve (AUC) were improved by the EGA treatment (Athukuri & Neerati, 2017). In a separate study by Shaik & Vanapatla, EGA through the inhibition of ABCB1 was reported to significantly improve the C_{max}, AUC and increase the bioavailability of oral linagliptin in rats (Shaik & Vanapatla, 2019). EGCG at both 3 and 10 mg/kg significantly increase the bioavailability of tamoxifen (Shin & Choi, 2009). The bioavailability of tamoxifen was approximately twice greater than that of the control group and the AUC was significantly increased in the presence of EGCG. The study suggested that the increase in bioavailability of tamoxifen is due to the decrease in first-pass metabolism in the intestine and liver by the inhibition of ABCB1 and CYP3A4 (Shin & Choi, 2009).

It is therefore essential to source natural compounds that can inhibit the activities of these drug-metabolism proteins to boost the bioavailability of PIs in the plasma and sanctuary sites. This study, therefore, investigated the inhibitory potentials of these PCs and their mechanism of inhibiting the PI-metabolizing proteins (CYP3A4 and ABCB1) using computational tools.

Methods

P-glycoprotein transporter and CYP3A4 enzyme, ligand acquisition and preparation

The X-ray crystal structures of the P-glycoprotein 1 (PDB code: 6C0V) (Kim & Chen, 2018) and CYP3A4 (PDB code:

4NY4 (Branden et al., 2014)) were obtained from publicly available RSCB Protein Data Bank. The structures of the proteins were then prepared on the UCSF Chimera software package. Two drugs reported to be inhibitors of CYP3A4 and ABCB1, Lopinavir (Storch et al., 2007; Weemhoff et al., 2003), and Ritonavir (Drewe et al., 1999; Storch et al., 2007), as well as the four antiviral PCs, were accessed from PubChem (Kim et al., 2016) and the 3-D structures prepared on the Avogadro software package (Hanwell et al., 2012). The two FDA-approved drugs were used as positive controls.

Before the docking, redocking was performed to validate the docking protocol used. The crystalized structures of the natural substrate of the proteins and the ligand-complexes were superimposed to demonstrate binding of the ligands at the same region or site on the proteins and their respective RMSD values evaluated (Figure 1).

Molecular docking

The Molecular docking software utilized in this study was the Autodock Vina Plugin available on Chimera (Yang et al., 2012), with default docking parameters. The structure of the proteins were prepared removing water molecules, nonstandard naming, protein residue connectivity. The missing atoms of side-chains and protein backbone were added in the protein structure before the molecular docking. Gasteiger charges were added to the compounds, and the non-polar hydrogen atoms were merged to carbon atoms. The PCs were then docked into the nucleotide-binding domain pocket of ABCB1 and the active site of CYP3A4 (by defining the grid box with a spacing of 1 Å and size of 106 × 112 × 64 and 52 × 38 × 52 pointing in x, y and z directions respectively). The two FDA-approved drugs (Lopinavir and Ritonavir) systems, as well as the four PCs systems, were then subjected to molecular dynamics simulations. Studies have reported both Lopinavir and Ritonavir to be inhibitors of CYP3A4 and ABCB1 (Drewe et al., 1999; Storch et al., 2007; Weemhoff et al., 2003).

Molecular dynamic (MD) simulations

The MD simulation was performed as described by Idowu et al. (2019). The simulation were performed using the GPU version provided with the AMBER package (AMBER 18), in which the FF18SB variant of the AMBER force field (Nair & Miners, 2014) was used to describe the systems.

ANTECHAMBER was used to generate atomic partial charges for the compounds by utilizing the Restrained Electrostatic Potential (RESP) and the General Amber Force Field (GAFF) procedures. The Leap module of AMBER 18 allowed for the addition of hydrogen atoms, as well as Cl⁻ counter ions for neutralization all (both ABCB1 and CYP3A4) systems. The amino acids were numbered, numbering residues 1-1242 for ABCB1 and 1-484 for CYP3A4. The systems were then suspended implicitly within an orthorhombic box of TIP3P water molecules such that all atoms were within 8 Å of any box edge (Jorgensen et al., 1983).

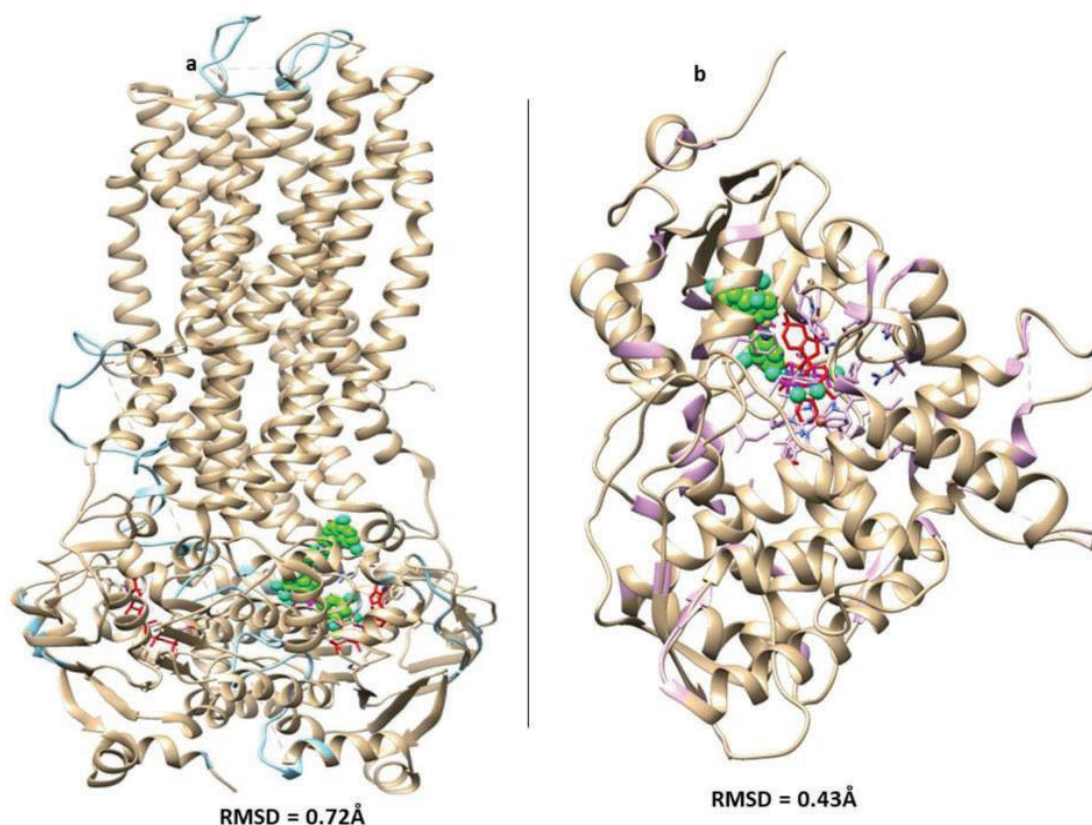


Figure 1. Superpositions of the crystalized structures of the natural substrates (in red) of the proteins and the ligand-complexes (in green). a) ABCB1 b) CYP3A4 and their respective RMSD values.

An initial minimization of 2000 steps were carried out with an applied restraint potential of 500 kcal/mol for both solutes, were performed for 1000 steps using the steepest descent method followed by 1000 steps of conjugate gradients. An additional full minimization of 1000 steps was further carried out using the conjugate gradient algorithm without restraint. A gradual heating MD simulation from 0 K to 300 K was executed for 50ps, such that the systems maintained a fixed number of atoms and fixed volume. The solutes within the systems were imposed with a potential harmonic restraint of 10 kcal/mol and collision frequency of 1.0ps. Following heating, an equilibration estimating 500ps of each system was conducted; the operating temperature was kept constant at 300 K. Additional features such as several atoms and pressure were also kept constant mimicking an isobaric-isothermal ensemble. The system's pressure was maintained at 1 bar using the Berendsen barostat (Basconi & Shirts, 2013; Gonnet, 2007).

The total time for the MD simulations conducted were 100ns. In each simulation, the SHAKE algorithm was employed to constrict the bonds of hydrogen atoms (Ryckaert et al., 1977). The step size of each simulation was 2fs, and an SPFP precision model was used. The simulations coincided with the isobaric-isothermal ensemble (NPT), with randomized seeding, the constant pressure of 1 bar maintained by the Berendsen barostat (Basconi & Shirts, 2013), a pressure-coupling constant of 2ps, a temperature of 300 K

and Langevin thermostat (Izaguirre et al., 2001) with a collision frequency of 1.0ps.

Post-dynamic analysis

Analysis of root means square deviation (RMSD), root means square fluctuation (RMSF), Solvent accessible surface area (SASA) and Radius of Gyration (RoG) was done using the CPPTRAJ module employed in the AMBER 18 suit (Shunmugam & Soliman, 2018). All raw data plots were generated using the Origin data analysis software (Seifert, 2014).

Binding free energy calculations

To estimate and compare the binding affinity of the systems, the free binding energy was calculated using the Molecular Mechanics/GB Surface Area method (MM/GBSA) (Ylilauri & Pentikäinen, 2013). Binding free energy was averaged over **100000** snapshots extracted from the 100 ns trajectory. The free binding energy (ΔG) computed by this method for each molecular species (complex, ligand, and receptor) can be represented as:

$$\Delta G_{\text{bind}} = G_{\text{complex}} - G_{\text{receptor}} - G_{\text{ligand}} \quad (1)$$

$$\Delta G_{\text{bind}} = E_{\text{gas}} + G_{\text{sol}} - TS \quad (2)$$

$$E_{\text{gas}} = E_{\text{int}} + E_{\text{vdw}} + E_{\text{ele}} \quad (3)$$

$$G_{\text{sol}} = G_{\text{GB}} + G_{\text{SA}} \quad (4)$$

$$G_{SA} = \gamma SASA \quad (5)$$

The term E_{gas} denotes the gas-phase energy, which consists of the internal energy E_{int} ; Coulomb energy E_{ele} and the van der Waals energies E_{vdw} . The E_{gas} was directly estimated from the FF14SB force field terms. Solvation free energy, G_{sol} , was estimated from the energy contribution from the polar states, GGB, and non-polar states, G. The non-polar solvation energy, SA. GSA, was determined from the solvent-accessible surface area (SASA), using a water probe radius of 1.4 Å. In contrast, the polar solvation, GGB, the contribution was estimated by solving the GB equation. S and T denote the total entropy of the solute and temperature, respectively.

Results and discussions

Stability and flexibility of proteins apo and bound systems

To discover the dynamic stability of the systems and to evaluate the MD simulations, root means square deviation (RMSD) values of alpha carbon ($C\alpha$) atoms were monitored along the entire MD trajectory for both the apo and the bound systems (Figure 2). RMSD is a measure of system convergence and stability (Hess, 2002) and the deviation produced by a protein during MD simulation is a factor determining its stability; the lower the deviation produced the more stable the protein. As shown in Figure 1(a–d), the overall RMSD values of the complexes of the four PCs and the two drugs are lower than the RMSD value of the ABCB1 apoenzyme implying that the binding of the ligand brings more stability to the enzyme. The result showed that the binding of inhibitors drastically influences the dynamic of P-glycoprotein, which can be reflected in the function of the protein (Shekari et al., 2015). Unlike the RMSD pattern observed in the apo and bound systems of ABCB1, the binding of the four ligands raised the RMSD values higher than the value of the apo for CYP3A4, while the values of the two FDA-approved drugs are lower than that of the apo. However, the higher RMSD values observed in the four PCs complexes showed that the binding of ligands does not disrupt the stability of the enzymes (CYP3A4), and the functions of the proteins were not altered.

The radius of gyration (RoG)

Graphical plots of the radius of gyration were plotted for the systems after 100 ns MD simulation. The RoG was carried out to evaluate the overall structural compactness of the systems (McGillewie et al., 2017; Salleh et al., 2012; Sindhu & Srinivasan, 2015). The plots of RoG for the apoenzymes and the bound ligands for both CYP3A4 and ABCB1 are shown in Figure 3. For the P-glycoprotein complexes, the average values for the RoG of the PCs were compared to the average values of the two FDA-approved inhibitors of the two enzymes. The result showed that the apo has an average value of 38.467 Å. Values of 38.012 Å, 38.253, 38.398 Å, 38.501 Å, 38.689 Å and 38.872 Å were recorded for LUT, EGA, EGCG, K7G, LPV and RTV respectively. K7G showed RoG

values that are most similar to the average values recorded for LPV and RTV. These results suggested that the binding of the three compounds induced conformational changes similar to both LPV and RTV. In complex with the CYP3A4 enzyme, the average RoG values for EGA, apo, RTV, LUT, K7G, EGCG and LPV are 22.862 Å, 23.013 Å, 23.113 Å, 23.232 Å, 23.254 Å, 23.223 Å and 23.652 Å respectively. Similar degrees of structural compactness were observed between RTV and LUT and K7G. The study therefore suggests that conformational changes that occurred in K7G, EGCG and LUT induced a more favourable structural compactness that enhances the stability of the protein in a similar way with RTV.

Root means square fluctuation (RMSF) plots (Figure 4) showed the effect of the binding of the ligands on the behaviour of the active residue. Higher fluctuation values indicated more flexible movements, and in contrast, reduced values expressed restricted fluctuations during the simulation (Kumar et al., 2014). From the RMSF plots, the apo (ABCB1) showed the overall highest fluctuation value of 5.53 Å. However, the binding of ligands at the active sites of the protein lowered the overall fluctuation values for the respective ligands. This agrees with the study of Pan and Stephen, that also reported decreased in the RMSF values after ligand binding to ABCB1 (Pan & Aller, 2015). RTV and LPV showed average values of 4.52 Å and 5.11 Å respectively. K7G (4.301 Å) and EGCG (4.33 Å) showed average RMSF values of similar to RTV (4.52 Å). EGA (3.51 Å) and LUT (3.07 Å) showed RMSF values lower than that the recorded values for the two inhibitors (Figure 4(a–d)). The decrease in fluctuation observed in all the compounds strongly indicated that their binding lowered dynamic residual fluctuations of the enzyme, thus inducing stability of the complex state (Kumar et al., 2014; Shunmugam & Soliman, 2018).

Figure 4(e–h) showed the RMSF plots of both the apo and the bound systems of CYP3A4. Similar protein fluctuation and flexibility were observed in the CYP3A4 system when compared to the P-gp. Generally, higher fluctuation and flexibility in the amino acid residues 140–240 was observed in all the PCs and the two drugs bound systems of CYP3A4, and the average fluctuation values for all the ligands (RTV 4.43 Å, LPV 3.4 Å, K7G 4.5 Å, EGCG 4.34 Å, EGA 4.43 Å and LUT 4.23 Å) are lower than the Apo values (5.77 Å). When compared with the two inhibitors, K7G, EGCG, LUT and EGA showed similar RMSF values with RTV.

Solvent accessible surface area (SASA)

In addition to the RMSD, RoG and RMSF plots, SASA is also a vital parameter to examine the impact of the binding of the different ligands to the two enzymes (CYP3A4 and ABCB1). The SASA quantifies the enzyme exposure to solvent molecules (Boyce et al., 2014).

In the ABCB1 system (Figure 5(a–d)), the average SASA values for EGA, LUT, APO, LPV, RTV, K7G and EGCG were 45,333.53 Å², **45,8212** Å², 46,333.63 Å², 47,500.00 Å², 47,8333.33 Å², 48,166.67 Å² and 48,723.73 Å² respectively. Decline in the exposure of LPV (at approximately 20 ns), and both EGCG and K7G (at approximately 60 ns) was observed,

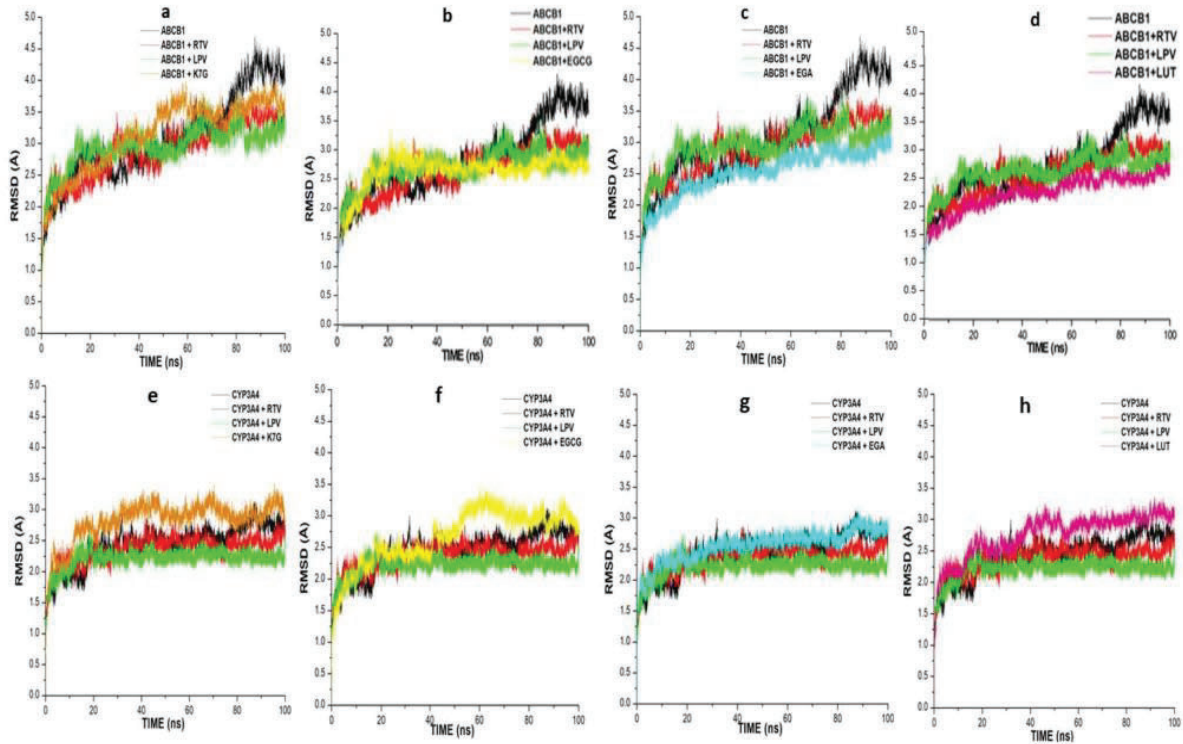


Figure 2. Comparative RMSD profile plots of C- α atoms of the ABCB1, RTV and LPV with ligands, a) K7G, b) EGCG, c) EGA and d) LUT systems and CYP3A4, RTV and LPV with e) K7G, f) EGCG, g) EGA and h) LUT calculated throughout 100 ns molecular dynamics simulation.

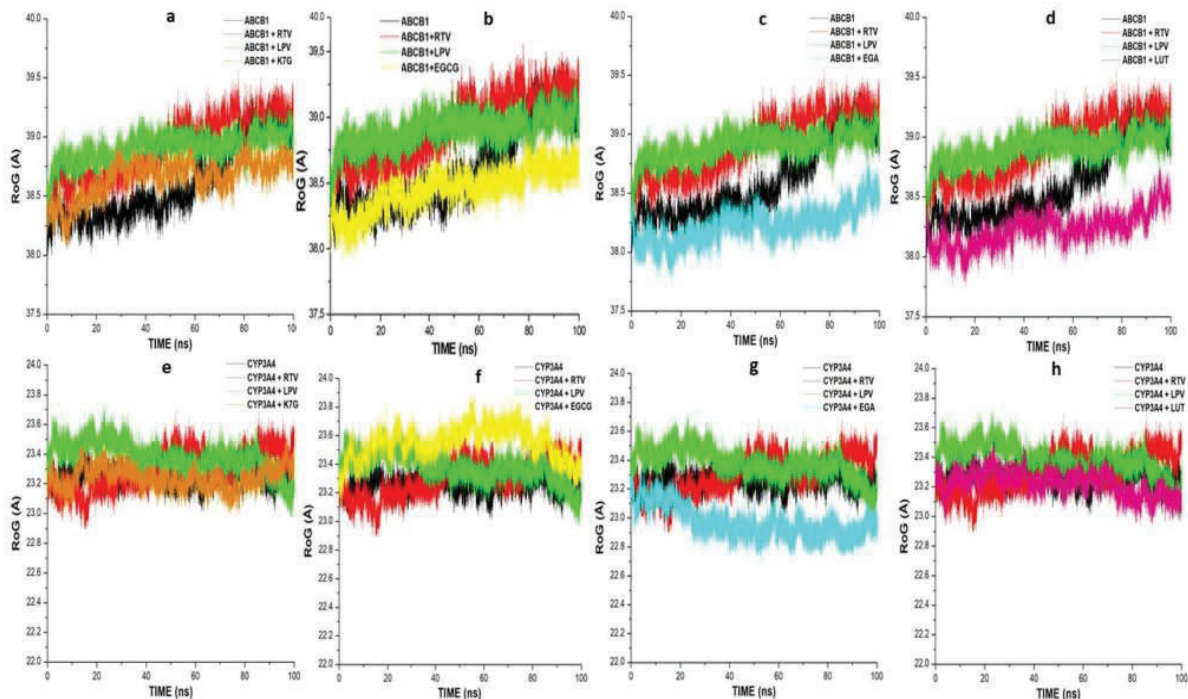


Figure 3. RoG profile of protein backbone atoms calculated throughout 100 ns molecular dynamics simulation of ABCB1 bound RTV, LPV and ligands, a) K7G, b) EGCG, c) EGA and d) LUT and CYP3A4 bound to RTV, LPV and ligands, e) K7G, f) EGCG, g) EGA and h) LUT.

followed by consistent exposure to the solvent molecules. This is an indication that the structural integrity of the protein was altered after 20 ns for LPV and 60 ns for both EGCG and K7G respectively. However, the progressive increase in

the SASA plots after 20 ns for LPV and stable plots for EGCG and K7G, indicated that the enzyme structural integrity is not altered (Boyce et al., 2014). When compared to the inhibitors, EGCG and K7G showed more similarity in SASA values with

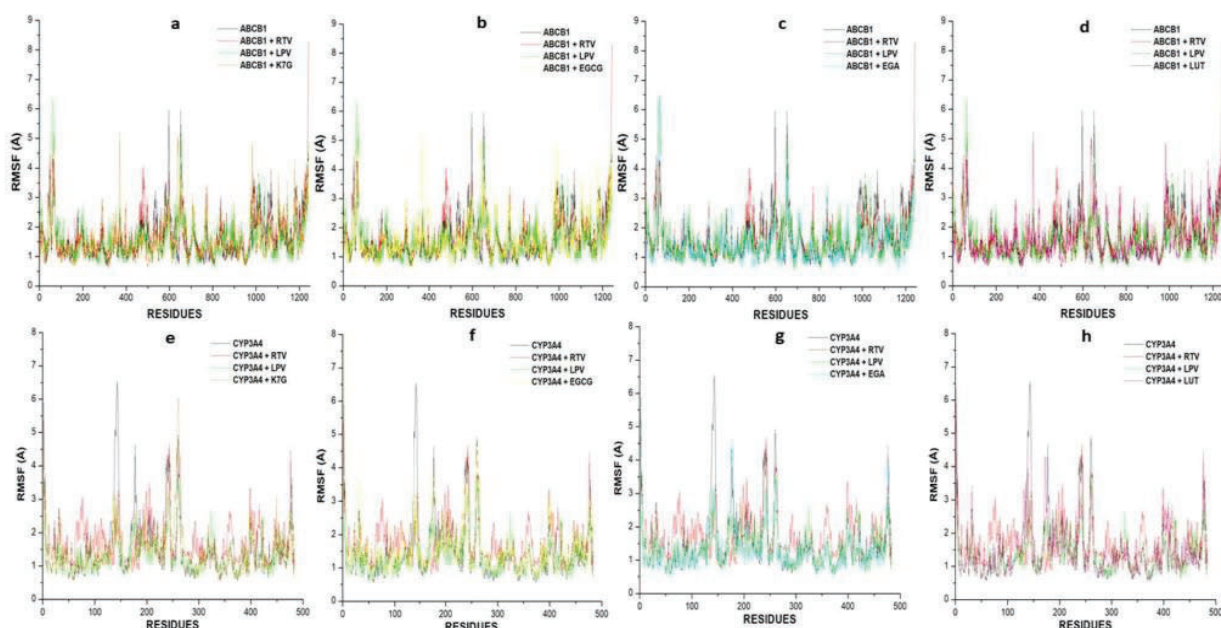


Figure 4. Comparative RMSF plots of Residue-based average C- α fluctuations of the apo (ABCB1), and bound with RTV, LPV and ligands, a) K7G, b) EGCG, c) EGA and d) LUT and CYP3A4 bound to RTV, LPV and ligands, e) K7G, f) EGCG, g) EGA and h) LUT systems calculated throughout 100 ns molecular dynamics simulation.

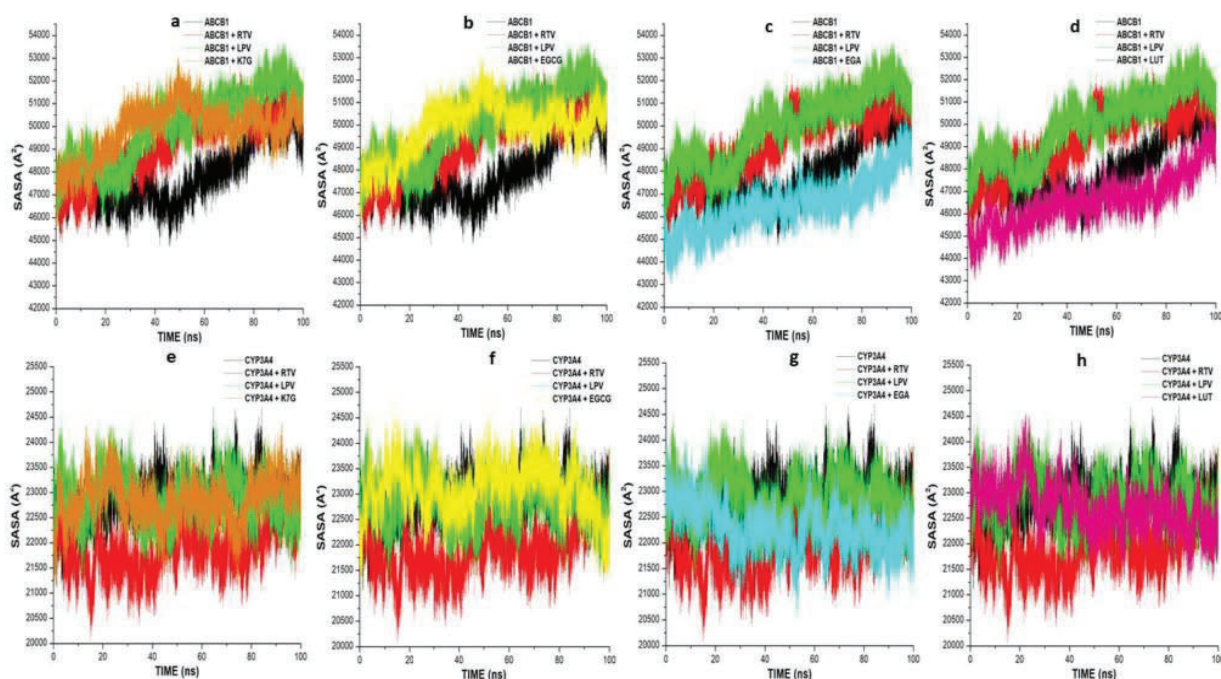


Figure 5. Solvent accessible surface area of apo (ABCB1) RTV, LPV and ligands, a) K7G, b) EGCG, c) EGA and d) LUT, and CYP3A4 bound to RTV, LPV and ligands, e) K7G, f) EGCG, g) EGA and h) LUT systems calculated throughout 100 ns molecular dynamics simulation.

both RTV and LPV. In the CYP3A4 systems (Figure 5(e-h)), EGA (22,000.00 Å²) shows the average SASA values similar to RTV (21,833.33 Å²), while EGCG (22,821.33 Å²), K7G (22,333.33 Å²) and LUT (22,166.62 Å²) showed similar values with LPV (22,333.33 Å²).

Thermodynamic binding free energy of the inhibitor drugs and PCs to CYP3A4 and ABCB1

After the 100 ns MD simulation, the binding free energy (ΔG_{bind}) was calculated using the MM/GBSA method. The MM/GBSA calculations have been widely used to evaluate

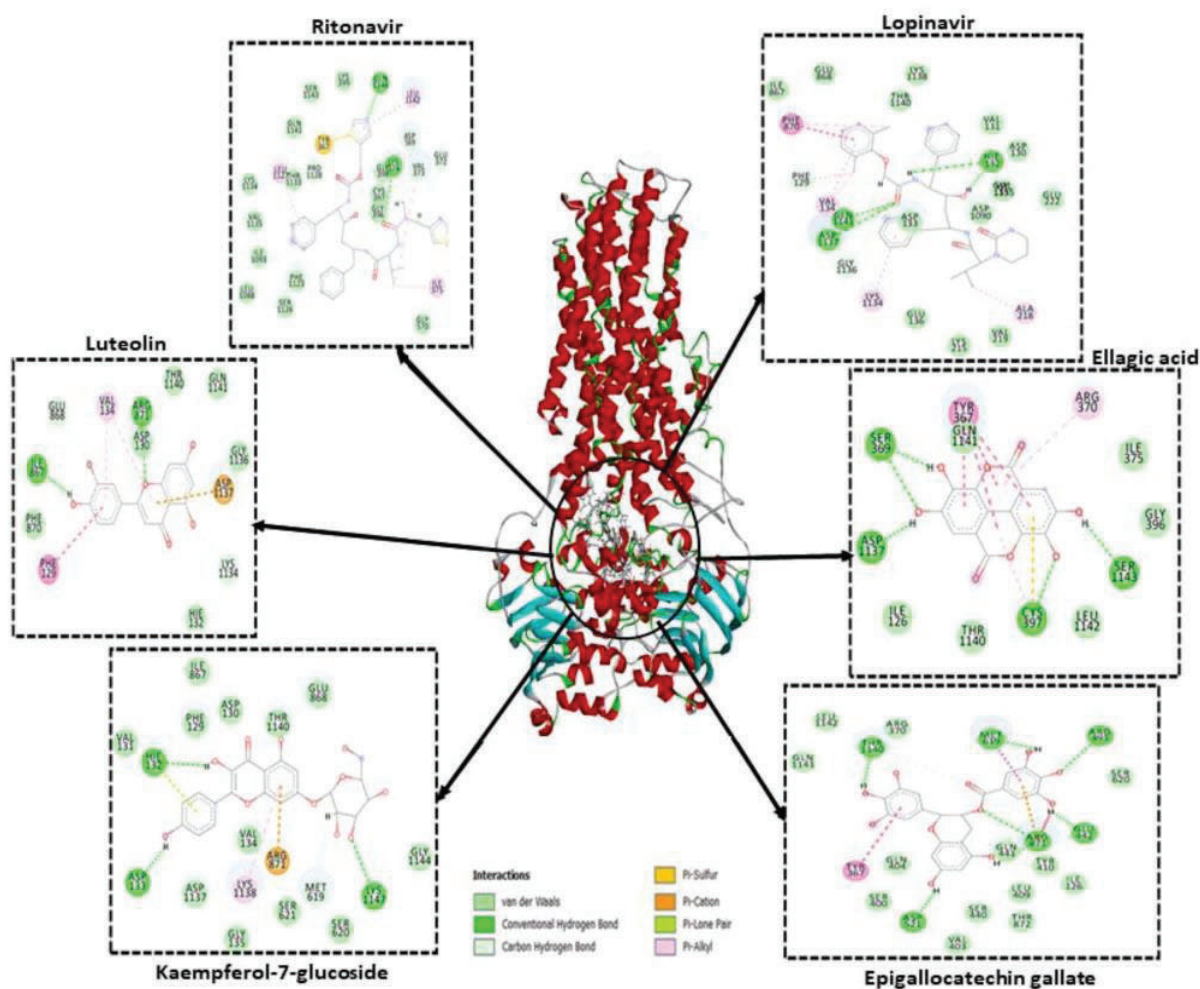


Figure 7. Representation of Protein (ABC1)-ligand interactions plots with different amino acid residues.

plots were assessed. Figure 6 showed the amino acid residues at the nucleotide binding domain (NBD) of ABCB1 (Figure 6(a)) and the catalytic site of CYP3A4 (Figure 6(b)).

Protein-ligand interaction has been used widely to examine the molecular interactions between residues at the active sites of a protein and bound ligands (Chetty et al., 2016; Idowu et al., 2019; Moonsamy et al., 2014; Ndagi et al., 2017). The effect of the binding of the different ligands on ABCB1 and CYP3A4 was analysed and the interactions between the critical residues at the binding sites in the presence of the two known inhibitors (RTV and LPV) and the four tested PCs was plotted. Figures 7 and 8 not only shows a 2D visualisation of the interactions between the ligands and the proteins, but also showed different types of interactions observed in the protein-ligand plots. Interactions such as hydrogen bond, ionic interaction, π -Sulfur, π -cation interaction, and Van der Waals (vdW) overlaps can be observed.

In P-glycoprotein (ABCB1) apo and bound systems (Figure 7), more interactions were observed in RTV (24) than LPV (22) and the tested PCs (EGA 12, LUT 13, K7G 18 and EGCG 20). This correlates with the highest binding free binding energy recorded for RTV (Table 1). LPV only showed similar types of interactions with RTV at amino residues Leu1141,

Val1135, and Lys1134, however there were less number of interactions in total amino residues in LPV when compare with RTV, which also correlates with the lower binding energy recorded for LPV when compared with RTV.

K7G and LUT showed similar type of interactions with LPV at amino residues Glu868, Val134, Thr1140, Asp130, Ile867, Phe870, Phe129, Hie132, and Asp1137. At residues Cys397, Leu1142, Ser1143, Gly396, Ile375, and Tyr367, EGA showed similar interactions with RTV. EGCG showed no similarity in protein-ligand interactions with LPV, however, it showed some similarity with RTV at amino acid residues Thr367, Gln1141 and Leu1142, suggesting that EGCG and EGA inhibit ABCB1 in a related mechanism to RTV.

As shown in Table 1, RTV has the highest free binding energy, higher than LPV and the four PCs complexes. This is due to the number and type of interactions between the individual RTV and the active site amino acids of the CYP3A4 (Figure 8). As shown in the ligand-protein interaction plots, there is a total of 28 interactive bonds (19 hydrogen and Van der Waal bonds, 2 Pi-cation bonds, 6 Pi-alkyl bonds and 1 Pi-Pi bond) between RTV and the active site amino residues of CYP3A4. These bonds significantly contributed to its overall binding energy.

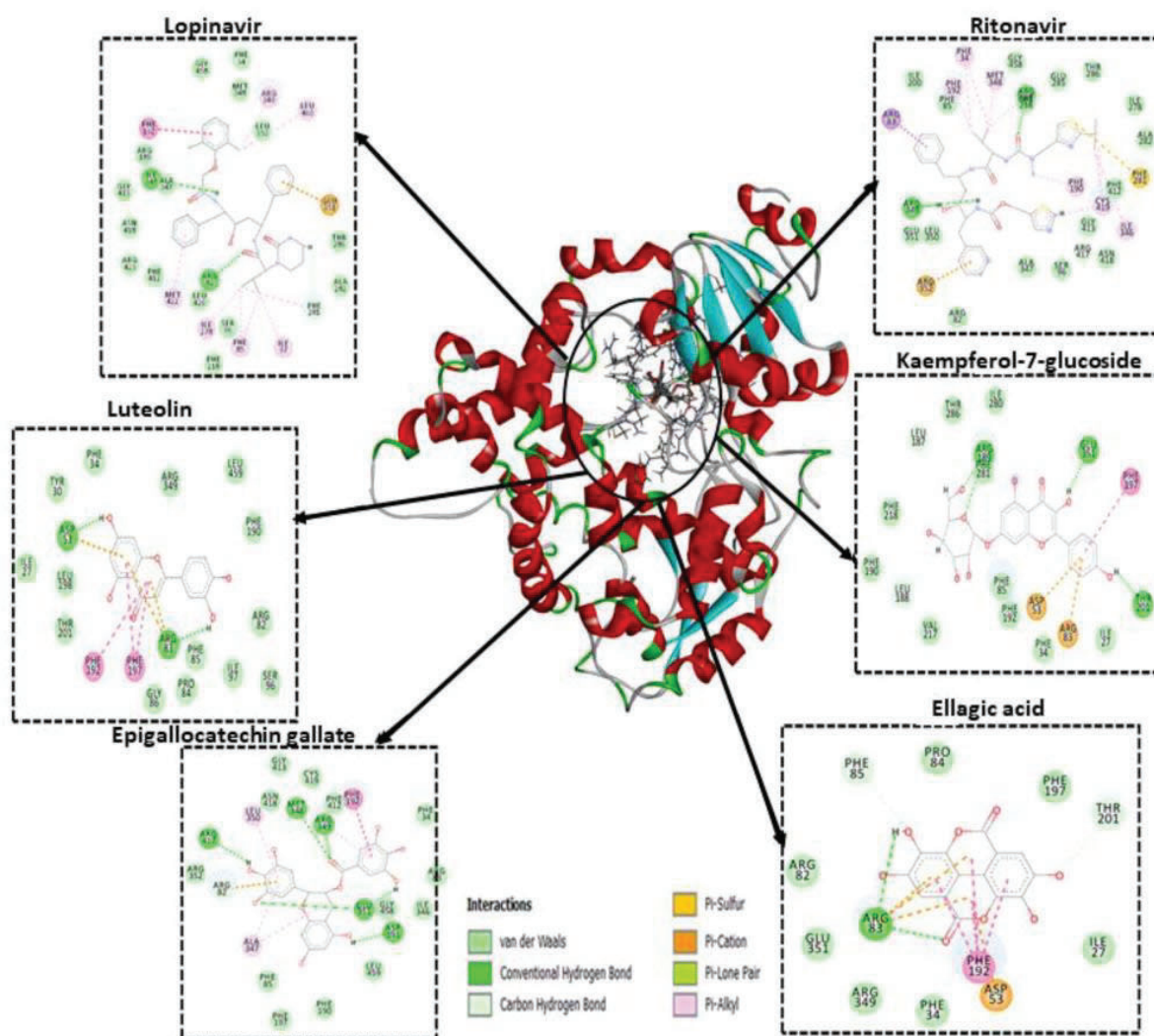


Figure 8. Representation of Protein (CYP3A4)-ligand interaction plots with different amino acid residues.

RTV has the highest number of interactions, higher than EGCG (22 bonds), K7G (18 bonds), LUT (18 bonds) and EGA (12 bonds). While K7G and LUT showed the same number of bonds (18 bonds) they showed different binding affinity (-48.769 kcal/mol and -46.214 kcal/mol, respectively). This can be attributed to two pi-cation bonds in K7G compared to one Pi-cation bond in LUT. Similar interactions were observed at amino acid residues Phe34, Arg82, Phe85, Arg189, Phe192, Phe281, Ala282, Ile346, Met348, Arg349, Leu350, Glu351, Gly413, Asn418 and Gly458 between LPV and RTV. The four PCs showed some similarity in term of interactions with both inhibitors: K7G (Phe34, Arg82, Phe85, Arg189, Phe192 and Phe281 for LPV and Arg83, Phe190, Phe218 and Thr286 for RTV), EGCG (Arg82, Phe192, Ile346, Phe34, Phe85, Met348, Arg349, Leu350, Glu351, Gly413, Asn418 and Gly458 for LPV and Phe34, Arg82, Arg83, Phe85, Phe192, Ile346, Ala347, Met348, Arg349, Leu350, Glu351, Arg352, Phe412, Gly413, Arg417,

Asn418, Cys419 and Gly458 for RTV). The interaction plot showed that EGCG has similar type of interactions with RTV than LPV. This therefore suggests that it could inhibit

CYP3A4 in similar way with RTV. The numbers of interactions of LUT and EGA with CYP3A4 are lower than that of RTV and LPV, however, they showed some similar interactions (Phe34, Arg82, Arg83, Phe85, Ser96, Ile97, Phe190, Phe192, Arg349 and Glu351) with the two inhibitors, indicating they could be moderate inhibitors of CYP3A4.

Conclusion

P-glycoprotein and CYP3A4 have been reported to play essential roles in controlling plasma concentrations of drugs, absorption and excretion. The inhibitory potentials of four phytochemical compounds and their mechanism(s) of inhibiting ABCB1 and CYP3A4 enzymes were examined using a combination of MD simulation and MM/GBSA free energy calculations. The MM/GBSA binding free energies showed that the binding energies (ΔG_{bind}) of both EGCG and K7G for the two proteins (ABCB1 and CYP3A4) are higher than LUT and EGA and fall between the ΔG_{bind} of the standard inhibitors (RTV and LPV) of both proteins. Structural analysis of the bound systems and the apo of the two proteins also

confirmed that the binding of the compounds (EGCG and K7G) at the active sites of the two proteins does not alter the structural integrity of the proteins. The results further showed that there are similar interactions between the drugs and the compounds, suggesting potential inhibitory similarities between the drugs and compounds. This study, therefore, suggests that EGCG, EGA and K7G showed more similarity with RTV in their interaction with CYP3A4, and K7G and EGCG showed similar interactions with LPV and RTV respectively in P-glycoprotein systems, thereby suggesting that EGCG and K7G might be a suitable substitute for RTV in its use as a booster for HIV protease drugs where it is known to increase the optimal concentration of PIs in the systemic circulation by inhibiting the pumping out and the rate of metabolism of PIs from the circulating system thereby, enhancing the therapeutic effect of the PI drugs.

Disclosure statement

The authors declare no conflict of interest.

Funding

This work was supported by College of Health Sciences, University of KwaZulu-Natal Scholarship.

References

- Athukuri, B. L., & Neerati, P. (2017). Enhanced oral bioavailability of diltiazem by the influence of gallic acid and ellagic acid in male wistar rats: Involvement of CYP3A and P-gp inhibition. *Phytotherapy Research: PTR*, 31(9), 1441–1448. <https://doi.org/10.1002/ptr.5873>
- Basconi, J. E., & Shirts, M. R. (2013). Effects of temperature control algorithms on transport properties and kinetics in molecular dynamics simulations. *Journal of Chemical Theory and Computation*, 9(7), 2887–2899. <https://doi.org/10.1021/ct400109a>
- Bierman, W., George, L., Scheffer, A. S., Gerrit, J., Michiel, A. A., Sven, A. D., & Rik, J. S. (2010). Protease inhibitors atazanavir, lopinavir and ritonavir are potent blockers, but poor substrates, of ABC transporters in a broad panel of ABC transporter-overexpressing cell lines. *The Journal of Antimicrobial Chemotherapy*, 65(8), 1672–1680.
- Boyce, S. E., Tirunagari, N., Niedziela-Majka, A., Perry, J., Wong, M., Kan, E., Lagpacan, L., Barauskas, O., Hung, M., Fenaux, M., Appleby, T., Watkins, W. J., Schmitz, U., & Sakowicz, R. (2014). Structural and regulatory elements of HCV NS5B polymerase- β -loop and C-terminal tail are required for activity of allosteric thumb site II inhibitors. *PLoS One*, 9(1), e84808. <https://doi.org/10.1371/journal.pone.0084808>
- Branden, G., Sjogren, T., Schnecke, V., & Xue, Y. (2014). Structure-based ligand design to overcome CYP inhibition in drug discovery projects. *Drug Discovery Today*, 19(7), 905–911.
- Chetty, S., Bhakat, S., Martin, A. J. M., & Soliman, M. E. S. (2016). Multi-drug resistance profile of PR20 HIV-1 protease is attributed to distorted conformational and drug binding landscape: Molecular dynamics insights. *Journal of Biomolecular Structure & Dynamics*, 34(1), 135–151. <https://doi.org/10.1080/07391102.2015.1018326>
- Cory, T. J., Schacker, T. W., Stevenson, M., & Fletcher, C. V. (2013). Overcoming pharmacologic sanctuaries. *Current opinion in HIV and AIDS*, 8(3), 190–195.
- Danielson, P. B. (2002). The cytochrome P450 superfamily: Biochemistry, evolution and drug metabolism in humans. *Current Drug Metabolism*, 3(6), 561–597. <https://doi.org/10.2174/1389200023337054>
- Dhananjay, P., Deep, K., Mukul, M., Durga, K., Paturi, B., & Ashim, K. M. (2011). Efflux transporters and cytochrome P-450-mediated interactions between drugs of abuse and antiretrovirals. *Life Sciences*, 88(21–22), 959–971.
- Drewe, J., Gutmann, H., Fricker, G., Török, M., Beglinger, C., & Huwyler, J. (1999). HIV protease inhibitor ritonavir: A more potent inhibitor of P-glycoprotein than the cyclosporin analog SDZ PSC 833. *Biochemical Pharmacology*, 57(10), 1147–1152.
- Farrokhzadeh, A., Akher, F. B., & Soliman, M. E. S. (2019). Probing the dynamic mechanism of uncommon allosteric inhibitors optimized to enhance drug selectivity of SHP2 with therapeutic potential for cancer treatment. *Applied Biochemistry and Biotechnology*, 188(1), 260–281. <https://doi.org/10.1007/s12010-018-2914-0>
- Fromm, M. F. (2004). Importance of P-glycoprotein at blood-tissue barriers. *Trends in Pharmacological Sciences*, 25(8), 423–429. <https://doi.org/10.1016/j.tips.2004.06.002>
- Gonnet, P. (2007). P-SHAKE: A quadratically convergent SHAKE in O(n²). *Journal of Computational Physics*, 220(2), 740–750. <https://doi.org/10.1016/j.jcp.2006.05.032>
- Hanwell, M. D., Curtis, D. E., Lonie, D. C., Vandermeersch, T., Zurek, E., & Hutchison, G. R. (2012). Avogadro: An advanced semantic chemical editor, visualization, and analysis platform. *Journal of Cheminformatics*, 4(8), 1–17.
- Hess, B. (2002). Convergence of sampling in protein simulations. *Physical Review*, 65(3), 31910.
- Idowu, K., Ramharack, P., Nlooto, M., & Gordon, M. (2019). The pharmacokinetic properties of HIV-1 protease inhibitors: A computational perspective on herbal phytochemicals. *Heliyon*, 5(10), e02565. <https://doi.org/10.1016/j.heliyon.2019.e02565>
- Izaguirre, J. A., Catarello, D. P., Wozniak, J. M., & Skeel, R. D. (2001). Langevin stabilization of molecular dynamics. *The Journal of Chemical Physics*, 114(5), 2090–2098. <https://doi.org/10.1063/1.1332996>
- Janneh, O., Jones, E., Chandler, B., Owen, A., & Khoo, S. H. (2007). Inhibition of P-glycoprotein and multidrug resistance-associated proteins modulates the intracellular concentration of lopinavir in cultured CD4 T cells and primary human lymphocytes. *The Journal of Antimicrobial Chemotherapy*, 60(5), 987–993. <https://doi.org/10.1093/jac/dkm353>
- Jorgensen, W. L., Chandrasekhar, J., Madura, J. D., Impey, R. W., & Klein, M. L. (1983). Comparison of simple potential functions for simulating liquid water. *The Journal of Chemical Physics*, 79(2), 926–935.
- Kim, S., Thiessen, P. A., Bolton, E. E., Chen, J., Fu, G., Gindulyte, A., Han, L., He, J., He, S., Shoemaker, B. A., Wang, J., Yu, B., Zhang, J., & Bryant, S. H. (2016). PubChem substance and compound databases. *Nucleic Acids Research*, 44(D1), D1202–D1213.
- Kim, Y., & Chen, J. (2018). Molecular structure of human P-glycoprotein in the ATP-bound, outward-facing conformation. *Science (New York, N.Y.)*, 359(6378), 915–919. <https://doi.org/10.1126/science.aar7389>
- Konig, J., Muller, F., & Fromm, M. F. (2013). Transporters and drug-drug interactions: Important determinants of drug disposition and effects. *Pharmacological Reviews*, 65(3), 944–966. <https://doi.org/10.1124/pr.113.007518>
- Kumar, C. V., Swetha, R. G., Anbarasu, A., & Ramaiah, S. (2014). Computational analysis reveals the association of threonine 118 methionine mutation in PMP22 resulting in CMT-1A. *Advances in Bioinformatics*, 2014, 1–10.
- Liyue, H., Stephen, A. W., Woolley, J. L., Brouwer, K. R., Serabjit-Singh, C., & Joseph, W. P. (2001). Induction of P-glycoprotein and cytochrome P450 3A by HIV protease inhibitors. *Drug Metabolism and Disposition*, 29(5), 754–760.
- Loscher, W., & Potschka, H. (2005). Role of drug efflux transporters in the brain for drug disposition and treatment of brain diseases. *Progress in Neurobiology*, 76(1), 22–76.
- Mahmood, N., Piacente, S., Pizza, C., Burke, A., Khan, A. I., & Hay, A. J. (1996). The anti-HIV activity and mechanisms of action of pure compounds isolated from *Rosa damascena*. *Biochemical and Biophysical Research Communications*, 229(1), 73–79. <https://doi.org/10.1006/bbrc.1996.1759>
- Massova, I., & Kollman, P. A. (2000). Combined molecular mechanical and continuum solvent approach (MM-PBSA/GBSA) to predict ligand binding. *Perspectives in Drug Discovery and Design*, 18(1), 113–135. <https://doi.org/10.1023/A:1008763014207>

- McGillewie, L., Ramesh, M., & Soliman, M. E. (2017). Sequence, structural analysis and metrics to define the unique dynamic features of the flap regions among aspartic proteases. *The Protein Journal*, 36(5), 385–396. <https://doi.org/10.1007/s10930-017-9735-9>
- Meintjes, G., Moorhouse, M. A., & Carmona, S. (2017). Adult antiretroviral therapy guidelines. *Southern African Journal of HIV Medicine*, 18(1), a776.
- Moonsamy, S., Dash, R. C., & Soliman, M. E. (2014). Integrated computational tools for identification of CCR5 antagonists as potential HIV-1 entry inhibitors: Homology modeling, virtual screening, molecular dynamics simulations and 3D QSAR analysis. *Molecules (Basel, Switzerland)*, 19(4), 5243–5265. <https://doi.org/10.3390/molecules19045243>
- Nair, P. C., & Miners, J. O. (2014). Molecular dynamics simulations: From structure function relationships to drug discovery. *In Silico Pharmacology*, 2(1), 1–4. <https://doi.org/10.1186/s40203-014-0004-8>
- Ndagi, U., Mhlongo, N. N., & Soliman, M. E. (2017). The impact of Thr91 mutation on c-Src resistance to UM-164: Molecular dynamics study revealed a new opportunity for drug design. *Molecular Biosystems*, 13(6), 1157–1171. <https://doi.org/10.1039/c6mb00848h>
- Osterberg, F., Morris, G. M., Sanner, M. F., Olson, A. J., & Goodsell, D. S. (2002). Automated docking to multiple target structures: Incorporation of protein mobility and structural water heterogeneity in AutoDock. *Proteins*, 46(1), 34–40.
- Pan, L., & Aller, S. G. (2015). Equilibrated atomic models of outward-facing P-glycoprotein and effect of ATP binding on structural dynamics. *Scientific Reports*, 5(1), 343–355.
- Pang, X., Baoyue, Z., Guangyan, M., Jie, X., Qian, X., Xia, Z., Ailin, L., Guanhua, D., & Yimin, C. (2018). Screening of cytochrome P450 3A4 inhibitors via in silico and in vitro approaches. *RSC Advances*, 8(61), 34783–34792. <https://doi.org/10.1039/C8RA06311G>
- Ramharack, P., & Soliman, M. E. S. (2018). Zika virus NS5 protein potential inhibitors: An enhanced in silico approach in drug discovery. *Journal of Biomolecular Structure and Dynamics*, 36(5), 1118–1133. <https://doi.org/10.1080/07391102.2017.1313175>
- Ryckaert, J.-P., Ciccotti, G., & Berendsen, H. J. (1977). Numerical integration of the Cartesian equations of motion of a system with constraints: Molecular dynamics of n-alkanes. *Journal of Computational Physics*, 23(3), 327–341. [https://doi.org/10.1016/0021-9991\(77\)90098-5](https://doi.org/10.1016/0021-9991(77)90098-5)
- Salleh, A. B., Rahim, A. S., & Rahman, R. N. (2012). The role of Arg157Ser in improving the compactness and stability of ARM lipase. *Journal of Computer Science and Systems Biology*, 5, 38–46.
- Seifert, E. (2014). OriginPro 9.1: Scientific data analysis and graphing software-software review. *Journal of Chemical Information and Modeling*, 54(5), 1552–1552.
- Shaik, M., & Vanapatla, S. R. (2019). Enhanced oral bioavailability of linaagliptin by the influence of gallic acid and ellagic acid in male Wistar albino rats: Involvement of p-glycoprotein inhibition. *Drug Metabolism and Personalized Therapy*, 34(2). <https://doi.org/10.1515/dmpt-2018-0020>.
- Shekari, F., Sadeghpour, H., Javidnia, K., Saso, L., Nazari, F., Firuzi, O., & Miri, R. (2015). Cytotoxic and multidrug resistance reversal activities of novel 1,4-dihydropyridines against human cancer cells. *European Journal of Pharmacology*, 746, 233–244. <https://doi.org/10.1016/j.ejphar.2014.10.058>
- Shin, S. C., & Choi, J. S. (2009). Effects of epigallocatechin gallate on the oral bioavailability and pharmacokinetics of tamoxifen and its main metabolite, 4-hydroxytamoxifen, in rats. *Anti-Cancer Drugs*, 20(7), 584–588.
- Shunmugam, L., & Soliman, M. E. (2018). Targeting HCV polymerase: A structural and dynamic perspective into the mechanism of selective covalent inhibition. *RSC Advances*, 8(73), 42210–42222. <https://doi.org/10.1039/C8RA07346E>
- Sindhu, T., & Srinivasan, P. (2015). Exploring the binding properties of agonists interacting with human TGR5 using structural modeling, molecular docking and dynamics simulations. *RSC Advances*, 5(19), 14202–14213.
- Storch, C. H., Theile, D., Lindenmaier, H., Haefeli, W. E., & Weiss, J. (2007). Comparison of the inhibitory activity of anti-HIV drugs on P-glycoprotein. *Biochemical Pharmacology*, 73(10), 1573–1581. <https://doi.org/10.1016/j.bcp.2007.01.027>
- Tripoli, E., Maurizio, L., Santo, G., Danila, D., & Marco, G. (2007). Food chemistry citrus flavonoids: Molecular structure, biological activity and nutritional properties: A review. *Food Chemistry*, 104, 466–479.
- Van Waterschoot, R., Ter Heine, R., Wagenaar, E., Van Der Kruijssen, C., Rooswinkel, R., Huitema, A., Beijnen, J., & Schinkel, A. (2010). Effects of cytochrome P450 3A (CYP3A) and the drug transporters P-glycoprotein (MDR1/ABCB1) and MRP2 (ABCC2) on the pharmacokinetics of lopinavir. *British Journal of Pharmacology*, 160(5), 1224–1233.
- Varatharajan, L., & Thomas, S. A. (2009). The transport of anti-HIV drugs across blood-CNS interfaces: summary of current knowledge and recommendations for further research. *Antiviral Research*, 82(2), A99–A109.
- Walubo, A. (2007). The role of cytochrome p450 in antiretroviral drug interactions. *Expert Opinion on Drug Metabolism & Toxicology*, 3(4), 583–598.
- Weemhoff, J. L., von Moltke, L. L., Richert, C., Hesse, L. M., Harmatz, J. S., & Greenblatt, D. J. (2003). Apparent mechanism-based inhibition of human CYP3A in-vitro by lopinavir. *The Journal of Pharmacy and Pharmacology*, 55(3), 381–386. <https://doi.org/10.1211/002235702739>
- Weiss, J., & Haefeli, W. E. (2010). Impact of ATP-binding cassette transporters on human immunodeficiency virus therapy. In *International review of cell and molecular biology* (pp. 219–279). Academic Press.
- Weiss, J., Rose, J., Storch, C. H., Ketabi-Kiyanvash, N., Sauer, A., Haefeli, W. E., & Efferth, T. (2007). Modulation of human BCRP (ABCG2) activity by anti-HIV drugs. *The Journal of Antimicrobial Chemotherapy*, 59(2), 238–245. <https://doi.org/10.1093/jac/dkl474>
- Yamaguchi, K., Honda, M., Ikigai, H., Hara, Y., & Shimamura, T. (2002). Inhibitory effects of (-)-epigallocatechin gallate on the life cycle of human immunodeficiency virus type 1 (HIV-1). *Antiviral Research*, 53(1), 19–34. [https://doi.org/10.1016/S0166-3542\(01\)00189-9](https://doi.org/10.1016/S0166-3542(01)00189-9)
- Yang, Z. F., Bai, L., Wen, B. H., Xu, Z. L., Sui, S. Z., Nan, S. Z., & Zhi, H. J. (2014). Comparison of in vitro antiviral activity of tea polyphenols against influenza A and B viruses and structure-activity relationship analysis. *Fitoterapia*, 93, 47–53. <https://doi.org/10.1016/j.fitote.2013.12.011>
- Yang, Z., Lasker, K., Schneidman-Duhovny, D., Webb, B., Huang, C. C., Pettersen, E. F., Goddard, T. D., Meng, E. C., Sali, A., & Ferrin, T. E. (2012). UCSF chimera, MODELLER, and IMP: An integrated modeling system. *Journal of Structural Biology*, 179(3), 269–278.
- Ylilauri, M., & Pentikäinen, O. T. (2013). MMGBSA as a tool to understand the binding affinities of filamin-peptide interactions. *Journal of Chemical Information and Modeling*, 53(10), 2626–2633.

Appendix G



26 September 2018

Mr KA Idowu (218068180)
School of Laboratory Medicine and Medical Sciences
College of Health Sciences
Kidowu93@yahoo.com

Protocol: Pharmacological and toxicological effects of chemical components of COA herbal medicine on enzymes and transporters involved in the metabolism of commonly prescribed protease inhibitor drugs used by HIV positive patients in South Africa.

Degree: PhD

BREC Ref No: BE566/18

EXPEDITED APPLICATION: APPROVAL LETTER

A sub-committee of the Biomedical Research Ethics Committee has considered and noted your application received on 06 September 2018.

The conditions have now been met and the study is given **full ethics approval** and may begin as from 26 September 2018. Please ensure that site permissions are obtained and forwarded to BREC for approval before commencing research at a site.

This approval is valid for one year from **26 September 2018**. To ensure uninterrupted approval of this study beyond the approval expiry date, an application for recertification must be submitted to BREC on the appropriate BREC form 2-3 months before the expiry date.

Any amendments to this study, unless urgently required to ensure safety of participants, must be approved by BREC prior to implementation.

Your acceptance of this approval denotes your compliance with South African National Research Ethics Guidelines (2015), South African National Good Clinical Practice Guidelines (2006) (if applicable) and with UKZN BREC ethics requirements as contained in the UKZN BREC Terms of Reference and Standard Operating Procedures, all available at <http://research.ukzn.ac.za/Research-Ethics/Biomedical-Research-Ethics.aspx>.

BREC is registered with the South African National Health Research Ethics Council (REC-290408-009). BREC has US Office for Human Research Protections (OHRP) Federal-wide Assurance (FWA 678).

The sub-committee's decision will be noted by a full Committee at its next meeting taking place on **13 November 2018**.

We wish you well with this study. We would appreciate receiving copies of all publications arising out of this study.

Yours sincerely



Prof V Rambiritch
Chair: Biomedical Research Ethics Committee

Supervisor: tarinm@ukzn.ac.za Co Supervisor: nlooto@ukzn.ac.za Postgrad admin: mabasonpz@ukzn.ac.za

Biomedical Research Ethics Committee

Professor V Rambiritch (Chair)

Westville Campus, Govan Mbeki Building

Postal Address: Private Bag X54001, Durban 4000

Telephone: +27 (0) 31 260 2486 **Facsimile:** +27 (0) 31 260 4609 **Email:** brec@ukzn.ac.za

Website: <http://research.ukzn.ac.za/Research-Ethics/Biomedical-Research-Ethics.aspx>



1910 - 2010
100 YEARS OF ACADEMIC EXCELLENCE

Founding Campuses: ■ Edgewood ■ Howard College ■ Medical School ■ Pietermaritzburg ■ Westville